UNIVERSITAT DE BARCELONA

From ultrafine to coarse particles: variability and source apportionment of atmospheric aerosol levels in the urban Mediterranean climate

Mariola Brines Pérez

CSIC
Consejo Superior de Investigaciones Científicas

idaea
Institut de Diagnosi Ambiental i Estudis de l'Aigua

Universitat de Barcelona
Departament d'Astronomia i Meteorologia

From ultrafine to coarse particles: variability and source apportionment of atmospheric aerosol levels in the urban Mediterranean climate

Mariola Brines Pérez

PhD thesis

Barcelona, August 2015

Supervisors:

Dr. Xavier Querol Carceller

Dr. Manuel Dall'Osto

Tutor:

Dr. Jeroni Lorente Castelló

Front and back covers courtesy of Xavier Querol.

Programa de doctorat en Física

From ultrafine to coarse particles: variability and source apportionment of atmospheric aerosol levels in the urban Mediterranean climate

Memòria presentada per

Mariola Brines Pérez

per optar al grau de
Doctor per la Universitat de Barcelona

Barcelona, agost 2015

Directors de tesi:

Dr. Xavier Querol Carceller

Dr. Manuel Dall'Osto

Tutor:

Dr. Jeroni Lorente Castelló

Als meus pares Carme i Joan

Abstract

Air pollution is a major environmental and public health concern, especially in urban areas where both emission sources and population are concentrated. The association between atmospheric particulate matter mass levels (PM) and particle number concentration (N) with respiratory and cardiovascular morbidity and mortality has been demonstrated by many epidemiological studies. Thus, aerosol sources and processes are being thoroughly investigated in order to identify those contributing to an increase in N and PM and develop according abatement strategies.

The sources and evolution of aerosols and gaseous pollutants once emitted into the atmosphere vary in each region, depending on geographical, climatological and meteorological conditions. This is applicable to Europe, with varying features from the cold and rainy northern countries to the warmer and drier southern regions. In particular, the Western Mediterranean Basin, and the coastal city of Barcelona (Spain) in particular are characterized by a warm dry climate, with scarce precipitation and high urban density and being geographically constrained by the coastal range it is also affected by the sea breeze regime.

Within this context, the intensive SAPUSS (Solving Aerosol Problems by Using Synergistic Strategies) campaign was developed in autumn 2010 in Barcelona (1 month duration), which consisted on concurrent aerosol measurements at different sites in the city region. The spatial distribution of the sites allowed the study of the aerosol temporal variability as well as the spatial distribution, progressively moving away from urban aerosol sources. The sites used in this thesis are: Road Site (RS) and Urban Background (UB) were located on ground levels, whereas Torre Mapfre (TM) and Torre Collserola (TC), representative of the urban/suburban environment were located at certain height above the city (150 m a.s.l. and 415 m a.s.l., respectively). Finally the Regional Background site (RB) located 50 km from the city allowed for the study of the transport of urban emissions outside the city.

Simultaneous sampling of aerosol size distributions during SAPUSS at the RS, UB, TC and RB with a Scanning Mobility Particle Sizer (SMPS) sites were studied after performing a k-means cluster analysis on the combined data sets. This allowed the

classification of all size distributions in 9 clusters which could be grouped in 3 main categories: "Traffic" (Traffic 1 "T_{clus_1}" - 8%, Traffic 2 "T_{clus_2}" - 13%, Traffic 3, "T_{clus_3}" - 9%), "Background Pollution" (Urban Background 1 "UB_{clus_1}" - 21%, Regional Background 1, "RB_{clus_1}" - 15%, Regional Background 2, "RB_{clus_2}" - 18%) and "Special cases" (Nucleation "NU_{clus}" - 5%, Regional Nitrate, "NIT_{clus}" - 6%, and Mix "MIX_{clus}"- 5%). As expected, the frequency of traffic clusters (T_{clus_1-3}) followed the order RS_{site}, UB_{site}, TC_{site}, and RB_{site}. These showed typical traffic modes mainly distributed at 20-40 nm and the shrinking of freshly emitted particles was detected as they were transported from the traffic hot spots towards urban background environments. The urban background sites (UB_{site} and TC_{site}) reflected also as expected urban background number concentrations (average values, N = $1.0 \cdot 10^4$ cm^{-3} and N = $5.5 \cdot 10^3$ cm^{-3}, respectively, relative to $1.3 \cdot 10^4$ cm^{-3} seen at RS_{site}). The cluster describing the urban background pollution (UB_{clus_1}) could be used to monitor the sea breeze circulation towards the regional background study area. Overall, the RB_{site} was mainly characterised by two different regional background aerosol size distributions: whilst both exhibited low N ($2.7 \cdot 10^3$ for RB_{clus_1} and $2.2 \cdot 10^3$ cm^{-3} for RB_{clus_2}), RB_{clus_1} had average PM_{10} concentrations higher than RB_{clus_2} (27 vs 23 µg m^{-3}). As regards the minor aerosol size distribution clusters, the "Nucleation" cluster was observed during daytime whilst the "Regional Nitrate" was mainly seen at night. The ninth cluster ("Mix") was the least well defined and likely composed of a number of aerosol sources. When correlating averaged values of N, NO_2 and PM for each *k*-means cluster, a linear correlation between N and NO_2 with values progressively increasing from the regional site RB_{site} to the road site RS_{site} was found. This points to vehicular traffic as the main source of both N and NO_2. By contrast, such an association does not exist for the case of the nucleation cluster, where the highest N is found with low NO_2 and PM. Within the measurement range of SMPS ($N_{15\text{-}228\ nm}$) and Condensation Particle Counters (CPC, $N_{>5\ nm}$), ultrafine particles within the range 5-15 nm in urban areas were found the most dynamic, being a complex ensemble of primary evaporating traffic particles, traffic tailpipe new particle formation and non-traffic new particle formation.

Road traffic emissions are often considered the main source of ultrafine particles (diameter smaller than 100 nm) in urban environments. However, this thesis and other

recent studies worldwide have shown that - in high-insolation urban regions at least - new particle formation events can also contribute to UFP. In order to quantify such events three cities located in predominantly sunny environments were systematically studied: Barcelona (Spain), Madrid (Spain) and Brisbane (Australia). Three long term datasets (1-2 years) of fine and ultrafine particle number size distributions (measured by SMPS) were analysed. By applying the same *k*-means clustering analysis, the collected aerosol size distributions we categorized as: "Traffic" (prevailing 44-63% of the time), "Nucleation" (14-19%) and "Background pollution and Specific cases" (7-22%). Measurements from Rome (Italy) and Los Angeles (USA) were also included to complement the study. The daily variation of the average UFP concentrations for a typical nucleation day at each site revealed a similar pattern for all cities, with three distinct particle bursts. A morning and an evening spike reflected traffic rush hours, whereas a third one at midday showed nucleation events. The photochemically nucleated particles burst lasted 1-4 hours, reaching sizes of 30-40 nm. On average, the occurrence of particle size spectra dominated by nucleation events was 16% of the time, which represented 22% of the annual average N, showing the importance of this process as a source of UFP in urban environments exposed to high solar radiation. On average, nucleation events lasting for 2 hours or more occurred on 55% of the days, this extending to >4hrs in 28% of the days, demonstrating that atmospheric conditions in urban environments are not favourable to the growth of photochemically nucleated particles.

The composition of the fine particulate matter fraction (PM_1, PM mass levels below 1 μm) was studied during the SAPUSS campaign in Barcelona. The samples collected at the RS and UB sites were analysed for organic and inorganic compounds, and the PMF EPA v5.0 (Possitive Matrix Factorization versión 5.0 from US-EPA) was applied to the data. This yielded 9 factors which apportioned the main pollution sources to PM_1 levels in the Barcelona urban environment: (1) Fresh traffic (RS: 2.9 μgm^{-3}, 18% of PM_1; UB: 1.2 μgm^{-3}, 10% of PM_1), (2) Organic urban mix (RS: 3.5 μgm^{-3}, 21%; UB: 0.2 μgm^{-3}, 2%), (3) Nitrate (RS: 2.8 μgm^{-3}, 17%; UB: 1.3 μgm^{-3}, 11%), (4) Industrial NE & sea salt (RS: 2.5 μgm^{-3}, 16%; UB: 2.2 μgm^{-3}, 18%), (5) Industrial SW & pin (RS: 0.8 μgm^{-3}, 5%; UB: 1.3 μgm^{-3}, 11%), (6) Shipping (RS: 2.4 μgm^{-3}, 15%; UB: 2.6

μgm^{-3}, 22%), (7) SIA (RS: 0.4 μgm^{-3}, 2%; UB: 0.6 μgm^{-3}, 5%), (8) Bio SOA (RS: 0.9 μgm^{-3}, 6%; UB: 2.3 μgm^{-3}, 19%) and (9) Biomass burning (RS: 0.1 μgm^{-3}, 1%; UB: 0.2 μgm^{-3}, 2%). The analysis of both inorganic and organic species made possible the identification of the industrial NE & sea salt source for the first time in the study area in the PM_1 fraction. Moreover, the joint study of inorganic and organic species resulted in a more complete and realistic study with a higher number of identified sources, as opposed to traditional studies limited to one kind of species. Industrial and shipping emissions accounted on average for 42% of the PM_1 mass, being the most relevant contributor to this size fraction, followed by secondary aerosols (29% on average) and traffic sources (28% on average). The biomass burning contribution was very low (1% on average), as previously reported in the study area. A clear decrease in concentration levels was detected with the distance to the emission sources; while the RS was dominated by traffic emissions (39% of PM_1), the UB was heavily impacted by industrial sources (51% of PM_1). Secondary aerosols were also more relevant at the UB than at the RS (RS: 25% of PM_1; UB: 35% of PM_1).

The sources contributing to the PM_{10} fraction (PM mass levels below 10 μm) were also analysed during the SAPUSS campaign. In this case the focus was set on evaluating the sources affecting this size fraction in both the horizontal and vertical levels. For this purpose, concurrent sampling at two ground sites (RS and UB) and two tower sites elevated above the city ground (TM and TC) was carried out. PM_{10} concentrations decreased from the traffic hot spots to the city background (RS 30.7 μg m^{-3}, UB 25.9 μg m^{-3}, TM 24.8 μg m^{-3} and TC 21.8 μg m^{-3}). Further sources apportionment of the inorganic species at the four sites by means of PMF v3.0 and ME-2 (Multilinear Engine-2) produced 8 factors: (1) Vehicle exhaust and wear (2-9 μgm^{-3}, 20-27% on average), (2) Road dust (2-4 μgm^{-3}, 9-12%), (3) Mineral dust (around 5 μgm^{-3}, 14-26%), (4) Aged marine (3-5 μgm^{-3}, 13-20%), (5) Heavy oil (0.4-0.6 μgm^{-3}, 2%), (6) Industrial (around 1.0 μgm^{-3}, 3-5%), (7) Sulphate (3-4 μgm^{-3}, 11-17%) and (8) Nitrate (4-6 μgm^{-3}, 17-21%). The concentrations registered at the ground sites (RS and UB) were two times higher than at the tower sites (TM and TC) for the vehicle exhaust and wear, road dust and industrial factors, evidencing the influence of the distance to emission sources. The factors contribution were relatively homogeneous both in horizontal and vertical

levels. However, proximity to the emission sources, air mass origin and meteorological parameters played a key role in influencing the variability of the factors concentrations. The mineral dust and "aged marine" (due to chemical reaction with anthropogenic pollutants) factors were found to be a mixture of natural and anthropogenic components and were thus further investigated.

Overall, 3 types of dust were identified to affect the urban area: road dust (35% of the dust load, 2-4 μgm^{-3} on average), Saharan dust (28%, 2.1 μgm^{-3}) and background mineral dust (37%, 2.8 μgm^{-3}). As regards of the aged marine factor, anthropogenic marine sulphate of regional origin (44% of the marine load, 1.8 μgm^{-3} on average, related with the SO_2 shipping emissions near the catalan coast) was found to be internally mixed with this factor. This marine sulphate did not correlate with the PMF sulphate factor, thus being attributed to the intense regional shipping emissions in the Western Mediterranean Basin, whereas the sulphate factor was attributed to mainland power generation and industrial sources. Our results evidence that although the city shows a homogeneous distribution of PM_{10} pollution sources, primary vehicle emissions and road dust are found to decrease in concentration with the distance to the emission points.

Overall, the complete study of aerosol fractions affecting the urban area of Barcelona and similar urban environments (Madrid, Brisbane, Roma and Los Angeles), from ultrafine to coarse particles, enables the identification of the main sources affecting each size fraction in particular and aerosol pollutants in general. Owing to the results obtained and the different techniques applied, some recommendations regarding air pollution studies and air quality measures are proposed:

- Although road traffic is the main source of ultrafine particles, due to the influence of nucleation events in highly insolated urban environments (on average 22% of the total particle number concentration), BC measurements are proposed as a more accurate parameter to monitor road traffic emissions.
- Regarding epidemiological studies, it would be advisable to study the morbidity and mortality associated with the daily N concentration,

differentiating between the nucleation particles and the traffic related ones, as they are thought to affect human helth differently.

- The inclusion of both organic and inorganic species in the source apportionment studies leads to a better understanding of the complex pollution scenario affecting urban environments and a higher number of resolved emission factors.
- Regarding the PM_{10} fraction, it is recommended to study effective abatement strategies to reduce the mineral dust of anthropogenic urban origin and to further investigate the regional sulphate concentrations due to the intense maritime traffic in the Mediterranean basin, as they both represent a relevant contribution to the mineral load and the total sulphate, respectively (38% of the mineral load and 32% of the sulphate load).

Resum

La contaminació atmosfèrica s'ha convertit en un motiu de preocupació degut al seu impacte en el medi ambient i en la salut de les persones, especialment en zones urbanes on es concentren les principals fonts d'emissió així com una alta densitat de població. Diversos estudis epidemiològics han demostrat la relació existent tant entre els nivells de massa de matèria particulada atmosfèrica (PM), com de la concentració del nombre de partícules (N), amb la incidència de malalties respiratòries i cardiovasculars. Per aquest motiu, s'està investigant de forma exhaustiva les fonts d'emissió i els processos que afecten als aerosols atmosfèrics, amb la finalitat d' identificar aquells que hi contribueixen a incrementar els nivells d'aquests contaminants i poder desenvolupar-hi mesures mitigadores efectives.

Les fonts d'emissió i l'evolució dels aerosols un cop emesos a l'atmosfera varien a cada regió en funció de les condicions geogràfiques, climàtiques i meteorològiques. A Europa, els països del nord es caracteritzen per un ambient més fred i plujós, mentre que al sud el clima és més temperat i sec. En la conca Mediterrània Occidental, i més concretament en la ciutat costanera de Barcelona, el clima es caracteritza per ser càlid i amb escassa precipitació. A més a més, la ciutat es troba molt densament poblada a més d'estar limitada geogràficament per la serralada litoral i trobar-se sota la influència de la brisa marina.

En aquest context es va desenvolupar la campanya intensiva SAPUSS (Solving Aerosol Problems by Using Synergistic Strategies) durant la tardor de 2010 a Barcelona (1 mes de durada), que va consistir en mesures simultànies d'aerosols a diferents ambients de la ciutat. La distribució espacial de les estacions de mesura va permetre estudiar la variabilitat espacial i temporal dels aerosols a mesura que un s'allunyava del centre de la ciutat. Les estacions de mesura utilitzades en aquesta tesi són: l'estació de trànsit "Road Site" (RS) i la de fons urbà "Urban Background" (UB) estaven situades a nivell de carrer, mentre que "Torre Mapfre" (TM) i "Torre Collserola" (TC), representatives d'escenaris urbans/suburbans, es trobaven a una certa alçada (150 m a.s.l. i 415 m a.s.l., respectivament). Per últim, l'estació de fons regional "Regional

Background" (RB), situada a 50 km de Barcelona permeté l'estudi del transport de les emissions urbanes a zones rurals properes.

La mesura de nivells d'aerosols en funció de la mida de partícula simultàniament a RS, UB, TC i RB amb Scanning Mobility Particle Sizer (SMPS) i la posterior aplicació de tècniques estadístiques de k-means clustering han permès fer-ne un estudi conjunt combinant les dades recollides a les 4 estacions. Així doncs, els 9 clústers o categories en que s'han classificat les distribucions de mida es poden agrupar en tres categories principals: "Trànsit" (Traffic 1 "T_{clus_1}" - 8%, Traffic 2 "T_{clus_2}" - 13%, Traffic 3, "T_{clus_3}" - 9%), "Contaminació de fons" (Urban Background 1 "UB_{clus_1}" - 21%, Regional Background 1, "RB_{clus_1}" - 15%, Regional Background 2, "RB_{clus_2}" - 18%) i "Casos especials" (Nucleation "NU_{clus}" - 5%, Regional Nitrate, "NIT_{clus}" - 6%, and Mix "MIX_{clus}"- 5%). Tal com era d'esperar, la freqüència dels clústers de trànsit (T_{clus_1-3}) segueix l'ordre RS_{site}, UB_{site}, TC_{site}, and RB_{site}. Aquests clústers mostren les modes típiques del trànsit distribuïdes entre 20-40 nm. També s'observa una disminució de la mida de les partícules "fresques" emeses pel trànsit mentre es transporten dels llocs d'emissió cap a ambients de fons urbans. Les estacions de fons urbà (UB_{site} i TC_{site}) reflecteixen concentracions de N més baixes que les més properes al trànsit (valors mitjans, N = $1.0 \cdot 10^4$ cm^{-3} i N = $5.5 \cdot 10^3$ cm^{-3}, respectivament, comparat amb $1.3 \cdot 10^4$ cm^{-3} registrat a RS_{site}). El clúster que descriu la contaminació de fons urbana (UB_{clus_1}) es pot emprar per a descriure la circulació de la brisa marina que transporta la contaminació cap a l'estació de fons regional. En general, l'estació RB_{site} es caracteritza pels dos clústers representatius de la contaminació de fons regional, que mostren diferències entre ells: encara que ambdós es caracteritzen per un baix N ($2.7 \cdot 10^3$ el RB_{clus_1} i $2.2 \cdot 10^3$ cm^{-3} el RB_{clus_2}), RB_{clus_1} mostra una mitjana de concentració de PM_{10} més alta que RB_{clus_2} (27 vs 23 μg m^{-3}). Pel que respecta els clústers minoritaris, "Nucleation" s'observa durant el migdia, mentre "Regional Nitrate" s'observa normalment durant la nit. El novè clúster ("Mix") es troba poc definit i probablement es tracta d'una mescla de diverses fonts de contaminants. En fer les correlacions entre les concentracions mitjanes de N, NO_2 i PM i cadascú dels clústers, s'observen correlacions lineals entre N i NO_2, amb valors augmentant progressivament de l'estació regional RB_{site} a l'estació de trànsit RS_{site}, posant en evidència que el trànsit rodat és la principal font d'N i NO_2. Pel

contrari, no s'observa aquesta relació per al clúster de nucleació, donat que les altes concentracions de N estan inversament relacionades amb les de NO_2 i PM. Dins del rang de mesura de l'SMPS ($N_{15\text{-}228\ nm}$) i dels Condensation Particle Counters (CPC, $N_{>5\ nm}$), les partícules ultrafines en el rang 5-15 nm en ambients urbans són molt dinàmiques, ja que contenen una complexa mescla de partícules primàries del trànsit que poden evaporar, partícules de nova formació en els tubs d'escapament i altres de nova formació no relacionades de forma directa amb el trànsit.

Es considera doncs, en el nostre estudi i en d'altres que les emissions del trànsit rodat són la principal font de partícules ultrafines (diàmetre inferior a 100 nm) en ambients urbans. No obstant, aquesta treball i altres estudis recents han mostrat que almenys, en regions exposades a alts nivells d'insolació, els episodis de formació de noves partícules poden contribuir als nivells de partícules ultrafines. Amb l'objectiu de quantificar aquests episodis es van escollir tres ciutats situades en climes caracteritzats per una elevada insolació: Barcelona, Madrid i Brisbane (Australia). Per aquest motiu es van analitzar tres sets de dades de llarga durada (1-2 anys) de distribució de mida de partícules fines i ultrafines (mesurades amb un SMPS). Mitjançant la mateixa tècnica estadística del k-means clustering foren classificades en tres categories principals: "Trànsit" (prevalença del 44-63% del temps), "Nucleació" (14-19%) i "Contaminació de fons i casos específics" (7-22%). Per tal de complementar l'estudi també s'han inclòs mesures de Roma (Itàlia) i Los Angeles (EEUU). La variació mitjana de les partícules ultrafines durant un dia típic de nucleació presenta similituds entre totes les ciutats, mostrant clarament tres puntes de nivells de N, dos d'ells relacionats amb les emissions del trànsit rodat a les hores punta del matí i del vespre i un tercer pic al migdia associat a episodis de nucleació. Els pics de partícules originades per processos de nucleació fotoquímica tenen una durada de 1-4 hores i les partícules assoleixen mides de 30-40 nm. De mitjana, els episodis de nucleació dominen la distribució de mida de partícula un 16% del temps, que representa un 22% de l'N mitjà anual, fet que demostra la importància d'aquest procés com a font de partícules ultrafines en ambients urbans exposats a alts nivells de radiació solar. Típicament, aquests processos tenen una durada superior o igual a 2 hores el 55% dels dies, mentre que la xifra es redueix al 28% dels dies per a durades superiors a 4 hores. Aquest fet demostra

que les condicions atmosfèriques que es troben en ambients urbans no afavoreixen el creixement de les partícules fruit de processos de nucleació fotoquímica.

La composició de la fracció fina de la matèria particulada (PM_1, nivells de massa de PM inferior a 1 μm de grandària) també fou objecte d'estudi durant la campanya SAPUSS en Barcelona. Les mostres foren recollides a les estacions de trànsit RS i fons urbà UB i analitzades per a compostos orgànics i inorgànics. Posteriorment es va aplicar el model de contribució de fonts PMF EPA v5.0 (Possitive Matrix Factorization versió 5.0 de la US-EPA) que va donar com a resultat 9 factors que contribueixen als nivells de PM_1 en aire ambient a Barcelona: (1) Fresh traffic (RS: 2.9 μgm^{-3}, 18% de PM_1; UB: 1.2 μgm^{-3}, 10% de PM_1), (2) Organic urban mix (RS: 3.5 μgm^{-3}, 21%; UB: 0.2 μgm^{-3}, 2%), (3) Nitrate (RS: 2.8 μgm^{-3}, 17%; UB: 1.3 μgm^{-3}, 11%), (4) Industrial NE & sea salt (RS: 2.5 μgm^{-3}, 16%; UB: 2.2 μgm^{-3}, 18%), (5) Industrial SW & pin (RS: 0.8 μgm^{-3}, 5%; UB: 1.3 μgm^{-3}, 11%), (6) Shipping (RS: 2.4 μgm^{-3}, 15%; UB: 2.6 μgm^{-3}, 22%), (7) SIA (RS: 0.4 μgm^{-3}, 2%; UB: 0.6 μgm^{-3}, 5%), (8) Bio SOA (RS: 0.9 μgm^{-3}, 6%; UB: 2.3 μgm^{-3}, 19%) i (9) Biomass burning (RS: 0.1 μgm^{-3}, 1%; UB: 0.2 μgm^{-3}, 2%). L'anàlisi tant d'espècies inorgàniques com orgàniques va permetre la identificació de la font industrial NE & sea salt per primer cop a la fracció PM_1 en aquesta àrea d'estudi. A més a més, l'estudi conjunt d'ambdós tipus d'espècies va permetre la identificació d'un nombre major de fonts, donat que els estudis tradicionals fets fins ara que només inclouen un dels dos tipus d'espècies. Les emissions de fonts industrials i del transport marítim són les més rellevants i representen un 42% de la massa de PM_1, seguides dels aerosols secundaris (29% de mitjana) i del trànsit rodat (28% de mitjana). La contribució de la crema de biomassa fou molt baixa (1% de mitjana), tal com es va trobar en estudis previs. S'ha observat una clara disminució dels nivells de concentració amb la distància a les fonts emissores; mentre l'estació de trànsit RS estava dominada per les emissions del trànsit rodat (39% de PM_1), l'estació de fons urbà UB presentava un major impacte de les fonts industrials (51% de PM_1). També es destaca que els nivells d'aerosols secundaris eren més elevats al fons urbà que al centre de la ciutat (RS: 25% of PM_1; UB: 35% of PM_1).

Les fonts que contribueixen a la fracció PM_{10} (nivells de massa de PM inferiors a 10 μm) també van ser estudiades durant la campanya SAPUSS. En aquest cas, l'estudi es

va centrar en avaluar les fonts que influencien aquesta fracció tant a nivell horitzontal com vertical sobre l'atmosfera de Barcelona. Amb aquest propòsit es van recollir mostres a dues estacions a nivell de carrer (RS i UB) i a una certa alçada (TM i TC). Els nivells de PM_{10} presenten una clara disminució de concentració des dels ambients més propers al trànsit fins als més nets (RS 30.7 μg m^{-3}, UB 25.9 μg m^{-3}, TM 24.8 μg m^{-3} i TC 21.8 μg m^{-3}). L'anàlisi de contribució de fonts mitjançant PMF v3.0 i ME-2 (Multilinear Engine 2) d'espècies inorgàniques obtingudes a les 4 estacions han resultat en 8 factors: (1) Vehicle exhaust and wear (2-9 μgm^{-3}, 20-27% de PM_{10} de mitjana), (2) Road dust (2-4 μgm^{-3}, 9-12%), (3) Mineral dust (al voltant 5 μgm^{-3}, 14-26%), (4) Aged marine (3-5 μgm^{-3}, 13-20%), (5) Heavy oil (0.4-0.6 μgm^{-3}, 2%), (6) Industrial (al voltant d' 1.0 μgm^{-3}, 3-5%), (7) Sulphate (3-4 μgm^{-3}, 11-17%) i (8) Nitrate (4-6 μgm^{-3}, 17-21%). Els factors relacionats amb el trànsit rodat així com el factor industrial mostren el doble de concentració a les estacions RS i UB en comparació amb les torres (TM i TC), mentre la resta de factors mostren una distribució homogènia a nivells horitzontals i verticals. Així i tot, la proximitat a les fonts d'emissió, l'origen de les masses d'aire i els paràmetres meteorològics també influencien les concentracions dels factors. Els factors de la pols mineral i aerosols marins "envellits" (per reacció química amb contaminants antropogènics) han resultat ser una mescla de fonts naturals i antropogèniques, i per aquest motiu han estat analitzades en més profunditat.

S'han identificat 3 tipus de pols mineral que afecten l'ambient urbà: la pols de carretera o rodament (35% dels pols mineral; 2-4 μgm^{-3} de mitjana), la pols Sahariana (28%, 2.1 μgm^{-3}) i la pols mineral de fons (37%, 2.8 μgm^{-3}). Pel que respecta a l'aerosol marí, es va trobar que el sulfat marí d'origen antropogènic regional (degut a les emissions d'SO_2 del trànsit marítim enfront de les costes catalanes) estava inclòs en aquest factor (44% de l'aerosol marí, 1.8 μgm^{-3} de mitjana). Aquest sulfat marí no presentava cap correlació amb el factor sulfat, i per tant es va associar a l'intens trànsit marítim, mentre que el factor sulfat s'associa a fonts de generació elèctrica i industrials. Els resultats d'aquesta tesi posen en evidència que encara que la ciutat mostra una distribució relativament homogènia de les fonts d'emissió de PM_{10}, les concentracions relacionades amb emissions primàries de vehicles i la pols de rodament disminueixen amb la distància als focus emissors.

L'estudi complet de les diferents fraccions d'aerosols que afecten l'àrea urbana de Barcelona i ambients urbans similars (Madrid, Brisbane, Roma i Los Angeles), cobrint des de les partícules ultrafines fins a les més grolleres, ha permès la identificació de les principals fonts que afecten a cada fracció en particular i als aerosols en general. Considerant els resultats obtinguts en aquesta tesi i gràcies a les diferents tècniques emprades, es proposen les següent recomanacions referents als estudis sobre contaminants atmosfèrics i les conseqüents mesures de millora de la qualitat de l'aire aplicables:

- Encara que el trànsit rodat és la font principal de partícules ultrafines en ambients urbans, donada la influència dels processos de nucleació en ambients urbans sota alta insolació (de mitjana 22% de la concentració mitjana anual del numero total de partícules), les mesures de BC constitueixen un paràmetre més adequat per a monitoritzar les emissions del trànsit rodat.
- Per a estudis epidemiològics, s'aconsella estudiar la mortalitat i morbiditat associada a la concentració diària del numero de partícules, però també la diferenciant entre el numero de partícules de nucleació i de trànsit, donat que els efectes en la salut seran molt diferents.
- El fet d'incloure espècies orgàniques i inorgàniques en l'anàlisi de contribució de fonts a PM millora l'anàlisi del complex escenari d'emissions que afecten els ambients urbans, a més de resoldre un major nombre de fonts.
- Pel que respecta a la fracció de PM_{10}, es recomana la implementació de mesures de control efectives per a reduir la concentració de pols mineral de fons d'origen antropogènic i continuar investigant la contribució del sulfat d'origen regional lligat a la intensa activitat marítima al Mediterrani, donat que ambdues representen una fracció important de la fracció mineral i de sulfat totals, respectivament (38% de la fracció mineral i 32% del sulfat total).

Resumen

La contaminación atmosférica se ha convertido en un motivo de preocupación dado su impacto en el medio ambiente y en la salud de las personas, especialmente en zonas urbanas donde se concentran las principales fuentes de emisión así como una alta densidad de población. Numerosos estudios epidemiológicos han demostrado la relación existente tanto entre los niveles de masa de materia particulada atmosférica (PM) como de la concentración del número de partículas (N), con la incidencia de enfermedades respiratorias y cardiovasculares. Por este motivo, se está investigando de forma exhaustiva las fuentes de emisión y los procesos que afectan a los aerosoles atmosféricos, con la finalidad de identificar a aquellos que contribuyen a incrementar los niveles y así poder desarrollar medidas mitigadoras efectivas.

Las fuentes de emisión y la evolución de los aerosoles atmosféricos varían en cada región en función de las condiciones geográficas, climáticas y meteorológicas. En el caso de Europa, los países del norte se caracterizan por un ambiente más frio y lluvioso, mientras que los del sud se disfrutan de un clima más templado y seco. En la cuenca Mediterránea Occidental, y más concretamente en la ciudad costera de Barcelona (España), el clima se caracteriza por ser cálido y seco, con escasas precipitaciones y alta densidad de población, además de estar limitado geográficamente por la cordillera litoral y estar bajo la influencia de la brisa marina.

En este contexto se desarrolló la campaña intensiva SAPUSS (Solving Aerosol Problems by Using Synergistic Strategies) durante el otoño de 2010 a Barcelona (1 mes de duración), que consistió en medidas simultáneas de aerosoles en diferentes ambientes de la ciudad. La distribución espacial de las estaciones de medida permitió estudiar la variabilidad espacial y temporal de los aerosoles a medida que uno se aleja del centre de la ciudad. Las estaciones de muestreo utilizadas en esta tesis son: la estación de tráfico “Road Site” (RS) y la de fondos urbano “Urban Background” (UB) están situadas a nivel de calle, mientras que “Torre Mapfre” (TM) y “Torre Collserola” (TC), representativas de escenarios urbanos/suburbanos se encontraban a una cierta altitud (150 m a.s.l. y 415 m a.s.l., respectivamente). Por último, la estación de fondo

regional “Regional Background” (RB), situada a 50 km de Barcelona permitió el estudio del transporte de las emisiones urbanas en zonas rurales cercanas.

La medida de niveles de aerosoles en función del tamaño de partícula simultáneamente en RS, UB, TC y RB con el Scanning Mobility Particle Sizer (SMPS) y la posterior aplicación de técnicas estadísticas de k-means clustering han permitido realizar un estudio conjunto combinando los datos recogidos en las 4 estaciones. Así pues, los 9 clústeres o categorías en las que se han clasificado las distribuciones por tamaño se pueden agrupar en tres categorías principales: “Tráfico” (Traffic 1 "T_{clus_1}" - 8%, Traffic 2 "T_{clus_2}" - 13%, Traffic 3, "T_{clus_3}" - 9%), "Contaminación de fondo" (Urban Background 1 "UB_{clus_1}" - 21%, Regional Background 1, "RB_{clus_1}" - 15%, Regional Background 2, "RB_{clus_2}" - 18%) and "Casos especiales" (Nucleation "NU_{clus}" - 5%, Regional Nitrate, "NIT_{clus}" - 6%, and Mix "MIX_{clus}"- 5%). Como era de esperar, la frecuencia de los clústeres de tráfico ($T_{clus\_1\text{-}3}$) sigue el orden RS_{site}, UB_{site}, TC_{site}, y RB_{site}. Estos clústeres muestran las modas típicas del tráfico distribuidas entre 20-40 nm. También se observa una disminución del tamaño de las partículas “frescas” emitidas por el tráfico mientras son transportadas de los sitios de emisión hacia ambientes de fondo urbano. Las estaciones de fondo urbano (UB_{site} y TC_{site}) reflejan concentraciones de N más bajas que las más cercanas al tráfico (valores promedio, N = $1.0\cdot10^4$ cm^{-3} y N = $5.5\cdot10^3$ cm^{-3}, respectivamente, comparado con $1.3\cdot10^4$ cm^{-3} registrado en RS_{site}). El clúster que describe la contaminación de fondo urbana (UB_{clus_1}) se puede utilizar para describir la circulación de la brisa marina que transporta la contaminación hacia el fondo regional. En general, la estación RB_{site} se caracteriza por dos clústeres representativos de la contaminación de fondo regional, aunque se pueden observar diferencias entre ambos: aunque los dos se caracterizan por un N bajo ($2.7\cdot10^3$ el RB_{clus_1} y $2.2\cdot10^3$ cm^{-3} el RB_{clus_2}), RB_{clus_1} muestra una concentración promedio de PM_{10} más alta que RB_{clus_2} (27 vs 23 $\mu g\ m^{-3}$). Por lo que respecta a los clústeres minoritarios, “Nucleation” se observa durante el mediodía, mientras que “Regional Nitrate” se observa normalmente por la noche. El noveno clúster (“Mix”) es el que está menos definido y probablemente se trata de una mezcla de varias fuentes de contaminantes. Las correlaciones entre las concentraciones promedio de N, NO_2 y PM y cada uno de los clústeres, muestran correlaciones lineales entre N y NO_2, y los valores aumentan

progresivamente de la estación regional RB_{site} a la estación de tráfico RS_{site}, quedando en evidencia que el tráfico rodado es la principal fuente de N y NO_2. Por el contrario esta relación no se cumple para el clúster de nucleación, dado que las altas concentraciones de N están inversamente relacionadas con NO_2 y PM. Dentro del rango de medida del SMPS ($N_{15\text{-}228\ nm}$) y de los Condensation Particle Counters (CPC, $N_{>5\ nm}$), las partículas ultrafinas en el rango 5-15 nm en ambientes urbanos son muy dinámicas, dado que contienen una compleja mezcla de partículas primarias de tráfico que poden evaporarse, partículas de nueva formación en los tubos de escape y otras de nueva formación no relacionadas con el tráfico de forma directa.

Así pues, se considera en nuestro estudio y en muchos otros, que las emisiones del tráfico rodado son la principal fuente de partículas ultra finas (diámetro inferior a 100 nm) en ambientes urbanos. No obstante, este trabajo y otros estudios recientes han mostrado que al menos, en regiones expuestas a altos niveles de insolación, episodios de formación de nuevas partículas pueden contribuir a los niveles de partículas ultra finas. Con el objetivo de cuantificar la incidencia de estos episodios se escogieron tres ciudades situadas en climas caracterizados por una alta radiación solar: Barcelona (España), Madrid (España) y Brisbane (Australia). Por este motivo se analizaron tres sets de datos (1-2 años) de distribución por tamaño de partículas finas y ultra finas (medidas mediante un SMPS). Aplicando la misma técnica estadística del k-means clustering se han clasificado en tres categorías principales: “Tráfico” (prevalencia del 44-63% del tiempo), “Nucleación” (14-19%) y “Contaminación de fondo y casos específicos” (7-22%). Para complementar el estudio también se han incluido datos de Roma (Italia) y Los Angeles (EEUU). La variación promedio de las partículas ultra fines durante un día típico de nucleación presenta similitudes en todas las ciudades, mostrando claramente tres picos niveles de N, dos de ellos relacionados con las emisiones del tráfico rodado en les horas punta de la mañana y la tarde y un tercer pico al mediodía asociado a episodios de nucleación. Los brotes de partículas originados por procesos de nucleación fotoquímica tienen una duración de 1-4 horas y las partículas crecen hasta los 30-40 nm. En promedio, los episodios de nucleación dominan la distribución por tamaños un 16% del tiempo, que representa un 22% del promedio anual de N, lo que demuestra la importancia de este proceso como fuente

de partículas ultra fines en ambientes urbanos expuestos a altos niveles de radiación solar. Típicamente, estos procesos tienen una duración superior o igual a 2 horas el 55% de los días, mientras que la cifra se reduce al 28% de los días para duración superiores a 4 horas. Este hecho demuestra que las condiciones atmosféricas que se encuentran en ambientes urbanos no favorecen el crecimiento de las partículas fruto de procesos de nucleación fotoquímica.

La comparación de la fracción fina de la materia particulada (PM_1, niveles de masa de PM inferior a 1 μm de tamaño) también fue objeto de estudio durante la campaña SAPUSS en Barcelona. Las muestras fueron recogidas en las estaciones de tráfico RS y fondo urbano UB y analizadas para compuestos orgánicos e inorgánicos. Posteriormente se aplicó el modelo de contribución de fuentes PMF EPA v5.0 (Possitive Matrix Factorization versión 5.0 de la US-EPA) que dio como a resultado 9 factores que contribuyen a los niveles de PM_1 en aire ambiente de Barcelona: (1) Fresh traffic (RS: 2.9 μgm^{-3}, 18% del PM_1; UB: 1.2 μgm^{-3}, 10% del PM_1), (2) Organic urban mix (RS: 3.5 μgm^{-3}, 21%; UB: 0.2 μgm^{-3}, 2%), (3) Nitrate (RS: 2.8 μgm^{-3}, 17%; UB: 1.3 μgm^{-3}, 11%), (4) Industrial NE & sea salt (RS: 2.5 μgm^{-3}, 16%; UB: 2.2 μgm^{-3}, 18%), (5) Industrial SW & pin (RS: 0.8 μgm^{-3}, 5%; UB: 1.3 μgm^{-3}, 11%), (6) Shipping (RS: 2.4 μgm^{-3}, 15%; UB: 2.6 μgm^{-3}, 22%), (7) SIA (RS: 0.4 μgm^{-3}, 2%; UB: 0.6 μgm^{-3}, 5%), (8) Bio SOA (RS: 0.9 μgm^{-3}, 6%; UB: 2.3 μgm^{-3}, 19%) and (9) Biomass burning (RS: 0.1 μgm^{-3}, 1%; UB: 0.2 μgm^{-3}, 2%). El análisis tanto de especies inorgánicas como orgánicas permitió la identificación de la fuente industrial NE & sea salt por primera vez en la fracción PM_1 en esta área de estudio. Además, el estudio conjunto de ambos tipos de especies permitió la identificación de un mayor número de fuentes que los estudios tradicionales realizados hasta ahora que sólo incluyen uno de los dos tipos de especies. Las emisiones de fuentes industriales y del transporte marítimo son las más relevantes y representan un 42% de la masa de PM_1, seguidas de los aerosoles secundarios (29% en promedio) y del tráfico rodado (28% en promedio). La contribución de la quema de biomasa fue muy baja (1% en promedio), de acuerdo con estudios previos. Se ha observado una clara disminución de los niveles de concentración con la distancia a las fuentes emisoras; mientras la estación de tráfico RS estaba dominada per las emisiones del tráfico rodado (39% de PM_1), la estación de fondo urbano UB

presentaba un mayor impacto de las fuentes industriales (51% de PM_1). También se destaca que los niveles de aerosoles secundarios eran más elevados en el fondo urbano que en el centro de la ciudad (RS: 25% of PM_1; UB: 35% of PM_1).

Las fuentes que contribuyen a la fracción PM_{10} (niveles de masa de PM inferior a 10 μm de tamaño) también fueron objeto de estudio durante la campaña SAPUSS. En este caso, el estudio se centró en evaluar las fuentes que influyen esta fracción tanto a nivel horizontal como vertical sobre la atmosfera de Barcelona. Con este propósito se recogieron muestres en dos estaciones al nivel de la calle (RS y UB) y a una cierta altitud (TM y TC). Los niveles de PM_{10} presentan una clara disminución de concentración desde los ambientes más influenciados por el tráfico hasta los más limpios (RS 30.7 μg m^{-3}, UB 25.9 μg m^{-3}, TM 24.8 μg m^{-3} and TC 21.8 μg m^{-3}). El análisis de contribución de fuentes PMF v3.0 y ME-2 (Multilinear Engine-2) de especies inorgánicas obtenidas en las 4 estaciones han resultado en 8 factores: (1) Vehicle exhaust and wear (2-9 μgm^{-3}, 20-27% de PM_{10} en promedio), (2) Road dust (2-4 μgm^{-3}, 9-12%), (3) Mineral dust (around 5 μgm^{-3}, 14-26%), (4) Aged marine (3-5 μgm^{-3}, 13-20%), (5) Heavy oil (0.4-0.6 μgm^{-3}, 2%), (6) Industrial (alrededor de 1.0 μgm^{-3}, 3-5%), (7) Sulphate (3-4 μgm^{-3}, 11-17%) y (8) Nitrate (4-6 μgm^{-3}, 17-21%). Los factores relacionados con el tráfico rodado así como el factor industrial muestran el doble de concentración en las estaciones RS y UB en comparación con les torres (TM y TC), mientras que el resto de factores muestran una distribución homogénea a niveles horizontales y verticales. Aun así, la proximidad a les fuentes de emisión, el origen de las masas de aire y parámetros meteorológicos també influyen en los niveles de concentración de los factores. Los factores del polvo mineral y los aerosoles marinos "envejecidos" (por reacción química con contaminantes antropogénicos) han resultado ser una mezcla de fuentes naturales y antropogénicas, y por este motivo han sido analizados en más profundidad.

Se han identificado 3 tipos de polvo mineral que afecten al ambiente urbano: el polvo de carretera o rodamiento (35% del polvo mineral; 2-4 μgm^{-3} en promedio), el polvo Sahariano (28%, 2.1 μgm^{-3}) y el polvo mineral de fondo (37%, 2.8 μgm^{-3}). Por lo que respecta al aerosol marino, se ha encontrado que sulfato marino de origen antropogénico regional (debido a las emisiones de SO_2 del tráfico marítimo frente a las

costas catalanas) estaba incluido en este factor (44% del aerosol marino, 1.8 μgm^{-3} en promedio). Este sulfato marino no presentaba ninguna correlación con el factor sulfato, y por lo tanto se asoció con el intenso tráfico marítimo frente a las costas catalanas, mientras que el factor sulfato se asocia a las fuentes de generación eléctrica e industriales. Los resultados de esta tesis ponen en evidencia que aunque la ciudad muestra una distribución relativamente homogénea de las fuentes de emisión de PM_{10}, las concentraciones relacionadas con las emisiones primarias de vehículos y el polvo de rodamiento disminuyen con la distancia a los focos emisores.

El estudio completo de las diferentes fracciones de aerosoles que afectan al área urbana de Barcelona y a ambientes similares (Madrid, Brisbane, Roma y Los Angeles), cubriendo desde las partículas ultra finas hasta las más gruesas, permite identificar las principales fuentes que afectan a cada fracción en particular y a los aerosoles en general. Considerando los resultados obtenidos en esta tesis y gracias a las diferentes técnicas empleadas, se proponen las siguientes recomendaciones referentes a los estudios sobre contaminantes atmosféricos y sus consiguientes medidas de mejora de la calidad del aire aplicables:

- Aunque el tráfico rodado es la fuente principal de partículas ultra finas en ambientes urbanos, dada la influencia de los procesos de nucleación en ambientes urbanos bajo alta insolación (un 22% de la concentración promedio anual de N), las medidas de BC constituyen un parámetro más adecuado para monitorizar las emisiones del tráfico rodado.
- Para estudios epidemiológicos se aconseja estudiar la mortalidad y morbilidad asociada a la concentración diaria del número de partículas pero también diferenciando entre el número de partículas de nucleación y las de tráfico, ya que seguramente sus efectos en la salud serán muy diferentes.
- El hecho de incluir especies orgánicas e inorgánicas en el análisis de la contribución de fuentes a PM mejora el estudio del complejo escenario de emisiones que afectan a los ambientes urbanos, además de resolver un mayor número de fuentes.

- Por lo que respecta a la fracción de PM_{10}, se recomienda la implementación de medidas de control efectivas para reducir la concentración de polvo mineral de fondo de origen antropogénico y continuar investigando la contribución del sulfato de origen regional ligado a la intensa actividad marítima en el Mediterráneo, dado que ambas representan una fracción importante de la fracción mineral y de sulfato total, respectivamente (38% de la fracción mineral y 32% del sulfato total).

Index

Chapter 1

Introduction

1. Introduction

1.1 Air pollution

Air pollution is a major environmental concern, especially in urban agglomerations where anthropogenic emissions are an important source. The pollutants (gases or particulate matter, PM) can be emitted to the atmosphere either by anthropogenic sources like industry, traffic or agriculture or by natural sources such as sea spray, mineral dust and volcanic emissions; however, in urban areas the first largely prevails over the second. Particulate pollutants are commonly referred to as aerosols, which are found suspended in the atmosphere in liquid or solid phase (Mészarós, 1999). Aerosol sizes vary from 1 nm to 10^5 nm and they have been historically classified into different categories regarding their mass concentration. PM_{10} represents the mass concentration ($\mu g\ m^{-3}$) of particles with a diameter below 10 μm, $PM_{2.5}$ includes particles with diameter smaller than 2.5 μm and PM_1 accounts for particles below 1 μm, while ultrafine particles (UFP) refer to those under 0.1 μm and are usually reported in number concentration (cm^{-3}). The formation mechanisms of atmospheric particles can be primary or secondary (Seinfeld and Pandis, 2006). Primary particles are those emitted directly to the atmosphere while secondary particles are generated through chemical reactions, such as gas to particle conversion, and represent an indirect emission. The study of ambient PM concentrations in urban environments has been of particular interest due to its adverse effects on human health (Pope and Dockery, 2006; Lim et al., 2012), such as respiratory and cardiovascular diseases (McCreanor et al. 2007; Pope et al., 2009)). Additionally, aerosols influence the Earth's radiative balance, either directly or indirectly, through their effect on the albedo and lifetimes of clouds (IPCC, 2007).

1.2 Natural and anthropogenic sources

Aerosols have a natural or an anthropogenic origin and may be emitted to the atmosphere directly or formed as a result of different atmospheric processes. Natural

sources include sea spray, mineral dust, volcanic emissions, biomass burning, biogenic emissions and organic matter. On the global scale, these sources account for 98% (12 100 Tg y^{-1}) of total global emissions, whereas anthropogenic emissions are estimated to be around 300 Tg y^{-1} (Andreae and Rosenfeld 2008; Durant et al., 2010). The most abundant natural aerosols are sea spray and mineral dust (10130 Tg y^{-1} and 1600 Tg y^{-1}, respectively as seen in Figure 1.1). The sea water bubbles are ejected from the sea surface and incorporated to the atmosphere, being typically found in the PM_{10} fraction. The interaction between sea salt and other anthropogenic components that might have a local or regional origin, such as sulphate and nitrate causes an ageing of the sea salt and increases the contribution of marine aerosols to the PM load (Amato et al., 2009, 2011). Mineral dust largest emission source are deserts, mainly located in a broad "dust belt" that extends from the west coast of North Africa, over the Middle East, Central and South Asia, to China in the Northern Hemisphere (Prospero et al., 2002). These crustal particles are injected in the atmosphere due to wind resuspension and may be transported long distances in high atmospheric layers (Ginoux et al., 2012). Local and regional soil resuspension by strong winds as well as anthropogenic activities such as construction and demolition works, mining and agriculture also contribute to the mineral load of PM (Querol et al., 2001, 2004b). Additionally, primary bioaerosols (pollen, spores and sulphates from biogenic gases), biogenic secondary organic aerosols (BSOA) from oxidation of biogenic volatile organic compounds (BVOCs) and volcanic emissions (crustal material and sulphates from volcanic SO_2) complete the contribution of natural aerosols (Seinfeld and Pandis, 2006).

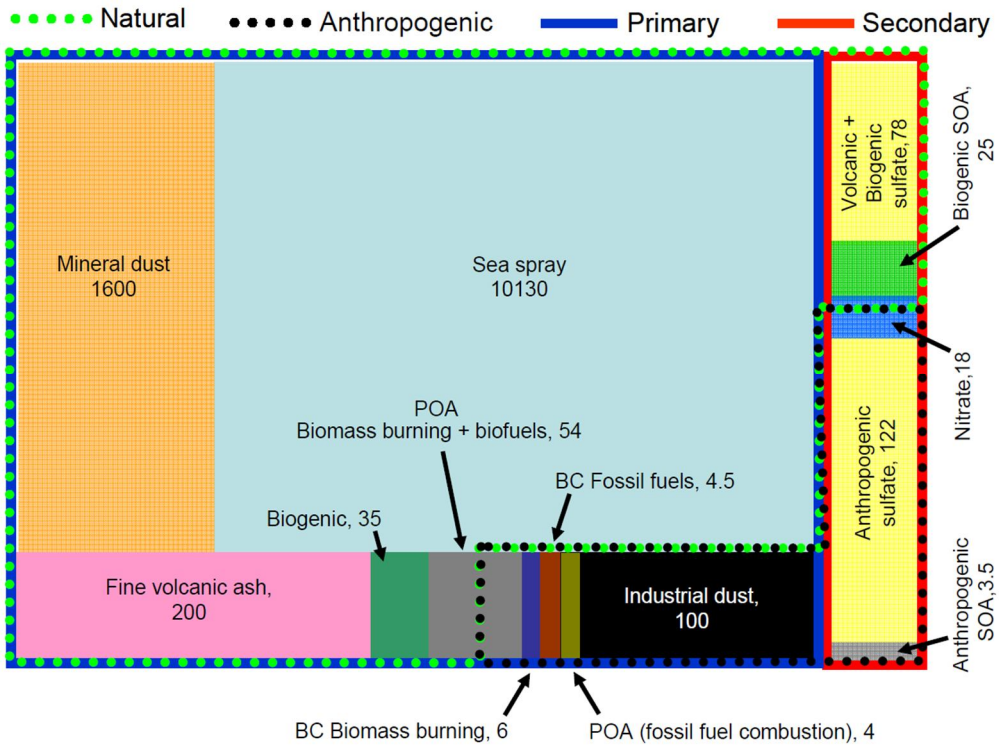

Figure 1.1: Global fluxes of primary and secondary atmospheric particulate matter (total of 12,400 Tg y^{-1}). The area of each square proportionally represents the contribution to the total loading. POA = primary organic aerosol; SOA = secondary organic aerosol; BC = black carbon. Obtained from Gieré and Querol (2010).

Although natural sources remain the main contributors to global aerosols concentrations, anthropogenic emissions may be very intense in highly populated areas and industrialized regions (Putaud et al., 2004). Natural emissions might also affect urban areas, depending on geographical and meteorological features. Some of the naturally formed aerosols might be long range transported to urban areas, adding to the already complex urban scenario of pollution sources (Figure 1.2). Reversely, anthropogenic emissions might also be transported to rural areas (Lelieveld et al., 2002).

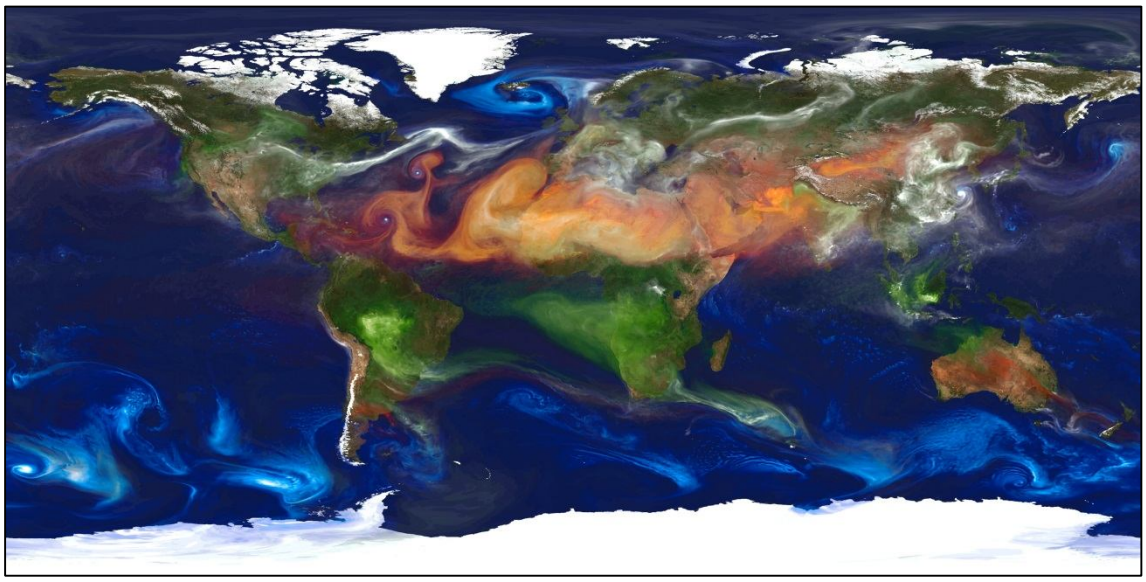

Figure 1.2: Global aerosols distribution produced by a GEOS-5 simulation at a 10-kilometer resolution. Aerosols sources emissions may be distinguished: dust lifted from the surface (red), sea salt (blue), smoke from biomass burning and forest fires (green), and sulfate particles (white) stream from volcanoes and fossil fuel emissions. Source: http://www.nasa.gov/multimedia/imagegallery/image_feature_2393.html#.VYk_6Ua3vgV

Within urban environments, road traffic is found to be the main source through both exhaust and non-exhaust emissions (Amato et al., 2009; Kumar et al., 2011; Pant and Harrison, 2013; Pey et al., 2009). Vehicle exhausts emit both primary particles (mainly in the UFP range) and gaseous pollutants which may later form new particles or condense onto pre-existing ones (mostly in the fine range). Domestic and residential heating, cooking, construction and demolition, shipping emissions as well as air traffic and harbours also contribute to the source apportionment in the city environment (EMEP/EEA air pollution inventory guidebook, 2013). Brake and pavement wear and road dust resuspension (coarse mode) also contribute to urban pollution. Additionally, the transport of pollution plumes from nearby industrial facilities may also add to the urban pollution load.

In addition to the natural and anthropogenic emissions, in the last years it is becoming relevant the so called “enhanced” formation of BSOA aerosols due to the interaction of BVOCs with other anthropogenic pollutants such as NO_x and O_3 (Hoyle et al., 2011). Thus, although the origin of BVOCs is natural the causes of the formation of enhanced biogenic secondary organic aerosols (eBSOA) is attributed to anthropogenic factors.

1.3 Aerosol formation and transformation processes

Primary sources are those that directly emit aerosols to the atmosphere (Seinfeld and Pandis, 2006). In urban environments they are mainly related to tailpipe emissions as a result of incomplete combustion (Kumar et al., 2011; Pant and Harrison, 2013). Also relevant are non-exhaust emissions linked to road traffic, such as brake and pavement wear (Amato et al., 2009). Industrial facilities involving high temperature processes such as smelters, waste incineration plants, power generation plants and other industrial combustion sources (Yang et al., 1998) as well as construction and demolition activities also emit primary particles (Amato et al., 2009; Dorevitch et al., 2006).

Secondary aerosols are those derived from gaseous precursors emitted directly to the atmosphere (Seinfeld and Pandis, 2006). They undergo different chemical processes in the atmosphere that lead them to particle formation. The most common precursor gases are NO_x, SO_2, NH_3 and VOCs. Homogeneous nucleation due to a gas to particle conversion process and condensation of gaseous pollutants onto pre-existing particles, as well as coagulation between particles are the most common aerosol transformation processes. All these physical and chemical transformations lead to varying aerosols sizes, chemical composition and structure, resulting in aerosol aging (see Figure 1.3). Removal of particles from the atmosphere is usually done through wet and dry deposition on surfaces (Mészáros, 1999). Aerosols may also result in cloud nuclei onto which water vapor condenses, forming cloud droplets and thus entering the water cycle (IPCC, 2013). Wet deposition remains as the main removal mechanism for atmospheric aerosols (Levin and Cotton, 2009). Dry deposition, on the other hand, is heavily influenced by external factors such as wind dispersion and diffusion depending on aerosol size (Knippertz and Stuut, 2014). For the UFP, coagulation and agglomeration accounts for a drastic reduction of life times of the finest UFP (Seinfeld and Pandis, 2006). As a consequence, the lifetime of atmospheric aerosol varies widely from hour to weeks, depending on their physico-chemical characteristics, their size and the meteorological factors (Seinfeld and Pandis, 2006).

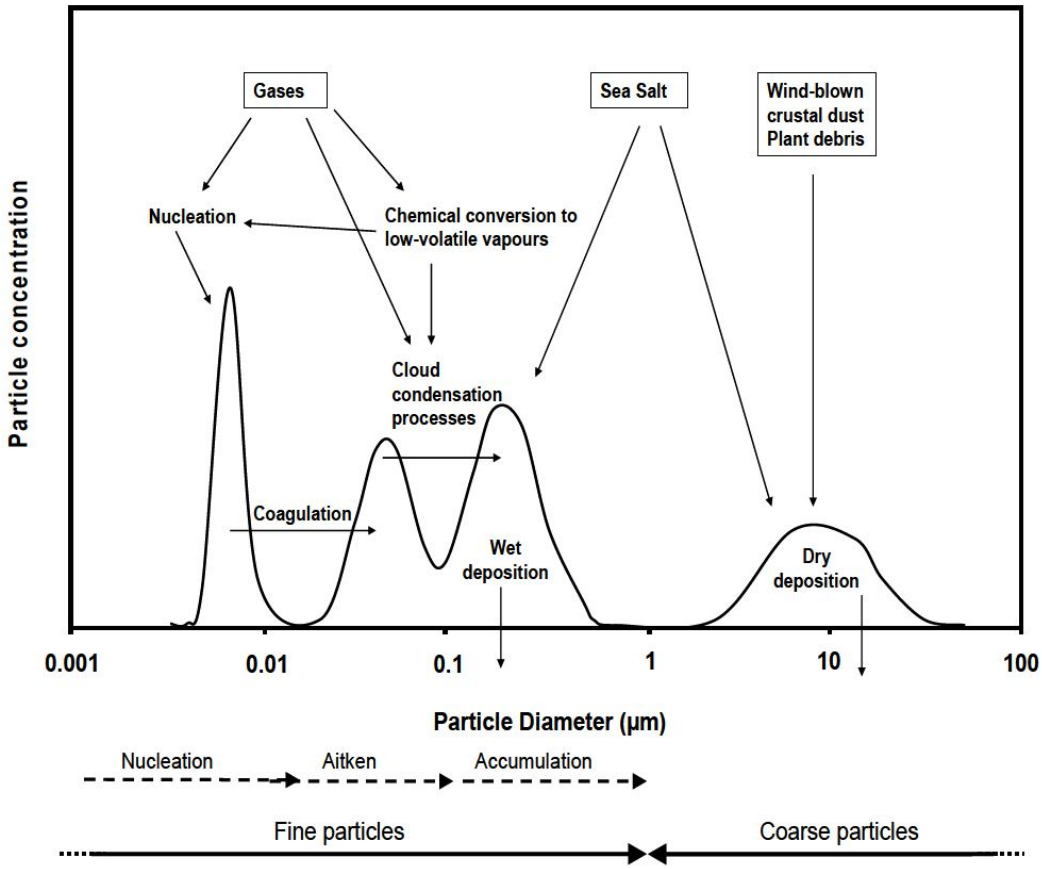

Figure 1.3: A simplified schematic illustration of atmospheric aerosols, sources, transformation processes and removal mechanisms (Cusack, 2013).

1.4 Aerosol chemical composition

Chemical composition of atmospheric aerosols is known to be varied, mainly depending on the emission sources and the atmospheric formation processes and interaction with other particles or gaseous precursors (Finlaysson-Pitts and Pitts, 2000). Meteorological conditions as well as the location may cause a wide variation both in spatial and temporal scales. Mineral matter, carbonaceous compounds, sea spray and secondary inorganic species such as sulphate, nitrate and ammonium, as well as some metals and water are the main chemical species found in atmospheric aerosols (Seinfeld and Pandis, 2006).

Mineral matter has a primary origin and its chemical composition varies depending on the emission area of crustal components (type of soils) and anthropogenic emissions such as mining, agriculture or construction related activities. The major components are Si, Al, Ca, Fe, Ti, K and Mg, while a number of trace

elements such as Co, Rb, Ba, Sr, Li, Sc, Cs and Rare Earth Elements (REEs) are present in trace concentrations (Chester et al., 2006). The main mineral composition of PM is quartz, calcite, dolomite, clay minerals and feldspars. In minor concentrations are also found calcium sulphate and iron oxides (Querol et al., 2002).

Sea spray is made up of NaCl, with minor contributions of $MgCl_2$, $MgSO_4$ and Na_2SO_4 (Mészáros, 1999). The oxidation of biogenic dimethyl sulphite (DMS) emitted by phytoplancton produces secondary organic sulphur compounds (Simpson et al., 1999). Other trace elements like Al, Co, Cu, Fe, Mn, Pb, V and Zn might contribute to this type of aerosols.

Carbonaceous aerosols are mainly composed by carbon with variable proportions of O, H and other hetero-atoms; although mineral carbon from carbonate minerals is not included in this category as it constitutes mineral matter. Carbonaceous aerosols are divided in elemental carbon (EC) and organic carbon (OC). EC is a primary graphitized material emitted by incomplete combustion from fossil fuels or biomass (Goldberg, 1985). Vehicle emissions constitute the main source of EC in urban environments, although power generation, industrial combustion processes and anthropogenic biomass combustion also contribute to this load (Bond et al., 2013). It accounts for a high light absorbance, directly influencing the warming effect of aerosols on climate (Hendricks et al., 2004), as well as for significant health outcomes (Health effects of BC WHO report, 2012). Anthropogenic OC is mainly due to fossil fuels combustion or biomass burning as well as agricultural activities. Polycyclic aromatic hydrocarbons (PAHs), alkanes, alkenes and several organic acids are also OC components (Seinfeld and Pandis, 2006). Bioaerosols, pollen, spores, windborne plant debris among other natural organic compounds constitute primary organic aerosols, whereas the secondary ones result through photochemical oxidation and condensation of VOCs (Jimenez et al., 2009). The condensed low volatility gases onto pre-existing particles may later evaporate, causing a shift to lower particle sizes (Dall'Osto et al., 2011b).

Secondary inorganic aerosols (SIA) refer to the main inorganic compounds in the atmosphere: sulphate (SO_4^{2-}, nitrate (NO_3^-) and ammonium (NH_4^+). They are formed

through gas-to particle conversion processes from their precursor species such as SO_2, NO_x and NH_3 (Hidy, 1994).

The emission of SO_2 to the atmosphere as a result of industrial processes such as energy generation, domestic and residential emissions, shipping, road traffic and natural sources such as volcanoes is found to oxidize in the atmosphere and react with other gaseous precursors to form PM (Mészáros., 1999). The most common atmospheric reaction is that which involves sulphuric acid and ammonia to form ammonium sulphate (Hidy, 1994). Additionally but in a minor proportion, sulphuric acid can also react with calcium carbonate and sodium chlorine to form calcium or sodium sulphate (Querol et al., 1998a, 1998b) . Ammonium sulphate is found in the fine fraction, while calcium and sodium sulphate show a coarser size (>1µm, Mildford and Davidson, 1987).

Nitrogen oxides (NOx) are emitted to the atmosphere as NO (mainly primary) or NO_2 (primary and secondary sources) from combustion sources. In urban environments road traffic is the main emission source, although other industrial and residential combustion sources also contribute (EEA, 2014). As a result of an atmospheric chemical reaction, nitrogen oxides convert to nitric acid, which is also highly reactive and can be neutralized to originate (fine) ammonium, (coarse) sodium or (coarse) calcium nitrate (Mészáros, 1999).

1.5 Size distribution and PM fractions

Given that aerosol sizes cover five orders of magnitude (1 to 10^5 nm) and in some measure reflect their formation mechanisms, particles have been classified into different size modes (Seinfeld and Pandis, 2006). Particle size is also directly related to the CCN efficiency (Andreae and Rosenfeld, 2008).

UFP (<100nm) include nucleation mode (<20nm) and Aitken mode particles (20-100 nm). Accumulation mode particles (100 nm-1 µm) link the UFP with the fine aerosols (<1 µm), while the coarse mode corresponds to particles 1-10 µm (Seinfeld and Pandis, 2006). UFP are very abundant in number but have little aerosol mass

(Harrison and Yin, 2000), whereas fine and coarse particles are scarce in number but have high aerosol mass.

The *nucleation mode* includes particles below 20 nm, which are usually dominated by the gas-to-particle conversion mechanism (Seinfeld and Pandis, 2006). In urban environments road traffic exhaust emissions are the main contributors to this factor as these particles can be formed in the engine or in the atmosphere after emission from the tailpipe (Charron and Harrison, 2003; Morawska et al., 1999; Shi and Harrison, 1999). Primary particles related to traffic are emitted during the dilution and cooling of road vehicle exhaust (Charron and Harrison, 2003; Kittelson et al., 2006) or as carbonaceous soot agglomerates formed by fuel combustion (Kittelson, 1998; Shi et al., 2000). Secondary particles related to traffic are formed behind the exhaust tailpipe as the exhaust gases are diluted and cooled with ambient air (Charron and Harrison, 2003). The most crucial aspect of particle formation behind the exhaust tailpipe is the three-dimensional representation of the dilution pattern, which involves varying length and time scales (Huang et al., 2014; Uhrner et al., 2007; Wehner et al., 2009; Zhu et al., 2002).

Additionally, new particle formation (NPF) can be originated through photochemical reactions enhanced by gaseous precursors such as H_2SO_4, NH_3 and VOCs (Kulmala et al., 2000). Low volatility vapours nucleate into neutral molecular clusters that are stabilized by amines, ammonia and organic vapours, and are activated by condensation of low-volatility organic compounds (Kulmala et al., 2013; see Figure 1.4). High insolation and wind speed, low relative humidity, available SO_2 and low pre-existing particle surface area are common features that enhance new particle formation events (Kulmala and Kerminen, 2008), characterised by a great increase in N in the nucleation mode and subsequent particle growth, if conditions are favourable.

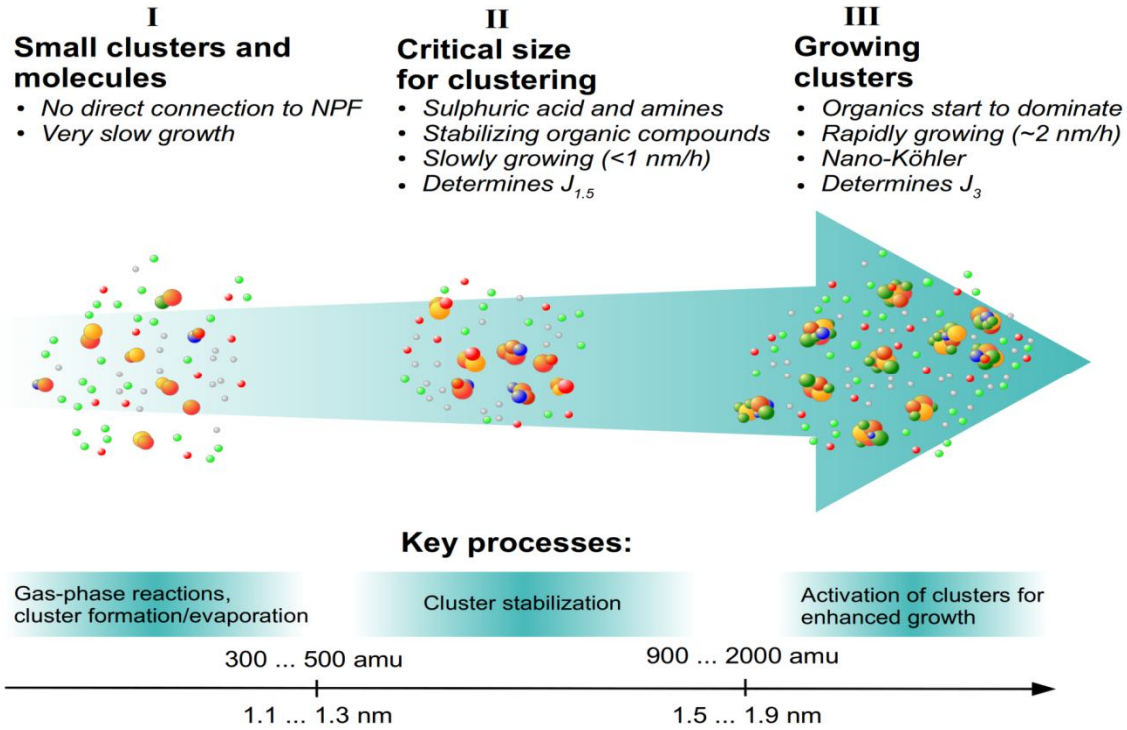

Figure 1.4: Schematic description of main size regimes of atmospheric neutral clusters and the main processes related to those size ranges (Kulmala et al., 2013).

NPF of regional origin due to photochemical reactions (Costabile et al., 2009; Kulmala et al., 2004; Wehner et al., 2007) has also been detected in urban areas. This is in contrast to what was assumed in the past, which is that photonucleation events only occur in background and regional environments such as clean coastal (O'Dowd et al., 2010), forest areas (Boy and Kulmala, 2002), semi-clean savannah (Vakkari et al., 2011), high altitude locations (Sellegri et al., 2010) and regional background sites (Wiedensohler et al., 2002). This is usually attributed to the fact that such natural environments are characterised by a low condensation sink (CS), thus facilitating nucleation. By contrast, urban environments are often characterised by high CS, so that a lower frequency of nucleation events is expected. Nevertheless, there are studies showing that these events in fact can be detected in urban areas, as originally demonstrated in Atlanta, USA (Woo et al., 2001), Birmingham, UK (Alam et al., 2003) and Pittsburgh, USA (Stanier et al., 2004), and subsequently in many cities worldwide (Betha et al., 2013; Cheung et al., 2013; Costabile et al., 2009; Dall'Osto et al., 2013; Pey et al., 2008, 2009; Rimnácová et al., 2011; Salma et al., 2011; Wu et al., 2008).

The *Aitken mode* refers to particles with diameters from 20-100 nm. This mode is dominated in urban areas by traffic-related particles, as both diesel and gasoline

vehicle emissions have been found to emit primary carbonaceous particles in the range 30-120 nm (Charron and Harrison, 2003). Moreover, growth, coagulation and condensation of nucleation mode particles contribute to this mode. The continuation of such processes lead to particles occasionally reaching the accumulation mode (Seinfeld and Pandis, 2006).

The *accumulation mode* particles comprehends those with sizes 0.1-1 μm and are usually dominated by former Aitken particles that have undergone further atmospheric processes such as coagulation onto pre-existing particles and condensation of semi-volatile compounds causing an increase in particles diameter (Seinfeld and Pandis, 2006). As a result, particle number concentrations decrease whereas an increase in particle mass is detected. These aged aerosols are found to be easily transported to distant areas, both urban originated aerosols being transported to rural areas (Cusack et al., 2013b) and rural aerosols, such as biomass burning particles reaching urban environments (Salimi et al., 2014). These particles, contrarily to UFP are found in low number concentration in the atmosphere but are characterised by higher mass concentrations.

Coarse aerosols are those with a particle diameter higher than 1 μm. Most of them have a primary origin and usually derive from mechanical processes, such as marine aerosols, mineral dust, road dust and biogenic debris. In addition to the primary dominant load of coarse PM, a secondary contribution may arise from the interaction of gaseous precursors such as NO_x and SO_2 (easily transformed to HNO_3 and H_2SO_4) with mineral matter (mainly $CaCO_3$) and sea salt (mainly NaCl), yielding to the formation of $CaSO_4$, $Ca(NO_3)_2$, Na_2SO_4 and $NaNO_3$. The importance of quantifying the sources affecting the mineral dust load and marine aerosols in PM_{10} resides in the need to distinguish natural from anthropogenic contributions and develop effective abatement strategies to improve air quality. Despite the efforts in reducing the exhaust and the emissions of gaseous precursors of secondary PM like NO_x and SO_2, non-exhaust emissions have not been targeted yet and contribute to non-compliance of the established PM_{10} limit values (Harrison et al., 2008).

1.6 Effects of aerosols

Atmospheric aerosols are ubiquitous in ambient air and have played a key role in the development of the Earth's atmosphere. Without them rainfall would not occur and the world climate would be very different (Mészáros, 1999). However, atmospheric chemical composition has changed over time due to various anthropogenic emissions, mainly derived from combustion sources, such as power plants, road vehicles and domestic stoves (Brimblecombe, 2001). Moreover, the increased anthropogenic emissions of certain condensable gaseous species such as sulphur dioxide, nitrogen dioxides and volatile organic compounds also have a large impact on local pollution problems. For example, the interaction between atmospheric aerosols and solar radiation has an impact on visibility, due to the scattering and absorption of radiation. In polluted urban environments the high concentration of anthropogenic particles may reduce the visibility to a few meters (Blumenthal et al., 1978; Deng et al., 2008; Husar et al., 1981; Wu et al., 2005). Additionally, atmospheric particulate matter deposition on buildings produces the degradation of exposed construction materials, such as stone, cement and metallic structures (Alastuey, 1994; Torfs and Van Grieken, 1997).

The interaction between aerosols and ecosystems can lead to aerosol deposition on plant leaves and soils as well as acid rain production, causing an acidification of the environment. On the other hand, the transport of mineral dust from arid areas over long distances has also important positive effects on biogeochemical cycles, as it represents an important source of primary nutrients like calcium, iron, nitrogen, potassium and phosphorus (Ávila et al., 1998; Prospero, 1999; Jickells, 2005) to both continental and marine ecosystems.

One of the most important negative effects of aerosols is the deterioration of human health, especially for those living in dense urban environments, which represents around 50% of the global population (UN World Urbanization Report: 2009 Revision). The high concentration of anthropogenic emissions due to transport and industrial activities generate a negative impact in populations' health and also affect the global radiation budget. Therefore, these effects will be further discussed in the following sections.

1.6.1 Health effects

Epidemiological studies have evidenced that exposure to fine and UFP are related with an increase of respiratory and cardiovascular diseases and premature mortality (Dockery et al., 1993; Dockery and Pope, 1994; Schwartz et al., 1996). Development impairments due to air pollution have also been reported (Bobak et al., 1999; Ritz et al., 2002). Some investigations indicate that PM can induce inheritable mutations in mice (Somers et al., 2004), while it is related to lung cancer in humans (Pope et al., 2002). Laden et al. (2000) found that an increase of 10 μgm^{-3} in $PM_{2.5}$ from mobile sources accounted for a 3.4% increase in daily mortality and the equivalent increase from coal combustion sources accounted for a 1.1% increase, while crustal particles were not associated with daily mortality. Pope et al. (1995) reported an association between increased mortality and sulphate and $PM_{2.5}$ concentrations. Particle surface area, UFP concentrations, bioavailable transition metals, PAHs, and other particle-bound organic compounds are suspected to be more important than particle mass in determining the health effects of air pollution (Lighty et al., 2000). There is growing evidence that the most harmful effects of PM are related to particle size, as smaller particles are hypothesized to increase acidity and penetrate into the lower airways (Kim et al., 2015). The health effects of PM sources were analysed in the city of Barcelona (Ostro et al., 2011). This work found that traffic, sulphate from shipping and long-range transport, and construction dust are important contributors to the adverse health effects linked to PM.

UFP are ubiquitous in urban environments (Kumar et al., 2014), and are very abundant in number but have little aerosol mass (Harrison and Yin, 2000). Because of their small size they are suggested to be more toxic than coarser particles per unit mass (Davidson et al., 2005; Seaton et al., 1995). Epidemiological studies have shown that particle number concentration is directly related to cardiovascular mortality (Atkinson et al., 2010) and they have a great potential for lung deposition (Oberdörster et al., 2005). Oberdörster et al. (2005) showed that they can penetrate the cell membranes, enter into the blood and even reach the brain. There is increasing scientific evidence that removal of particles deposited in the lung is size-related (Salma et al., 2015; Kim et al., 2015).

Although evidence of a relationship between mortality and fine aerosols in urban areas has been stronger than for coarse particles, coarse PM has been suggested to be linked with hospital admissions due to cardiovascular and respiratory diseases (Brunekreef and Forsberg, 2005 and references therein). There is evidence for effects of coarse aerosols on mortality, especially in dry regions due to resuspension of mineral dust (Ostro et al., 2000; Perez et al., 2008). Given the frequent outbreaks of Saharan dust in the Mediterranean region, adverse health effects of coarse particles during Saharan dust outbreaks were found in a study in Madrid, Spain (Tobías et al., 2011). In a study in 5 cities in the Mediterranean environment, the association between main chemical species of PM_{10} and $PM_{2.5}$ aerosols and hospital admissions and mortality was investigated (Basagaña et al., 2015). EC and Ni were mainly related to an increase in morbidity, although many other species showed increased percent changes, while also EC, Ni and SO_4^{2-} were found to have the highest association with respiratory mortality.

1.6.2 Effects on climate

Atmospheric aerosols play a key role in global atmosphere, as they are directly related to the radiative balance due to their absorbing, reflecting and dispersive nature (IPCC, 2013). Although their variation in time and space has always been dynamic, due to intensive natural point emissions, such as volcanic eruptions and occasional wildfires, anthropogenic emissions have provoked a dramatic change (IPCC, 2013). The scattering and reflection of aerosols add to the negative radiative forming, contributing to cool the Earth's surface (Figure 1.5). On the other hand, absorbing aerosols such as black carbon, greenhouse gases and clouds absorb radiation and thus have a warming effect (Bond et al., 2013). According to the IPCC fifth assessment report (IPCC, 2013) and shown in Figure 1.5 the warming effect caused by greenhouse gases and short-lived gases is estimated in 3.0 Wm^{-2}, whereas the cooling effect of aerosols directly and through cloud effects is estimated in -0.82 Wm^{-2}. The total radiative budget leaves a warming global effect of 2.29 Wm^{-2}. The total contribution of aerosols to the radiative budget is still poorly understood, due to the high uncertainty in the measurements and modelling (IPCC, 2013). This has important implication also for the weather and climatic prediction models, which present limitations due to this

insufficient knowledge. The great dynamism of aerosols in the atmosphere, including multiple transformation processes, varying sources, spatial distribution and lifetime, make this a challenging topic.

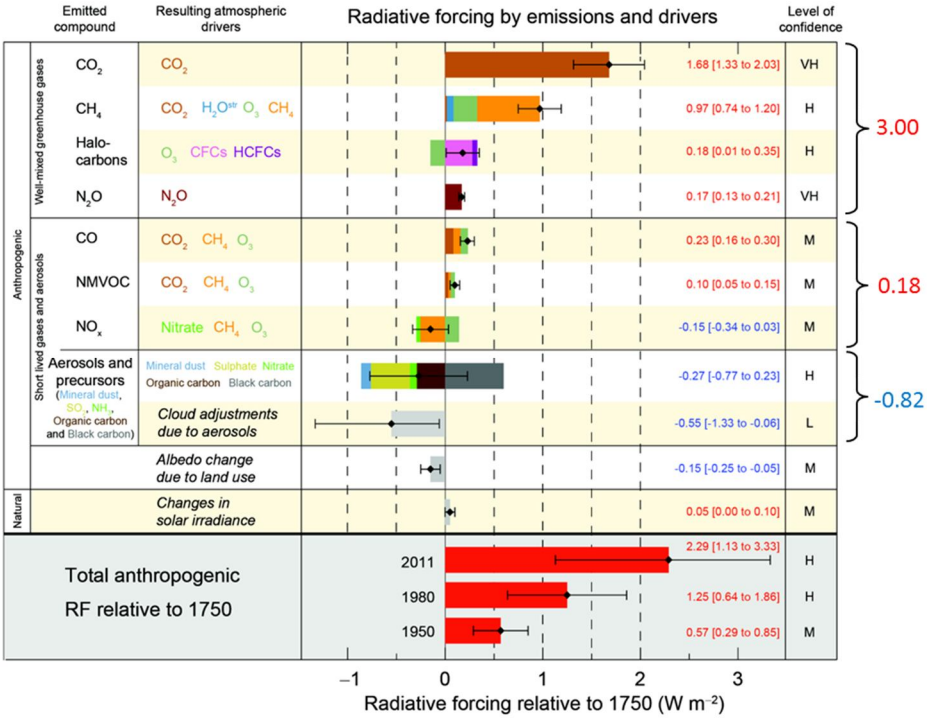

Figure 1.5: Radiative forcing estimates in 2011 relative to 1750 and aggregated uncertainties for the main drivers of climate change (IPCC, 2013).

1.6.3 Air quality regulations

The main objective of the regulations is to protect human health and the natural environment from the hazardous effects of aerosols. Therefore, the current European policies aim to improve air quality and strengthen the emissions control. The actual air quality European directives 2008/50/CE and 2004/107/CE establish the annual, daily and hourly or 8-hours limits or target values that should not be surpassed of the following pollutants: PM_{10}, $PM_{2.5}$, O_3, BaP, Pb, As, Cd, Hg, Ni, BaP, SO_2, NO_2, CO and NO_x. Both European directives have been transposed in Spain into a Royal Decree RD 102/2011. They require the implementation of air pollution monitoring sites, which should be located close to road traffic sources, in urban background environments, industrial and rural areas.

For PM_{10} concentrations, the annual value should not exceed 40 μm^{-3}, whereas the daily limit value of 50 μm^{-3} should not be exceeded more than 35 times a year. Regarding $PM_{2.5}$, the annual limit value is 25 μm^{-3}, which should be reduced to 20 μm^{-3} by 2020. Annual average of Pb contained in PM_{10} aerosols should not exceed 500 ngm^{-3}, whereas annual targets As, Cd, Ni and BaP should not exceed 6, 5, 20 and 1 ngm^{-3}, respectively.

All the members of the European Union must comply with these directives. To this end they should implement the emission directives and apply additional actions, such as low emission zones, to further improve air quality in their countries/regions (Holman et al., 2015). Both NO_x (mostly associated with traffic sources) and SO_x levels (mostly of industrial origin) EU emissions have followed a decreasing trend for the last 10 days, especially since the in deep implementation of the Large Combustion Plants (LCP) and the Integrated Pollution Prevention and Control (IPPC) directives in 2008 (Figure 1.6). However, PM_x emissions levels have slightly increased, probably due to the widespread use of biomass burning for domestic heating. Currently, due to the advances in scientific research, BC measurements and N are being proposed as additional parameters to control air pollution. BC is a main contributor to climate forcing and has also been related to adverse health effects (WHO, 2012). As previously discussed, particle mass is not a suitable parameter for controlling the ambient air UFP due to their abundance in number but little mass. Moreover, these have been related to harmful effects on populations' health (HEI Review Panel, 2013).

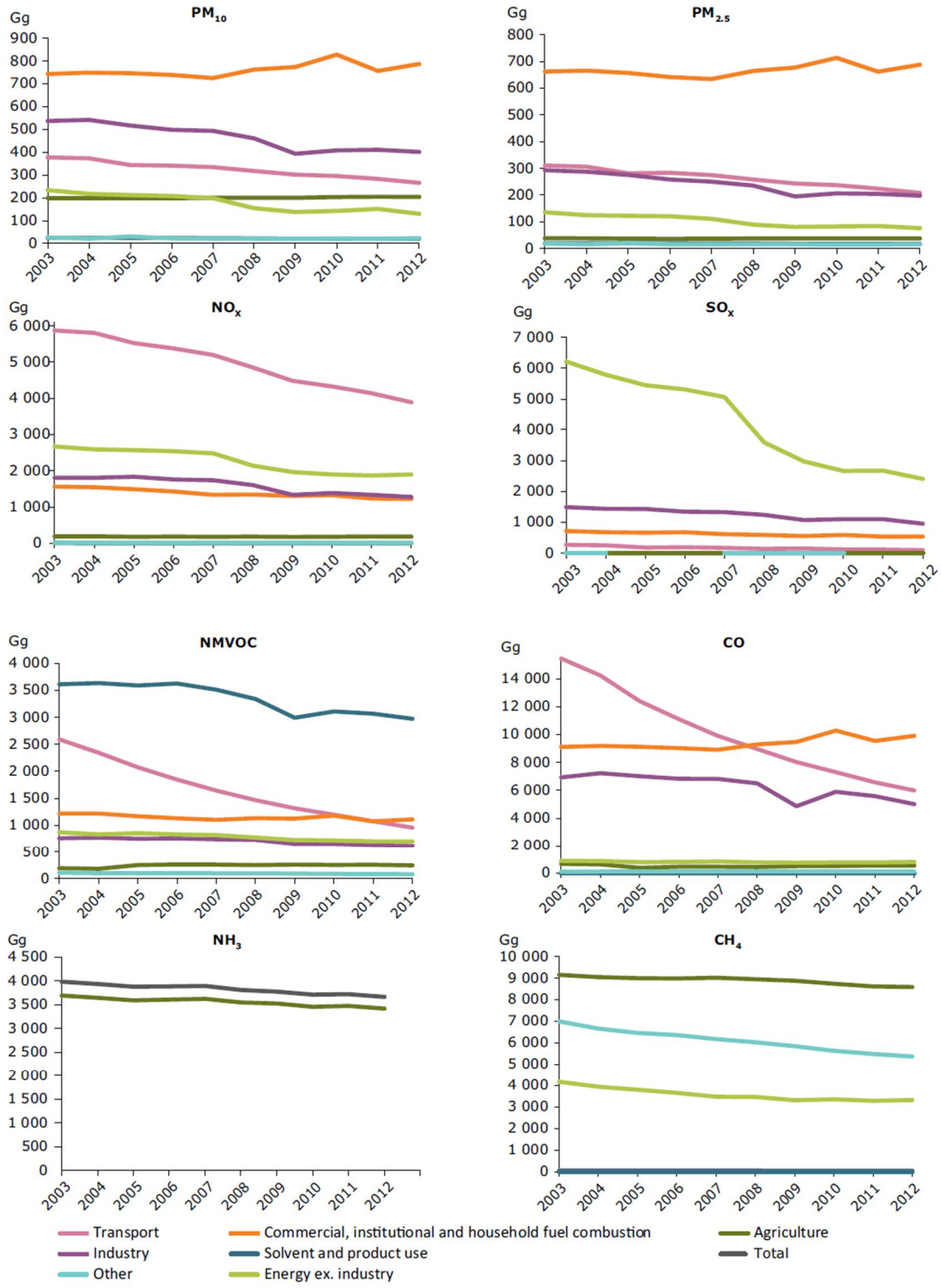

Figure 1.6: Contribution to EU emissions from main sources sectors (Gg/year=1000 tonnes/year) of PM_{10}, $PM_{2.5}$, NO_x, SO_x, NMVOC, CO, NH_3 and CH_4 (EEA Report Air Quality in Europe, 2014).

1.7 Specifics of southern European countries

Current regulations address the amount of ambient particulate matter expressed as a mass concentration of particles (PM), and not N concentrations. However, the European Union (EU) has recently taken initial steps to set N concentrations emission regulations for vehicular emissions (EU, 2012).

Regarding UFP, the variability of particle levels in urban ambient air is not only dependent on the number of vehicles but it is also influenced by the geographical, climatological and the meteorological features of the study area (Birmili et al., 2000; Hussein et al., 2006; Olivares et al., 2007). A large gradient of N is found within urban areas of Europe. In northern European countries N is usually correlated with primary traffic markers during all seasons (Hussein at al., 2004), whereas in the Southern European countries the scenario is far more complex. Indeed, Reche et al. (2011) showed that the high insolation registered in Mediterranean cities enhances nucleation events, thus increasing N.

Within Northern Europe, nucleation events in many urban areas are not very often detected (Alam et al., 2003; Wegner et al., 2012; von Bismarck-Osten et al., 2013). However, Reche et al. (2011) showed that a different behaviour was observed in southern European cities, where new particle formation processes at midday did occur with higher frequency than in northern European cities. The main cause for this difference is likely to be the higher intensity of solar radiation in the Southern European areas, and/or possible site specific chemical precursors.

The intermediate fine fraction (PM_1 or $PM_{2.5}$) presents a wide variation with Europe depending on the type of site and the different regions (Querol et al., 2004b). It is usually dominated by combustion and photochemical processes in urban environments (Morawska et al., 2008). When moving away from the traffic hot spots to more remote sites, an increase in organic aerosols and a decrease in EC is recorded in the fine fraction (Yin and Harrison, 2008). Additionally, air mass origin and seasonality heavily influences the formation of secondary organic and inorganic aerosols in remote environments (Ripoll et al., 2015). Industrial processes emissions also contribute to PM_1 aerosols, especially thermal processes (Ehrlich et al., 2007).

Regarding coarse particles, in southern European countries, due to the drier climate conditions, mineral dust resuspension and Saharan dust outbreaks substantially contribute to increase PM concentrations. Overall, higher PM_{10} levels were recorded for southern European countries in comparison to central EU regions, mainly due to the mineral dust input (Putaud et al., 2010; Querol et al., 2004b). However, the factors influencing aerosol mass concentrations and the contributing sources are many, causing a high variability in PM levels within Europe input (Eeftens et al., 2012; Putaud et al., 2010; Querol et al., 2004b). In northern European countries, the road dust originated by pavement abrasion due to the use of studded tires (Norman and Johansson, 2006), high sea salt concentrations in the coastal areas (Yin et al., 2005) and the use of biomass burning for heating purposes (Puxbaum et al., 2007) are significant sources of PM.

Additionally, the low dispersion and recirculation of air masses in summer mainly in coastal areas increase PM concentrations (Millan et al., 1997). The intense maritime transport in the Mediterranean Sea and related harbour activities contribute to degrade air quality in southern European coastal areas due to PM_x, NO_x, SO_2, PAH and N emissions (Pandolfi et al., 2011; Viana et al., 2014). High pollutants emissions from urban and industrial agglomerates are also relevant (El Haddad et al., 2013; Rodríguez et al., 2004; Tolis et al., 2014), whose dispersion is disfavoured by the high density of urban structures (Sicard et al., 2011).

1.8 Western Mediterranean Basin

In the areas surrounding the Western Mediterranean Basin (WMB) the low dispersion conditions due to scarce rainfall (concentrated in spring and autumn), the long-range transport of natural aerosol and the intense anthropogenic emissions in the basin present a complex pollution scenario (Rodríguez et al., 2002). The low precipitation rates favours road resuspension, as well as the dense urban structure, difficulting pollutants dispersion. Winter anticyclonic episodes are associated with stagnant atmospheric conditions, favouring the accumulation of pollutants in the mixing layer on a regional scale (Jorba et al., 2013). As a consequence an increase in

pollutants levels is observed. The mild Mediterranean climate accounts for high insolation levels, thus activating sea breezes in coastal areas that have a direct influence in pollution sources concentrations as they transport marine aerosols from the coastal areas further inland (Minguillón et al., 2014; Pandolfi et al., 2013). This is reflected in the high pollution levels recorded in the WMB respect some other European areas (Putaud et al., 2010).

The intensified solar radiation induces photochemical nucleation processes, which can have either an urban or regional origin (Dall'Osto et al., 2013b). Photochemical nucleation episodes in the Barcelona urban environment were first reported by Pey et al. (2009) and further investigated by Perez et al. (2010). Since then, several studies have deepened in the knowledge of this events characteristics and frequency (Dall'Osto et al., 2012; Reche et al., 2011). It should be kept in mind that the Mediterranean climate is not exclusive of the Mediterranean Basin and can be encountered in other worldwide cities like Los Angeles (Hudda et al., 2010). Additional effects of intense solar radiation is the oxidation of biogenic emissions due to the abundance of coniferous forest areas spread across the Basin, enhancing the formation of secondary organic aerosols in the rural areas of the WMB (Minguillón et al., 2011).

In the Barcelona urban environment, carbonaceous aerosols (related to road traffic, among other sources) have been reported to dominate the PM_1 fraction, followed by secondary inorganic compounds such as sulphate, nitrate and ammonia (Pérez et al., 2010). Mineral matter, sea spray and trace elements contribution were minimal. Additionally, fuel oil combustion and industrial sources were identified by using a positive matrix factorization model (Amato et al., 2009).

The main sources of PM_{10} in the Barcelona urban environment are mineral dust and road traffic emissions (Amato et al., 2009; Pérez et al., 2010; Querol et al., 2001). Mineral sources include both natural (Saharan dust) and anthropogenic emissions (road dust) (Escudero et al., 2005; Querol et al., 2004a). Other minor sources comprise shipping (being V and Ni common tracers; Viana et al., 2014), both locally due to the city harbour and regional sources in the Mediterranean Basin (Pey et al., 2010; Querol et al., 2009a). Industry (heavy industry emissions traced by Mn, Pb, As, Cd, Cu and Sb)

represents usually less than 10% of PM_{10} mass (Amato et al., 2009, 2014). Biomass burning contribution to PM_{10} is relatively low in the Barcelona area (Minguillón et al., 2011; Reche et al., 2012). Secondary aerosol components affect PM_{10} especially during regional recirculation episodes, were the stagnant conditions lead to the accumulation of pollutants (Pandolfi et al., 2014). In addition, due to the coastal location of the study area, sea breeze (during the day) and mountain breeze (during the night) also influence pollution transport from/towards the urban area.

Three main components of mineral dust in the WMB have been reported in the literature: road dust, Saharan dust and urban or regional background dust (Querol et al., 2004a). Road dust is associated with resuspended road dust by passing vehicles and wind, and is traced by Fe, Ca, Al, Si, Ti, Cu, Sb, Sn, Ba, Zn, OC and EC (Schauer et al., 2006). A background source rich in Ca, Si, Al and Ti was attributed to regional anthropogenic and natural resuspension such as urban dust from construction/demolition works, unpaved areas and parks, among other sources (Amato et al., 2009). Querol et al. (2001) reported a urban/regional background mineral dust factor enriched in Al and Ca, which presented higher concentrations in summer than in winter. In addition, Saharan dust outbreaks transporting dust (made of quartz, clays, calcium carbonate and iron oxide and traced by Al, Si, Ti among others) regularly impact the study area (Querol et al., 2001). Efforts have focused on quantifying this contribution to the average mineral loading, both for air quality purposes (Pey et al., 2013; Querol et al., 2009b) and its impact on population's health (Perez et al., 2008).

1.9 Previous studies

The Environmental Inorganic Geochemistry research group at IDAEA-CSIC has focused its research on the characterisation of atmospheric aerosols in the Iberian Peninsula (IP), especially in the WMB.

The measurements of TSP and PM_{10} levels and chemical speciation started in 1995 at the Teruel coal-fired power station. The influence of Saharan dust and resuspension processes on coarse aerosols were also reported (Querol et al., 1996, 1998a and b).

Querol et al., (2001) reported that hourly levels of $PM_{2.5}$ and PM_1 reflected the daily cycle of road traffic gaseous pollutants in Barcelona. The impact of meteorology on PM levels was investigated by Rodriguez (2002), as well as the impact of dust sources in the urban environment. The measurements carried out in the urban environment revealed annual exceedances of the daily limit values, mainly caused by local sources (Viana, 2003). Escudero (2006) found an important influence of Saharan dust outbreaks to the regional background, while Castillo (2006) studied the impact on levels and chemical speciation of aerosols in NE Spain.

Minguillón (2007) studied levels, composition and sources of PM in the industrial ceramic area of Castelló and possible abatement strategies. A reduction of 3-5 μgm^{-3} in PM_{10} for urban areas was proposed, especially aiming to decrease the mineral fraction.

For the first time, Pey (2007) monitored N and size distributions in Spain, concluding that UFP concentrations directly depended on vehicle exhaust emissions, although secondary processes such as photochemical nucleation also contributed, especially to the nucleation mode.

Pérez (2010) collected a long PM data series until 2007, introducing PM_1 as a relevant fraction in Barcelona urban environment. It also included BC as a complementary measure to monitor vehicle emissions. Amato (2009) investigated road dust emissions by means of a PMF, highlighting the contribution of non-exhaust emisssions to urban pollution sources. In order to reduce such emissions, the effectiveness of several abatement strategies was evaluated.

Reche (2012) highlighted the importance of intense solar radiation in the occurrence of photochemical nucleation processes that were thus enhanced in Southern European urban environments in comparison to Northern regions. This work also further evaluated several sources impacting the urban environment such as NH_3 and biomass burning as well as the toxicological effects of urban particles.

Cusack (2013) further investigated the PM characteristics of the WMB regional background environment using long term PM data series. Photochemical nucleation regional events and their evolution in the rural atmosphere were also analysed.

Alier (2014) investigated the sources of submicron organic aerosols in the urban background environment of Barcelona of both biogenic and anthropogenic origin. Among the organic compounds analysed were PAHs, dicarboxilic acids and isoprene and α-pinene oxidation products. Van Drooge et al. (2012) also analysed the impact of natural emissions in the WMB, considering only the organic fraction.

Ripoll (2015) studied the impact of natural and anthropogenic sources in the WMB continental background, using both online and offline PM chemical speciation instruments. Additionally, physical and optical aerosol properties were investigated.

1.10 The SAPUSS and VAMOS projects

Abundant studies and PhD thesis have been carried out in the research group as described in the previous section. However, there are still gaps of knowledge that should be covered. Regarding UFP, the sources and processes influencing nucleation events in a Mediterranean environment need to be further investigated, especially regarding the evolution of freshly nucleated particles. The origin and variation of atmospheric aerosols in the WMB have been previously analysed; however concurrent measurements at both horizontal and vertical levels of PM was lacking, as well as an inclusive study of organic and inorganic chemical speciation. With the aim of filling these gaps, the VAMOS (Combination of new generation aerosol measurements at surface to interpret their time and spatial variability in the Western Mediterranean) and SAPUSS (Solving Aerosol Problems by Using Synergistic Strategies) projects were developed.

The present PhD is carried out in the framework of the SAPUSS and VAMOS projects and it is done with the support of a doctorate grant (BES-2011-046110) sponsored by the National Plan of Research from the Spanish Ministry of Economy and Competitiveness assigned to the VAMOS project (CGL2010-19464). The VAMOS project focuses on studying the source origin and atmospheric processes controlling aerosol levels and characteristics during the winter and summer PM pollution episodes in NE Spain. It aims at studying the origin and variability of PM and N over the city of Barcelona, by simultaneously measuring in diverse urban scenarios at different

heights. Special emphasis is given to the sources of organic and mineral matter in urban and regional aerosols, as well as the temporal and spatial variations of NH_3 levels in urban and rural areas. Finally, it also aims at characterising the high nucleation midday summer episodes occurring in the WMB. This project was aimed at providing long-term aerosol measurements in the Barcelona area, such as particle number size distribution. It also included the SAPUSS project, an intensive sampling campaign aimed at monitoring the Barcelona urban environment by deploying state-of-the-art aerosol instrumentation at several sampling sites.

The SAPUSS project is a Marie Curie EU Action that was developed in order to address several knowledge gaps in the urban agglomerate of Barcelona (NE of Spain). The city is located in the WMB, showing high population (1.7 million inhabitants) and car densities (6100 cars km^{-2}) and very dense urban structure as it is geographically confined by the coastal range of Collserola to the north, the Mediterranean Sea to the south-east and two river valleys, the Besòs River to the north-east and the Llobregat River to the west. All this factors contribute to a complex and multi-faceted pollution scenario. As described in previous sections, several atmospheric sources had already been targeted as important contributors to atmospheric aerosols (i.e. photochemical nucleation events to UFP, industrial sources to the fine fraction, dust sources to the coarse fraction), although further knowledge of formation and/or transformation processes as well as the 3D variation of PM_x and N concentrations was lacking. Therefore, several sampling sites were chosen within the urban area both in horizontal and vertical levels (Dall'Osto et al., 2013a). Concurrent measurements in up to 6 sites took place from 20 September to 20 October 2010, including a road traffic site, two urban background sites, a regional background site and two tower sites (150 m a.s.l. and 545 m a.s.l., respectively). In each site, multiple instruments working under different techniques and principles were simultaneously deployed to characterise particulate matter, gaseous pollutants and meteorological scenarios, aiming for a better understanding of the atmospheric chemistry and physics governing the Mediterranean urban environment.

1.11 Objectives

The specific objectives of this PhD thesis are:

1- To identify the atmospheric processes and sources affecting the size selected aerosol concentrations simultaneously detected at four different monitoring sites in the Barcelona area during the SAPUSS campaign.

2- To categorise sources of UFP in urban environments situated in temperate regions affected by high solar radiation levels. Specifically, we aim to assess the frequency and influence of nucleation events on UFP levels and variability, as well as the atmospheric conditions facilitating such events.

3- To characterise the main sources contributing to PM_1 urban aerosols by a source apportionment study of both inorganic and organic species, as previous source apportionment studies in the area had been carried out separately for inorganic and organic species. The differences in sources concentrations between a traffic road side and the urban environment are also investigated.

4- To assess the main sources contributing to PM_{10} aerosols fraction both in horizontal and vertical levels (4 sites in total) in the urban agglomerate of Barcelona. Specifically we aim to study the main factors influencing the variability of aerosol sources over the whole area.

1.12 Structure of the thesis

Following the introduction, the methodology section will describe the main study areas and the monitoring sites in detail, and outline the sampling instruments and the data treatment tools applied. The results section will be divided in four parts, ranging from ultrafine particles to coarse particles in the Barcelona urban environment. A brief introduction and state-of-the-art will introduce each of the different subsections of this chapter. The first two parts will focus on the characteristics of aerosol size distributions in Barcelona during the intensive SAPUSS campaign and in several worldwide cities sharing a similar climate to Barcelona, respectively. Then, the source apportionment for the PM_1 and PM_{10} fractions at several sites during SAPUSS will be

analysed, with special emphasis on the organic fraction (PM_1) and the mineral and marine aerosols (PM_{10}). Afterwards, a common discussion ranging from the finest UFP to the coarse aerosols and the dominating sources and processes affecting each fraction will be presented. A conclusion chapter will sum up the main conclusions regarding air pollution in a WMB urban environment and include some remarks and implications for air quality. Finally, future work and literature references will be listed.

Chapter 2

Methodology

2. Methodology

The methodology section is divided in five main sections. The two first sections describe the study areas and the sampling sites used during the long-term measurements and the intensive SAPUSS campaign. After that, the measurements performed at each sampling site are presented, followed by a detailed description of the air pollution sampling instruments. Finally, a description of the data treatment tools applied is given.

In order to clarify the structure of the thesis and the sampling sites discussed in this section, Table 2.1 describes the data that has been used in each chapter.

Table 2.1: Sampling sites used in each of the chapters of this thesis. l.t.m. stands for long term measurements and i.c. for intensive campaign.

Sites	Chapter 3 (Results)				Chapter 4 (Discussion)		Chapter 5 (Conclusions)
	3.1	3.2	3.3	3.4	4.1	4.2	5
Barcelona (l.t.m.) -BCN		X			X		X
Barcelona (i.c. SAPUSS)							
- RS	X		X	X	X	X	X
- UB	X		X	X	X	X	X
- TM				X		X	X
- TC	X			X	X	X	X
- RB	X				X		X
Madrid (l.t.m.) - MAD		X			X		X
Brisbane (l.t.m.) - BNE		X			X		X
Rome (l.t.m.) - ROM		X			X		X
Los Angeles (l.t.m.) - LA		X			X		X

2.1 Study areas

The Mediterranean climate is categorised as *dry-summer subtropical* (type Csa/b in the Köppen climate classification) due to its mild winters and warm summers with scarce rainfall. It is characterised by annual average temperatures of 12-18°C, with

dominant clear sky conditions (annual global irradiance intensity of 180-190 Wm^{-2}). Precipitation is concentrated in autumn and spring and is very scarce during summer; its annual average is about 600 mm. Although it prevails in the coastal Mediterranean Sea Basin areas, it is also present in other parts of the world, such as south-western USA, the west and southern Australian coast, south-western South Africa and central Chile (see Figure 2.1).

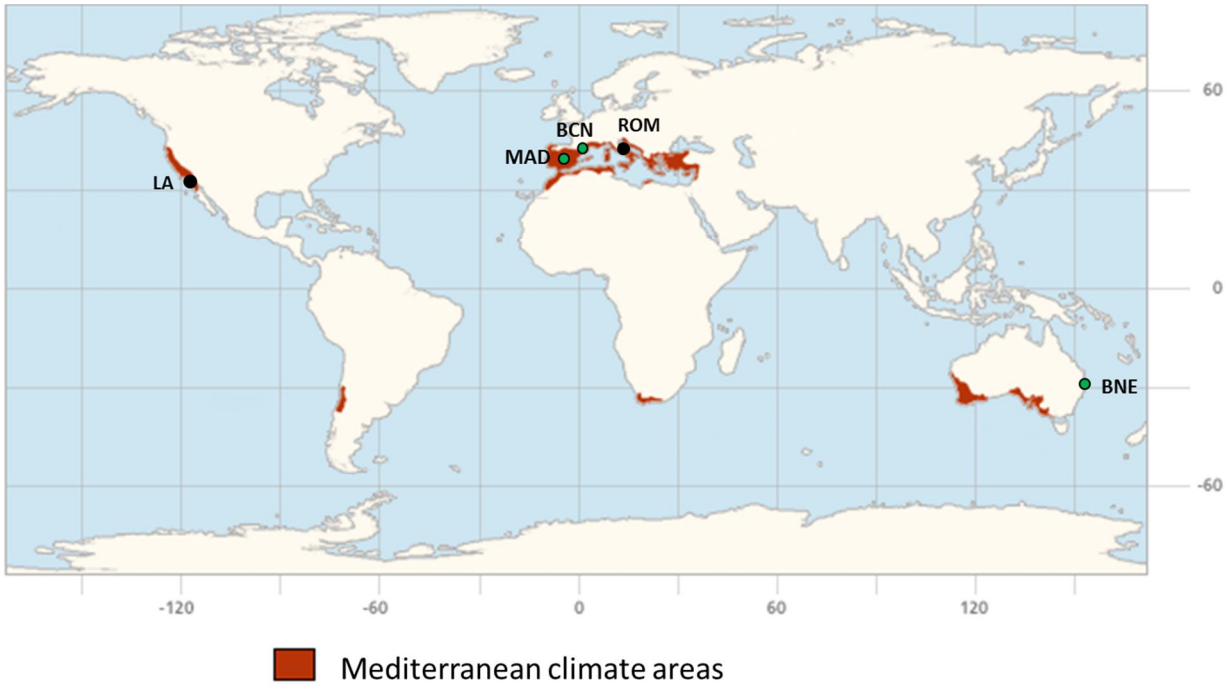

Figure 2.1: Location of the cities selected for the study. The 3 main cities Barcelona (BCN), Madrid (MAD) and Brisbane (BNE) are marked in green, whereas the supporting cities of Los Angeles (LA) and Rome (ROM) are shown in black. The cities of BCN, MAD, ROM and LA are located in Mediterranean climate regions, whereas BNE has a humid subtropical climate. Image source: US National Park Service California Mediterranean Research Learning Center.

With the objective of categorising sources of UFP in urban environments similar to that encountered in the Barcelona study area, a number of cities situated in temperate regions affected by high solar radiation levels were chosen. In addition to Barcelona, two more cities in the western Mediterranean Basin were selected for this study: Madrid and Rome. For the American continent the city of Los Angeles was chosen (it is also located in a Mediterranean climate region). Finally, the city of Brisbane (Australia) was also included. Its climate is categorised as *humid subtropical* (type Cfa) due to the higher mean annual rainfall (1150 mm versus 600 mm for the Mediterranean climate),

although otherwise presents many climatological similarities to the Mediterranean regions with mild winters and warm summers with prevalent sunny days (average annual global irradiance of 208 Wm^{-2}, see Table 2.2).

Table 2.2**:** Average annual meteorological parameters for each site during the respective study periods. Due to the reduced data availability in Los Angeles, values in parentheses represent annual values provided by NOAA or NASA.

City	T (°C)	RH (%)	Rain (mm)	Solar radiation (Wm^{-2})
Barcelona	18±6	68±16	432	190±270
Madrid	15±7	66±23	438	182±265
Brisbane	20±5	72±20	1072*	240±337
Rome	19±7	59±17	732[#]	203±274
Los Angeles	19±6 (19[$])	58±20 (71[$])	126 (452[$])	(225[+])

* Australian Government Bureau of Meteorology
[#] http://www.weatherbase.com/weather/weatherall.php3?s=124261&refer=&units=metric
[$] National Oceanic and Atmospheric Admisnistration (NOAA)
[+] National Aeronatics and Space Sdmisnistration (NASA)

Although the selected cities are located in similar climatic environments, some differences regarding meteorological conditions were encountered (see Table 2.2). All cities show mild annual temperatures, ranging from 15°C in Madrid (due to its inland location) to 20°C in Brisbane (due to its latitude, closer to the equator, see Figure 2.1). Relative humidity varies by 10% across the cities, showing highest values in Brisbane (72%). This is probably related to the higher precipitation rate registered in this city (1072 mm), two times higher than in BCN, MAD or LA (430-450 mm). As expected, the highest average annual values of solar radiation are recorded in Brisbane and the lowest in Madrid (240±337 Wm^{-2} and 182±265 Wm^{-2}, respectively).

In addition to meteorological features, other factors influence UFP emission sources in these urban areas, especially regarding traffic-related pollutants. The vehicle fleet composition is not homogeneous among the sampling sites, as a tendency towards dieselization has been experienced in some European countries over the last years, especially in Spain (Amato et al., 2009), where 55% of vehicles are diesel-

powered versus 44% gasoline (Dirección General de Tráfico, 2015). In Italy 37% of the vehicles used diesel fuel and 62% used gasoline in 2007 (Istituto Nazionali di Statistica, 2009). On the other hand, in the USA or Australia the diesel share represents only around 20% (Gentner et al., 2012; Australian Bureau of Statistics, 2014). Diesel vehicle engines are known to emit much higher N than gasoline ones (Harris and Maricq, 2001), which might imply a higher concentration of primary UFP in European countries in comparison to the USA and Australia. Another relevant difference between the cities relates to their urban structure. While both Brisbane and Los Angeles are extensively suburbanised cities with relatively low population densities, favouring dilution and diffusion of pollutants, southern European cities are dense urban agglomerates that favour the trapping and accumulation of pollutants. Given these differences between the cities, we nevertheless view the climatic similarities to be strong enough to consider the urban background environments in which the data have been sampled to be broadly comparable.

2.1.1 Barcelona

The city of Barcelona has 1.7 million inhabitants and around 4 million counting the metropolitan area, being the second largest city in Spain. It is located in the North East of Spain in the WMB, confined by the coastal range of Collserola to the North, the Mediterranean Sea to the South-East and two river valleys, the Besòs River to the North East and the Llobregat River to the West (Figure 2.2). Along the river valleys there is a relevant industrial structure including cement kilns, metallurgy among others, resulting in its pollution plume often reaching the city (Amato et al., 2009; Minguillón et al., 2014). Nonetheless, the major PM pollution source is traffic, as the city has a high vehicle density (5800 cars km^{-2}, Anuari Estadístic de la Ciutat de Barcelona, 2011).

Due to its location in a coastal area, the transport and dispersion of atmospheric pollutants within the study area is dominated by the sea-breeze during the day and the less strong land-breeze at night. Moreover, due to its geographical location, the WMB is affected by the influence of the Azores high-pressure system, which depending on its latitudinal location favours or blocks the passing of low-pressure systems over the

Iberian Peninsula. The renewal of air masses is more favoured in winter due to the southerly position of the Azores anticyclone, favouring the transport of clean Atlantic air masses. On the other hand, from late spring until autumn the intensity of the high pressure system enhances the development of local and mesoscale circulations favouring the recirculation of polluted air masses (Jorba et al., 2013; Sicard et al., 2011). Additionally, during summer African air masses loaded with Saharan dust frequently reach the study area, contrarily to advection episodes from central-Europe, which usually affect the WMB on autumn, spring and winter (Pey, 2007).

The development of the sea breeze and the boundary layer plays a key role not only in the city but in the surrounding areas as well. In the urban environment, emissions from the city harbour are transported inland, while a higher boundary layer enhances pollutants dilution at midday (Reche et al., 2011). In the rural environment both the sea and mountain breezes transport inland anthropogenic pollutants from the coastal industrial facilities and urban nucleuses increasing the pollution load in rural areas (Cusack et al., 2013).

2.1.2 Madrid

Madrid is the Spanish capital city, located in the centre of the IP in a plateau about 650 m a.s.l., it features 3.3 million inhabitants although the metropolitan area accounts for more than 6 million. It is constrained to the north-northwest by a high mountain range (Sierra de Guadarrama, 40 km distant) and to the northeast and east by lower mountainous terrain (Gómez-Moreno et al., 2007). The weather in Madrid corresponds to a typical mid-latitude continental area, with cold winters, hot dry summers and mostly sunny days. Mean annual precipitation is around 400 mm, mainly concentrated during spring and autumn (Gómez-Moreno et al., 2011). It shows intense seasonal contrasts concerning temperature and rainfall, causing seasonal patterns for specific pollutants.

Madrid industrial activities consist of light industry and therefore most emissions arise from road traffic and residential and domestic sources (cooking and winter heating systems based on fossil fuels, including a small proportion based on coal) (Gómez-Moreno at al. 2011). Although the IP is usually under stable atmospheric

conditions due to the Azores anticyclone, Atlantic and north advections are also common. In winter the stagnant anticyclonic conditions and the appearance of radiative nocturnal surface inversions lead to persistent pollution episodes over the city. On the other hand, thermal convective activity dominates during summer thus contributing to the mixing layer development (Gómez-Moreno at al. 2011).

2.1.3 Brisbane

Brisbane is located on the eastern Australian coast; it has two million inhabitants although the metropolitan area accounts for 3 million. The city is centred along the Brisbane river, close to its estuary and is surrounded by mountains from south to north, facing the Pacific ocean to the east (Cheung et al., 2011). This city's climate is classified as *humid subtropical* (type Cfa in the Köppen classification). The main difference with the Mediterranean climate is the higher mean annual rainfall (1150 mm versus 600 mm for the Mediterranean climate), as otherwise they are both characterised by sunny days, mild winters and warm summers.

Traffic exhaust emissions are the main pollution source, although plumes coming from the airport, harbour and industrial facilities can also contribute. The region is governed by SE synoptic flows, although a NE breeze is also a daily feature (Morawska et al., 1998). The recirculation of polluted air masses under certain atmospheric conditions (coincident NW synoptic flow with overnight SW drainage) can lead to photochemical smog events (Cheung et al., 2011).

2.1.4 Rome

Rome is the Italian capital, located 24 km inland from the Mediterranean Sea and features 2.7 million inhabitants although the metropolitan area accounts for 4 million. The city is located in the Tiber valley, and the river crosses the city before flowing into the Mediterranean. Being a Mediterranean climate city, the city has cool humid winters and hot dry summers.

Air pollution in Rome originates mostly from motor vehicle traffic. As a result, concentrations of CO, NO_2, O_3 and airborne particles are generally high, but with different seasonal patterns, whereas SO_2 levels are usually low (Fusco et al., 2001).

However, the anthropogenic urban pollutants may be transported further inland to rural locations. This aspect has been studied at the suburban site of Montelibretti, which is exposed to the urban plume of Rome whenever the sea-land breeze system drives the air mass circulation in the Tiber Valley (Costabile et al., 2010). Photochemical smog episodes can be detected from March to late October when cyclonic weather is established in central Italy or when southeastern flow advects warm air from the African continent (Ciccioli et al., 1999).

2.1.5 Los Angeles

The city of Los Angeles is located on the Pacific coast of the USA and it is a metropolitan area that exceeds 15 million inhabitants. The Los Angeles basin is surrounded by mountains on three sides and opens to the Pacific Ocean in the southwest, tending to confine pollutants within the coastal basin (Lu and Turco, 1995). It shares the mild winters and hot summers, with rainfall concentrated in spring and autumn with the other Mediterranean climate cities.

Primary direct emissions (mainly from road traffic) and transported aged aerosols from upwind locations contribute to PM loadings in Los Angeles Basin (Hudda et al., 2010). Due to its location in a coastal area surrounded by elevated terrain, sea and land-breezes govern the transport and distribution of pollutants. It is characterised by frequent anti-cyclonic atmospheric conditions leading to the accumulation of both primary and secondary pollutants (Alier et al., 2014). The strong subsidence inversion layer, frequently present in winter and almost permanent in the summer, limits vertical dispersion of air pollutants (Hudda et al., 2010).

2.2 Monitoring sites

2.2.1 Intensive SAPUSS campaign

In order to investigate the sources and processes of atmospheric pollutants in the WMB as outlined in the objectives, 6 monitoring sites were positioned in the surroundings of the Barcelona area both at ground level and at certain height above

the city environment during the SAPUSS campaign (20th September to 20th October 2010).

The setup of the SAPUSS campaign aimed at monitoring the variability of pollution sources in the city environment (see Figure 2.2). Therefore, to study the intensity of the impact of pollution sources within the city environment monitoring sites were located both at ground level and at certain height. Two sites were located at ground level, one reflecting a road traffic environment (RS_{site}) and the other one representative of the Urban Background (UB_{site}). Two more sites within the city area were located at certain height in an urban and suburban environment, respectively (TM_{site} and TC). TC_g was located close to TC at ground level on a hill and both sites constituted the TC_{site}. Finally, the nearby regional background environment was monitored with the RB_{site}. It is important to stress that this spatial lay-out allows us to study point source emissions at the RS_{site} being transported to the urban background sites (UB_{site}, TM_{site} and TC_{site}) and later on to the RB_{site} (Figure 2.2).

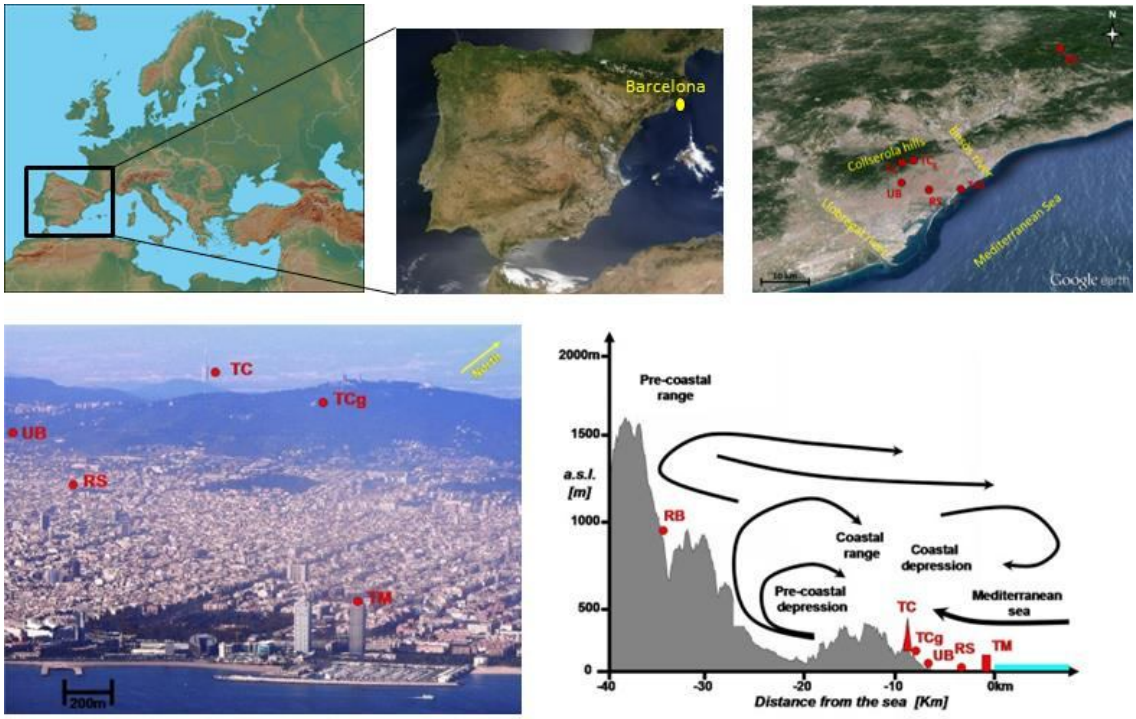

Figure 2.2: SAPUSS monitoring sites specific location within the Barcelona area (adapted from Dall'Osto et al., 2013a).

2.2.1.1 Road site (RS_{site})

The RS_{site} was located in the car park of Escola Tècnica d' Enginyeria Industrial in the Urgell Street (41°23'18'' N, 02°09'0'' E, elevation 40 m a.s.l.), a street canyon with four vehicle lanes (one direction) and two cycling lanes in both directions. This street is representative of the urban traffic related to commercial activity, and during the SAPUSS campaign the approximate vehicle intensity was 17 000 cars day^{-1}. Three parked vans located 4 m from the kerb housed the majority of instruments (see Figure 2.3). Ambient air was drawn through several inlets located at the roof of the vehicle at an approximated height of 4 m. Several trees, a fence and a pedestrian path separated the road from the instruments. Two traffic lights are found 50 m on the right side (close to a subway entrance) and 150 m on the left side. Several restaurants and shops are also located in the surroundings.

Figure 2.3: RS_{site} monitoring site lay-out. Instruments were located inside the vans with their sampling inlets located on the roof.

2.2.1.2 Urban Background site (UB_{site})

The UB_{site} was located in a park of a residential area at the North-West of the city centre (41°23'15'' N, 02°07'05'' E, elevation 80 m a.s.l). It was also close to the busy Diagonal Avenue (9 lane road) that crosses the city from East to West and is primarily used by commuters. It reflects the rush hour traffic peaks and has a traffic volume of about 62 000 cars day^{-1} (Dall'Osto et al., 2013a). Two cabins contained the monitoring

instruments, with inlets also located on the roof about 4 m height, with additional PM samplers located outside (Figure 2.4).

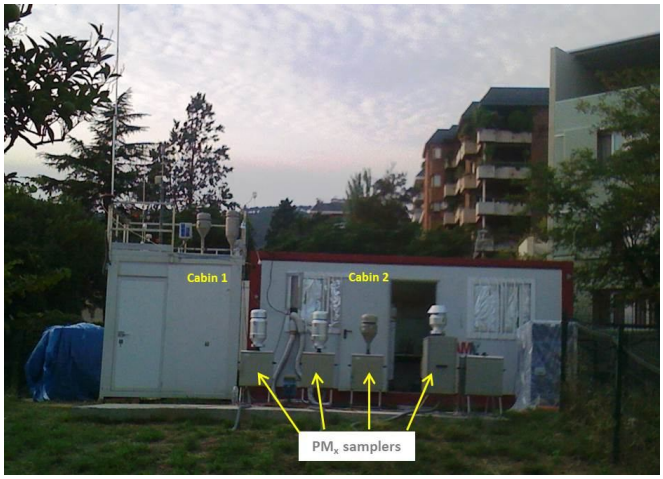

Figure 2.4: UB_{site} monitoring site lay-out. Instruments were located inside two conditioned cabins with their sampling inlets located on the roof. Additionally PM samplers were located outside the cabins.

2.2.1.3 Torre Mapfre site (TM_{site})

The TM_{site} was located on the rooftop of a skyscraper (41°23'16'' N, 02°11'51'' E, 150 m a.s.l.) 200 m from the coast in the Olympic Port of Barcelona, close to a recreational harbour and leisure area (to the south). North of the tower there is a tunnelled motorway ring road (four lanes) at 50 m distance from the building and two three-lane roads at ground level. Several instruments were deployed on the tower's terrace while some others were placed inside a room at the top floor, with an inlet (Figure 2.5).

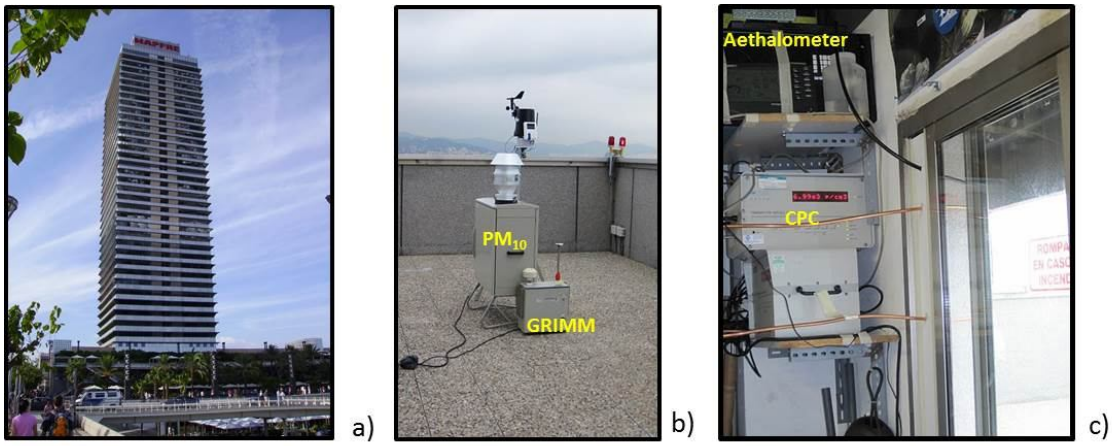

Figure 2.5: TM_{site} monitoring site lay-out: a) Torre Mapfre skyscraper, b) instruments placed at the rooftop terrace of the building and c) instruments placed inside a room at the top floor with an inlet to sample ambient air.

2.2.1.4 Torre Collserola site (TC_{site})

Collserola mountain range is part of the Catalan coastal range, and limits the city of Barcelona to the NE between the Llobregat and the Besòs rivers (located south and north of the city, respectively). This forested area is a natural park, being its highest peak at 512 m a.s.l.. The main telecommunication tower of Barcelona (Torre Collserola, TC) is located on one of its hills (41°25'02'' N, 02°06'51'' E, 445 m a.s.l.), and on its fourth floor some instruments were deployed (80 m a.g.l). Due to the limited space available in the tower, several instruments were placed in the nearby Fabra astronomical observatory (41°25'56'' N, 02°07'27'' E, 415 m a.s.l), and located about 450 m (900 m road distance) from the tower Collserola site (TC_g). Therefore, two different monitoring sites were used to characterise the Torre Collserola site: TC_g at ground level and TC at the top of the tower (Dall´Osto et al., 2013). In summary, meteorological data and N were measured at TC, whereas PM and N size distribution were sampled at TC_g (see Figure 2.6). Regardless of these location differences, both sampling sites are considered to represent the same environment and will be further referred to as TC_{site}. This site characterizes the suburban environment of the city and is affected by the boundary layer daily cycle and the sea/mountain breeze circulation.

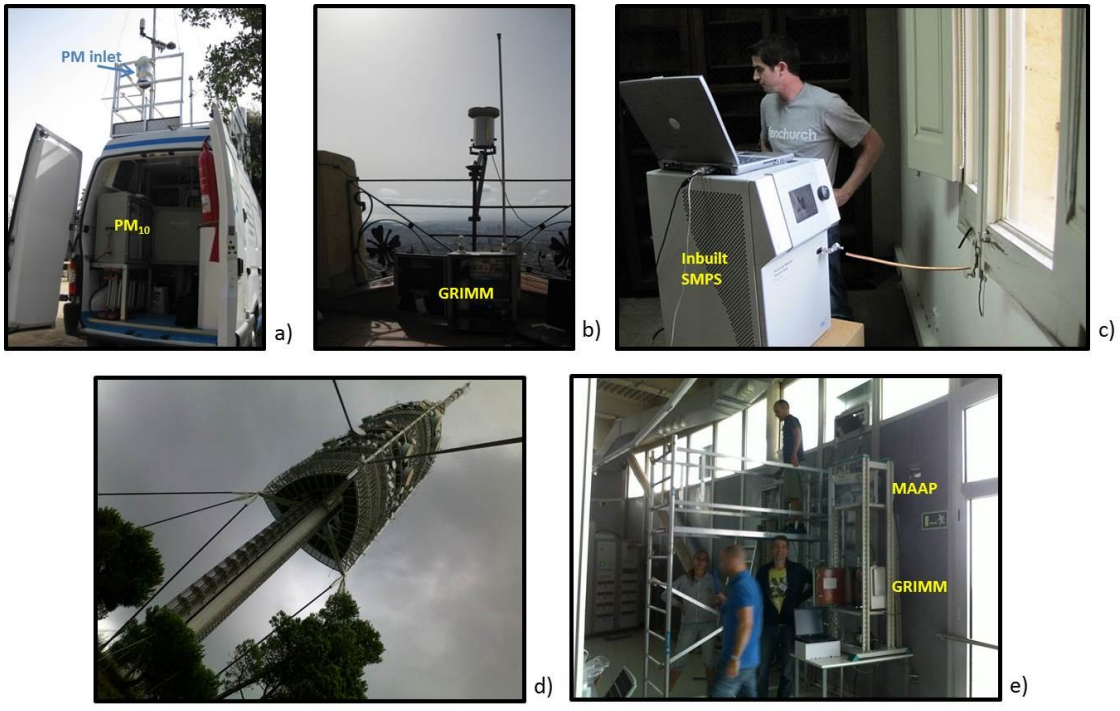

Figure 2.6: TC_{site} monitoring site lay-out: instruments located at TC_g (a-c) and TC (d-e).

2.2.1.5 Regional Background site (RB_{site})

The RB_{site} is located in the Montseny natural park (41°46'45'' N, 02°21'29'' E, 720 m a.s.l.), about 50 km to the North-North East of Barcelona. This measuring station is part of the ACTRIS network (Aerosols, Clouds, and Trace gases Research InfraStructure Network; formerly EUSAAR) under the abbreviation MSY. It is located 30 km from the Mediterranean coast and is regularly affected by a diurnal mountain breeze (Cusack et al., 2013a; Pérez et al., 2008a; Pey et al., 2010). The monitoring site lay-out can be seen in Figure 2.7.

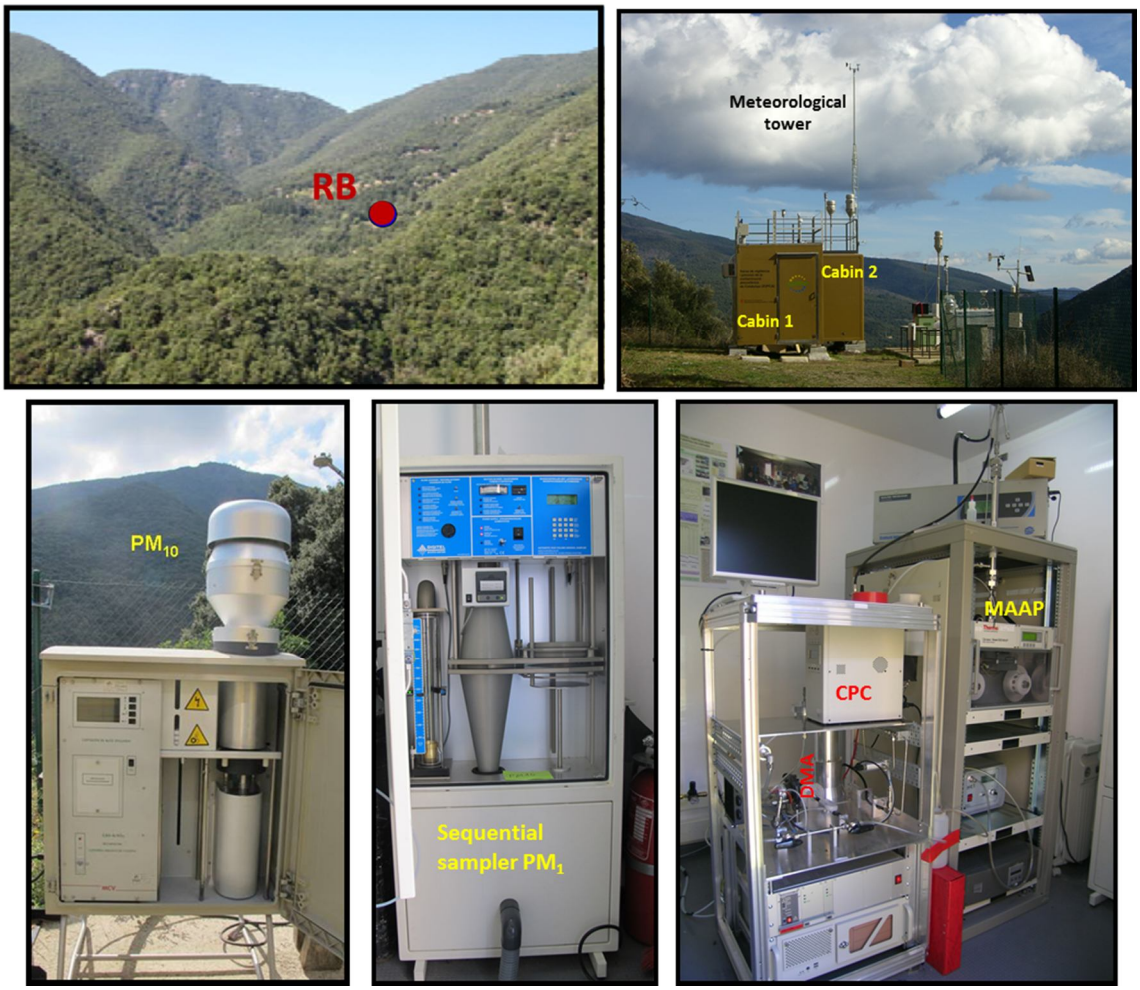

Figure 2.7: RB_{site} monitoring site lay-out. Two conditioned cabins contained the aerosol instruments, which sampled ambient air through inlets placed in the cabins' roof. Addtionally, PM samplers were located outside the cabins.

2.2.2 Long term measurements in worldwide cities

2.2.2.1 Barcelona (BCN)

Long term PM measurements in the urban background of Barcelona have been carried out since 1999, with varying locations within the city. In 2011 the site was definitely established at Palau Reial, located close (350 m) to a major highway (Diagonal Avenue: 90 000 vehicles per working day), which is primarily used by commuters (see Table 2.3). This current site is 200m distant to the UB_{site} used during the intensive SAPUSS campaign (autumn 2010), therefore being both fully comparable. For simplicity, this sampling site will be further referred to in the text as Barcelona or BCN.

2.2.2.2 Madrid (MAD)

The SMPS sampling site was located at the CIEMAT (Centro de Investigaciones Energéticas, Medioambientales y Tecnológicas) facilities, NW of the city centre and considered as a suburban background area (see Table 2.3). It is situated close to two green areas, with an extensive forested area spreading to the north, although it is close (around 1 km) to the ring road M30 and the highway A6.

2.2.2.3 Brisbane (BNE)

The monitoring site was located in the campus of the Queensland University of Technology (QUT), located to the SE of the city centre, with a major highway (the Pacific Motorway) situated along the SW side of the campus. Measurements were performed about 10 m a.g.l. on the top floor of a campus building, in an area considered as urban background (see Table 2.3).

2.2.2.4 Rome (ROM)

The sampling site is located in Montelibretti, 30 km NE from the Rome city centre (Table 2.3). Although considered as a regional background site, it is regularly impacted by pollutants transported from the area of Rome, due to the sea-breeze circulation (Ciccioli et al., 1999). Additional emissions sources are the town of Monterotondo (35 000 inhabitants, 5 km to the WSW) and a four-lane highway (10 000 veh day^{-1}, 2km to the W; Costabile et al., 2010).

2.2.2.5 Los Angeles (LA)

The data were sampled in downtown Los Angeles at the University of Southern California (USC) site, representative of the urban background pollution of the city (see Table 2.3).The site is influenced by the freeway I-110 (120 m distance).

Table 2.3: Exact locations of the selected worldwide sampling sites, their elevation and site type.

City	Site	Latitude	Longitude	Elevation (m a.s.l.)	Site type
Barcelona, Spain	Palau Reial	41°23'14"N	2°6'56"E	78 m	Urban background
Madrid, Spain	CIEMAT	40°27'30"N	3°43'30"W	655 m	Suburban background
Brisbane, Australia	QUT	27°28'43"S	153°1'44"E	10 m	Urban background
Rome, Italy	Montelibretti	42°06'38"N	12°38'05"E	47 m	Regional background
Los Angeles, USA	USC	34°1'9"N	118°16'39"W	61 m	Urban background

2.3 Measurements

The following table broadly describes the type of measurements carried out at each site. For more detailed information on the sampling periods and instrument techniques and models used see the tables in this section.

Table 2.4: Main aerosol measurements carried out at all monitoring sites. The abbreviation l.t.m. stands for long term measurements and i.c. for intensive campaign.

Sites	Particle number		Off-line PM		Other parameters			
	SMPS	CPC	PM_1	PM_{10}	Meteorology	Gaseous pollutants	On-line PM	BC
Barcelona (l.t.m.) -BCN	X	X	X		X	X	X	X
Barcelona (i.c. SAPUSS)								
- RS	X	X	X	X	X	X	X	X
- UB	X	X	X	X	X	X	X	X
- TM				X	X		X	X
- TC	X	X	X	X	X	X	X	X
- RB	X	X	X		X	X	X	
Madrid (l.t.m.) - MAD	X		X		X	X	X	
Brisbane (l.t.m.) - BNE	X	X	X		X	X	X	
Rome (l.t.m.) - ROM	X		X		X	X		
Los Angeles (l.t.m.) - LA	X	X	X		X	X	X	

2.3.1 SAPUSS campaign measurements

2.3.1.1 Size segregated aerosol concentrations

Four different Scanning Mobility Particle Sizer (SMPS) instruments with 5 minute time resolution were simultaneously deployed at four sites (RS_{site}, UB_{site}, TC_{site} and RB_{site}). Although the use of aerosol drier is advisable (Colbeck and Lazaridis, 2014, Swietlicki at al., 2008) in future studies, unfortunately it was not possible to use during this campaign. The instrument specifications at each site are as follows:

- RS_{site}: Differential Mobility Analyser (DMA) TSI 3080 and a TSI Condensation Particle Counter (CPC) 3010 (size measuring range of 11-322 nm for a total of 511 hours).

- UB_{site}: DMA TSI 3080 coupled with a TSI CPC 3775 (size measuring range of 15-228 nm for 424 hours).

- TC_{site}: DMA TSI 3034 with an inbuilt CPC (size measuring range of 10-470 nm for 585 hours).

- RB_{site}: the SMPS deployed was a EUSAAR IfT Model coupled with a TSI CPC 3772 (size measuring range of 10-470 nm for 486 hours).

The size ranges and the number of size bins were different for each SMPS (RS_{site} 48 bins, UB_{site} 39 bins, TC_{site} 54 bins, RB_{site} 54 bins). In order to harmonize the data, they were averaged at hourly resolution to the size ranges of the UB_{site}, in order to obtain a homogeneous data set that could allow an intercomparison between all sites. This resulted in a data matrix of particle size distributions ranging from 15 to 228 nm (39 bins) that contained 2006 hours of measurements distributed across the four sites. All SMPS instruments were calibrated and intercompared beforehand, resulting in excellent agreement as shown in Dall'Osto et al. (2013a). They also provided an excellent temporal overlap (85%, see Table 2.5).

Table 2.5: SMPS instrument models used at the monitoring sites and their data availability during the SAPUSS.

Site	SMPS model	SMPS measurements availability
RS	TSI 3080 DMA and TSI CPC 3010	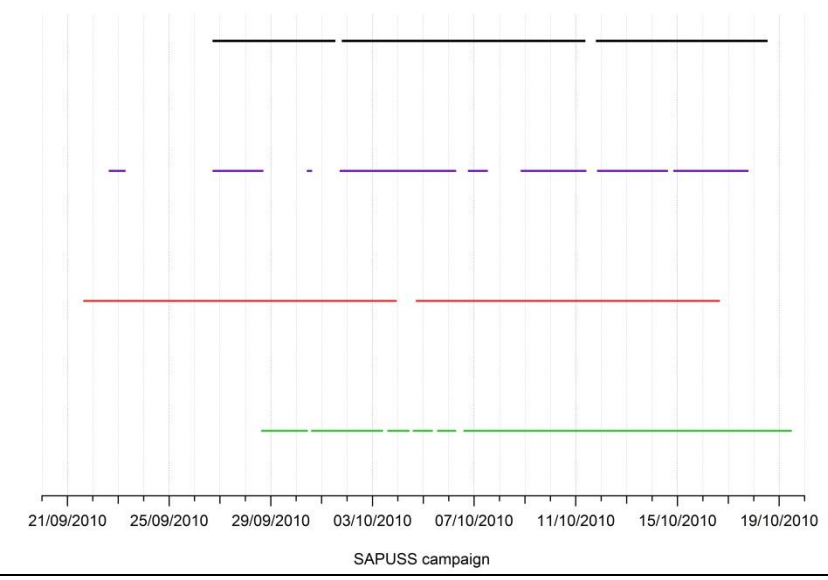
UB	TSI 3080 DMA and TSI CPC 3775	
TC_g	TSI 3030 DMA with inbuilt CPC	
RB	EUSAAR IfT Model and TSI CPC 3772	

2.3.1.2 Particle mass concentrations

Gravimetric PM measurements were carried out by high volume samplers DIGITEL DHA-80 and MCV CAV-A/mSb ($30 m^3 h^{-1}$) equipped with PM_{10} and PM_1 heads that collected 12 h samples (from 11:00 to 23:00 and from 23:00 to 11:00, local time) on quartz fibre filters (Pallflex 2500QAT-UP).

PM_{10} samples were collected at five monitoring sites (RS_{site}, UB_{site}, TM_{site}, TC_g and RB_{site}). Due to technical problems, the amount of data collected at the RB site for PM_{10}

was not considered sufficient, therefore these data were not considered for this study (Table 2.6). A total of 221 filter samples were collected, from which 93% were sampled simultaneously at the four monitoring sites (54 concurrent samples per site). Regarding PM_1 samples, they were concurrently collected at the RS_{site} and UB_{site}, resulting in 98% concurrent samples (53 concurrent samples per site).

Table 2.6: Particulate matter off-line data availability at the monitoring sites during the sampling period.

Site	Particulate matter off-line measurements availability
RS UB TM TC_g RB	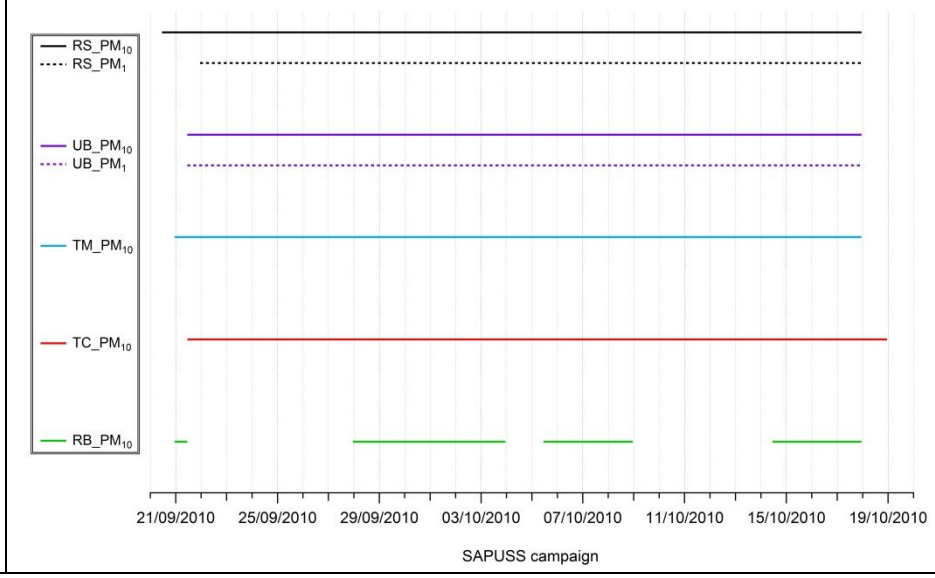

2.3.1.3 PM chemical analysis

2.3.1.3.1 Inorganic chemical analysis

PM_{10} and PM_1 mass concentrations from filter samples were determined gravimetrically. Subsequently, the samples were analysed following the methodology described by Querol et al. (2001). Briefly, a quarter of the filter was acid digested (HNO_3:HF:$HClO_4$), and the resulting solution was analyzed for Al, Ca, K, Mg, Fe, Ti, Mn, P, S, Na and 25 trace elements by Inductively Coupled Plasma Atomic Emission and Mass Spectrometry (ICP-AES and ICP-MS), respectively; a quarter of the filter was water-extracted and the concentrations of SO_4^{2-}, NO_3^- and Cl^-, and NH_4^+ were determined by ion chromatography (IC) and selective electrode, respectively. A section of 1.5 cm^2 of the filter was used to determine organic carbon (OC) and elemental carbon (EC) by a thermal–optical transmission technique (Birch and Cary, 1996) using a Sunset Laboratory OCEC Analyzer following the EUSAAR2 temperature protocol (Cavalli

et al., 2010). Laboratory and field blanks were analysed following the same procedure. Ambient concentrations were calculated based on the samples and the blanks concentrations.

2.3.1.3.2 Organic chemical analysis

Additionally, the PM_1 filter samples were also analysed for organic aerosols (Alier et al., 2013; van Drooge and Grimalt, 2015), preserving an 1/8 section of each filter for this purpose. This section was ultrasonically extracted with (2 : 1, v/ v) dichloromethane : methanol (3×5 mL; Merck, Germany) for 15 min. Before extraction 25 µL of the surrogate standards levoglucosan-d_7, n-$C_{24}d_{50}$ (Cambridge Isotopic Laboratories, UK), succinic acid-d_4 (Sigma Aldrich), anthracene-d_{10}, benz[a]anthrancene-d_{12}, benzo[k]fluoranthene-d_{12} and benzo[ghi]perylene-d_{12} (Dr. Ehrenstorfer) were added. The extracts were filtered over 0.45 µm teflon membrane filters (Whatman) in order to remove insoluble particles. Then, they were concentrated to 1mL under a gentle N_2-gas stream.

Anhydro saccharides, acids, polyols and nicotine were analyzed following a procedure that was similar to others described previously (El Haddad et al., 2011; Medeiros and Medeiros, 2007; van Drooge et al., 2012a). Briefly, an aliquot of the extract (25 µL) was evaporated under a gentle N_2 stream until dryness. Then, 25 µL of bis(trimethylsilyl)trifluoroacetamide (BSFTA)+trimethylchlorosilane (99 : 1) (Supelco) and 10 µL of pyridine (Merck) were added for derivatization of the saccharides, acids and polyols to their trimethylsilyl esters at 70 °C during 1 h. Before injection into a gas chromatograph coupled to a mass spectrometer (GC-MS), 25 µL of the internal standard, pyrene-d_{10}, were added to the vial.

For the analysis of polycyclic aromatic hydrocarbons and hopanes, the remaining extract was evaporated to almost dryness under a gentle N_2-gas stream and re-dissolved in 0.5mL hexane+dichloromethane (9 : 1 v/v) (Merck, Germany). Then, it was cleaned up by adsorption column chromatography on 1 g of aluminum oxide (Merck, Germany) that was activated overnight at 120 °C. The analytes were eluded with 4mL of (9 : 1 v/v) hexane:dichloromethane and 4mL of (1 : 2 v/v) hexane:dichloromethane, respectively (Merck, Germany). The collected fraction was concentrated under a gentle

N_2-gas stream to 50 μL, and the internal standard, pyrene-d_{10}, was added before injection into GC.

Sample extracts were injected into a Thermo GC/MS (Thermo Trace GC Ultra – DSQ II) equipped with a 60m fused capillary column (HP-5MS 0.25mm × 25 μm film thickness). The oven temperature program started at 60 °C held for 1 min, and then it was heated to 120 °C at 12 °C min^{-1} and to 310 °C at 4 °C min^{-1} where it was held for 10 min. The injector, ion source, quadrupole and transfer line temperatures were 280 °C, 200 °C, 150 °C and 280 °C, respectively. Helium was used as a carrier gas at 0.9mLs^{-1}. The MS selective detector was operated in fullscan (m/z 50– 650) and electron impact (70 eV) ionization modes.

Besides comparison of retention times, levoglucosan and mannosan were identified with ion m/z 204, galactosan with ion m/z 217 and nicotine with ion m/z 84. Acids, polyols and 2-methyltetrols were identified with the following ions: malonic acid (m/z 233), succinic acid (m/z 247), glutaric acid (m/z 261), pimelic acid (m/z 289), suberic acid (m/z 303), azelaic acid (m/z 317), glyceric acid (m/z 292), malic acid (m/z 233), tartaric acid (m/z 292), phthalic acid (m/z 295), tricarballytic acid (m/z 377), cispinonic acid (m/z 171), 3-hydroxyglutaric acid (m/z 349), 3- methyl-1,2,3-butanetricarboxylic acid (MBTCA) (m/z 405), 2-methylglyceric acid (m/z 219), C5-alkene triols (m/z 231), 2-methylthreitol and 2-methylerythritol (m/z 219). Quantification was performed with the external standard calibration curves. All concentrations were corrected by the recoveries of the surrogate standard succinic acid (m/z 251) and levoglucosan-d7 (m/z 206). No standards were available for 3-hydroxyglutaric acid, MBTCA, 2-methylglyceric acid, C5 alkene triols, 2-methylthreitol and 2-methylerythritol. Their chromatographic peaks were identified by comparison of their mass spectra to literature and library data (Claeys et al., 2007; Kourtchev et al., 2005; Clements and Seinfeld, 2007), and they were quantified with the calibration curve of succinic acid. Application of the calibration curves of other standards leads to lower concentrations with a maximum variation of factor of 3. Therefore, caution should be taken when comparing these results with those from other studies.

PAH were identified by retention time comparison of the peaks with the following ions in SIM mode: phenanthrene (m/z 178), anthracene (m/z 178), fluoranthene (m/z 202), pyrene (m/z 202), benz[a]anthracene (m/z 228), chrysene+triphenylene (m/z 228), benzo[b]fluoranthene (m/z 252), benzo[k]fluoranthene (m/z 252), benzo[e]pyrene (m/z 252), benzo[a]pyrene (m/z 252), indeno[1,2,3- cd]pyrene (m/z 276), benzo[ghi]perylene (m/z 276) and coronene (m/z 300). 17(H)α-21(H)β-29-Norhopane and 17(H)α-21(H)β-hopane were identified in the m/z 191 mass fragmentogram and the corresponding retention times. Quantification was also performed by the external standard method, and the calculated concentrations were corrected for the recoveries of the abovementioned surrogates: anthracene-d_{10} (m/z 188), benz[a]anthrancene-d_{12} (m/z 240), benzo[k]fluoranthene-d_{12} (m/z 264) and benzo[ghi]perylene-D_{12} (m/z 288).

In all cases the recoveries of the surrogate standards were higher than 70 %. Field blank levels were between 1% and 30% of the sample levels. All concentrations were corrected for blank levels. Limits of quantification (LOQ) were calculated by dividing the lowest measured levels in the standard calibration curves by the volumes of the analyzed sample fraction. These were 0.1 ngm^{-3} for the anhydrosaccharides, 0.06 ngm^{-3} for the acids and 0.005 ngm^{-3} for PAHs and hopanes (Alier et al., 2013).

2.3.1.4 Meteorological parameters

Meteorological parameters (temperature, relative humidity, solar radiation, atmospheric pressure and wind components) were recorded at five sites (RS_{site}, UB_{site}, TM_{site}, TC_g and RB_{site}). The meteorological instrumentation was located in the same monitoring sites with the exception of the UB site, which data were obtained from a close meteorological station located on the roof terrace of the Physics Faculty of the Universitat de Barcelona.

As can be seen in Table 2.7 however, the wind components were not measured at TM_{site} and at the RS_{site} they were compromised due to the street canyon conditions of the sampling location.

Table 2.7: Meteorological parameters data availability at the monitoring sites during the sampling period. *Meteo* refers to temperature, relative humidity, solar radiation and rain, whereas *wind* refers to the wind components.

Site	Meteorological parameters measurements availability
RS UB TM TC_g RB	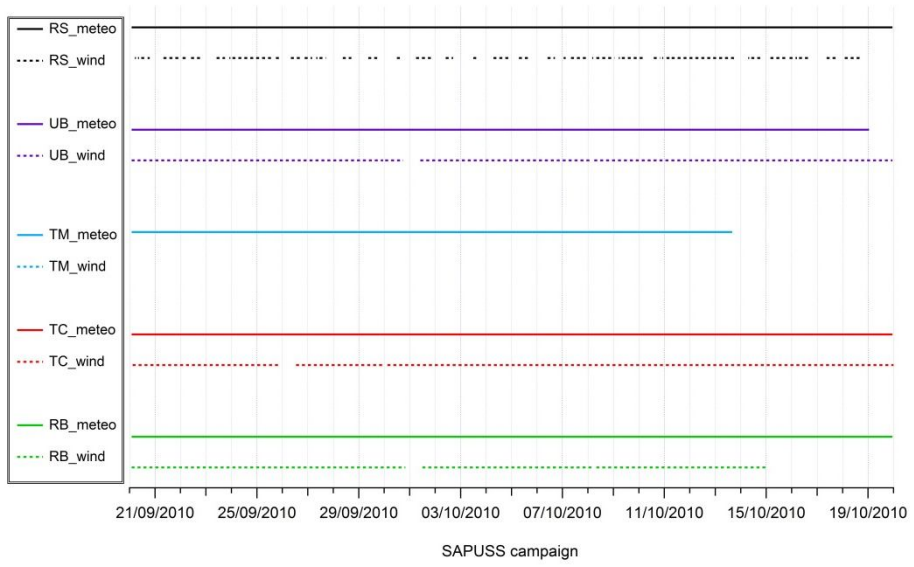

2.3.1.5 Gaseous pollutants

Gaseous pollutants such as NO, NO_2, O_3, SO_2, CO were also measured using the standard air quality reference techniques. NO and NO_2 were obtained by chemiluminescence, O_3 by UV absorption, SO_2 by UV fluorescence and CO by IR absorption. Data coverage was very high for all gaseous pollutants at all sites (see Table 2.8).

Table 2.8: gaseous pollutants measurement availability at the sampling sites during the sampling period.

Site	Gaseous pollutants measurements availability
RS UB TC RB	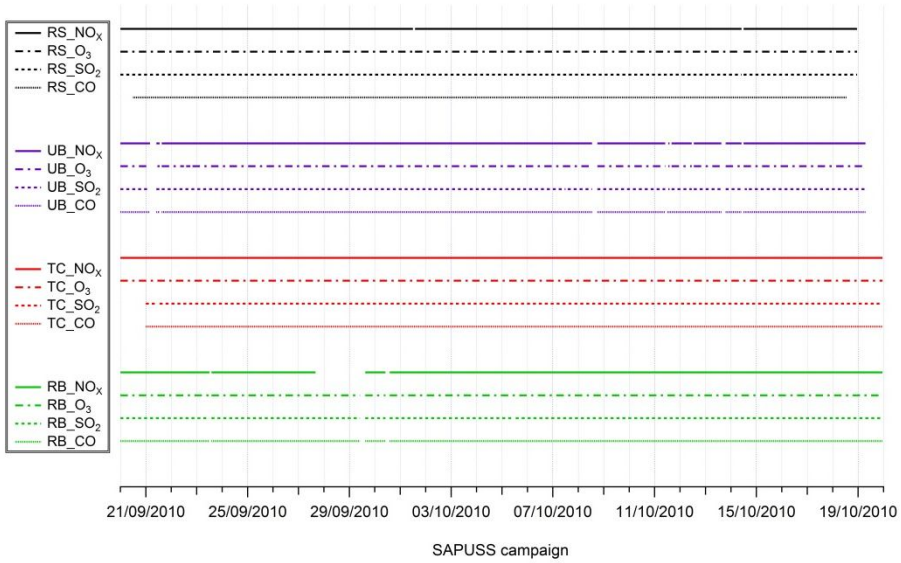

2.3.1.6 Black carbon

Levels of Black Carbon (BC) were measured with a Multi-Angle Absorption Photometer (MAAP) or a Magee Aethalometer (see Table 2.7). MAAP instruments were deployed at the RS_{site}, UB_{site}, and TC sites whereas an Aethalometer was placed at TM_{site}. MAAP instruments were found to give excellent agreement between them as reported by Dall'Osto et al. (2013a). The intercomparison between these instruments and the Aethalometer yielded and R^2=0.98 (Dall'Osto et al., 2013a). However, the data availability at the RS and UB was scarce, as the instruments operated correctly less than 50% of the duration of the campaign (Table 2.9).

Table 2.9: Black carbon instruments used at the sampling sites and their data availability during the sampling period.

Site	BC instrument	BC measurements availability
RS	MAAP	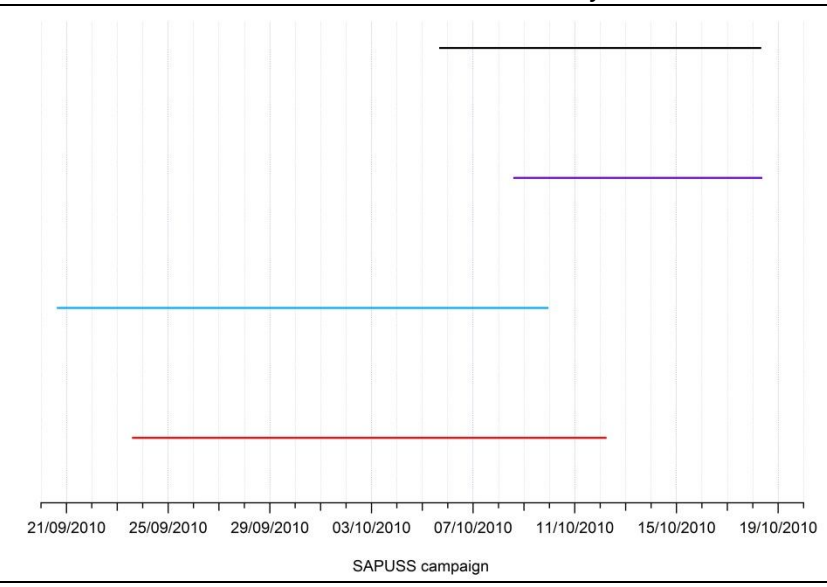
UB	MAAP	
TM	Magee AE-16 Aethalometer	
TC	MAAP	

2.3.1.7 Particle number concentration

In addition to particle number size distribution, total particle number concentrations were measured at five monitoring sites (RS_{site}, UB_{site}, TM_{site}, TC and RB_{site}). At the RS_{site} and TC the CPC deployed was a buthanol-based TSI Model 3022A with a 50% cut-point at 7 nm while at the UB and RB_{site} the CPC deployed was a water-based TSI Model 3785 with a lower cut-point at 5 nm. The CPC's were intercompared before and after the campaign, giving excellent overlap, with uncertainties around 5% both times (Dall'Osto et al., 2013a). Biswas et al. (2005) intercompared both water-based and buthanol-based instruments and concluded that they showed a similar

response, always within the uncertainty of the manufacturer (±10%). See Table 2.10 for the instruments availability at the sampling sites.

Table 2.10: CPC instruments used at the sampling sites and their data availability during the sampling period.

Site	CPC instrument	CPC measurements availability
RS	TSI 3022 CPC	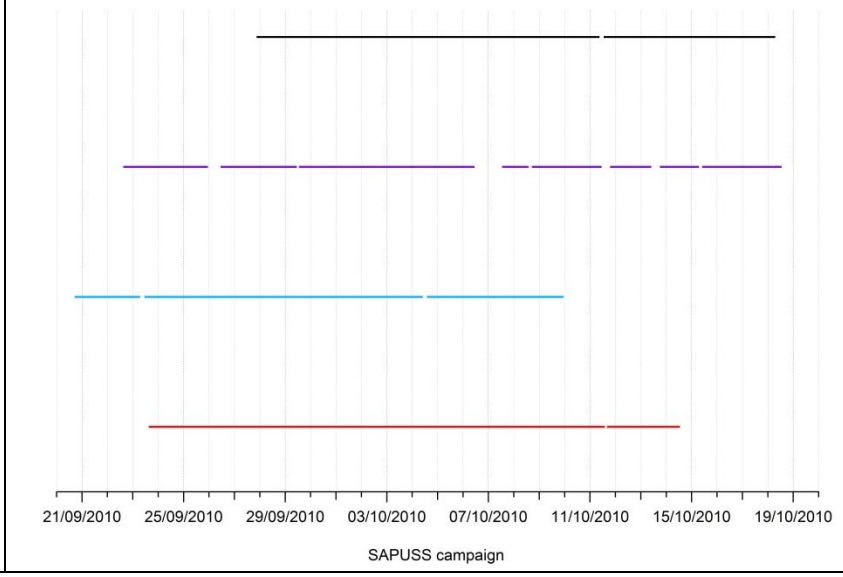
UB	TSI 3785 CPC	
TM	TSI 3022 CPC	
TC	TSI 3022 CPC	

2.3.1.8 On-line PM measurements

Simultaneously with sampling, PM_{10}, $PM_{2.5}$ and PM_1 were continuously online measured with optical dust monitors (Grimm Labortechnik Model 1107). Table 2.11 shows that the data coverage ranged between 70-100% of the campaign at the different sites. These values were corrected by the gravimetric PM concentrations.

Table 2.11: On-line PM instruments used at the sampling sites and their data availability during the sampling period.

Site	PM online	PM on-line measurements availability
RS	Grimm 1107	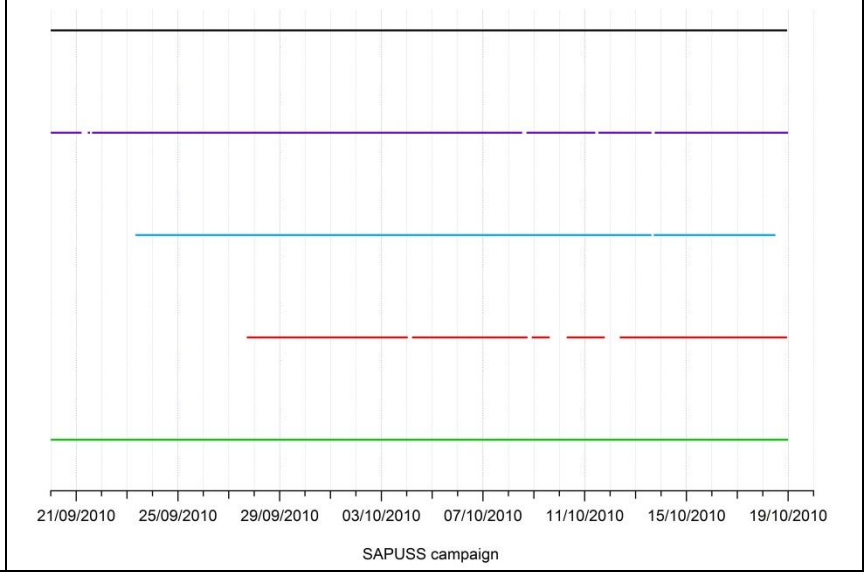
UB	Grimm 1107	
TM	Grimm 1107	
TC_g	Grimm 1107	
RB	Grimm 1107	

2.3.2 Measurements at the complementary study areas

2.3.2.1 Particle number size distributions

The detailed characteristics of the sampling periods, SMPS models and size ranges at each city can be seen in Tables 2.12 and 2.13. Although the use of aerosol drier is advisable (Swietlicki at al., 2008; Colbeck and Lazaridis., 2014), it was not possible at the time of sampling. Nevertheless, data were thoroughly checked to avoid possible humidity influences (Costabile et al., 2010). The SMPS low-cut point ranged from 10.2 nm to 17.5 nm whereas the SMPS high-cut point varied from 101.8 to 615.3 nm. The lack of measurements below 10 nm does not allow for proper identification of the start of new particle formation events, therefore our so-called "nucleation events" reflect photochemically nucleated particles that have grown over the low-cut detection limits of each instrument. In addition, such events were evaluated visually by inspecting the trends of the SMPS size distributions. More information reporting a detailed analysis of the aerosol size distributions used in this work can be found in previous studies (Madrid: Gómez-Moreno et al., 2011; Brisbane: Cheung et al., 2011; Rome: Costabile et al., 2010; Los Angeles: Hudda et al., 2010). Due to the different time resolution of each instrument, all measurements were averaged to 1 hour resolution. All data herein reported should be read as local time.

Table 2.12: Sampling period of the SMPS instruments and their characteristics and size range at each selected city.

City	Sampling period	SMPS model	SMPS size range	Size bins
Barcelona (BCN)	30/07/2012-04/08/2013 (7295 h)	TSI (DMA 3081, CPC 3772)	11.3-358.7 nm	97
Madrid (MAD)	10/01/2007-12/12/2008 (12482 h)	TSI (DMA 3071, CPC 3022)	17.5-572.9 nm	34
Brisbane (BNE)	01/01/2009-31/12/2009 (6227 h)	TSI (EC 3080, CPC 3781)	10.2-101.8 nm	65
Rome (ROM)	26/09/2007-07/05/2009 (3373 h)	TSI (DMA 3081, CPC 3775)	15.1-224.7 nm (10.2-615.3 nm)	76 (87, 93, 104)
Los Angeles (LA)	04/09/2009-10/12/2009 (2184 h)	TSI (DMA 3081, CPC 3022A)	15.7-371.8 nm	89

Table 2.13: SMPS data availability at the five selected sites: Barcelona (BCN), Madrid (MAD), Brisbane (BNE), Rome (ROM) and Los Angeles (LA).

Site	Long-term SMPS measurements availability
Barcelona (BCN) Madrid (MAD) Brisbane (BNE) Rome (ROM) Los Angeles (LA)	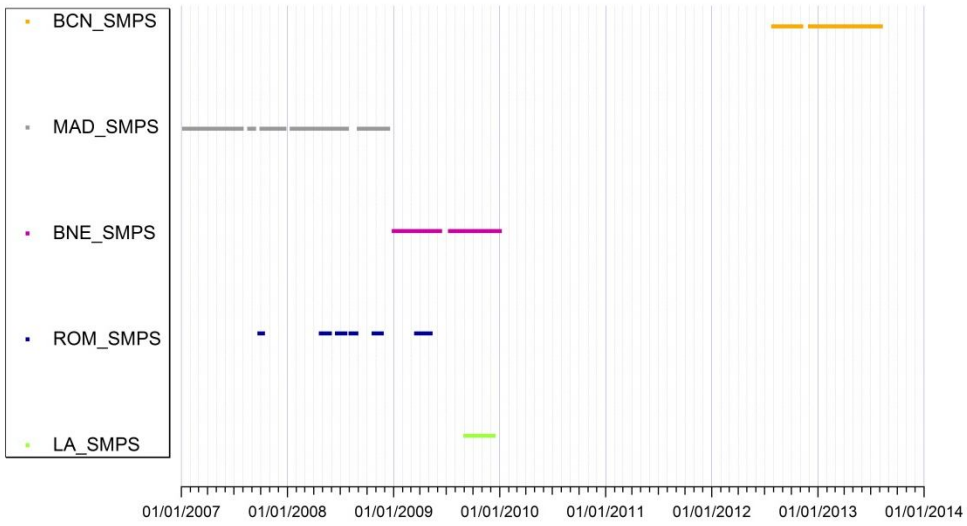

2.3.2.2 Meteorological parameters and other air pollutants

Meteorological (temperature, relative humidity, wind components and solar radiation), gaseous pollutants (NO, NO_2, O_3, CO, SO_2) and other parameters (PM_x, N, BC and particulate nitrate concentrations) were obtained at the site or from the closest available air quality station (see Table 2.14). These data were averaged to 1 hour resolution to match the SMPS measurements.

Table 2.14: Summary of the online measured parameters at the selected cities. V^+ indicates the measurement site is different to the SMPS site.

City	Ancillary data site	Meteorological data					Gaseous Pollutants					Particulate Matter				Other	
		T	RH	ws/ wd	Rain	SR	NO	NO_2	O_3	CO	SO_2	PM_{10}	$PM_{2.5}$	PM_1	NO_3^-	N	BC
BCN	Palau Reial, Fac. of Physics$^+$	V^+	V^+	V^+	V^+	V^+	V	V	V	V	V	V	V	V		V	V
MAD	CIEMAT, Casa de Campo$^+$	V	V	V	V	V	V	V	V	V^+	V	V^+	V^+		V		
BNE	Rocklea$^+$	V^+	V^+	V^+	V^+	V^+	V^+	V^+	V^+			V^+	V^+			V^+	
ROM	Buf$^+$	V^+	V^+	V^+	V^+	V^+	V^+	V^+	V^+		V^+						
LA	South Coast AQMD$^+$	V^+	V^+	V^+	V^+		V^+	V^+	V^+	V^+	V^+		V^+			V	

2.4 Air pollution sampling instruments

2.4.1 Particle number concentration

The particle number concentration was measured using a Condensation Particle Counter (CPC). The most commonly used time resolution is 5 min and usually a PM_1 cyclone is placed at the airflow entrance to avoid the penetration of larger particles. The aerosol enters the sample inlet and reaches a wetted media soaked by either water or butanol, depending on the model. Due to the heater saturator placed in this first chamber and the following cooler condenser, the liquid condenses onto the particles causing them to increase their size and thus allowing its detection with an optical system (Figure 2.8). Different CPC models were used at the monitoring sites (see details in Table 2.10), usually with a low-cut diameter of 5-7 nm.

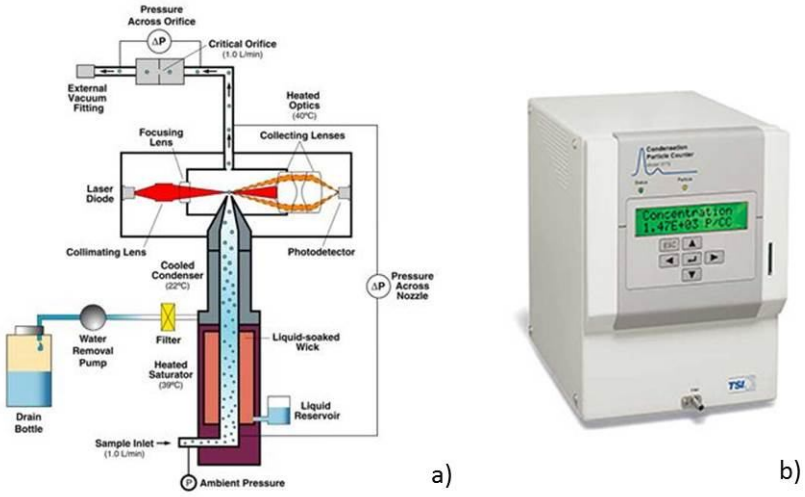

Figure 2.8: Condensation particle counter: a) schematic diagram of a TSI 3772/3771 model, b) TSI 3772 CPC instrument.

2.4.2 Particle number size distributions

Particle number size distributions were measured by means of a scanning mobility particle sizer (SMPS). This instrument consists of a differential mobility analizer (DMA) connected to a condensation particle counter (CPC). Ambient air is pumped through the sampling inlet, reaching a bipolar charger or neutralizer, which is usually a radioactive source such as Kr^{85}. Following their neutralization, aerosols then enter the DMA, where they are classified according to their electrical mobility. The selected monodisperse aerosols exit the DMA and reach the CPC, where their number

concentration is determined for that size range (Figure 2.9). The models used in each of the sampling sites as well as the size range are reported in Tables 2.4 and 2.12.

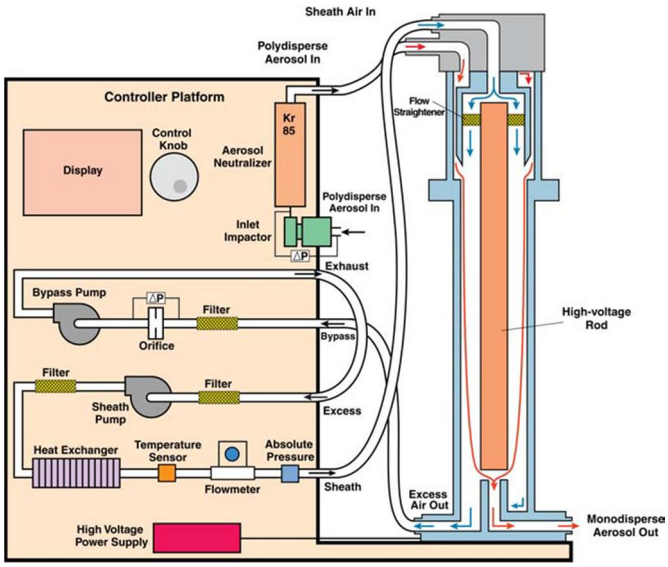

a) b)

Figure 2.9: SMPS for measuring on-line particle number particle concentration: a) schematic diagram of the functioning of the TSI 3081 DMA (TSI, 2009), b) SMPS consisting of a TSI DMA 3081 and a TSI 3772 CPC.

2.4.3 Off-line particle mass concentration

PM_{10} and PM_1 samples were collected every 12 h on 150 mm diameter quartz microfiber filters (Pallflex 2500QAT-UP) at most of the SAPUSS monitoring sites using DIGITEL or equivalent MCV CAV-A/MSb (Figure 2.10) equipped with PM_{10} and PM_1 cutt-off inlets, respectively. Before sampling, all filters followed a strict protocol to ensure data quality. First they were treated under high temperatures (200°C) in an oven for a minimum of 4 hours to eliminate volatile impurities. After that, they were placed in a temperature-controlled chamber at 20°C and 50% relative humidity for 48 hours. Then, the filters were weighted on three different days three times in the same climate-controlled chamber according to the EN 12341 standard (CEN, 1999). After sampling they remained 48 hours longer on the same chamber and were weighted again twice on two consecutive days under the same conditions. The mass concentration was determined from the increase in filter mass and air volume sampled for each filter.

Ambient air was sampled at a flow rate of 30 m^3 h^{-1} through the inlets and the nozzles of the sampling head by means of an in-built pump. The geometric design of the nozzles determines the cut-off diameter for the sampled particle size fraction, whereas larger particles are adhered to a vaseline daubed plate placed inside of the head, allowing for the desired particles to pass through and deposit on the filter. The PM_1 head is comprised of a 2-stage impactor, an upper one where particles larger than 2.5 μm are firstly removed and a lower one where particles in the range 2.5-1 μm are further removed. Regular maintenance such as cleaning sampling heads and flow rate control was done during the duration of the campaign.

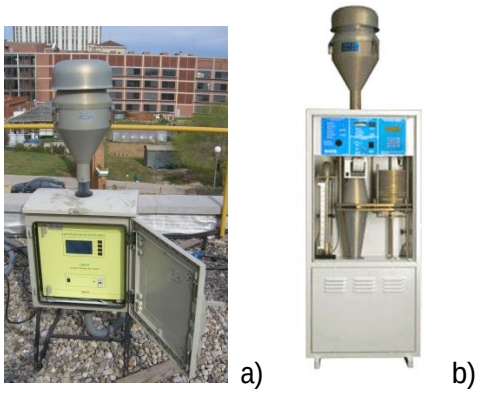

a) b)

Figure 2.10: High-volume samplers: a) MCV, b) Sequential Digitel.

2.4.4 On-line particle mass concentration

On-line measurement levels of PM_x fractions (PM_{10}, $PM_{2.5}$ and PM_1) were carried out by means of PM optical counters at most of the sites (see Table 2.11 and 2.14). During the SAPUSS campaign Grimm Labortechnik GmbH & Co. KG model 1107 was deployed at the monitoring sites, whereas in the BCN site the Grimm model 180 was used. The selected time resolution was either 30 min or 1 hour although all measurements were later averaged to 1 hour resolution.

The Grimm monitors measure light scattering by individual particles as they go through a narrow light beam. A fraction of the scattered light is collected at a 90 angles by a mirror and transferred to a photodetector (Figure 2.11), where it is converted to a proportional voltage pulse (McMurry et al., 2000). Particle size is determined from the number of single particle counts registered in each channel, and it is converted to mass by using a particle-density based equation thus obtaining PM_x concentrations. The

advantage of the model 180 is the lower maintenance required, as it has been designed for continuous, unattended automatic operation in a sheltered space.

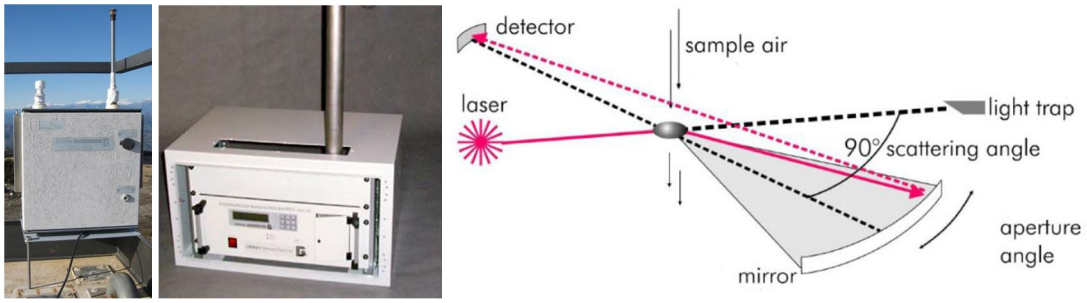

a) b) c)

Figure 2.11: GRIMM optical counter: a) model 1107, b) model 180, c) schematic operational diagram (GRIMM, 2007).

2.4.5 Aerosol absorption coefficient measurements

Levels of Black Carbon (BC) were monitored at all SAPUSS sites and at some of the cities (Tables 2.8 and 2.14). Most of the measurements were carried out using a multi-angle absorption photometer (MAAP, Thermo ESM Andersen Instruments) set to 1-5 min resolution with a PM_{10} inlet. This instrument determines the absorption properties of light of airborne aerosols, based on light attenuation by absorption, scattering and reflection of particles accumulated on a moving filter tape (Figure 2.12). The absorbance is converted to the mass concentration of BC ($\mu g m^{-3}$) using a mass absorption cross section at 637 nm (Müller et al., 2011) of 6.6 $m^2 g^{-1}$ recommended by the manufacturer.

At TM_{site} an Aethalometer AE-16 from Magee was deployed to measure BC. This instrument analyses BC measuring the attenuation of an 880 nm beam light transmitted through the sample when collected on a fibrous filter (Magee Scientific, 2005). We used in this case the Absorption/BC conversion factor provided by the manufacturers that was 16.6 $m^2 g^{-1}$.

Good agreement was found between the MAAPs and the AE-16 and correction factors were applied when necessary.

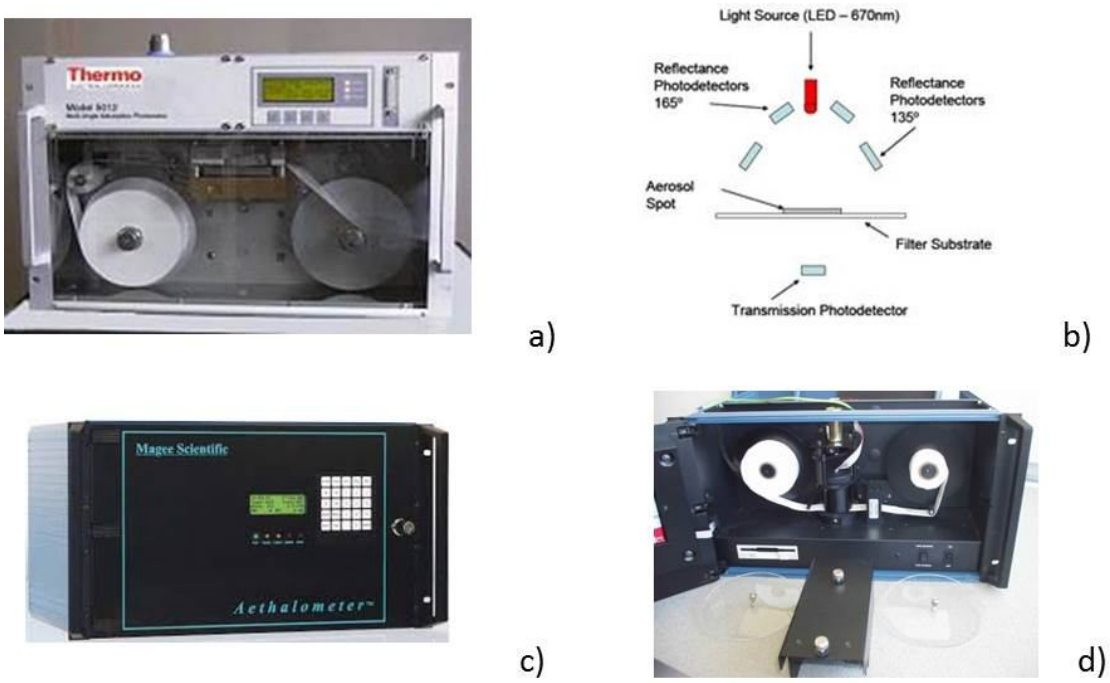

Figure 2.12: Black carbon monitoring instruments: a) MAAP, b) schematic diagram of the MAAP detector (Thermo, 2004), c) MAGEE AE-16 front panel and d) fibre filter of the AE-16 located in the rear inside part of the instrument (Magee, 2005 and 2008).

2.5 Data treatment

2.5.1 Particle number size distribution

Particle number size distribution data sampled by the SMPS usually generates large data matrixes that are complex to analyse without the use of statistical tool. For example, one year of continuous size distribution data with hourly resolution comprises 8760 size spectra. In order to address this issue, several techniques have been developed, being k-means the preferred one (Salimi et al., 2014). This technique has also been found very useful for studying aerosol dynamics and new particle formation events (Väänänen et al., 2013).

2.5.1.1 *k*-means clustering analysis

The k-means tool applied in this thesis is based on the technique developed by Beddows et al. (2009). This method classifies spectra with the highest degree of similarity into the same category or cluster therefore reducing the number of spectra to analyze. The number of clusters was conservatively chosen using the Dunn Index and the Silhouette Width. The larger the Dunn Index and Silhouette Width, the more

compact and well separated were the clusters and the more similar were the elements within each cluster (Beddows et al., 2009). Preference was given to a solution with a higher cluster number to reduce the likelihood that any one of the clusters grouped together spectra reflects more than one source. Although we reduce the possibility of losing information by 'over-clustering', it is likely that when comparing the average size distributions - together with the corresponding gaseous pollutants, meteorological parameters, and various temporal trends (daily, weekday-weekend, monthly) - that more than one size distribution may (or even may not) originate from a similar process/source. More often than not, when considering the average size distributions and auxiliary measurements from over-clustered data (e.g. similarly low NO concentrations among the clusters, similar daily trends, etc.), one or more clusters are combined together thus reducing the number of clusters in the final solution.

This methodology has already been successfully applied to a number of studies involving one (Dall'Osto et al., 2012) or multiple monitoring sites (Beddows et al., 2009, 2014; Dall'Osto et al., 2011b). In a nutshell, this method creates manageable groups of clusters that can be classified into aerosol size distributions types (i.e. characteristic of emission or formation processes) and permits a simplification of the data analysis that facilitates its interpretation.

To account for the uncertainty of the method, the uncertainty limits for all the clusters size distributions have been calculated using the confidence limits μ:

$$\mu = \text{mean}(x) \pm t\frac{\sigma}{\sqrt{n}}$$

where x are the size bin values $dN/d\log D_p$, n is the number of values used in the average, σ is the standard deviation, t is the Student t-value. We approximated the degrees of freedom to ∞, due to the high number of hours contributing to each cluster - in the range of hundreds to thousands. We considered 99.99% of the confidence level, obtaining a Student t-value of 3.291 according to http://www.webassign.net/harrischem/4-02tab.gif (last entry Dec 2014). The corresponding uncertainty bands have been plotted around each cluster size distribution.

During the SAPUSS campaign, particle number size distributions were collected at 4 different monitoring sites (RS_{site}, UB_{site}, TC_{site} and RB_{site}). All data were averaged to hourly resolution and the size range were harmonized to the common size range (15-228 nm, 39 size bins), resulting in a total of 2006 size spectra. The k-means clustering analysis was applied to the data matrix containing all four sites spectra, which allowed study of the transport and spatial evolution of aerosols in the urban environment of Barcelona and its region.

On the other hand, long-term measurements of particle number size distributions from BCN, MAD, BNE, ROM and LA, were collected over a longer time at each site (ranging from 2 years to 3 months), therefore a different approach was used. In this case, separate k-means clustering analyses for each city were carried out, and the specific resulting clusters were later compared.

2.5.2 PM chemistry

2.5.2.1 PM mass closure

In the PM_{10} fraction, the calculations for the crustal and sea salt aerosols concentration were performed carefully due to having some common elements contributing to both sources (Na, Mg and Ca). Moreno et al. (2006) reported the average composition of mineral dust originated in the North African region that later reached the WMB. Based on the average Na/Al ratio of the North African dust, the mineral Na (or non-sea salt Na, nss Na) can be calculated from the Al concentrations, hence the remaining Na is attributed to sea salt (ss Na). The sea salt load for each sample was calculated based on the ss Na and the standard sea salt composition which includes Na, Cl^-, ss Mg, ss Ca and ss SO_4^{2-} (Mészáros, 1999). Crustal matter was then calculated as the sum of SiO_2, CO_3^{2-}, Al_2O_3, nss Ca, Fe, K, nss Mg and nss Na. SiO_2 concentrations were estimated as $3*Al_2O_3$. CO_3^{2-} concentrations were estimated as 1.5*Ca, assuming that Ca is present as carbonates. Organic matter (OM) was estimated as OC multiplied by a factor 1.4 at the RS_{site}, 1.6 at the UB_{site} and TM_{site} and 2.1_{site} at the TC_{site}, according to Turpin and Lim (2001). Secondary Inorganic Aerosols (SIA) was calculated as the sum of SO_4^{2-}, NO_3^- and NH_4^+. The sum of OM, EC, crustal material, sea salt and trace elements accounted for the determined PM mass. The difference

between the weighted PM_x mass and that determined through chemical mass closure accounted for the undetermined mass, being attributed to formation, crystallization and moisture water that had not been removed during the sample conditioning.

2.5.2.2 Source apportionment by Positive Matrix Factorization (PMF)

With the chemical database obtained from the PM_{10} and PM_1 speciation during the intensive SAPUSS sampling campaign at several sites (RS_{site} and UB_{site} for PM_{10} and PM_1 and also TM_{site} and TC_{site} for PM_{10}) a source apportionment analysis to both PM fractions was performed in order to identify and quantify source contribution.

PMF is a widely used receptor model based on the mass conservation principle:

$$x_{ij} = \sum_{k=1}^{p} g_{ik} f_{jk} + e_{ij} \quad i=1,2,...,m \quad j=1,2,...,n \quad (1)$$

Where x_{ij} is the i^{th} concentration of the species j, g_{ik} is the i^{th} contribution of the source k and f_{jk} is the concentration of the species j in source k, and e_{ij} are the residuals. Equation (1) can be also expressed in matrix form as $\mathbf{X}=\mathbf{G}\mathbf{F}^{T}+\mathbf{E}$. PMF solves equation (1) minimizing the object function Q:

$$Q = \sum_{i=1}^{n} \sum_{j=1}^{m} (e_{ij} / s_{ij})^2 \quad (2)$$

Where s_{ij} are the individual data uncertainties. The uncertainty estimates were based on the approach by Escrig Vidal et al. (2009) and Amato et al. (2009) and provided a criterion to separate the species which retain a significant signal from the ones dominated by noise. This criterion is based on the signal-to-noise S/N ratio defined by Paatero and Hopke (2009). Species with S/N < 2 are generally defined as weak variables and downweighted by a factor of 3. Nevertheless, since S/N is very sensitive to sporadic values much higher than the level of noise, the percentage of data above detection limit was used as complementary criterion. The combination of both criteria permitted to select 27 inorganic and 35 organic species for PM_1 and 32 species out of the 61 available species for the PMF analysis in the case of PM_{10}. All the samples collected for each fraction were gathered in one data matrix. This data assembling allows exploring a larger area of the N-dimensional source contributions

space. The data matrix was uncensored, i.e. negative, zero and below detection limit values were included as such in the analyses to avoid a bias in the results (Paatero, 2007).

Two different constrained Positive Matrix Factorization (PMF, Paatero and Tapper, 1994) models were applied to the PM_{10} and PM_1 data matrices separately. In the case of PM_{10} the Multilinear Engine (ME-2) (Paatero, 1999) open script was applied with the opportune modifications (see below), whereas for the PM_1 data matrix the EPA PMF v5.0 software was chosen, which also implement ME-2 scripting but without access to the script. The differences between the two programmes are subtle.

Advantages of the ME-2 open script:

- Uncomplete datasets can be handled, without values imposition or case deletion.
- It is easier to implement constraints on G by means of loops, whereas for the EPA PMF each constraint needs to be imposed separately
- A species concentration in factor profiles can be easily incorporated, whereas species conentrations must be normalized in the EPA model, thus needing the total variable (PMx)

Advantages of the EPA PMF v5.0:

- It is more user friendly than the ME-2 open script, thus less time consuming
- It provides more methods to evaluate output errors: the Displacement (DISP) and Boostrapping Displacement (BS-DISP) techniques.

The displacement technique explicitly explores the rotational ambiguity in a PMF solution by assessing the largest range of source profile values without an appreciable increase in the Q-value, while bootstrapping (BS) is used to detect and estimate disproportionate effects of a small set of observations on the solution and also, to a lesser extent, effects of rotational ambiguity (EPA PMF 5.0 user guide).

2.5.2.2.1 Particularities of the PMF PM_1 source apportionment

A total of 107 samples (53 at the RS site, 54 at the UB site) were collected for the PM1 fraction, and each sample analysed for a total of 62 species (27 inorganic and 35 organic). The EPA PMF v5 model was run on the total data matrix and the variables Sn, Ba and Cl were marked as weak. Also, unrealistic differences between RS_{site} and UB_{site} for one of the industrial sources were minimized. A seed value of 23 was used with 20 runs. Rotational ambiguity was reduced by means of the implementations of the aforementioned and additional constraints in the chemical profiles (see Results section) and evaluated through bootstrapping. Fpeak rotations were not explored due to the fact that constraints already allow exploring matrixes rotations. An additional 7% uncertainty to all data was applied. The final number of factors was chosen based on several criteria: Q values, factors profiles and contributions, distribution of scaled residuals and G space plots.

2.5.2.2.2 Particularities of the PMF PM_{10} source apportionment

Regarding the PM10 source apportionment analysis, a total of 221 samples containing 32 different species were included in the PMF which was run by means of the programme-2 open script allowing to introduce a priori information as shown in the Results section A bootstrap technique was used to estimate the uncertainties of factor profiles, based on the EPA PMF v3.0 script. It consisted on three different steps: re-sampling, reweighting and random rotational pulling (Tukey, 1958; Efron and Tibshirani, 1986). A seed value of 7 was used with 20 runs. Rotational ambiguity was reduced by means of the implementations of the constraints and evaluated through bootstrapping. F_{peak} rotations were not explored due to the fact that the script does not implement it, however the implemented constraints already allow to explore matrixes rotations. The final number of factors was chosen based on several criteria: Q values, factors profiles and contributions, distribution of scaled residuals and G space plots.

2.5.2.3 African dust and sea salt concentrations to the PM_{10} fraction

The PMF model has been applied to a wide variety of areas with positive results. However, this statistical tool is usually unable to differentiate between natural and anthropogenic sources contributing to the same factor. This was the case for mineral dust in the PM_{10} fraction, as Saharan dust outbreaks impact regularly southern European countries, adding to the mineral load. In order to differentiate two distinct sources, other estimation methods have been developed. The methodology proposed by Escudero et al. (2007) for estimating the Saharan dust daily contribution for different mass fractions consists in subtracting to the average concentrations registered at the city (Barcelona) those measured at the nearest regional background site (Montseny, 720 m.a.s.l., 50 km NE of Barcelona). However, the Saharan dust loadings exceeded in some cases the concentrations registered at the SAPUSS sites, thus indicating the different impact of Saharan dust on the city and its surrounding area given the higher altitude of the rural reference site (Escudero et al., 2007). Therefore, a different methodology was applied for subtracting the Saharan dust load from the mineral factor. Thus, we calculated the in situ baseline of mineral dust levels at each site during the Saharan intrusions, taking into account the concentrations registered before and after the episodes, and extracted these from the mineral dust load for each sample at each site. The resulting concentration exceedance of mineral dust was interpreted as the Saharan dust contribution.

In the case of marine aerosols, sea salt can be internally mixed with other sources, such as sulphate (Waked et al., 2014). However, the primary natural sea salt can be extracted from this source by stoichiometrically calculating its contribution to the marine aerosols, as described in section 2.5.2.1.

2.5.3 Complementary methods

Several tools were used to complement the data analysis on aerosol pollutants and sources, by using statistical tools (Openair) and air mass back trajectories. This helped identify the main pollution sources and their possible origin/location as well as complementing the meteorological data analysis.

2.5.3.1 Openair

The statistical data management has been done with the OPENAIR package of R, providing with many useful graphs and figures of the meteorological and pollutant data (Carslaw and Ropkins 2012).

One of the most interesting functions is *polarPlot*, which plots pollutants concentrations and wind speed and direction simultaneously, helping to identify their sources and intensity. These plots represent the concentration (in our case of certain PMF factors extracted from PM_{10} and PM_1 filters) depending on the wind direction and speed. Note that for the sites located in the city (RS_{site}, UB_{site} and TM_{site}) the wind data used is that measured at the Faculty of Physics as it is representative of the city conditions. The wind components applied to the TC_{site} site are those measured at TC_g.

2.5.3.2 Air mass back trajectories during the SAPUSS campaign

To complete the study the back trajectories of the air masses arriving to Barcelona were calculated for each day of the duration of the campaign, depicting the path taken by the air masses over the previous five days. The back trajectories were run using the online HYSPLIT model developed by the National Oceanic and Atmospheric Administration (NOAA) (Draxler and Rolph, 2003). The classification into different air mass types was made also taking into account local meteorlogical conditions at the five sampling sites. Five air mass scenarios were found: Regional (REG), Atlantic (ATL), North African West (NAF_W), North African East (NAF_E) and European (EUR), as seen in Figure 2.15. Days with multiple air mass type within the same day were classified as transition.

The typical REG meteorological situation is shown in Figure 2.13. This type was characterized by a continental polar air mass, occurring for a total of 9 days (most frequent scenario during SAPUSS campaign). Three distinct episodes were found: 20–21 September, 29 September–1 October and 14–17 October. These air masses are typical of the summer months in the WMB, characterized by high temperatures and insolation (Millan et al., 1997). On a synoptic level, these scenarios were dominated by the Azores anticyclone, with the formation of thermal lows developing over the Iberian Peninsula (IP) along with strong land–sea breezes over the coasts (Millan et al., 2000).

These regional episodes are characterized by a lack of a significant synoptic air mass advection, leading to recirculation episodes and the accumulation of pollutants, consequently showing lower wind speeds (Dall'Osto et al., 2013a).

The ATL scenario (marine polar air mass type) occurred for a total of 7 days, being the second most frequent regime. Three distinct episodes were found: 25–28 September, 5 October and 18–19 October. This scenario is characterized by intense air mass advections from the Atlantic ocean, associated with cold fronts crossing the IP. Meteorological values for this air mass type showed the driest conditions recorded during the study associated with the coldest temperatures, sunny days and strong northerly winds (Dall'Osto et al., 2013a).

The EUR air mass is originated in Eastern Europe (continental polar air mass type), reaching the IP after having crossed all Europe and lasting for 2 days (11^{th}-13^{th} October). This air mass transported pollutants from mainland Europe to the sampling sites, although in this case being associated with rainy weather enhanced pollutants scavenging in the Barcelona area. Therefore, it was associated with low solar radiation, strong winds and high relative humidity (Dall'Osto et al., 2013a).

The NAF (North African) air masses are originated in the North African Saharan desert, being a continental/ marine tropical air mass type. A total of three events (six days in total) were identified under this regime. The advection of southerly air masses was associated with high temperature (Dall'Osto et al., 2013a), as well as resuspended dust from the the Saharan desert (Escudero et al., 2005). Escudero et al. (2005) found foure different meterological situations which originated the transport of African air masses towards the WMB: (1) a North African high located at surface levels (NAH-S), (2) an Atlantic depression (AD) located in front of Portugal, (3) a North African depression (NAD), and (4) a North African high located at upper atmospheric levels (NAH-A). During the SAPUSS campaign, two different NAF regimes: NAF_E and NAF_W depending on the origin and path described by the air masses before reaching the WMB (see Figure 2.15). While the NAF_W an air mass trajectory originated in the tropical Atlantic Ocean and arrived from the south-west to Barcelona (NAF_W), the

NAF_E has its origin in the Saharan region and arrived at Barcelona from the easterly wind sector (Figure 2.15).

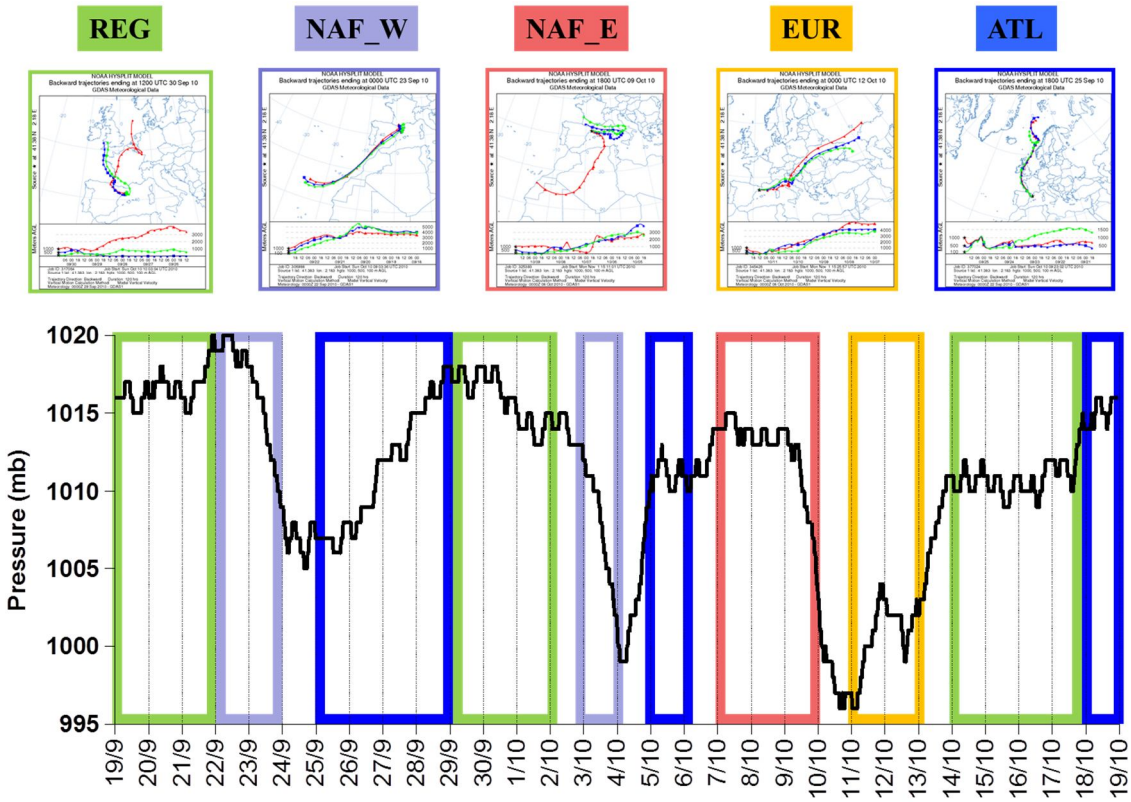

Figure 2.15: Atmospheric pressure and air mass origins during SAPUSS (adapted from Dall'Osto et al., 2013a).

Chapter 3

Results

3. Results

The results of this thesis are presented in four main sections, showing main outputs from research carried out from UFP to coarse particles measured and sampled in the study areas. The first two sections analyse the sources and processes affecting UFP in the Mediterranean urban environment of Barcelona during the intensive SAPUSS campaign (section 3.1) and more generally in developed cities under high insolation (section 3.2). The following two sections investigate the source apportionment of both PM_1 and PM_{10} fractions (section 3.3 and 3.4, respectively) during the SAPUSS campaign at multiple sites in the urban environment.

3.1 Aerosol size distributions over the area of Barcelona during SAPUSS

The Barcelona area presents a complex mixture of sources and processes affecting UFP. It is highly populated (population density 15810 people km^{-2}, Idescat 2014), shows a high density of vehicles (5800 vehicles km^{-2}, DGT 2015) and a compact urban structure, thus causing the accumulation of anthropogenic pollutants emissions and hampering their dispersion. Moreover, the geographical constraints and the sea-breeze circulation condition the evolution of pollutants over the study area.

Within urban environments, the main emission source is road traffic due to tailpipe emissions (Pey et al., 2009; Kumar et al., 2014). Vehicle exhausts emit both primary particles and gaseous pollutants that can lead to semi-volatile organic compounds rapidly converting into aerosols by secondary processes (Charron and Harrison, 2003). In addition to road traffic sources, geographical, climatological and meteorological features of the area under study also influence the variability of particle levels (Zwack et al., 2011). Indeed, in northern European countries, N concentrations are mostly related to traffic emissions (Wegner et al., 2012; Wehner et al., 2002) while in the southern countries, the different climatological conditions (higher solar radiation) enhance photochemical formation (Pey et al., 2009; Reche et al., 2011).

In order to study the sources and processes influencing N concentrations in the study area, four SMPS were simultaneously deployed at four sites during the intensive

SAPUSS campaign: a road side (RS_{site}), an urban background site located in the city (UB_{site}), an urban background located in the nearby hills of the city (Torre Collserola, TC_{site}) and a regional background site located about fifty km from the Barcelona urban areas (RB_{site}). The spatial distribution of sites allows study of the aerosol temporal variability as well as the spatial distribution, progressively moving away from urban aerosol sources.

3.1.1 *K*-means clustering analysis

The *k*-means clustering analysis performed on the SAPUSS SMPS data resulted in nine clusters. Cluster validation indices were used to choose the optimum number of spectra to divide the data as described elsewhere (Beddows et al., 2009; Dall'Osto et al., 2011a). This is solely a statistical optimisation, not accounting for the scientific context in which the data were collected, based on the shape of the spectra. To reduce the possibility that any clusters combined spectra from two different sources or processes, a higher optimum cluster number (in the range 10-20) was selected in the initial analysis. Having studied the cluster within a scientific context, common clusters were recombined (Dall'Osto et al., 2011a) and for our dataset this procedure resulted in a nine cluster solution. The results herein presented summarise all the particle size distributions acquired during SAPUSS at the four monitoring sites (Figure 3.1.1). The size distributions reported in Figure 3.1.1 are extrapolated to the largest size depending on the site, given the good agreement shown between the harmonized (resulting from the k-means clustering analysis) and the raw spectra.

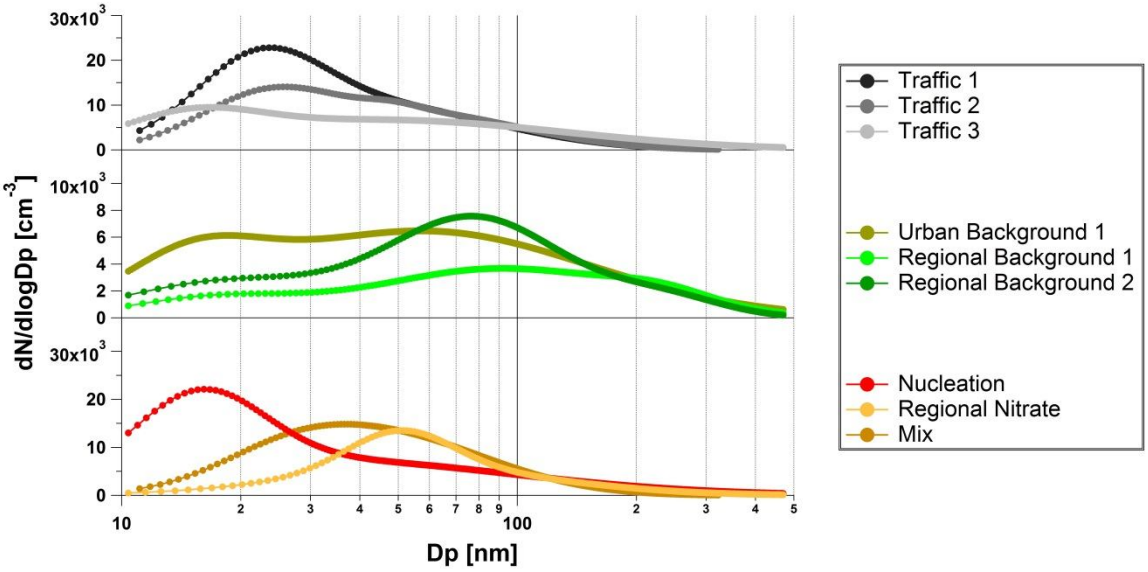

Figure 3.1.1: Aerosol size resolved distributions of the nine clusters result of the *k*-means analysis performed on the SMPS data at all SAPUSS monitoring sites.

The nine clusters show a very different frequency among the four different monitoring sites (Table 3.1.1). This is expected due to the different aerosol sources affecting each site.

Table 3.1.1: Overall occurrence (%) of each cluster and classified into different scenarios as well as in each site (RS_{site}, UB_{site}, TC_{site} and RB_{site}).

Type	Time (%)	*k*-means cluster	Road Site (RS_{site})	Urban Back. (UB_{site})	Torre Collserola (TC_{site})	Regional Background (RB_{site})
Traffic: 30%	8%	*Traffic 1* (T_{clus_1})	24%	1%	5%	2%
	13%	*Traffic 2* (T_{clus_2})	47%	1%	3%	1%
	9%	*Traffic 3* (T_{clus_3})	1%	22%	14%	0%
Background Pollution: 54%	21%	*Urban Back. 1* (UB_{clus_1})	15%	28%	26%	14%
	15%	*Reg. Back. 1* (RB_{clus_1})	0%	19%	18%	22%
	18%	*Reg. Back. 2* (RB_{clus_2})	3%	17%	15%	39%
Special Case: 16%	5%	*Nucleation* (NU_{clus})	1%	11%	6%	1%
	6%	*Reg. Nitrate* (NIT_{clus})	2%	1%	7%	14%
	5%	*Mix* (MIX_{clus})	7%	0%	6%	7%

Such a complex scenario can be broadly summarized in three main aerosol categories:

- Three of the clusters are associated with "Traffic" (T_{clus_1}, T_{clus_2} and T_{clus_3}) and prevailed during 30% of all measured hours. Within the Traffic category, the differences between clusters are due to the proximity to the traffic source and to the atmospheric processes affecting aerosols after emission, such as evaporation (Dall'Osto et al., 2011b; Harrison et al., 2012). As expected, the RS_{site} is the most affected by traffic emission as it is located close to traffic sources (Table 3.1.1). Indeed, T_{clus_1} and T_{clus_2} clusters are almost exclusive to the RS_{site} and account for 24% and 47% of the hours measured at this site, respectively (Table 3.1.1). In contrast, T_{clus_3} is associated with the urban background stations of UB_{site} (22%) and TC_{site} (14%) which are more distant from traffic sources. As expected, the regional RB_{site} is not characterised by primary traffic size distributions.

- Three clusters referred to the "Background Pollution" category (UB_{clus_1} - Urban Background 1, RB_{clus_1} - Regional Background 1 and RB_{clus_2} - Regional Background 2) characterised the overall aerosol population for 54% of the sampling time. They were predominantly found at the background sites of UB_{site}, TC_{site} and RB_{site}. Cluster UB_{clus_1} was found at all four sites and had very dynamic characteristics. It was found more frequently at the UB_{site} and the TC_{site} (around 25% of hours at each site) in contrast to the 15% of hours registered at both RS_{site} and RB_{site} (Table 3.1.1). On the other hand, clusters describing a Regional Background pollution environment (RB_{clus_1} and RB_{clus_2}) were found more commonly at the SAPUSS monitoring sites not affected by anthropogenic sources. This is the case of the RB_{clus_1} cluster, seen at the RB_{site}, UB_{site} and TC_{site} for 22%, 19%, and 18% of the time, respectively. RB_{clus_2} was also found frequently at the RB_{site} (39%), followed by UB_{site} (17%) and TC_{site} (15%).

- Three clusters (Nucleation - NU_{clus}, Regional Nitrate - NIT_{clus} and Mix - MIX_{clus}) associated with "Special Cases" accounted for the remaining 16% of the aerosol size distribution overall population. The NU cluster was seen primarily at the

urban background stations and rarely at the RS_{site} or the RB_{site}. The NIT cluster occurred mostly at the RB_{site} while the MIX cluster (the least characterised among all) was observed in almost the same proportion at all sites except for the UB_{site} (Table 3.1.1).

Figure 3.1.1 shows the particle size distribution for each of the nine clusters. In order to support the interpretation of this figure, the log-normal fitting modes of each cluster and their modal diameters and mode area percentages are presented in Figure 3.1.2 and Table 3.1.2, respectively.

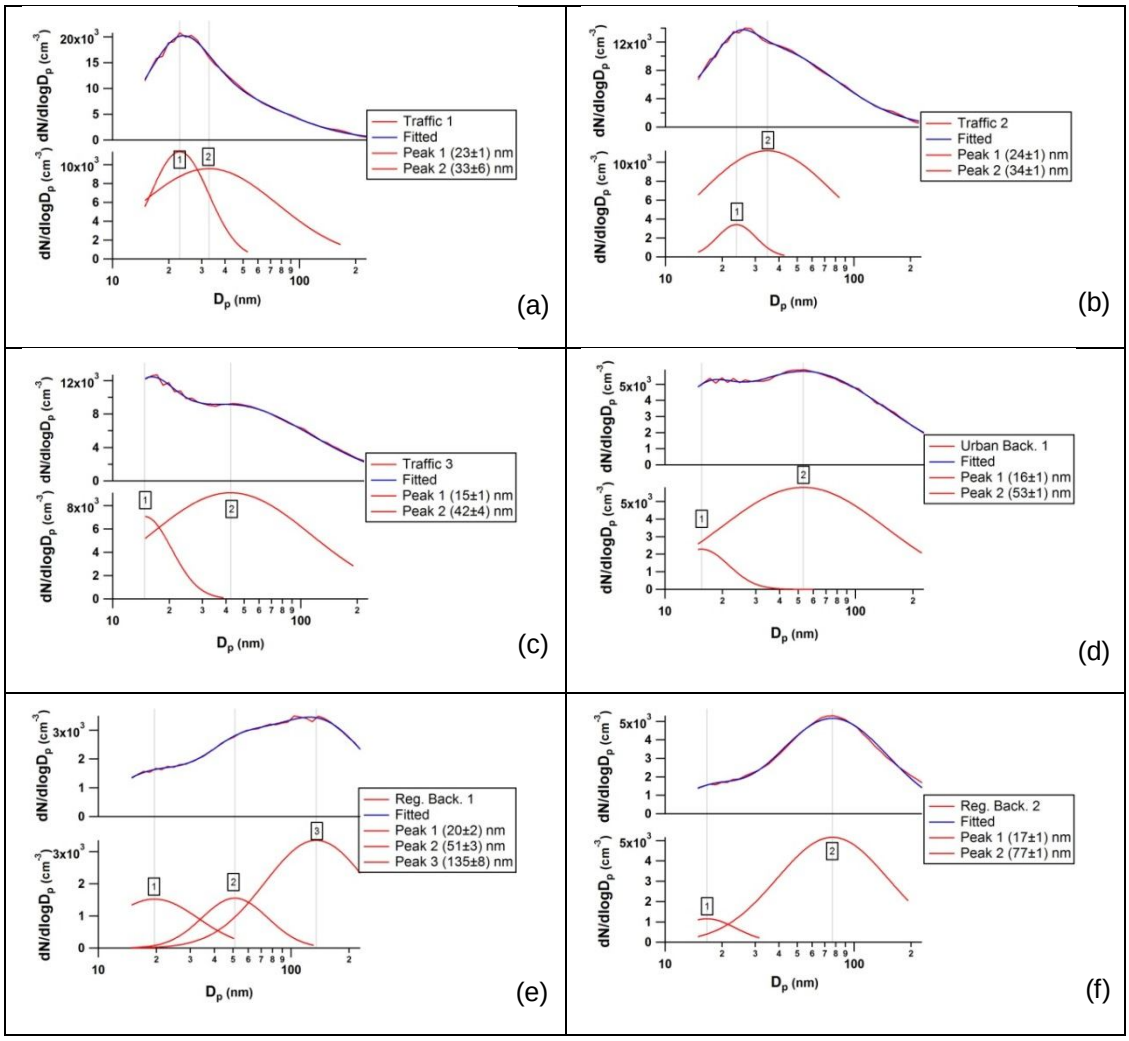

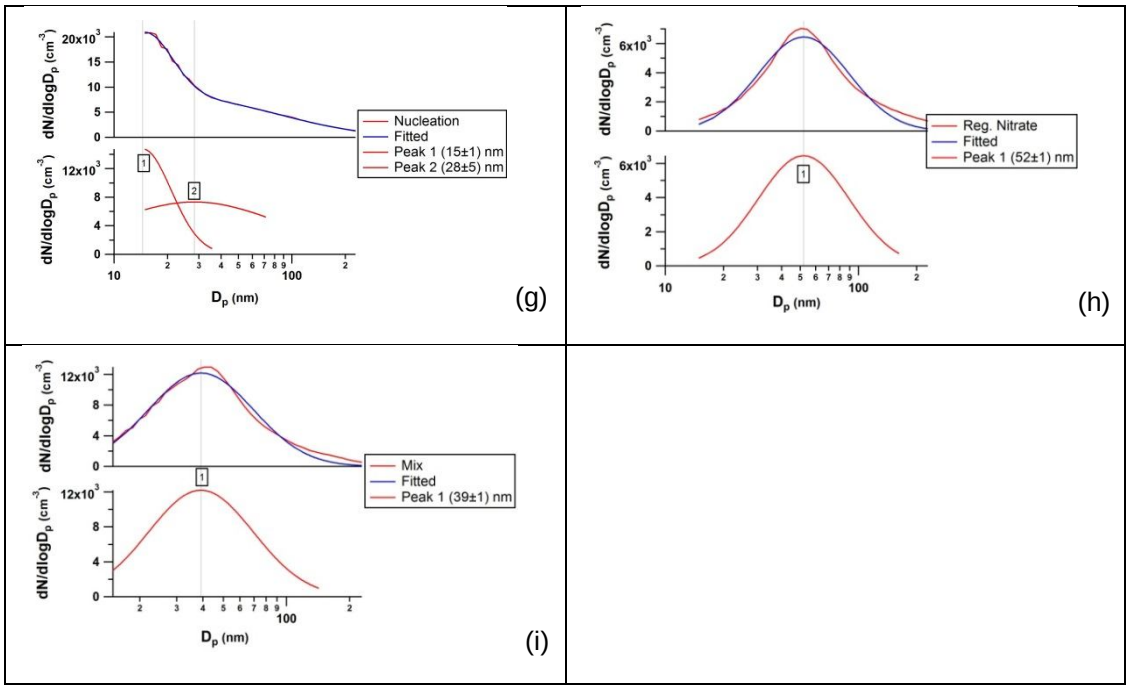

Figure 3.1.2: Log normal fitting curves and the peak values for each cluster: a) Traffic 1, b) Traffic 2, c) Traffic 3, d) Urban Background 1, e) Regional Background 1, f) Regional Background 2, g) Nucleation, h) Regional Nitrate, i) Mix.

Table 3.1.2: Summary of the lognormal fitting of the 9 clusters separated into the nucleation, Aitken and accumulation modes. Peak maximum values were found between 14-24 nm for the nucleation mode, 33-77 nm for the Aitken mode and particles larger than 100 nm correspond to the accumulation mode. The total area percentage for each peak is also indicated.

Type	*k*-means cluster	nucleation	Aitken	accumulation
Traffic	*Traffic 1*	23±1 nm (21%)	33±6 nm (79%)	-
	Traffic 2	24±1 nm (4%)	34±1 nm (96%)	-
	Traffic 3	15±1 nm (6%)	42±4 nm (94%)	-
Background Pollution	*Urban Background 1*	16±1 nm (2%)	53±1 nm (98%)	-
	Regional Background 1	20±2 nm (4%)	51±3 nm (9%)	135±8 nm (87%)
	Regional Background 2	17±1 nm (2%)	77±1 nm (98%)	-
Special Case	*Nucleation*	15±1 nm (16%)	28±5 nm (84%)	-
	Regional Nitrate	-	52±1 nm (100%)	-
	Mix	-	39±1 nm (100%)	-

Furthermore, Table 3.1.3 shows the dominant air mass for each cluster presented. This is achieved following the procedure described in Dall'Osto et al. (2013a), classifying the air mass origin of each day of the campaign as: Atlantic (ATL), European-Mediterranean (EUR), North African East (NAF_E), North African West (NAF_W) or Regional (REG), as explained in the Methodology section.

Table 3.1.3: Air mass origin dominating at each cluster (average percentage values). The air mass types are: Atlantic (ATL), Regional (REG), North African West (NAF W), North African East (NAF E) and European (EUR).

Type	*k*-means cluster	Dominant air mass
Traffic	*Traffic 1*	56% REG
	Traffic 2	39% REG
	Traffic 3	40% ATL
Background Pollution	*Urban Background 1*	35% REG
	Regional Background 1	57% REG
	Regional Background 2	49% NAF E
Special Case	*Nucleation*	78% ATL
	Regional Nitrate	50% REG
	Mix	63% ATL

Additionally, the average values of air pollutants and meteorological parameters for each cluster at each site can be found in Table 3.1.4, and the diurnal trends are shown in Figure 3.1.3.

Table 3.1.4: Average values for each of the nine SMPS clusters at each site with relevant occurrence (more than 30 counts) of air pollutants and meteorological parameters. In bold text are the relevant values for each cluster at the different sites.

Cluster name	Sites	$N_{15\text{-}30nm}$ (cm^{-3})	$N_{30\text{-}228nm}$ (cm^{-3})	$N_{15\text{-}228nm}$ (cm^{-3})	$N_{5(7)\text{-}1000nm}$ (cm^{-3})	NO ($\mu g\ m^{-3}$)	NO_2 ($\mu g\ m^{-3}$)	NO_x ($\mu g\ m^{-3}$)	O_3 ($\mu g\ m^{-3}$)	SO_2 ($\mu g\ m^{-3}$)	CO ($mg\ m^{-3}$)	BC ($\mu g\ m^{-3}$)	PM_{10} ($\mu g\ m^{-3}$)	$PM_{2.5}$ ($\mu g\ m^{-3}$)	PM_1 ($\mu g\ m^{-3}$)	T (°C)	RH (%)	SR ($W\ m^{-2}$)	WS ($m\ s^{-1}$)
Traffic 1	RS	**$2.1{\cdot}10^3$**	$2.4{\cdot}10^3$	$4.5{\cdot}10^3$	**$1.5{\cdot}10^4$**	**9±7**	**39±15**	52±22	44±20	3±2	0.4±0.2	**3.3±1.4**	**34±15**	18±9	16±8	20±4	54±16	68±60	0.7±1.6
Traffic 2	RS	$1.3{\cdot}10^3$	$2.1{\cdot}10^3$	$3.4{\cdot}10^3$	$1.4{\cdot}10^4$	**8±8**	**39±18**	51±28	42±20	3.4±2.5	0.4±0.2	**3.3±1.7**	**35±17**	20±8	17±7	21±3	**67±11**	69±66	0.6±0.6
Traffic 3	UB	$2.1{\cdot}10^3$	$3.7{\cdot}10^3$	$5.8{\cdot}10^3$	$1.6{\cdot}10^4$	**8±13**	**41±24**	54±41	50±27	1.6±1.7	0.4±0.2	2.4±1.7	25±8	15±5	12±3	19±4	67±16	171± 237	1.6±1
	TC	$1.0{\cdot}10^3$	$1.7{\cdot}10^3$	$2.7{\cdot}10^3$	$5.6{\cdot}10^3$	2±2	**19±10**	22±12	67±15	1.2±0.7	0.3±0.1	0.8±0.5	20±9	14±6	9±5	18±3	74±14	223±223	4±2
Urban Background 1	RS	$5.3{\cdot}10^2$	$1.4{\cdot}10^3$	$1.9{\cdot}10^3$	$8.2{\cdot}10^3$	4±4	25±15	31±19	52±20	2.6±1.5	0.3±0.1	2.0±1.2	**32±11**	22±7	**20±7**	20±3	74±10	50±51	1.3±1.1
	UB	$1.0{\cdot}10^3$	$2.6{\cdot}10^3$	$3.6{\cdot}10^3$	$1.0{\cdot}10^4$	4±4	**30±16**	35±20	57±23	1.3±0.7	0.3±0.1	1.6±1.2	29±11	19±9	14±5	18±4	68±15	140±200	2.6±1.7
	TC	$6.7{\cdot}10^2$	$1.7{\cdot}10^3$	$2.4{\cdot}10^3$	$4.7{\cdot}10^3$	2±2	**20±15**	22±17	68±16	1.4±1.4	0.3±0.1	0.8±0.5	25±11	18±7	13±6	17±3	78±11	160±200	4±3
	RB	$5.0{\cdot}10^2$	$1.5{\cdot}10^3$	$2.0{\cdot}10^3$	-	1.0±0.2	4±3	5±3	75±16	0.5±0.9	0.2±0.0	-	23±9	12±3	12±4	14±4	76±18	176±223	0.7±0.7
Regional Background 1	UB	$4.0{\cdot}10^2$	$1.6{\cdot}10^3$	$2.0{\cdot}10^3$	$5.9{\cdot}10^3$	2±3	17±10	20±14	60±18	1.0±0.0	0.3±0.1	1.2±0.6	**34±12**	**25±9**	**18±5**	15±3	71±14	125±210	**3.8±2.2**
	TC	$2.0{\cdot}10^2$	$1.0{\cdot}10^3$	$1.2{\cdot}10^3$	$2.5{\cdot}10^3$	1.1±0.5	9±6	10±6	76±15	1.1±0.2	0.3±0.0	0.5±0.2	**29±11**	**21±7**	**16±7**	15±3	84±8	50±100	**5±3**
	RB	$2.7{\cdot}10^2$	$2.0{\cdot}10^3$	$2.7{\cdot}10^3$	-	1.0±0.1	4±3	6±3	62±19	0.5±0.2	0.2±0.0	-	**27±10**	**14±4**	**15±5**	12±4	85±8	140±207	**0.8±0.8**
Regional Background 2	UB	$5.8{\cdot}10^2$	$2.9{\cdot}10^3$	$3.5{\cdot}10^3$	$7.2{\cdot}10^3$	1.6±1.4	15±8	17±10	64±18	1.2±0.7	0.3±0.1	0.6±0.3	24±11	16±7	12±3	18±5	75±20	87±167	2.8±1.7
	TC	$3.3{\cdot}10^2$	$1.7{\cdot}10^3$	$2.0{\cdot}10^3$	$4.2{\cdot}10^3$	1.2±0.9	13±12	15±12	79±18	3±4	0.3±0.1	0.7±0.5	21±9	15±5	11±5	17±2	81±9	88±172	4.2±2.6
	RB	$2.5{\cdot}10^2$	$1.9{\cdot}10^3$	$2.2{\cdot}10^3$	-	1.0±0.2	4±3	5±3	66±17	0.4±0.5	0.2±0.0	-	23±11	12±4	11±5	15±3	82±15	105±182	0.5±0.6
Nucleation	UB	**$2.4{\cdot}10^3$**	$2.0{\cdot}10^3$	$4.4{\cdot}10^3$	**$1.5{\cdot}10^4$**	2.4±1.8	23±15	27±16	**64±18**	1.0±0.2	0.3±0.1	-	23±5	10±2	9±1	20±2	47±13	**233±273**	2.6±1.6
	TC	**$2.1{\cdot}10^3$**	$1.7{\cdot}10^3$	$3.8{\cdot}10^3$	**$1.1{\cdot}10^4$**	1.5±0.8	14±7	16±8	**75±13**	1.2±0.6	0.2±0.1	0.7±0.4	16±3	11±2	7±2	19±3	63±16	**365±285**	3.5±1.4
Regional Nitrate	TC	$2.9{\cdot}10^2$	$2.2{\cdot}10^3$	$2.5{\cdot}10^3$	$5.1{\cdot}10^3$	1.0±0.0	12±11	14±11	86±17	**5±6**	0.2±0.0	0.4±0.3	15±11	10±4	7±2	16±1	72±13	23±79	5±3
	RB	$2.9{\cdot}10^2$	$1.7{\cdot}10^3$	$2.0{\cdot}10^3$	-	1.0±0.0	2±1	4±1	60±22	**0.5±0.3**	0.2±0.0	-	11±5	7±2	6±2	12±4	81±19	77±149	0.5±0.7
Mix	RS	$8.7{\cdot}10^2$	$2.0{\cdot}10^3$	$2.9{\cdot}10^3$	**$1.3{\cdot}10^4$**	**10±13**	**45±20**	60±40	37±20	**5±3**	0.4±0.2	**3±2**	26±10	15±4	14±4	20±2	66±9	56±83	0.2±0.1
	TC	$1.0{\cdot}10^3$	$2.8{\cdot}10^3$	$3.8{\cdot}10^3$	$8.0{\cdot}10^3$	1.2±0.6	14±11	16±12	78±18	2±2	0.2±0.0	0.5±0.3	14±3	9±1	5±1	17±3	61±14	107±153	3.8±1.5
	RB	$3.9{\cdot}10^2$	$1.3{\cdot}10^3$	$1.7{\cdot}10^3$	-	1.0±0.0	3±2	4±2	63±11	0.3±0.3	0.1±0.0	-	9±4	6±1	5±1	13±4	74±17	91±159	0.6±0.9

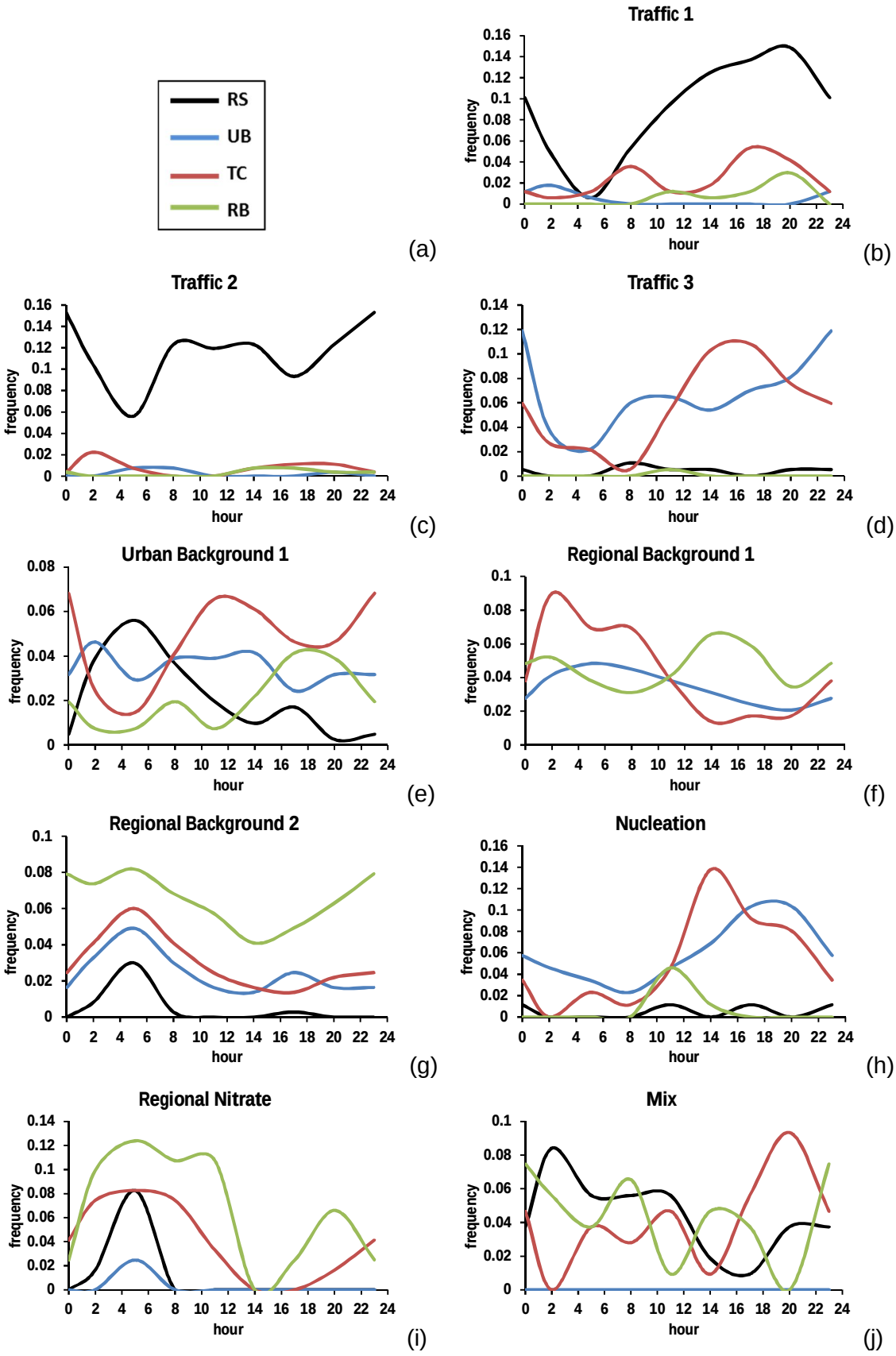

Figure 3.1.3: Daily trends for each k-means cluster at the 4 sites (RS_{site}, UB_{site}, TC_{site} and RB_{site}) a) legend, b) Traffic 1, c) Traffic 2, d) Traffic 3, e) Urban Background 1, f) Regional Background 1, g) Regional Background 2, h) Nucleation, i) Regional Nitrate and j) Mix.

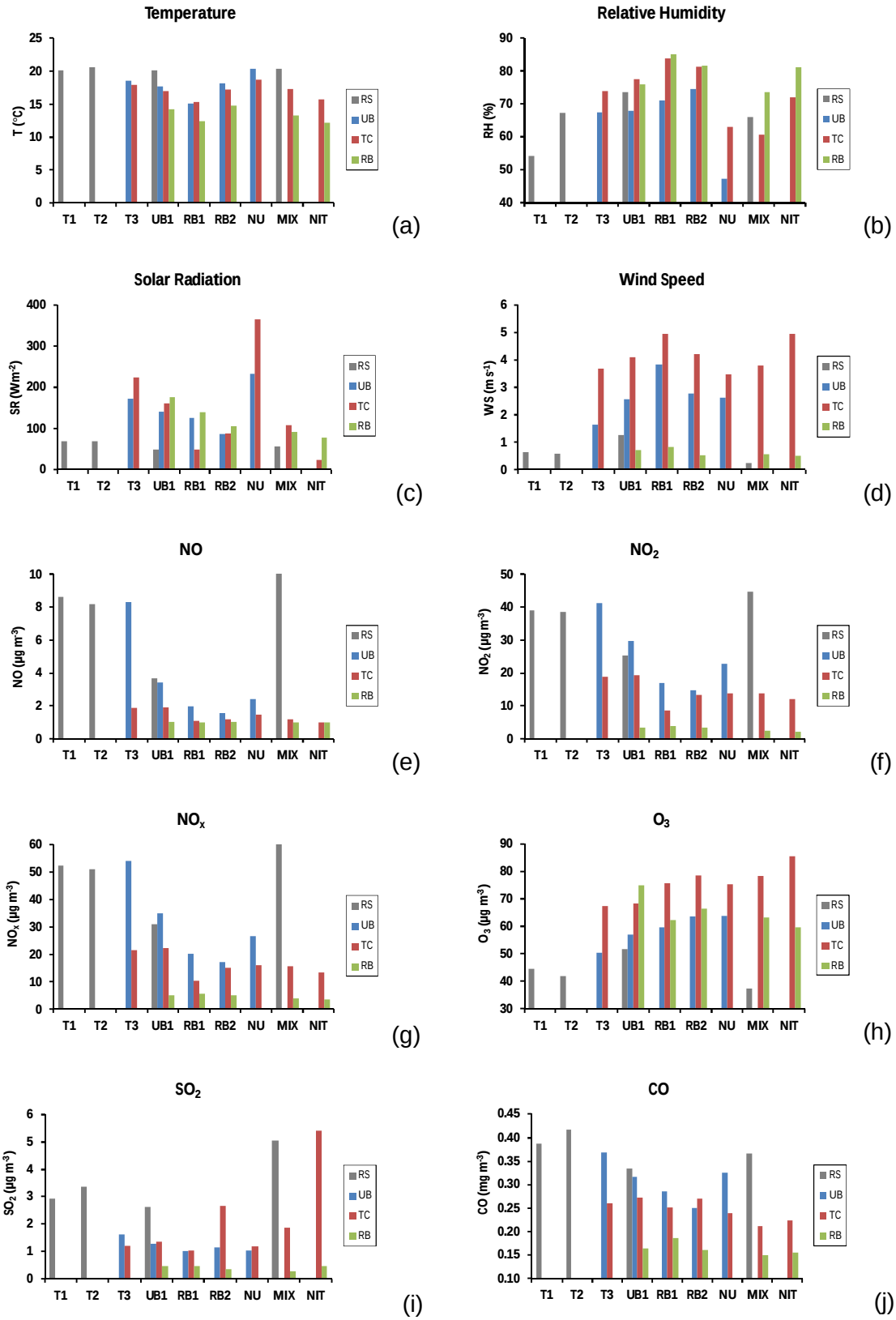

Figure 3.1.4: Comparison of meteorological factors and gaseous pollutants average values for each significant cluster at each site (RS_{site}, UB_{site}, TC_{site}, RB_{site}) : a) temperature, b) relative humidity, c) solar radiation, d) wind speed, e) NO, f) NO_2, g) NO_x, h) O_3, i) SO_2, j) CO.

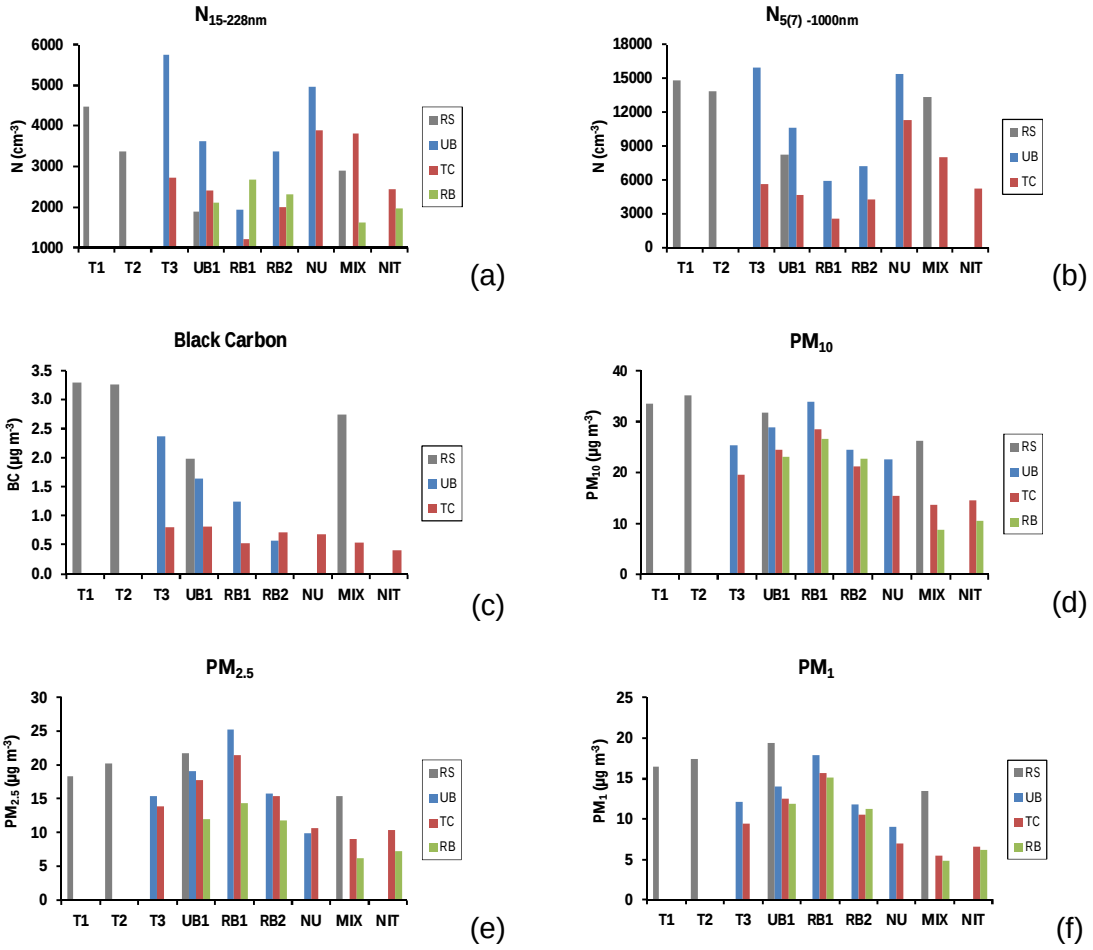

Figure 3.1.5: Comparison for each significant cluster at each site (RS, UB, TC, RB) of: a) particle number concentration measured with the SMPS ($N_{15\text{-}228nm}$), b) particle number concentration measured with the CPC ($N_{5(7)\text{-}1000nm}$), c) black carbon (BC), d) PM_{10}, e) $PM_{2.5}$, f) PM_1.

It should be noted that clusters showing a lower incidence than 30 counts (hours) at any site were not considered. According to the data obtained, each cluster can be described as follows:

3.1.1.1 Traffic related clusters

- T_{clus_1} represents 8% of the total sample and is exclusively observed at the RS_{site} (24%). It presents one of the highest N showing a bimodal size distribution with a well-defined nucleation size mode at 23±1 nm and a broad Aitken mode at 33±6 nm (Figures 3.1.1 and 3.1.2a, Table 3.1.2). It is associated with high concentration levels of traffic pollutants such as BC (3.3±1.4 µg m^{-3}), NO (9±7 µg m^{-3}) and NO_2 (39±15 µg m^{-3}, Figures 3.1.5c, 3.1.4e and f). Regarding particle mass it shows high

PM_{10} concentration values (34±15 µg m^{-3}) and also high N values in the nucleation mode $N_{15\text{-}30nm}$ (2.1 10^3 cm^{-3}), as shown in Table 3.1.4. It also has the lowest relative humidity (54±16 %) of all clusters at the RS_{site} and occurs mainly in the afternoon and early evening (Figure 3.1.3b).

- T_{clus_2} prevails during 13% of the time and is the dominant cluster at the RS_{site} (47%). Like cluster T_{clus_1}, it shows a bimodal particle size distribution peaking at 24±1 nm and 34±1 nm and it has similar concentration values of BC (3.3±1.7 µg m^{-3}), NO (8±8 µg m^{-3}) and NO_2 (39±18 µg m^{-3}). The most important difference between this cluster and the previous traffic cluster (T_{clus_1}) is that this one is associated with higher RH conditions (67±11 % versus 54±16 %). It also contains less particles in the nucleation mode range $N_{15\text{-}30nm}$ ($1.3{\cdot}10^3$ cm^{-3} and $2.1{\cdot}10^3$ cm^{-3}, respectively). This points to an opposite trend between RH and ultrafine particle concentrations, as further discussed in Section 4.1.2. This cluster correlates temporally with the morning rush hour (8 am) and is maintained until the afternoon (2 pm). Its frequency rises again coinciding with the evening rush hour (8 pm) as can be seen in Figure 3.1.3c.

- T_{clus_3} prevails 9% of the time and characterises the traffic environment detected at the urban background stations of UB_{site} (22%) and TC_{site} (14%). Like T_{clus_1} and T_{clus_2}, T_{clus_3} also shows a bimodal distribution with one peak in the nucleation size mode and a second in the Aitken mode, although with different size modes (a much reduced nucleation mode at 15±1 nm and broader Aitken mode at 42±4 nm, respectively, see Table 3.1.2). T_{clus_3} is associated with the highest levels of traffic pollutants at the urban background UB_{site} and TC_{site}, with traffic gaseous average concentrations similar to T_{clus_1} and T_{clus_2} (see Figure 3.1.4e, f and g). However, it presents the lowest N concentrations among the three traffic clusters (Table 3.1.4). Furthermore, T_{clus_3} is related to the predominance of Atlantic air masses. This is in contrast to T_{clus_1} and T_{clus_2} which are found under regional stagnant air mass conditions (see Table 3.1.3). T_{clus_3} occurred mainly during the daylight hours and late evening at UB_{site}, and reaches TC_{site} at midday due to transport by the sea

breeze circulation (Figure 3.1.3d). Further consideration on the difference among the three traffic related clusters is given in Section 4.1.1.

3.1.1.2 Background Pollution clusters

- Urban Background 1 (UB_{clus_1}) is the most prevalent of all clusters (21% of the time) as it has a significant occurrence at all the four monitoring sites (Table 3.1.1). However, it occurs more frequently at the urban background sites (UB_{site} 28% and TC_{site} 26%). Like the traffic clusters, it exhibits a bimodal distribution with a small nucleation size mode (16±1 nm) and a broader Aitken mode (53±1 nm). Nevertheless, it is important to note that the nucleation mode is less pronounced in comparison to the Traffic clusters and N concentrations are lower (Figure 3.1.1, Tables 3.1.2 and 3.1.4). This cluster is also affected by moderate levels of traffic pollutants: e.g. at the RS_{site} the level of NO_2 reached 25±15 μg m^{-3}. This background cluster is prevailing during night time at the RS_{site}, likely representing the cleanest conditions at the road monitoring site. By contrast, at the UB_{site} this cluster does not show a clear diurnal variation, confirming its urban background nature (Figure 3.1.3e). It is interesting to note that this cluster was monitored during the morning in the hilly background environment (TC_{site}) and later on in the afternoon at the regional RB_{site}. This suggests that the urban background pollution (represented by this cluster, hence named after it) can be transported by the sea breeze circulation from the city centre to the regional background (Figure 3.1.3e).

- The Regional Background Pollution 1 (RB_{clus_1}) cluster prevails 15% of the time and is present at all sites except at the RS_{site}. At the RB_{site} it accounts for 22% of the time while at the urban background UB_{site} and TC_{site} represents the 19% and 18%, respectively. This cluster was the only one to have a tri-modal size distribution, with size modes at 20±2 nm, 51±3 nm and 135±8 nm, the accumulation mode being the dominant one (Table 3.1.2). It shows the highest PM concentrations of all clusters for UB_{site}, TC_{site} and RB_{site} (e.g. at UB_{site} PM_{10} is 34±12 μg m^{-3}, $PM_{2.5}$ is 25±9 μg m^{-3} and PM_1 is 18±5 μg m^{-3}, Table 3.1.4). It is also associated with the highest wind speed values of all clusters at UB_{site} (3.8±2.2 ms^{-1}), TC_{site} (5±3 ms^{-1})

and RB_{site} (0.8±0.8 ms^{-1}). Figure 3.1.3f shows that it prevails during the night in TC_{site}, when the site is less influenced by the urban background. At the UB_{site} it occurs regardless of the hour, suggesting that regional background size distributions can also describe the lowest urban background conditions at the UB_{site}.

- The Regional Background Pollution 2 (RB_{clus_2}) cluster occurs more often at the regional background RB_{site} (39%) and then decreases in occurrence as we come close to the city: TC_{site} (15%) and UB_{site} (17%). It has a small nucleation size mode at 17±1 nm and a dominant Aitken mode at 77±1 nm. Regarding the diurnal trends (Figure 3.1.3g) it can be observed that it is similar at all four sites, peaking at night. The main differences between RB_{clus_1} and RB_{clus_2} clusters is that the first one accounts for aged and long-transport aerosols (highly loading of PM mass, Table 3.1.4) and is dominated by the accumulation mode (Table 3.1.2). By contrast, cluster RB_{clus_2} presents a broad peak in the Aitken mode with higher N and lower mass concentration levels.

3.1.1.3 Minor clusters

- The Nucleation cluster (NU_{clus}) represents only 5% of all observations and occurs mainly at the urban background UB_{site} and TC_{site} (11% and 6% respectively). It has a main nucleation size mode at 15±1 nm and a small Aitken mode at 28±5 nm (Figure 3.1.2g). This cluster prevails under intense solar radiation at both UB_{site} (233±273 Wm^{-2}) and TC_{site} (365±285 Wm^{-2}) as well as relatively high ozone concentrations at UB_{site} (64±18 µg m^{-3}) and TC_{site} (75±13 µg m^{-3}, Table 3.1.4, Figures 3.1.4 and 3.1.5). The high total N concentrations ($1.5 \cdot 10^4$ cm^{-3} at UB_{site} and $1.1 \cdot 10^4$ cm^{-3} at TC_{site}) and the concentration for the nucleation mode $N_{15\text{-}30nm}$ at both UB_{site} ($2.4 \cdot 10^3$ cm^{-3}) and TC_{site} ($2.\ 1 \cdot 10^3$ cm^{-3}) should also be noted. The diurnal trends also confirm that this cluster is associated with photochemical nucleation events peaking during the afternoon and early evening at the UB_{site} (14h-20h) and TC_{site} (12h-15h), respectively (Figure 3.1.3h). This cluster was found to describe well the nucleation events studied in detail by Dall'Osto et al. (2013b). However, it

should be noted that during this study only particles above 15 nm were monitored due to the SMPS configurations. Therefore, the NU_{clus} accounts for the nucleating particles that have grown to such detectable sizes - thus leading to an underestimation of the early stage nucleation processes. It is also of note that the frequency of this NU_{clus} increase in June-August (Dall'Osto et al., 2012) compared to September-October (this study).

- The Regional Nitrate cluster represents 6% of the total, and occurs predominantly at the TC_{site} (7%) and RB_{site} (14%). It exhibits a unimodal aerosol size distribution peaking at 52±1 nm (Figure 3.1.2h). It is found to peak mainly during night time (Figure 3.1.3i). This mode is smaller than a similar *k*-means cluster (cluster regional, 90±12 nm) found in the clustering analysis of Dall'Osto et al. (2012) for the whole year 2004 in the urban area of Barcelona. In this regard, it is interesting to note that the nitrate cluster of this study was found to occur mainly at the TC_{site} and RB_{site}, the two sites that are away from the urban city centre, suggesting different aerosol size distributions for urban background (Dall'Osto et al., 2012) and regional background nitrate (this study). Additionally, SAPUSS measurements were restricted to the autumn season, whereas the previous study included a whole year of measurements (Dall´Osto et al., 2012). It is likely that the larger size mode of the previous study reflects the winter time high nitrate mass loadings not monitored during this intensive SAPUSS field campaign.

- The Mix cluster occurs 6-7% of the time at the RS_{site}, TC_{site} and RB_{site}. It exhibits a unimodal size distribution with a peak in the Aitken mode at 39±1 nm (Table 3.1.2). The temporal trends and the average values of the air quality parameters were not well defined (Figure 3.1.3j, Table 3.1.4), likely due to a mix of sources and atmospheric processes describing this factor. This factor cannot be associated with any specific source and was found to be the least well defined of all the nine clusters. It is associated with high concentrations of traffic-related pollutants (NO, CO and black carbon) and SO_2, but is clearly not heavily influenced by fresh traffic emissions.

3.1.2 SMPS *k*-means clustering results explained by cluster proximity diagram during SAPUSS

The results described in the previous section (3.1.1) are graphically summarised by a Cluster Proximity Diagram (CPD) in Figure 3.1.6.

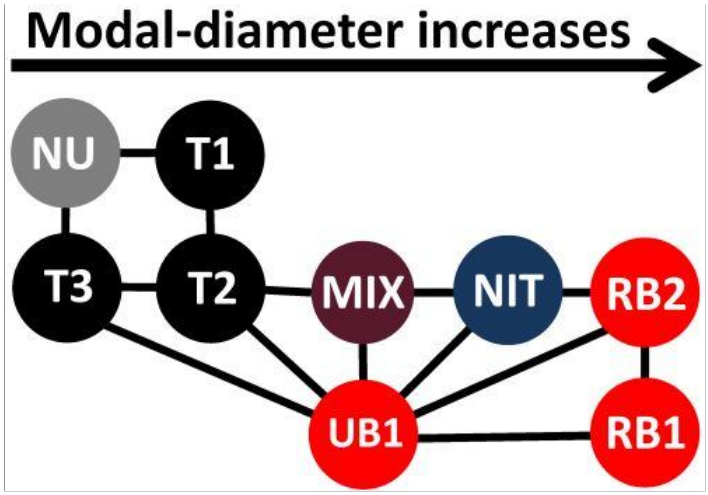

Figure 3.1.6: Cluster Proximity Diagram during SAPUSS. In black are traffic related clusters (T_{clus_1}, T_{clus_2}, T_{clus_3}), in red background clusters (UB_{clus_1}, RB_{clus_1}, RB_{clus_2}) and in grey, purple and blue the special cases (NU_{clus}, MIX_{clus} and NIT_{clus}).

The CPD displays how the clusters are arranged relative to each other based on the similarity of the elements in each cluster measured using the Silhouette Width (Beddows et al., 2009). While *k*-means clustering matches together the most similar spectra into the nine clusters (Figures 3.1.1 and 3.1.3), the CPD positions these clusters according to the degree of similarity within each cluster. The more similar the elements within a selection of clusters are, the closer the nodes representing those clusters are placed to each other in the diagram (e.g. T_{clus_1}, T_{clus_2} and T_{clus_3}). Using the optimum number of clusters (9), the elements of this selection (e.g. T_{clus_1}, T_{clus_2} and T_{clus_3}) are sufficiently similar to each other to be placed next to each other in the diagram but they are not sufficiently similar to form a new cluster. Likewise, pairs of nodes furthest apart in the diagram represent clusters whose elements are the most dissimilar (e.g. NU_{clus} and RB_{clus_1}). In particular, this is illustrated further in Figure 3.1.6 where the average modal diameter of the clusters increases from left to right.

Clusters T_{clus_1} and T_{clus_2} are associated with primary traffic aerosols and are positioned in the same vertical area of the diagram. Cluster NU_{clus} and cluster T_{clus_3} are confined in the smallest modal diameters, in the far left part of the CPD. This is due to the atmospheric sources and the processes affecting cluster NU_{clus} (new particle formation) and cluster T_{clus_3} (evaporation of traffic related particles $T_{clus\_1\text{-}2}$, Dall'Osto et al. (2011b). By contrast, the largest modal diameters detected (right part of CPD, Figure 3.1.6) are associated with regional background clusters (RB_{clus_1} and RB_{clus_2}, same vertical position in the CPD). Cluster MIX_{clus} - not well defined - stands in the middle of the CPD and is likely to be a mixture of all sources and processes. By contrast, NIT_{clus} stands in a position close to the RB clusters. Finally, it is interesting to note that cluster UB1 (which is associated with the urban background pollution) is linked to all but two (NU_{clus} and T_{clus_1}) of the clusters. This suggests that the sources/processes loading clusters T_{clus_3}, T_{clus_2}, MIX_{clus}, NIT_{clus}, RB_{clus_2} and RB_{clus_1} all consequently develop and contribute to urban background aerosol. Clusters T_{clus_1} and NU_{clus} are strong ultrafine aerosol sources which are somehow modified (for example by growth or evaporation) before contributing to the urban background aerosol population.

In summary, the main sources of the smallest UFP detected during SAPUSS are due to new particle formation (NU_{clus}) and the evaporation of traffic-related particles (T_{clus_3}, coming from T_{clus_1} and T_{clus_2}). The lowest N concentrations and the highest modal diameters are related to regional background conditions (RB_{clus_1}, RB_{clus_2}, NIT_{clus}). Finally, all these diverse clusters contribute directly into the urban background general aerosol particle spectra (UB_{clus_1}), which is indeed at the centre of Figure 3.1.6.

3.2 Aerosol size distributions in high insolation developed urban environments

As discussed in the Methodology section, the Mediterranean climate can be found in other worldwide regions in addition to the Mediterranean Basin (Figure 2.1). With the purpose of categorising sources of UFP in urban environments situated in temperate regions affected by high solar radiation levels, long-term aerosol size distributions were sampled in several worldwide cities. As seen in section 3.1, traffic emissions are the main contributors to UFP in urban environments. However, photochemical nucleation events have been detected in urban environments, such as in Barcelona (Pey et al., 2009; Dall'Osto et al., 2012), Madrid (Gómez-Moreno et al., 2011), Huelva (Fernández-Camacho et al., 2010), Marseille and Athens (Petäjä et al., 2007) where the high solar radiation levels registered in the Mediterranean Basin play a key role (Reche et al., 2011). The Mediterranean climate characteristics are also shared in other worldwide areas, where photochemical nucleation events in urban environments have also been reported (Los Angeles: Hudda et al., 2010; Brisbane: Cheung et al., 2010)

Hence, the objective is to study the sources and processes affecting UFP in worldwide developed urban environments under high insolation. Specifically we aim to assess the frequency and influence of nucleation events on UFP levels and variability, as well as the atmospheric conditions facilitating such events in. Therefore, long-term size-resolved particle number concentration measurements were carried out at several cities. The main databases are taken from two cities in Southern Europe (Barcelona and Madrid, Spain) and one in Eastern Australia (Brisbane). To complement the study, two additional datasets from high insolation areas (also located in temperate climatic areas) are analysed: two years of data from a regional background site regularly impacted by the Rome (Italy) pollution plume and three months of data from an urban background site in Los Angeles (USA). The complexity of the data is further reduced by applying *k*-Means clustering analysis to each data set separately (Beddows et al., 2009, 2014; Dall'Osto et al., 2011b, 2012; Sabaliauskas et al., 2013; Salimi et al., 2014). The identification of the main pollution sources contributing to UFP affecting urban environments enables quantitative estimation of the temporal prevalence of each source and a further comparison between the selected cities.

3.2.1 *k*-Means clustering

A *k*-Means clustering analysis was performed on each of the five SMPS data sets, resulting in a number of representative clusters for each city that ranged between 7 and 15. After careful consideration (see section 2.5.1.1), such results were further simplified to 4-7 clusters per monitoring site (see Figures 3.2.1 and 3.2.5). Additionally, the reduction to three more-generic classifications, while not based on statistics, is based on existing knowledge of distributions typically observed and associated with these categories. The uncertainty bands plotted for each cluster (Figures 3.2.1 and 3.2.5) show the 99.9% confidence limits for the hourly size distributions contained within each cluster. This means that with a probability of 99.9%, all hourly spectra contained in each cluster are found within the uncertainty bands. The fact that none of the uncertainty bands of the spectra overlap over the full size range at any of the sites reflects the robust cluster classification achieved by *k*-Means analysis. To further characterise each *k*-Means cluster, its corresponding size peaks were extracted; and hourly, weekly and annual cluster trends were analysed. Moreover, the corresponding average values of meteorological parameters and available air pollutants for each cluster at each site were calculated. The analysis of each cluster characteristics allows its classification into different categories depending on the main pollution source or process contributing to it.

The majority of the clusters were found common to most of the cities, although showing some site specific characteristics depending on the location of the site (proximity to pollution sources), the sampling size range (low-cut 10.2-17.5 nm and upper-cut 101.8-615.3 nm, see Table 2.10) and the particular emission and atmospheric features of each city (see Figures 3.2.1 and 3.2.5). To further simplify the results, the clusters have been carefully divided in three main categories: “Traffic”, “Nucleation” and “Background pollution and Specific cases”. The most relevant categories common to all sites are Traffic and Nucleation, which display very different characteristics. Broadly, Traffic clusters dominate the aerosol size distributions during rush hours, showing very high NO_x levels. In contrast, Nucleation clusters are seen at midday, under high temperature, solar radiation and ozone levels and low NO_x levels. Detailed features of each *k*-Means size distributions can be found in Tables 3.2.1 to

3.2.4 and Figures 3.2.1 and 3.2.5. Finally, it is important to remember that the clustering results can provide a much higher amount of information than that presented here. Nevertheless, the objective of this study is to present main aerosol size distribution categories in order to quantify the impact of photochemical nucleation processes in urban environments under high solar radiation. In order to show averaged annual results only the cities of Barcelona, Madrid and Brisbane were considered for several reasons. In Rome, the sampling site is not located in an urban environment, although it is affected by the Rome pollution plume. The monitoring sites in the cities of Barcelona, Madrid, Brisbane and Los Angeles were classified as urban background, whereas the one in Rome was further away from the city. Regarding Los Angeles only three months of measurements were available, which was not sufficient for studying the annual trends. However, we believe the sites of Rome and Los Angeles add some important supporting information to further validate our findings.

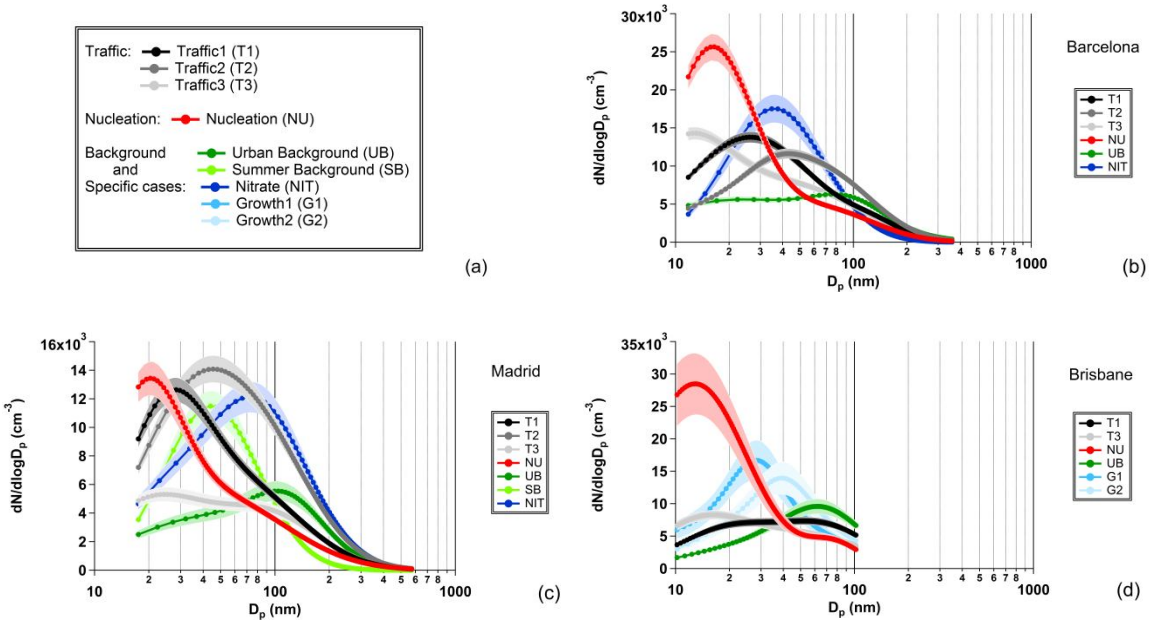

Figure 3.2.1: Aerosol size distribution results of the *k*-Means cluster analysis performed on the SMPS data at the main cities: a) legend, b) Barcelona, c) Madrid and d) Brisbane. Shaded areas around the curves represent the confidence limits μ calculated for 99.9% confidence level. Note the different scales for $dN/dlogD_p$.

Table 3.2.1: Log-normal fitting peaks for each cluster category *k*-Means size distribution at the main sites and the corresponding peak area percentage.

Category	Subcategory	Barcelona	Madrid	Brisbane
Traffic	*Traffic 1 (T1)*	26±1 nm (84%), 130±4 nm (16%)	25±1 nm (31%), 70±6 nm (69%)	21±1 nm (30%), 77±1 nm (70%)
	Traffic 2 (T2)	23±2 nm (31%), 36±1 nm (8%), 75±2 nm (61%)	31±3 nm (30%), 83±9 nm (70%)	-
	Traffic 3 (T3)	11±1 nm (21%), 48±1 nm (79%)	21±1 nm (24%), 92±3 nm (76%)	14±1 nm (18%), 52±4 nm (82%)
Nucleation	*Nucleation (NU)*	16±1 nm (53%), 69±2 nm (47%)	19±1 nm (24%), 48±2 nm (76%)	13±1 nm (74%), 77±1 nm (26%)
Background pollution and Specific case (SC)	*Urban Background (UB)*	22±1 nm (61%), 96±1 nm (39%)	40±1 nm (53%), 119±1 nm (47%)	63±2 nm (100%)
	Summer Background (SB)	-	44±1 nm (100%)	-
	Nitrate (NIT)	36±1 nm (100%)	63±1 nm (100%)	-
	Growth 1 (G1)	-	-	28±1 nm (100%)
	Growth 2 (G2)	-	-	37±1 nm (100%)

Table 3.2.2: Overall occurrence (%) of each cluster at each site, classified into different categories (Traffic, Nucleation and Background pollution and Specific cases).

Category	Subcategory	Barcelona	Madrid	Brisbane	Rome	Los Angeles
Traffic	*Traffic 1 (T1)*	27%	25%	24%	7%	36%
	Traffic 2 (T2)	24%	22%	-	27%	-
	Traffic 3 (T3)	12%	11%	20%	7%	25%
Nucleation	*Nucleation (NU)*	15%	19%	14%	6%	33%
Background pollution and Specific cases	*Urban Background (UB)*	15%	6%	22%	25%	6%
	Summer Background (SB)	-	7%	-	-	-
	Regional Background (RB)	-	-	-	28%	-
	Nitrate (NIT)	7%	10%	-	-	-
	Growth 1 (G1)	-	-	10%	-	-
	Growth 2 (G2)	-	-	10%	-	-
Total		100%	100%	100%	100%	100%

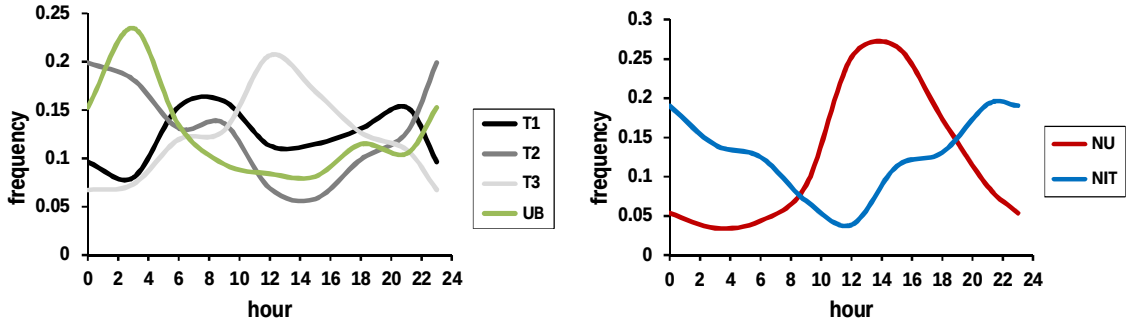

Figure 3.2.3: Diurnal trends for the main clusters: a) Traffic1 (T1), Traffic2 (T2), Traffic3 (T3) and Urban Background (UB); b) Nucleation (NU) and Nitrate (NIT). Although they are extracted from the results for Barcelona, they are representative of the rest of the cities.

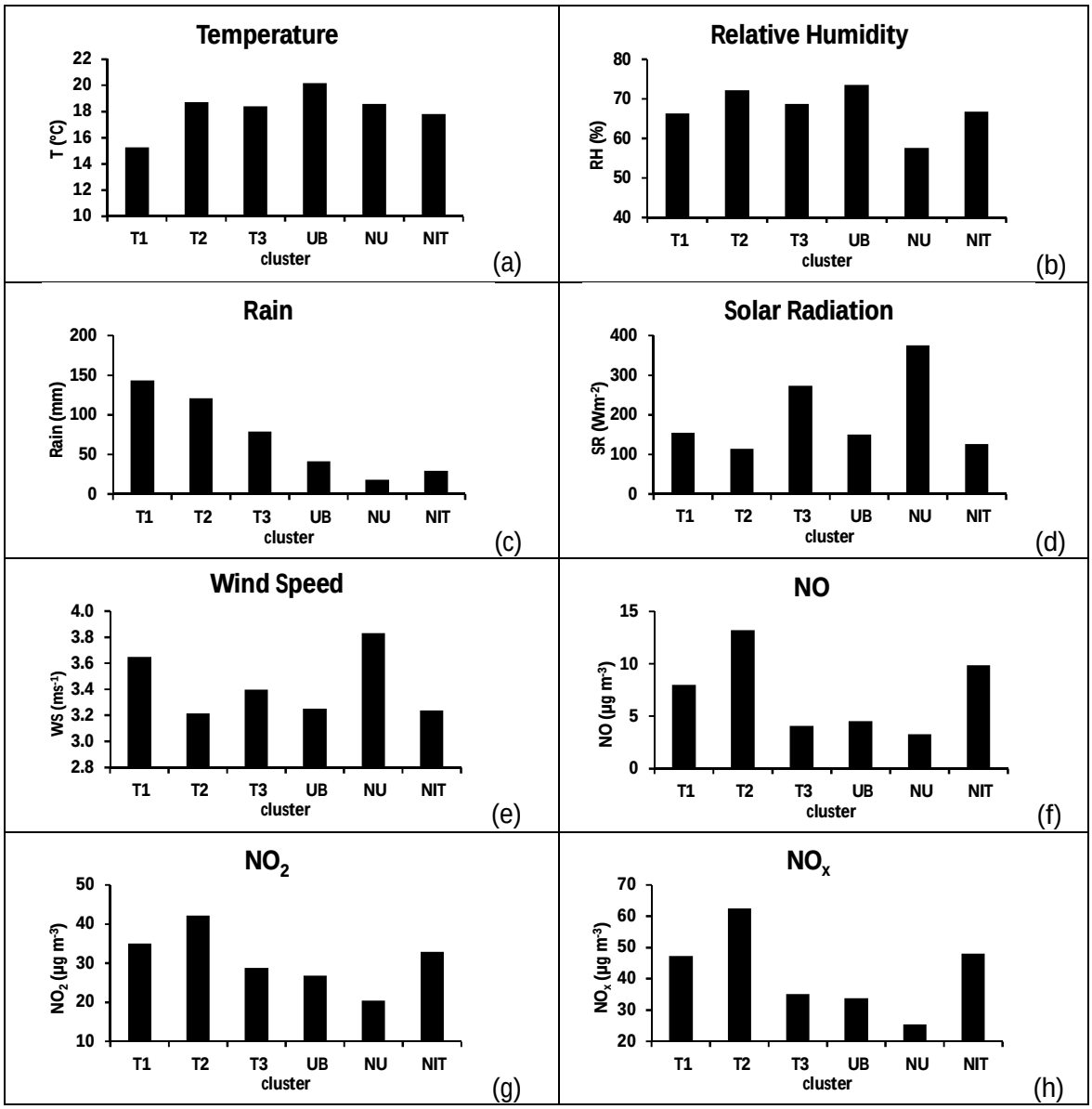

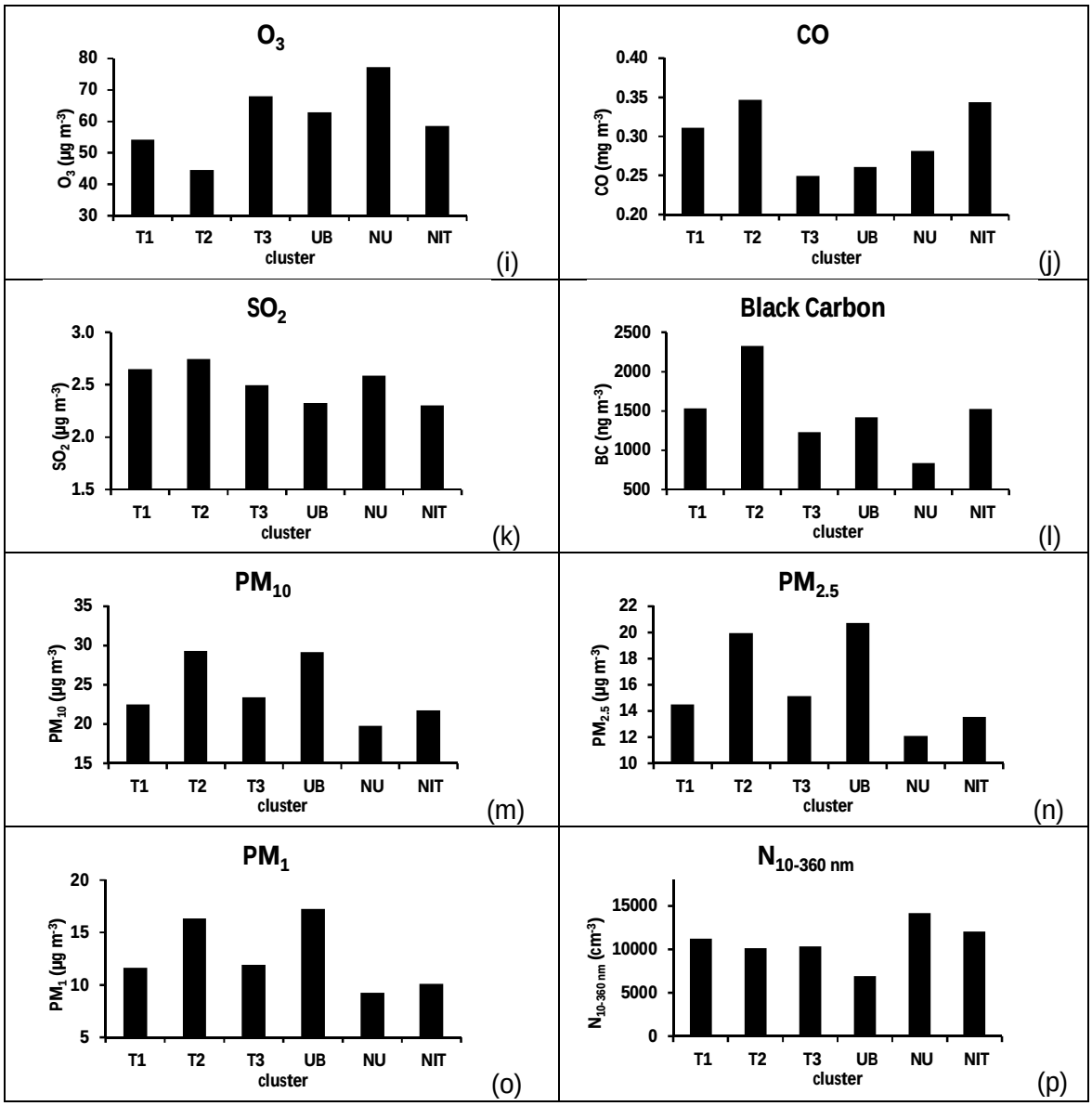

Figure 3.2.4: Meteorological parameters and gaseous pollutants for the main clusters: a) Temperature, b) Relative Humidity, c) Rain, d) Solar Radiation, e) Wind Speed, f) NO, g) NO_2, h) NO_x, i) O_3, j) CO, k) SO_2, l) Black carbon, m) PM_{10}, n) $PM_{2.5}$, o) PM_1, p) $N_{10\text{-}360}$. Although they are extracted from the results for Barcelona, the trend followed by clusters is representative of the rest of the cities.

3.2.1.1 Traffic-related clusters

- Traffic 1 (T1): this cluster can be seen at all monitoring sites, occurring 27-24% of the time (Table 3.2.2). It exhibits a bimodal size distribution, as typically found in vehicle exhausts, with a dominant peak at 20-40 nm (traffic-related nucleated particles) and another at 70-130 nm (soot particles) (see Table 3.2.1). Its diurnal trends are driven by traffic rush hours and display very high levels of traffic pollutants, such as NO, NO_2, BC and CO (see Figures 3.2.3a and 3.2.4).

Regarding particle mass concentrations, T1 is associated with high values of PM_{10} (see Figure 3.2.4). We attribute this cluster to freshly emitted traffic particles.

- Traffic 2 (T2): this cluster is seen in Barcelona and Madrid, occurring 22-24% of the time (Table 3.2.2). It shows a bimodal size distribution with a minor peak at 20-40 nm and a dominant one at 70-90 nm (see Table 3.2.1). It is usually observed during the evening and night, and contains high concentration of traffic pollutants, like T1 (see Figures 3.2.3a and 3.2.4). The main difference with T1 is that it accounts for particles with traffic origin that might have undergone physicochemical processes after being emitted, such as condensation or coagulation and that have resulted in a change of the size distribution with respect to T1. This change can be appreciated for each city in Figure 3.2.1. The evolution of this aerosol size distribution modes attributed to traffic have already been widely discussed in previous studies (Dall'Osto et al., 2011b, 2012).

- Traffic 3 (T3): this traffic-related cluster was found in all the monitored cities 11-20% of the time (see Table 3.2.2). It presents a bimodal size distribution, with a low peak in the nucleation mode at 10-20 nm and a main peak at 50-90 nm (see Table 3.2.1). It occurs throughout all day, with a peak during daytime, and it is associated with the lowest pollution levels of all the Traffic clusters (see Figure 3.2.3a). The shift to smaller sizes of the 20-40 nm peak of T1 and T2 towards the nucleation mode in T3 might indicate particle evaporation in Barcelona, Madrid and Brisbane (see Figure 3.2.1b-d). More information on the evolution of traffic-related cluster T1-T2 towards traffic-related cluster T3 can be found in section 3.1.1, where aerosol size distribution modes simultaneously detected at four monitoring sites during SAPUSS are reported. As recently discussed in Kumar et al. (2014), the volatile nature of the traffic nucleation mode particles raises issues in relation to their reliable measurement and may also enhance their spatio-temporal variability following their emission into the atmospheric environment (Dall'Osto et al., 2011b). A traffic-related cluster

peaking during noontime was also related to the extension of the morning traffic peak, which is similar to the diurnal variation of NO_x (Liu et al., 2014). The pattern of this factor is similar to the local traffic factor found in Beijing in a previous study (Wang et al., 2013a).

3.2.1.2 Nucleation cluster

- Nucleation (NU): the Nucleation cluster was found to be common to all sites - stressing the importance of the occurrence of new particle formation processes in high-insolation urban environments (see Table 3.2.2). It occurs between 14 and 19% of the measured periods and has a dominant nucleation mode peak in the range 10-20 nm and a minor size peak in the Aitken mode at 50-80 nm (see Table 3.2.1), the latter being attributed to background aerosols. NU is observed at midday or early afternoon more intensely during spring and summer (see Figure 3.2.3b). This cluster is generally characterised by very high solar irradiance, high wind speed and low concentration of traffic pollutants (see Figure 3.2.4). The N/NO_x ratio from 8 a.m. to 12 a.m. was calculated for the Nucleation and Traffic 1 clusters for each city. In all cases it was found to be higher for the Nucleation than for the Traffic 1 clusters, highlighting both the clean atmospheric conditions favouring nucleation (low NO_x levels) and the contribution of nucleated particles to N.

3.2.1.3 Background pollution and Specific cases clusters

- Urban Background (UB): the Urban Background cluster can be observed at all three sites 6-22% of the time (see Table 3.2.2). The size distributions present a bimodal peak at 20-40 nm and at 60-120 nm (see Table 3.2.1). At Barcelona and Madrid - cities highly influenced by road traffic emissions - the dominant peak is the finest one, whereas in Brisbane the larger peak prevails (see Table 3.2.1). Urban background clusters were usually observed during the night time, associated with relatively clean atmospheric conditions in the urban environment (see Figures 3.2.3a and 3.2.4).

- Summer Background (SB): this cluster occurred 7% of the time in Madrid (see Table 3.2.2). The unimodal size distribution shows a peak in the Aitken mode at 44±1 nm (see Table 3.2.1). It is seen during the summer nights and is thus influenced by low levels of traffic pollutants, pointing towards clean summer atmospheric conditions.

- Nitrate (NIT): this cluster was observed in the two Spanish cities, occurring 7% of the time in Barcelona and 10% of the time in Madrid. This cluster is characterised by its prevalence at night during the colder months (see Figure 3.2.3b). Moreover, in Madrid a minor peak was also seen during midday. Although the Nitrate cluster occurs more frequently at night, photochemically induced nitrate formation accounts for higher mass concentrations during the day, especially in winter in Madrid (Gómez-Moreno et al., 2007; Revuelta et al., 2012).

  The two size distributions associated with nitrate in Barcelona and Madrid are unimodal although presenting different modes. BCN_NIT shows a finer mode at 36±1 nm, whereas MAD_NIT shows a larger size mode at 63±1 nm. This might be due to the location of the sampling sites, closer to traffic sources in Barcelona (urban background) than in Madrid (suburban background).

- Growth 1 and 2 (G1, G2): these clusters were found to be exclusive to the Brisbane monitoring site and both accounted for 10% of the time. They show a unimodal peak at 28±1 and 37±1 nm, respectively. These are frequently seen in the afternoon after photonucleation occurs (BNE_G2 follows BNE_G1), and are likely related to further growth of nucleated or traffic particles (see section 3.2.3 and Figure 3.2.6c).

It is worthy of note that weekday/weekend ratios were calculated for each cluster at each city in order to analyse the impact of traffic/urban emissions on the clusters occurrence. The highest average ratio (1.3) was found for the T1 cluster, strengthening its relation to fresh traffic emissions. On the other hand, T2 and T3 clusters average ratio was 1-1.1, indicating relative independence on fresh traffic emissions, in contrast

to T1. The nucleation cluster was found to occur more often during weekends (average ratio 0.9). The lowest ratio was recorded for the UB cluster during weekends (average ratio 0.7) reflecting its background nature.

3.2.2 Supporting *k*-means cluster results from Rome and Los Angeles

Both Rome and Los Angeles clusters were classified into the same categories as the main cities, thus similar characteristics regarding meteorological parameters and gaseous pollutants as in the main cities apply.

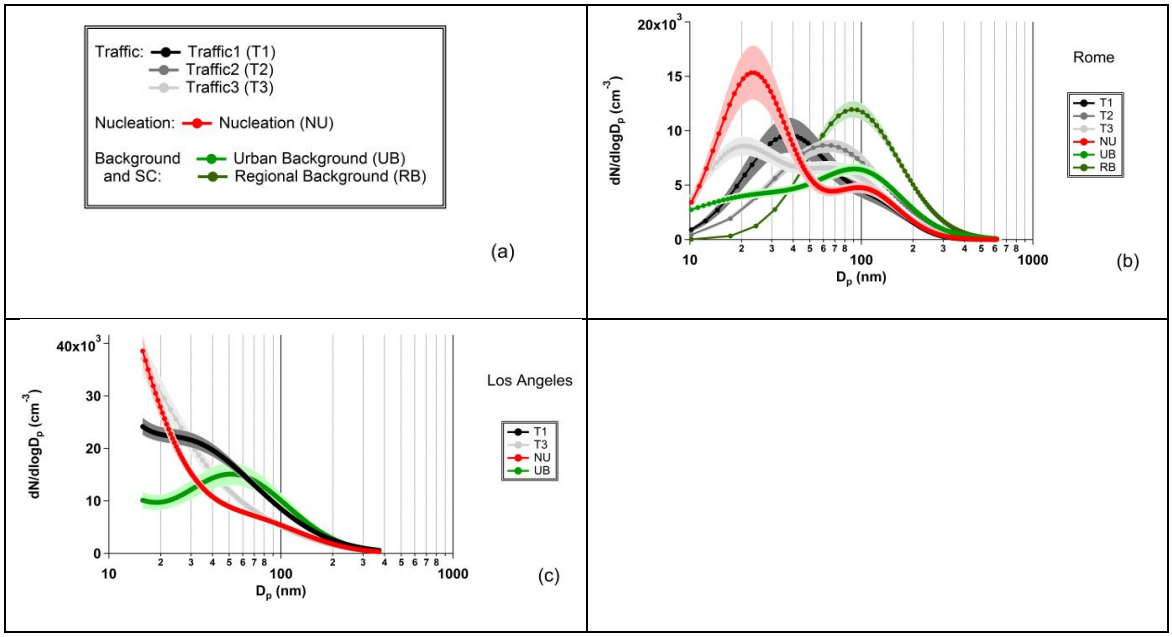

Figure 3.2.5: Aerosol size distribution results of the *k*-Means cluster analysis performed on the SMPS data at the selected complementary cities: a) legend, b) Rome and c) Los Angeles. Shaded areas around the curves represent the confidence limits calculated for 3 sigmas. Note the different scales for $dN/dlogD_p$.

Due to its location in a regional background area under the influence of the Rome pollution plume, the Rome clusters showed some differences with respect to those of Barcelona, Madrid and Brisbane. For Rome, the Traffic (T1-T3) and Nucleation clusters displayed a lower occurrence (41% and 6%, respectively) as well as a shift in its peaks to larger sizes, reflecting their aged nature (see Tables 3.2.3 and 3.2.4).

Table 3.2.3: Log-Normal fitting peaks for each cluster category *k*-Means size distribution at the supplementary sites and the corresponding peak area percentage.

Category	Subcategory	Rome	Los Angeles
Traffic	*Traffic 1 (T1)*	37±1 nm (65%), 130±7 nm (35%)	21±1 nm (100%)
	Traffic 2 (T2)	59±2 nm (91%), 102±8 nm (9%)	-
	Traffic 3 (T3)	19±1 nm (20%), 75±1 nm (80%)	<15 nm (73%), 66±1 nm (27%)
Nucleation	*Nucleation (NU)*	23±1 nm (43%), 102±2 nm (57%)	<15 nm (62%), 67±3 nm (38%)
Background pollution and Specific cases	*Urban Background (UB)*	27±2 nm (46%), 105±1 nm (54%)	45±1 nm (100%)
	Summer Background (SB)	-	-
	Regional Background (RB)	89±1 nm (100%)	-
	Nitrate (NIT)	-	-
	Growth 1 (G1)	-	-
	Growth 2 (G2)	-	-

Table 3.2.4: Cluster categories (Traffic, Nucleation and Background pollution and Specific cases) and their occurrence at the supplementary sites.

Category	Rome	Los Angeles
Traffic	41%	61%
Nucleation	6%	33%
Background	53%	6%
	100%	100%

Indeed, previous studies have showed that an aged nucleation mode of particles in the size range 20-33nm is related to photochemically nucleated particles downwind of Rome growing in size while being transported to the sampling site (Costabile et al., 2010). Moreover, in addition to the Urban Background cluster, a unique Regional Background cluster occurring 28% of the time (Table 3.2.2) was found specific to this site, and corresponded to the Regional Background PCA factor described in Costabile et al. (2010). Regarding Los Angeles, although this site was located in an urban background environment, aerosol size distributions were only measured from September to December (see Table 2.10). Two Traffic clusters and an Urban Background cluster were identified (representing 61% and 6% of the time, respectively), reflecting the proximity of the sampling site to main roads. The

Nucleation cluster was found to occur 33% of the time, due to the enhancement of photochemical nucleation events during warm months (see Table 3.2.2).

3.2.3 *k*-means clustering results explained by the cluster proximity diagram

Another way of looking at the *k*-Means results is through the Cluster Proximity Diagram (CPD), which is obtained using the Silhouette Width (Beddows et al., 2009). This diagram positions each cluster according to the similarity with the rest of the clusters (Figure 3.2.6). The closer nodes represent similar clusters, although not sufficiently alike to form a new cluster. Conversely, the more distant nodes represent the most dissimilar clusters. The average cluster modal diameter increases from left to right.

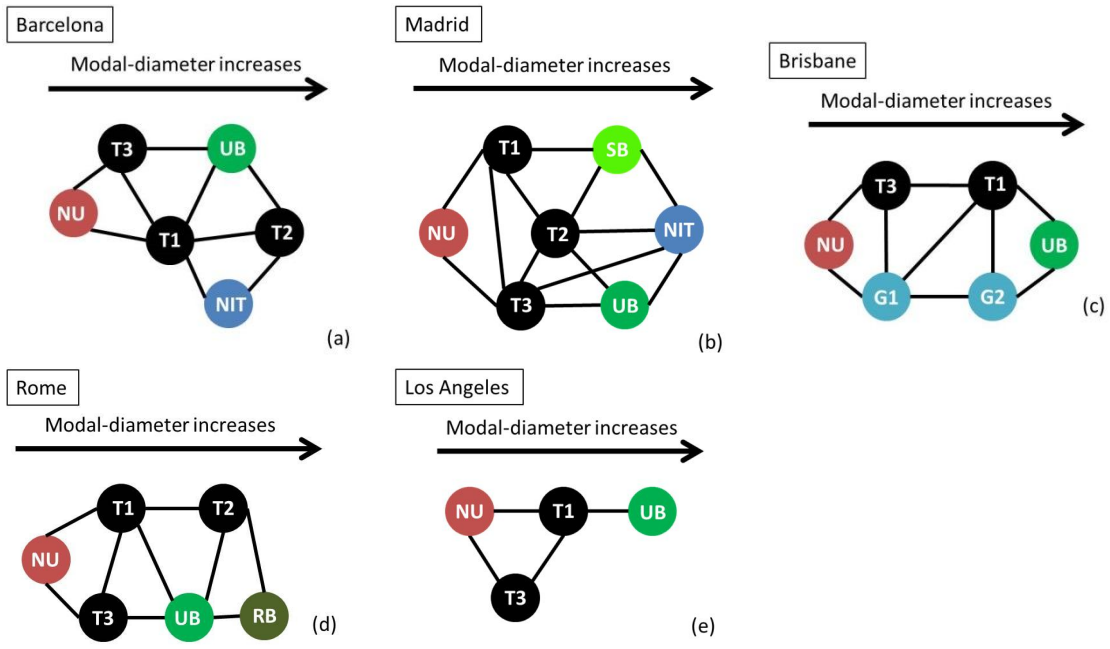

Figure 3.2.6: Cluster proximity diagram (CPD) for each selected city. In black are represented the Traffic clusters (T1, T2, T3); in green the background clusters (UB, SB, RB), in red the nucleation cluster (NU), in dark blue the Nitrate cluster (NIT) and in light blue the growth clusters (G1, G2) for: a) Barcelona, b) Madrid, c) Brisbane, d) Rome and e) Los Angeles.

Figure 3.2.6 shows the corresponding CPDs for the selected cities. The Nucleation clusters NU are located in the far left side of the diagram, as they account for a very fine size mode (see Tables 3.2.1 and 3.2.3). Traffic clusters (T1-T3) are positioned next to NU, although their location within the CPD varies depending on the city. In general, T3 and T1 are confined closer to the NU clusters than T2, given their association with

primary traffic emissions (T1) and evaporation of traffic particles or nucleation (T3). Clusters T2 are an intermediate step between fresh traffic emissions (T1) and the Urban Background clusters (UB). Regarding the Background Pollution clusters (UB and SB), their location on the right side of the graphs suggests that the sources/processes loading the Nucleation and Traffic clusters develop and contribute to this category. Barcelona and Madrid (Figures 3.2.6a and b, respectively) show site specific clusters. The SB cluster in Madrid is loaded with traffic particles from T1 and T2 before it contributes to the Nitrate (NIT) cluster. Other site specific clusters such as Nitrate (NIT) are only observed in Barcelona and Madrid (Figures 3.2.6a and b, respectively). In the case of Barcelona, NIT is linked to the Traffic clusters T1 and T2, highlighting its urban nature. On the other hand, although the Traffic clusters T2 and T3 contribute to the formation of Nitrate in Madrid, both Background Pollution clusters UB and SB add to its loading, thus resulting in a higher modal diameter for the NIT cluster in Madrid than in Barcelona (Table 3.2.1). The remaining Growth clusters in Brisbane (G1 and G2) are positioned in the centre of the CPD (Figure 3.2.6c) and represent particle growth from NU or the Traffic clusters (T1 and T3) before contributing to the UB. This is also supported by their time occurrence after the NU or T clusters.

3.3 PM_1 organic and inorganic species at traffic and urban sites during SAPUSS

The fine aerosol fraction (PM_1) in an urban environment is affected by several sources mainly with an anthropogenic origin (Pérez et al., 2010). Pollution sources contributing to the PM_1 fraction in the urban atmosphere of Barcelona include mainly road traffic, and secondary species (sulphate and nitrate), as well as industrial emissions and fuel oil (Amato et al., 2009). Reche et al. (2012) found that the contribution from biomass burning to PM_1 was relatively small (5% of the mass). Previous research in the study area by Pérez et al. (2008b) and Amato et al. (2009) focused on the inorganic fraction, while Van Drooge et al. (2012) and Alier et al. (2013) only analysed the organic fraction. For the first time in Barcelona, both inorganic and organic PM_1 species were simultaneously analysed and apportioned to different sources. To complement the study, an additional source apportionment analysis was performed considering only the inorganic elements at both sites, as Alier et al. (2013) had apportioned the organic fraction during SAPUSS. The concurrent sampling in two

city sites with different characteristics, representing a road site (RS) and urban background environment (UB) allowed studying the contribution and variability of the sources.

3.3.1 Source apportionment by means of PMF of organic and inorganic species

A positive matrix factorization analysis was applied to the PM_1 data matrix, containing 107 samples (53 at the RS, 54 at the UB) and 62 species (27 inorganic and 35 organic). The results of the PMF analysis yielded a 9 factors solution, with a Q (constrained) value of 7486, being the Q/Qexp ratio 1.49, and with an increase dQ of 3.5% with respect to the base run, due to the implementation of auxiliary equations. The nine factors yielded by the EPA PMF v5 were: fresh traffic, organic urban mix, nitrate, industrial NE & sea salt, industrial SW & pinene, shipping, SIA (Secondary Inorganic Aerosols), bio SOA and biomass burning (Tables 3.3.1 and 3.3.2 and Figure 3.3.1). The biomass burning factor was achieved with a K/EC constrained ratio of 0.48 obtained by Alves et al. (2010) for the Mediterranean shrubland. The pull down maximally option of the software was used for Ti and Sr in the bio SOA and for levoglucosan, mannosan and galactosan in the nitrate factor.

Table 3.3.1: Mean concentrations to PM_1 ($\mu g m^{-3}$) of the 9 PMF factors at the Road Site (RS), Urban Background (UB) and the average of both site. The relative contribution of each factor to PM_1 mass at each site can be found in parenthesis.

PM_1 ($\mu g\ m^{-3}$)	RS	UB	average
Fresh traffic	2.9 (18%)	1.2 (10%)	2.0 (15%)
Organic Urban Mix	3.5 (21%)	0.2 (2%)	1.9 (13%)
Nitrate	2.8 (17%)	1.3 (11%)	2.1 (15%)
Industrial NE & sea salt	2.5 (16%)	2.2 (18%)	2.4 (17%)
Industrial SW & pin	0.8 (5%)	1.3 (11%)	1.0 (7%)
Shipping	2.4 (15%)	2.6 (22%)	2.5 (18%)
SIA	0.4 (2%)	0.6 (5%)	0.5 (3%)
Bio SOA	0.9 (6%)	2.3 (19%)	1.6 (11%)
Biomass burning	0.1 (1%)	0.2 (2%)	0.1 (1%)
	16.3 (100%)	11.9 (100%)	14.1 (100%)

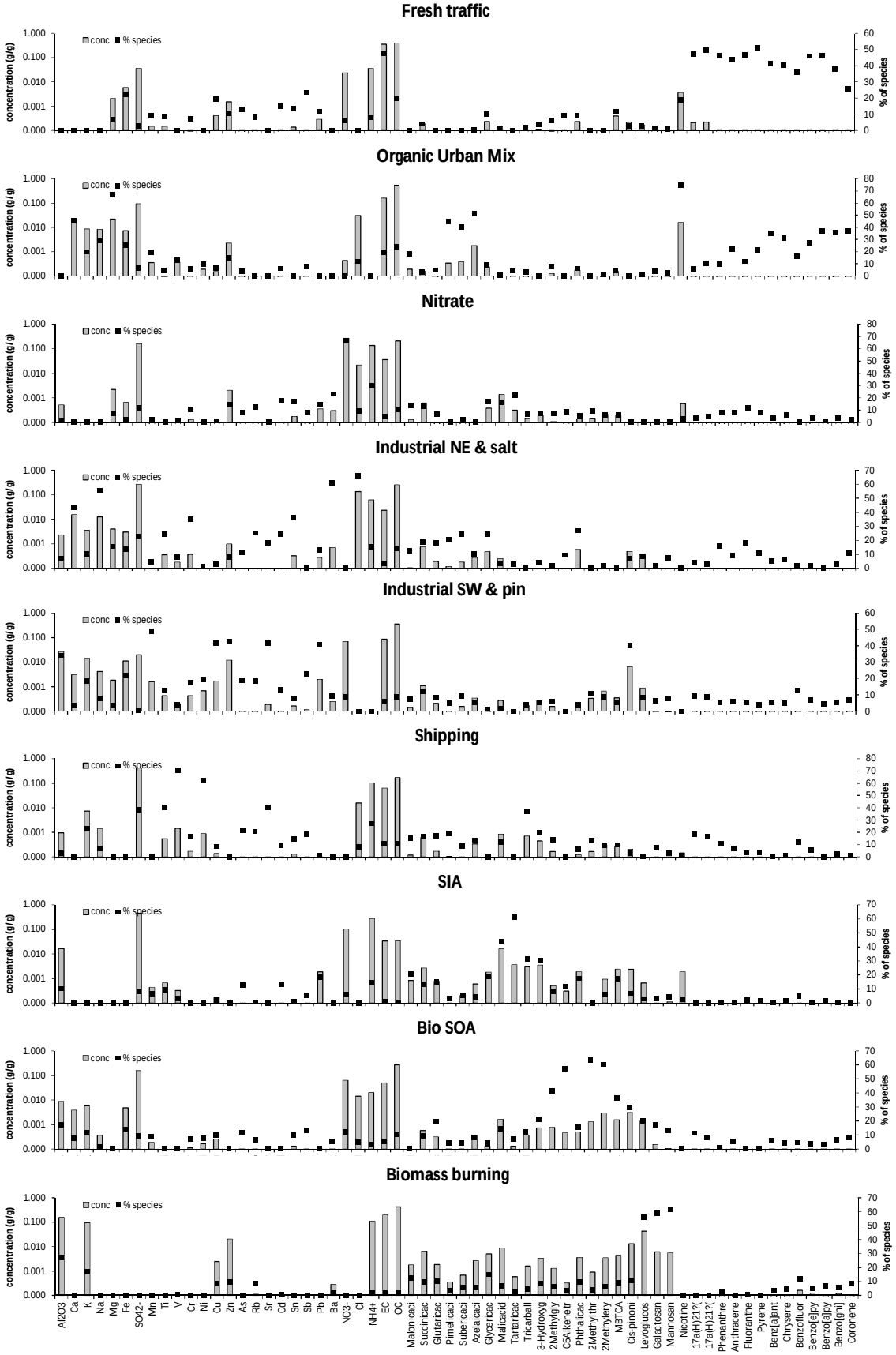

Figure 3.3.1: PMF sources profiles for PM_1 during the SAPUSS campaign.

Table 3.3.2: Contribution (%) of each specie to each of the 9 PMF factors.

% of species	Fresh traffic	Org. Urban Mix	Nitrate	Ind. NE & sea salt	Ind. SW & pin	Shipping	SIA	Bio SOA	Biomass burning
PM_1	14	13	15	17	7	18	3	11	1
Al_2O_3	0	0	1	7	34	3	10	17	**27**
Ca	0	46	0	43	4	0	0	7	0
K	0	20	0	10	18	23	0	12	**17**
Na	0	**29**	0	**56**	8	7	0	1	0
Mg	7	**67**	8	16	3	0	0	0	0
Fe	**22**	**25**	3	14	**22**	0	0	14	0
SO_4^{2-}	3	6	**12**	**23**	1	**38**	8	9	0
Mn	9	20	2	5	**49**	0	6	9	0
Ti	9	5	0	24	13	40	9	0	0
V	0	13	2	8	4	**70**	3	0	0
Cr	7	6	11	**35**	17	17	0	7	0
Ni	0	10	0	1	**20**	**62**	0	7	0
Cu	**20**	6	1	3	**41**	8	2	10	8
Zn	11	15	14	8	**42**	0	0	0	10
As	13	4	8	11	**19**	21	13	12	0
Rb	8	0	13	**25**	18	21	1	6	8
Sr	0	0	0	18	**42**	41	0	0	0
Cd	15	6	18	**24**	13	9	13	0	1
Sn	13	0	17	**36**	8	15	2	10	0
Sb	**23**	8	9	0	**23**	18	6	13	0
Pb	12	0	15	13	**41**	1	18	1	0
Ba	0	0	23	61	9	0	0	5	1
NO_3^-	6	0	**67**	0	9	0	6	12	0
Cl	0	12	9	**66**	0	8	0	5	0
NH_4^+	8	0	**30**	15	0	**27**	14	3	2
EC	**48**	**20**	5	4	6	10	1	5	2
OC	**20**	**24**	10	14	9	10	0	10	1
Malonicaci	0	18	14	12	8	15	21	0	13
Succinicac	4	3	13	19	12	16	14	10	10
Glutaricac	0	5	7	18	8	17	15	20	10
Pimelicaci	0	**45**	0	20	5	19	3	4	4
Subericaci	0	**40**	3	24	9	9	6	4	5
Azelaicaci	1	**51**	0	10	5	13	5	9	6

% of species	Fresh traffic	Org. Urban Mix	Nitrate	Ind. NE & sea salt	Ind. SW & pin	Shipping	SIA	Bio SOA	Biomass burning
Glycericac	10	9	17	**24**	1	0	19	4	15
Malicacid	2	0	16	3	2	12	**44**	15	7
Tartaricac	0	4	22	3	0	0	**61**	7	3
Tricarball	2	3	7	0	4	**37**	32	12	5
3-Hydroxyg	4	0	7	4	5	20	**31**	21	8
2Methylgly	7	8	8	2	6	14	9	**42**	6
C_5Alkenetr	9	0	9	9	0	0	12	**58**	4
Phthalicac	9	6	6	**27**	4	6	18	15	10
2Methylthr	0	0	9	0	11	13	0	**63**	4
2Methylery	0	1	6	2	9	10	6	**61**	6
MBTCA	12	4	6	0	5	10	17	**37**	9
Cis-pinoni	3	0	0	7	**40**	3	7	**29**	11
Levoglucos	3	1	0	8	8	1	3	20	**56**
Galactosan	1	4	0	2	6	8	3	17	**59**
Mannosan	1	3	0	8	7	3	4	13	**62**
Nicotine	**19**	**75**	3	0	0	1	2	0	0
17a(H)21β (H)-29-	**47**	6	4	4	9	18	0	11	0
17a(H)21β (H)	**50**	10	5	3	9	16	0	8	0
Phenanthrene	**46**	10	8	**16**	5	11	0	1	3
Anthracene	**44**	22	8	9	6	7	0	5	0
Fluoranthene	**47**	12	12	**18**	5	3	2	0	1
Pyrene	**51**	**21**	8	**11**	4	4	1	0	0
Benz[a]anthracene	**41**	**35**	3	5	5	1	1	6	3
Chrysene	**40**	**31**	6	6	5	1	1	5	5
Benzofluor	**36**	**16**	0	2	13	12	5	5	12
Benzo[e]pyrene	**46**	**27**	4	2	7	6	0	4	5
Benzo[a]pyrene	**46**	**37**	1	0	4	0	1	3	7
Benzo[ghi]perylene	**38**	**36**	3	3	5	2	0	6	6
Coronene	**26**	**37**	2	11	7	1	0	8	8

The average concentrations of each factor registered at each site are shown in Figure 3.3.2, where the traffic related factors (fresh traffic, organic urban mix and nitrate) show significantly higher concentrations at the RS that at the UB, as also observed on the concentrations temporal trend over the SAPUSS campaign (Figure 3.3.3). The polar plots presented in Figure 3.3.4 help identify the emission sources, by showing the prevalent wind and the factors concentrations.

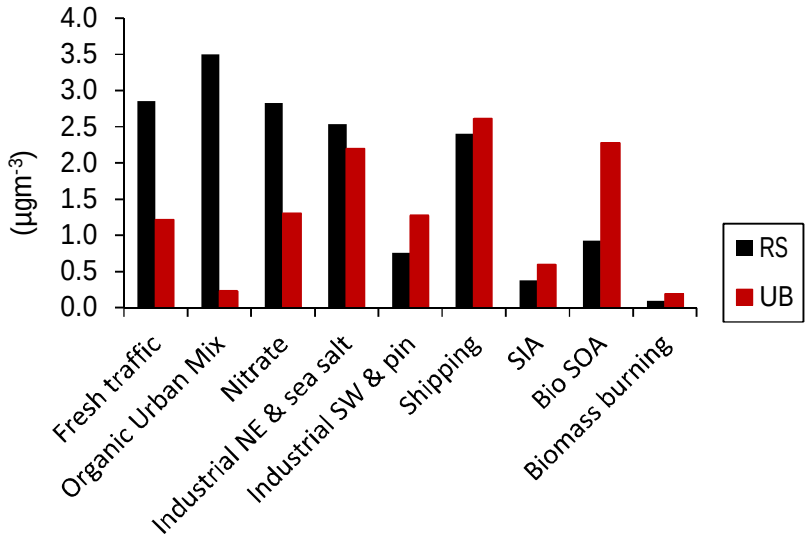

Figure 3.3.2: Contribution to PM_1 concentration levels of each of the nine factors at the Road Site (RS) and Urban Background (UB).

The nine factors obtained by PMF analysis can be described as follows:

- The fresh traffic factor was characterized by EC and OC originated from vehicle exhaust emissions (48% and 20% of the species, respectively), as well as Sb, Fe, Cu (23%, 22%, 20% of the species, respectively) as seen in Figure 3.3.1 and Table 3.3.2, that are usually related to brake and tyre wear (Sternbeck et al., 2002; Ntziachristos et al., 2007; Amato et al., 2009). It was also defined by strong contributions from Low Molecular Weight (LMW) PAH and hopanes, which pointed to primary emissions of diesel vehicles as a relevant source (Rogge et al., 1993; Zielinska et al., 2004). 19% of nicotine was contained in this factor, evidencing the relationship between heavily trafficked scenarios and tobacco smoke. Due to its direct traffic origin, this factor accounted for a higher mass contribution at the RS (18%, 2.9 µg m^{-3}) than at UB (10%, 1.2 µg m^{-3}), and the polar plots reflected the local origin of this factor (Figure 3.3.4).

- The organic urban mix factor (OUM) contained high concentrations of OC and EC (24% and 20% of the species, respectively) as well as Fe (25% of the specie) and several PAHs signal (12-37% of the species) as seen in Figure 3.3.1 and Table 3.3.2, reflecting the influence of road traffic emissions to this factor. Moreover, a strong association with pimelic (45%), suberic (40%) and azelaic acids (51%), which are related to oxidation of unsaturated fatty acids and food cooking emissions (Robinson et al., 2006) was also found. It also contained 75% of the nicotine signal. The high concentration difference between RS and UB site (21% at RS and 2% at UB of PM_1, Table 3.3.1) point towards local urban sources as the main contributors to the factor. Moreover, concentrations were on average 77% higher during the day than at night at the RS.

- The nitrate factor was mainly traced by NO_3^-, but NH_4^+ and SO_4^{2-} also contributed in a minor proportion (67%, 30%, 12% of the species, respectively). Contributions from organic species are found negligible as they are lower than 25% for all compounds (see Figure 3.3.1 and Table 3.3.2). Average concentrations doubled at the RS compared with the UB (RS: 2.8 μg m^{-3}, 17%; UB: 1.3 μg m^{-3}, 11%; see Table 3.3.1), pointing towards local urban traffic as the main source contributing to this factor. Concentrations were on average 60-80% higher during the night time and increased notably during the last days of the campaign coinciding with a strong regional recirculation episode.

- The industrial NE & sea salt factor was characterized mainly by Cl^-, Na, Sn, Cr, Rb, Cd, SO_4^{2-} (66%, 56%, 36%, 35%, 25%, 24%, 23%) and organic species such as phthalic and glyceric acid (27% and 24% of the specie, respectively) and the PAHs fluoranthene, phenanthrene and pyrene (18, 16 and 11%, respectively), as seen in Figure 3.3.1 and Table 3.3.2. Concentrations were similar at both sites (RS: 2.5 μg m^{-3}, 16%; UB: 2.2 μg m^{-3}, 18%). The Na/Cl^- ratio exceeded the sea salt ratio, thus indicating that the excess Cl^- could be attributed to an industrial source. Moreover, the contribution of both trace metals and organic combustion tracers in significant concentrations confirmed that an industrial combustion source was the main source contributing to this factor. Indeed,

fluoranthene, phenanthrene and pyrene have been previously associated with municipal waste incineration plants (Besombes et al., 2001; Liu et al., 2010; Maître et al., 2003). A waste incinerator plant and an industrial glass industry are located NE of the city, which considering the higher concentrations registered under NE winds (see Figure 3.3.4), points towards this industrial area as the main source contributing to this factor.

- The industrial SW & pinene traced by Mn, Zn, Sr, Pb, Cu, Fe, Ni and As (49%, 42%, 42%, 41%, 41%, 23%, 22%, 20% and 19% of the species, see Figure 3.3.1 and Table 3.3.2) was related to the smelters and cement kilns located along the nearby Llobregat valley, NW of the city (Amato et al., 2009; Moreno et al., 2011). Cis-pinonic acid showed 40% of the specie, which is a primary product of pinene oxidation (Claeys et al., 2007; Szmigielski et al., 2007), pointing towards the forested areas located along the Llobregat valley as the main sources of these biogenic emissions. The industrial emission plume was advected towards the city by the night land breeze, adding biogenic emissions to its load while being transported to the city area (see Figure 3.3.4). Concentrations at the UB site were higher than at RS due to its closeness to the industrial facilities (RS: 0.8 $\mu g\ m^{-3}$, 5%; UB: 1.3 $\mu g\ m^{-3}$, 11%) and also displayed an average increase by 40% at night time at the UB, while at the RS the difference was not significant.

- The shipping factor is mainly traced by V, Ni, SO_4^{2-} and NH_4^+ (70%, 62%, 38%, 27% of the specie, respectively, see Figure 3.3.1 and Table 3.3.2) pointing both towards direct harbour emissions and high-sulphate background pollution in the Mediterranean Basin due to intense maritime transport. Since the implementation of the Air Quality Plan in 2007, petcoke and fuel oil cannot be used for power generation in or around Barcelona (Decret 152/2007), therefore V and Ni are attributed to shipping emissions, as shown by Amato et al. (2009) and Minguillón et al. (2014). Although the relative contribution of this factor was higher at the UB (22%) compared to RS (15%), similar concentrations were detected at both sites (around 2.5 $\mu g\ m^{-3}$). Concentrations registered at the UB during daylight were on average 43% higher, whereas at the RS the

percentage reduced to 17%. The cruise and commercial port of the city is located south of the city, and thus under S-SW winds the highest shipping concentrations are recorded at both sites (see Figure 3.3.4).

- The secondary inorganic aerosols (SIA) factor is characterised by SO_4^{2-}, NO_3^- and NH_4^+ (Figure 3.3.1). Tartaric and malic acid (61% and 44% of the species, respectively, see Table 3.3.2) are also tracers of this factor, showing a contribution of secondary organic oxidation products. Although it showed higher concentrations at the UB site, the contributions to PM_1 mass at both sites were low (2-5%, see Table 3.3.2). Daylight concentrations were found on average 78% higher at the UB site, while an increase of 44% on average respect night time was detected at the RS.

- The biogenic secondary organic aerosols (Bio SOA) factor is characterised by SO_4^{2-} and NH_4^+ (Figure 3.3.1). Organic tracers such as 2Methylthreitol, 2Mehtylerythritol, C5 Alkene triols, 2Methylglyceric, MBTCA and Cis-pinonic acid (63%, 61%, 58%, 42%, 37%, 29% of the specie) also characterise this factor. Both first and second generation oxidation products of cis-pinonic acid are reflected in this factor, such as 2-methyltetrols (2-MT, first product, Claeys et al., 2004; Surrat et al., 2007) and MBTCA (second product, Claeys et al., 2007; Szmigielski et al., 2007) as seen in Figure 3.3.1 and Table 3.3.2. As a consequence of its secondary nature, it shows more than two times higher concentrations at the UB (2.3 μgm^{-3}) than at the RS (0.9 μgm^{-3}, see Table 3.3.1). Moreover, low NO concentrations enhance the photo oxidation of biogenic VOCs (such as isoprene) that lead to the formation of biogenic SOA (Hoyle et al., 2011; Lin and Surratt, 2012). Alier et al. (2013) reported two times higher concentration of 2-MT at the UB than at the RS, which were explained by the lower NO levels at UB respect RS. The daylight concentrations are on average 30% higher at the UB, whereas at the RS the day-night difference was not significant.

- The biomass burning factor is defined by mannosan, galactosan and levoglucosan (62%, 59% and 56% of the specie), generated by thermal alteration of cellulose and emitted in large quantities during biomass burning (Simoneit et al., 2002; Fine et al., 2004) and by a contribution of Al_2O_3 and K (27% and 17% of the specie, respectively) as seen in Figure 3.3.1 and Table 3.3.2. Although the contribution to PM_1 mass is limited to 1-2% at both sites, it is two times higher at the UB than at the RS (0.2 μgm^{-3} vs 0.1 μgm^{-3}) as seen in Table 3.3.2. The small contribution of this factor to PM_1 mass is in agreement with the results obtained by Reche et al. (2012) in the same study area (5% of PM_1). The highest concentrations of biomass burning were registered during a regional recirculation episode at the end of the campaign coinciding with the permission to burn stubble from the surrounding fields (DOGC, 1995).

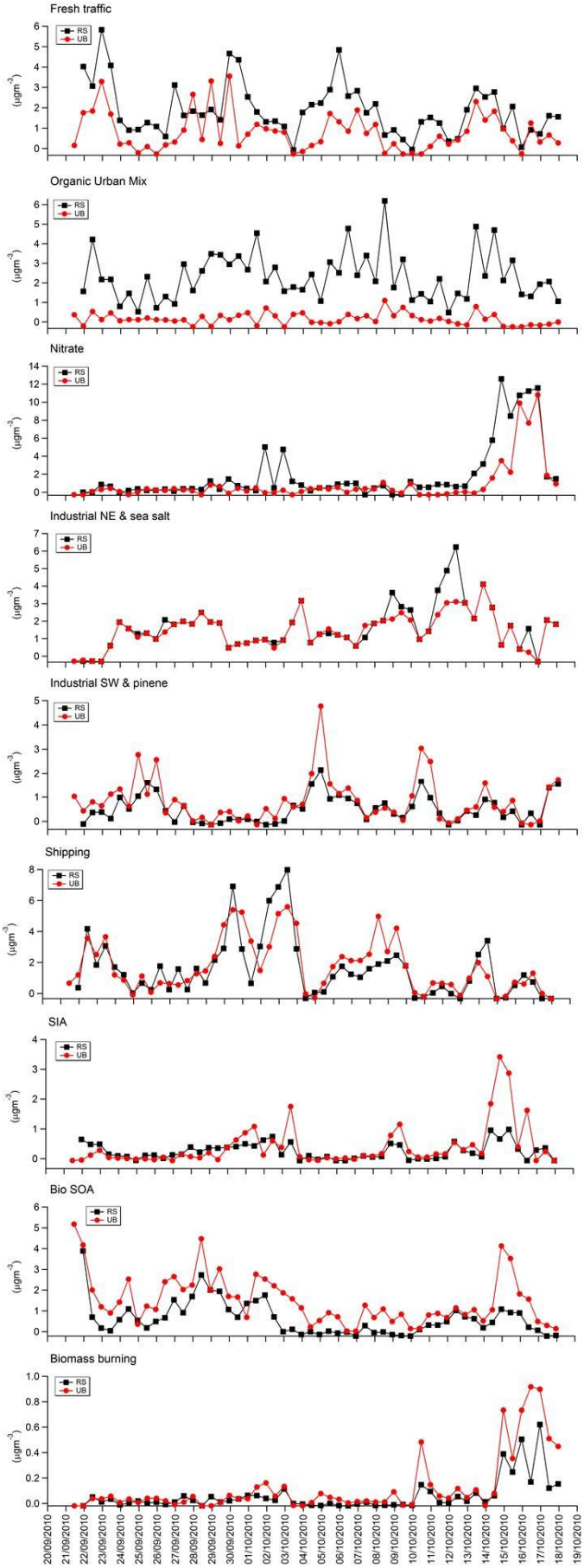

Figure 3.3.3: Temporal variation of each PMF factor at the RS and UB sites.

	RS	UB
Fresh traffic	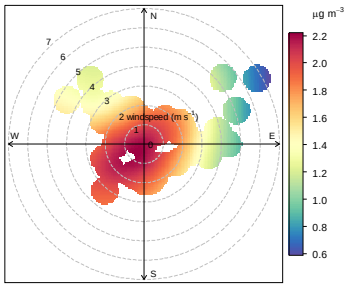	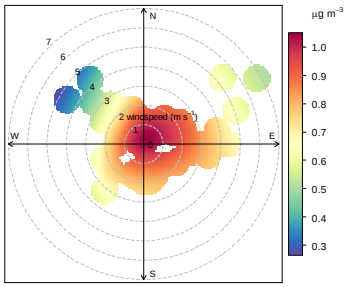
Organic Urban Mix	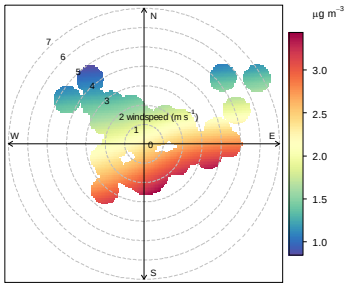	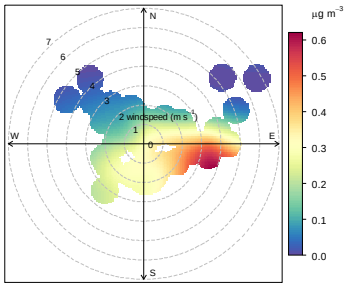
Nitrate	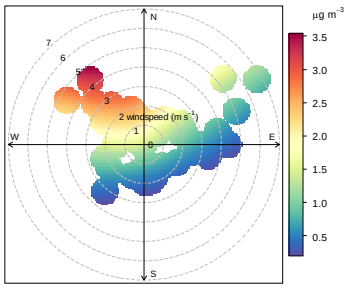	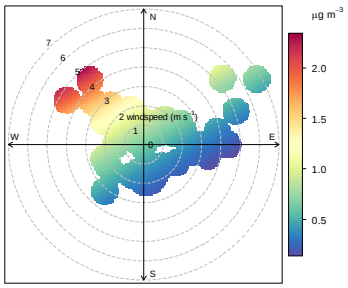
Industrial NE & sea salt	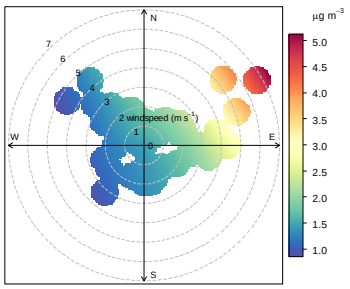	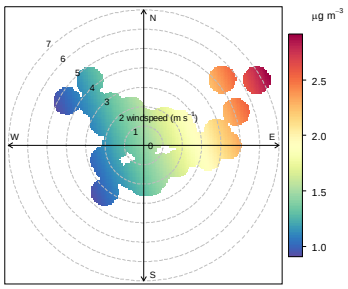
Industrial SW & pin	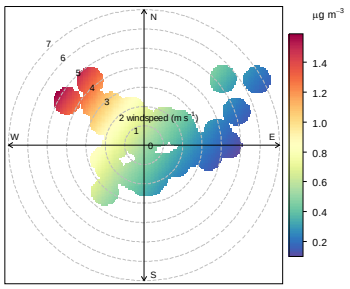	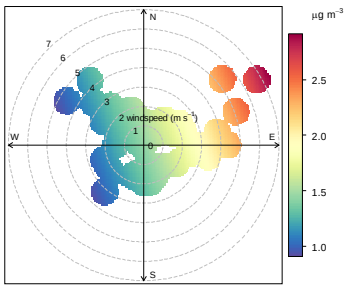

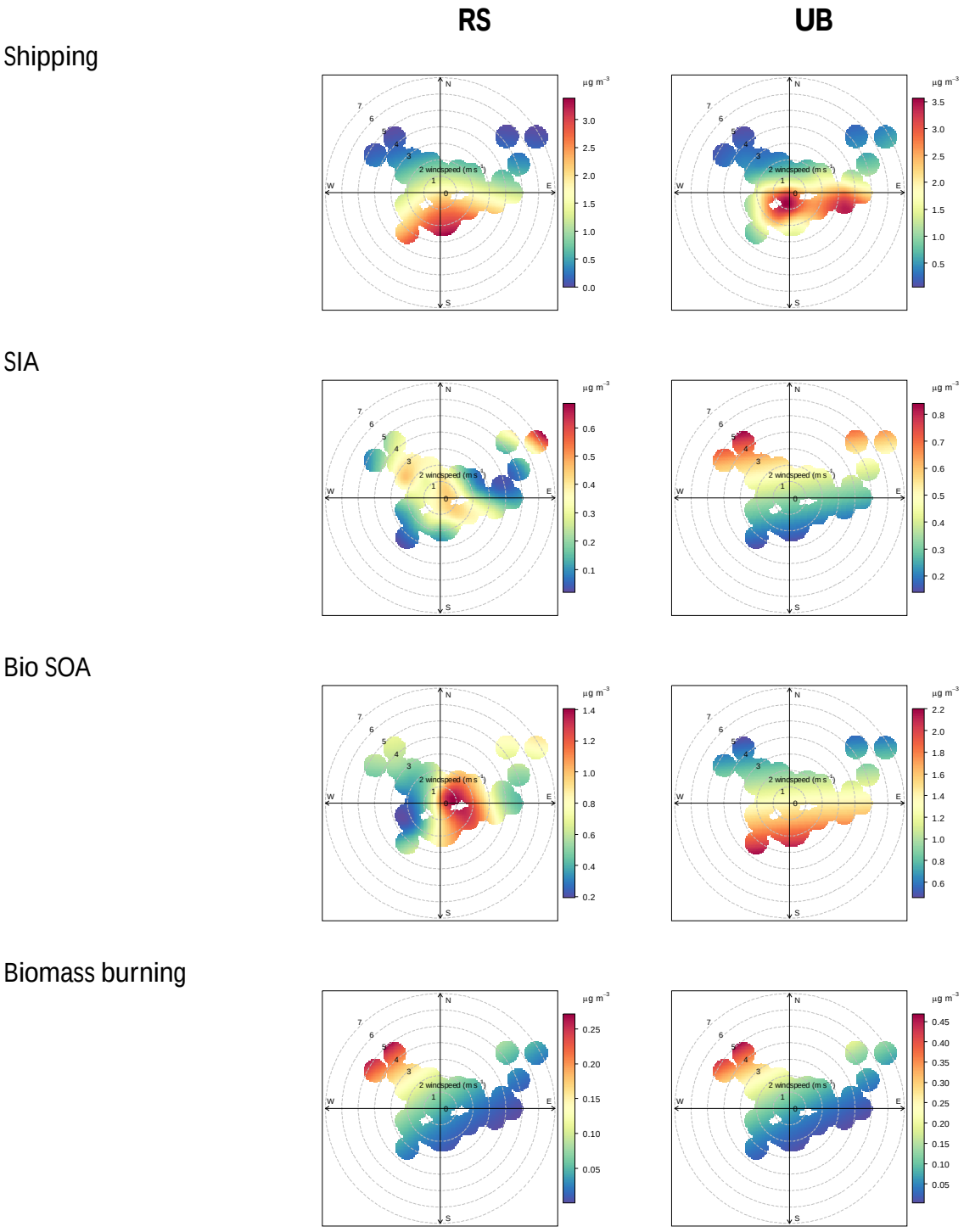

Figure 3.3.4: Polar plots of the nine PMF factors at both Road Site (RS) and Urban Background site (UB).

3.3.2 Source apportionment by means of PMF of the inorganic species only

A positive matrix factorization analysis was applied to the PM_1 data matrix, containing 107 samples (53 at the RS, 54 at the UB) and 27 inorganic species or elements. The results of the PMF analysis yielded a 5 factors solution obtained with the base run, with a Q (minimum) value of 2215, being the Q/Qexp ratio 1.12,. The five

factors yielded by the EPA PMF v5 were: Sulphate & industrial NE & aged sea salt$_{_i}$, Traffic$_{_i}$, Nitrate$_{_i}$, Shipping$_{_i}$ and Industrial SW$_{_i}$ (Table 3.3.3 and Figure 3.3.5).

Table 3.3.3: Mean concentrations to PM_1 (μgm^{-3}) of the 5 PMF inorganic factors at the Road Site (RS), Urban Background (UB) and the average of both site. The relative contribution of each factor to PM_1 mass at each site can be found in parenthesis.

PM_1 inorganics ($\mu g\ m^{-3}$)	RS	UB	average
Sul.&Ind. NE &aged sea salt$_{_i}$	3.3 (30%)	2.8 (36%)	3.0 (32%)
Traffic$_{_i}$	3.4 (31%)	1.1 (14%)	2.2 (24%)
Nitrate$_{_i}$	2.3 (21%)	1.8 (23%)	2.0 (22%)
Shipping$_{_i}$	1.3 (12%)	1.3 (16%)	1.3 (14%)
Industrial SW$_{_i}$	0.7 (6%)	0.8 (11%)	0.8 (8%)
	11.0 (100%)	7.8 (100%)	9.3 (100%)

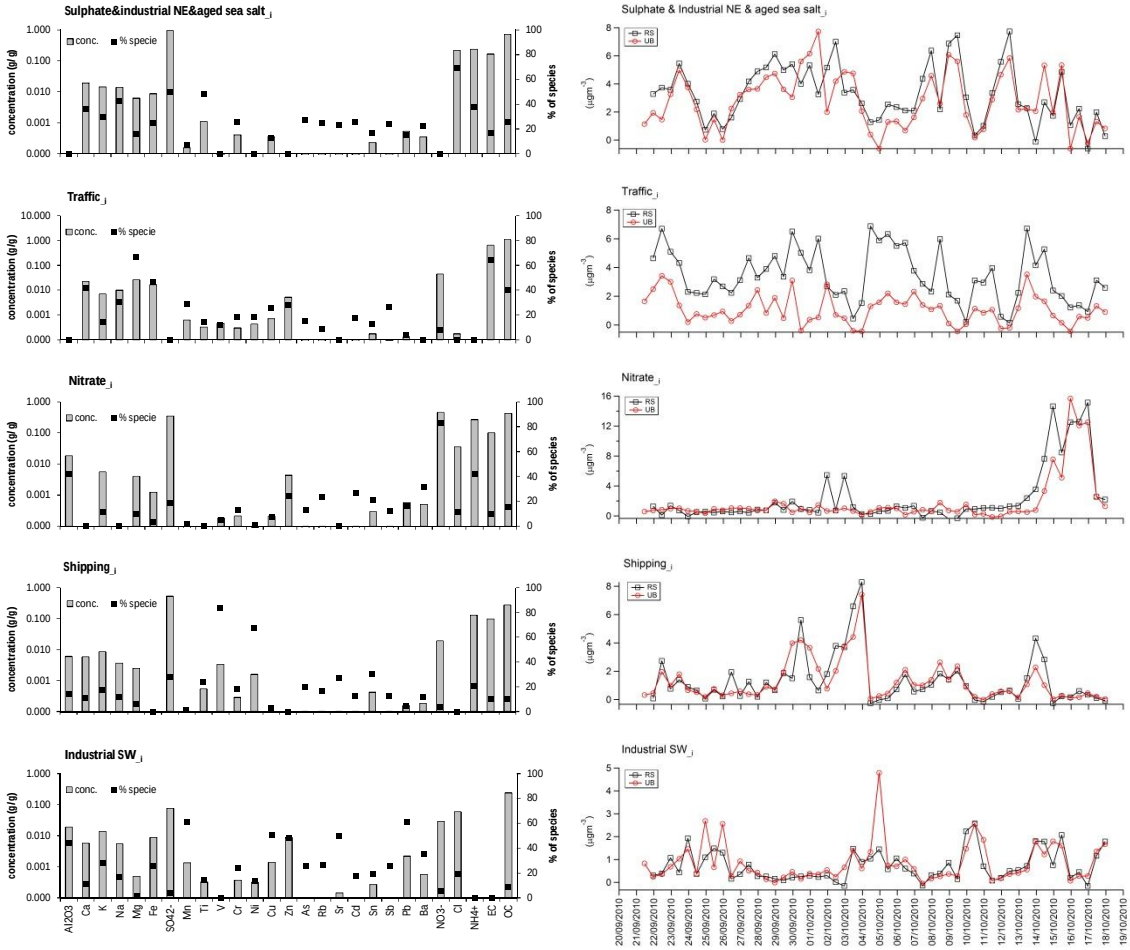

Figure 3.3.5: Source profiles and temporal variation of the PM_1 inorganic compounds source apportionment.

Table 3.3.4: Contribution (%) of each specie to each of the 5 PMF factors.

% of species	Sulphate &Industrial NE &aged sea salt $_i$	Traffic $_i$	Nitrate $_i$	Shipping $_i$	Industrial SW $_i$
PM_1	32	24	22	14	8
Al_2O_3	0	0	42	14	44
Ca	36	**42**	0	11	11
K	29	14	11	17	28
Na	42	30	0	11	17
Mg	16	**67**	10	6	1
Fe	25	**47**	4	0	25
SO_4^{2-}	**50**	0	**18**	**28**	4
Mn	7	28	2	2	**61**
Ti	**48**	14	0	23	14
V	0	11	5	**84**	0
Cr	**26**	19	13	18	24
Ni	0	18	1	**67**	13
Cu	13	26	8	3	**50**
Zn	0	**28**	24	0	**48**
As	**27**	15	13	20	26
Rb	**25**	9	24	17	26
Sr	**23**	0	0	27	**50**
Cd	**26**	17	27	13	17
Sn	17	13	21	30	19
Sb	**23**	27	12	12	26
Pb	15	4	16	4	**61**
Ba	22	0	31	11	35
NO_3^-	0	8	**83**	3	5
Cl	70	0	11	0	19
NH_4^+	**38**	0	**42**	20	0
EC	16	**64**	10	10	0
OC	26	**40**	15	10	9

The five inorganic factors obtained by PMF can be described as follows:

- The Sulphate & Industrial NE & aged sea salt_i was characterised by SO_4^{2-} and NH_4^+ (50% and 38%, respectively), industrial tracers such as Ti, As, Cd, Cr, Rb, Sr and Sb (48%, 27%, 27%, 26%, 25%, 23% and 23% of the species, respectively) and sea salt components Cl^- and Na (70% and 42% of the species, respectively) as can be seen in Table 3.3.4 and Figure 3.3.5. As seen in Table 3.3.3, this factor explains 32% (3.05 μg m^{-3}) of PM_1 inorganics mass on average, with higher concentrations at RS compared to UB (RS: 3.3 μg m^{-3}, 30%; UB: 2.8 μg m^{-3}, 36%). The excess Cl^- respect the Na/Cl^- ratio indicates that in addition to sea salt aerosols an industrial source also influences this factor, which is attributed to the industrial area NE of the city.

- The Traffic_i factor contained high concentrations of EC and OC (64% and 40% of the species, respectively), Mg, Fe, Ca and Zn (67%, 47%, 42%, 28% of the species, respectively) as seen in Table 3.3.4 and Figure 3.3.5, reflecting the influence of direct and indirect road traffic emissions (Amato et al., 2009). This factor contributed 24% (2.2 μg m^{-3}) to PM_1 inorganics mass on average, being the contributions at the RS more than two times higher than at the UB site (RS: 3.4 μg m^{-3}, 31%; UB: 1.1 μg m^{-3}, 14%).

- The Nitrate_i factor was dominated by NO_3^- representing 83% of the specie. NH_4^+ and SO_4^{2-} also contributed but in a lower proportion (42% and 18% of the species, respectively) as seen in Table 3.3.4 and Figure 3.3.5. It contributed on average to 22% (2.0 μg m^{-3}) of the total PM_1 inorganics mass, and showed higher concentrations at the RS than at the UB (RS: 2.3 μg m^{-3}, 21%; UB: 1.8 μg m^{-3}, 23%).

- The Shipping_i factor was mainly characterised by V, Ni and SO_4^{2-} (84%, 67% and 28% of the species, respectively) as seen in Table 3.3.4 and Figure 3.3.5, attributed to shipping emissions from the nearby city harbour. It contributed 14% (1.3 μg m^{-3}) to the PM_1 inorganics mass on average and despite showing

the same concentration at both sites, it displayed higher relative concentrations at the UB than at the RS (RS: 1.3 μg m^{-3}, 12%; UB: 1.3 μg m^{-3}, 16%), being the UB site located closer to the port area.

- The Industrial SW_i factor was characterised by industrial tracers such as Mn, Pb, Cu, Sr and Zn (61%, 61%, 50%, 50% and 48% of the species, respectively) as seen in Table 3.3.4 and Figure 3.3.5. It represents the lowest contribution to PM_1 inorganics mass on average (8%, 0.8 μg m^{-3}). The UB site was more impacted by this factor, being, located closer to the emission area SW of the city (RS: 0.7 μg m^{-3}, 6%; UB: 0.8 μg m^{-3}, 11%).

3.4 PM_{10} sources in horizontal and vertical levels during SAPUSS

The PM_{10} aerosol fraction in the Barcelona urban environment is affected both by anthropogenic and natural sources. In addition to the source contributions described for PM_1 in the prior chapter, mineral dust resuspension and Saharan dust intrusions are relevant sources to PM_{10}. Previous studies (Amato et al., 2009) have reported natural sources (mineral dust and aged sea salt) to represent 35% of the PM_{10} in an urban background environment. Vehicle exhaust and road dust were found to contribute 21% and 17% of PM_{10}, respectively. Secondary sulphate (13%) and nitrate (11%) as well as fuel oil combustion (5%) and industrial emissions (1%) completed the source apportionment. However, these values were obtained in a single urban background site and the sources evolution over the study area both in horizontal and vertical levels had not been studied. Therefore during the intensive SAPUSS campaign 4 sampling sites, two at ground level (RS and UB) and two at a certain height (TM, 150 m a.s.l. located close to the sea side and TC, 415 m a.s.l. located on the suburban hills) within the Barcelona urban area concurrently sampled PM_{10}, allowing to chemically characterizing aerosol loadings and sources in a three dimensional scenario. Using the source apportionment study, sources estimations were also carried out to account for the natural and anthropogenic sources.

3.4.1 PM_{10} concentration and chemical composition in a 3D scenario during SAPUSS

The average PM_{10} concentrations at the 4 monitoring sites during SAPUSS followed a decreasing trend from the site closest to traffic sources to the one located in the suburban background at 415 m a.s.l. (RS 30.7, UB 25.9 , TM 24.8 and 21.8 μgm^{-3} at TC; Figures 3.4.1 and 3.4.2). The UB concentrations were very close to the annual PM_{10} mean recorded at this site for 2010 (23 $\mu g\ m^{-3}$). The variability in PM_{10} concentrations and air mass scenario (according to the classification presented by Dall'Osto et al. (2013a)) during SAPUSS is shown in Figure 3.4.1. Indeed, air mass origin seems to play a key role in the temporal variability of PM_{10}. PM_{10} concentrations particularly increased under the influence of regional (REG) and North African air masses (West (NAF_W) and East (NAF_E)). On the other hand, changes in air mass origin, or transition periods usually led to a relative decrease in PM_{10} concentrations (Figure 3.4.1). In addition, the European air mass (EUR) episode, coinciding with rainfall during SAPUSS, contributed to lower PM levels.

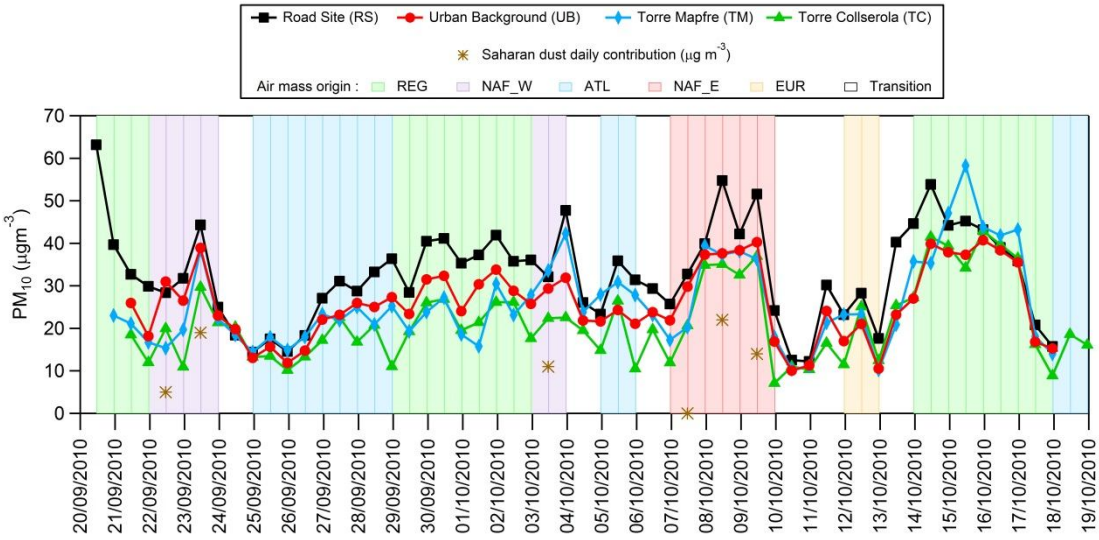

Figure 3.4.1: PM_{10} variation at the 4 sites (RS, UB, TM, TC) during the SAPUSS campaign under different air mass origin (Regional (REG), North African West (NAF_W), Atlantic (ATL), North African East (NAF_E), European (EUR)). Saharan dust daily contribution to PM_{10} is indicated.

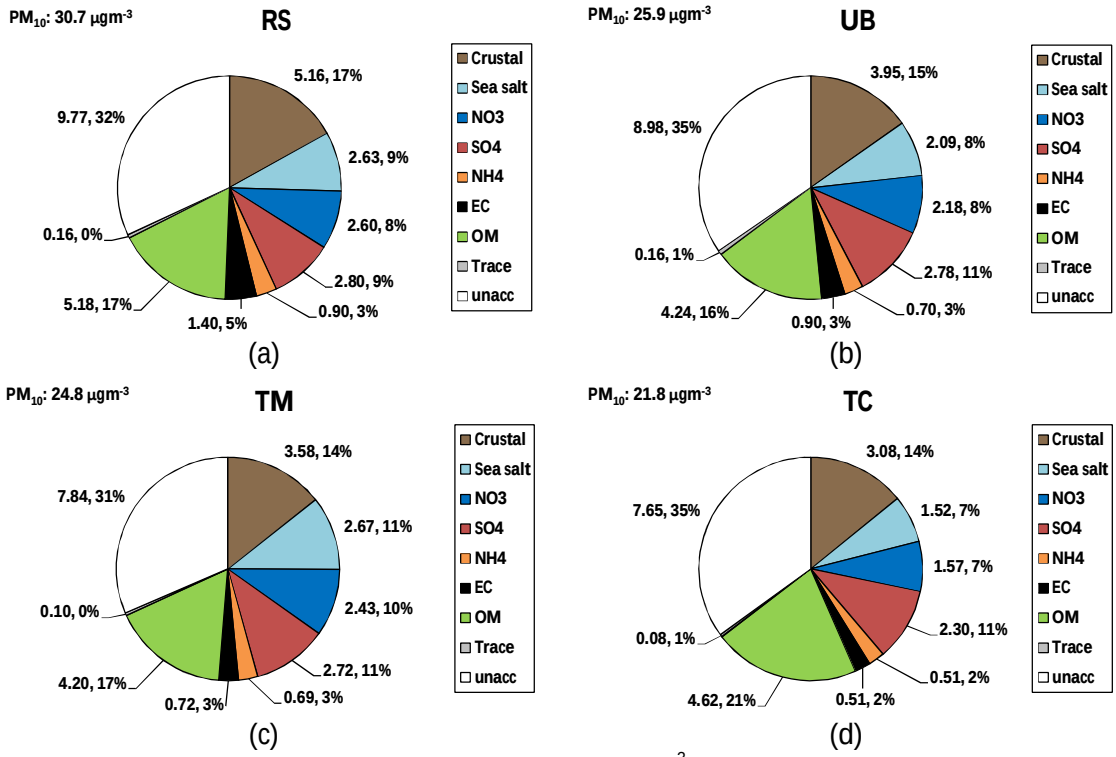

Figure 3.4.2: Mean composition of PM_{10} concentration in µg m^{-3} measured during the SAPUSS campaign at: a) Road Site (RS), b) Urban Background (UB), c) Torre Mapfre (TM) and d) Torre Collserola (TC). Data are given in µgm^{-3} and %. On the top right of each graph average gravimetric PM_{10} concentration are represented.

The major PM_{10} components are summarised in Figure 3.4.2, which show the absolute and relative contributions to PM_{10} at each site. The concentration of each analysed species (both major components and trace elements) is shown in Table 3.4.1 at each monitoring site. Several main and trace elements have been reported to be associated with different emission sources, thus Figure 3.4.3 summarises the most relevant ones at each sampling site.

Table 3.4.1: Average concentration of PM_{10} analysed species at each site (RS, UB, TM and TC).

	RS	UB	TM	TC
PM_{10} (μgm^{-3})	30.7	25.9	24.8	21.8
OC (μgm^{-3})	3.7	2.5	2.5	2.2
EC (μgm^{-3})	1.4	0.9	0.7	0.5
C_{total} (μgm^{-3})	5.8	3.4	3.1	2.7
EC+OM (μgm^{-3})	7.6	5.2	4.9	5.2
$CO_3^{=}$ (μgm^{-3})	1.1	0.9	0.7	0.6
SiO_2 (μgm^{-3})	1.9	1.3	1.5	1.3
Al_2O_3 (μgm^{-3})	0.6	0. 5	0.5	0.4
Ca (μgm^{-3})	0.7	0.6	0.5	0.4
Fe (μgm^{-3})	0.6	0.4	0.3	0.2
K (μgm^{-3})	0.3	0.2	0.2	0.2
Mg (μgm^{-3})	0.2	0.2	0.2	0.1
Na (μgm^{-3})	1.1	0.9	1.2	0.7
SO_4^{2-} (μgm^{-3})	2.8	2.8	2.7	2.3
NO_3^{-} (μgm^{-3})	2.6	2.2	2.4	1.6
Cl (μgm^{-3})	1.3	1.0	1.2	0.8
NH_4^{+} (μgm^{-3})	0.9	0.7	0.7	0.5
Li (ngm^{-3})	0.2	0.3	0.2	0.2
Be (ngm^{-3})	<0.1	<0.1	<0.1	<0.1
Sc (ngm^{-3})	0.1	<0.1	<0.1	<0.1
Ti (ngm^{-3})	20.1	19.9	15.4	13.8
V (ngm^{-3})	6.4	5.9	6.8	4.9
Cr (ngm^{-3})	6.7	4.6	1.9	1.0
Mn (ngm^{-3})	9.3	9.4	6.8	5.3
Co (ngm^{-3})	0.2	0.2	0.2	0.1
Ni (ngm^{-3})	4.8	5.2	2.9	2.5
Cu (ngm^{-3})	23.9	15.9	8.3	5.3
Zn (ngm^{-3})	41.1	61.9	27.9	23.8
Ga (ngm^{-3})	0.1	0.1	<0.1	0.1
Ge (ngm^{-3})	0.2	0.2	<0.1	<0.1
As (ngm^{-3})	0.4	0.4	0.3	0.3
Se (ngm^{-3})	0.5	0.5	0.5	0.4
Rb (ngm^{-3})	0.5	0.5	0.4	0.4
Sr (ngm^{-3})	2.9	2.3	2.2	1.5
Y (ngm^{-3})	0.5	0.3	<0.1	<0.1
Zr (ngm^{-3})	5.8	2.7	5.1	5.3
Nb (ngm^{-3})	<0.1	0.1	<0.1	<0.1
Mo (ngm^{-3})	6.1	4.8	3.8	<0.1
Cd (ngm^{-3})	0.1	0.1	0.1	0.1
Sn (ngm^{-3})	5.8	4.6	2.1	2.9
Sb (ngm^{-3})	2.5	1.8	1.3	0.8
Cs (ngm^{-3})	<0.1	<0.1	<0.1	<0.1
Ba (ngm^{-3})	10.9	13.0	5.6	4.1
La (ngm^{-3})	0.3	0.2	0.2	0.2
Ce (ngm^{-3})	0.7	0.5	0.4	0.4
Pr (ngm^{-3})	<0.1	<0.1	<0.1	<0.1
Nd (ngm^{-3})	0.2	0.2	<0.1	<0.1
Sm (ngm^{-3})	0.1	0.1	<0.1	<0.1

	RS	UB	TM	TC
Eu (ngm^{-3})	<0.1	<0.1	<0.1	<0.1
Gd (ngm^{-3})	0.1	0.1	<0.1	<0.1
Tb (ngm^{-3})	<0.1	<0.1	<0.1	<0.1
Dy (ngm^{-3})	0.1	0.1	<0.1	<0.1
Ho (ngm^{-3})	<0.1	<0.1	<0.1	<0.1
Er (ngm^{-3})	<0.1	<0.1	<0.1	<0.1
Tm (ngm^{-3})	<0.1	<0.1	<0.1	<0.1
Yb (ngm^{-3})	<0.1	<0.1	<0.1	<0.1
Lu (ngm^{-3})	<0.1	<0.1	<0.1	<0.1
Hf (ngm^{-3})	0.1	0.1	<0.1	<0.1
Ta (ngm^{-3})	<0.1	<0.1	<0.1	<0.1
W (ngm^{-3})	0.1	0.1	0.1	<0.1
Tl (ngm^{-3})	<0.1	<0.1	<0.1	<0.1
Pb (ngm^{-3})	6.6	6.8	4.9	5.1
Bi (ngm^{-3})	0.3	0.3	0.2	0.1
Th (ngm^{-3})	0.1	0.1	0.1	0.1
U (ngm^{-3})	0.1	0.1	<0.1	0.1

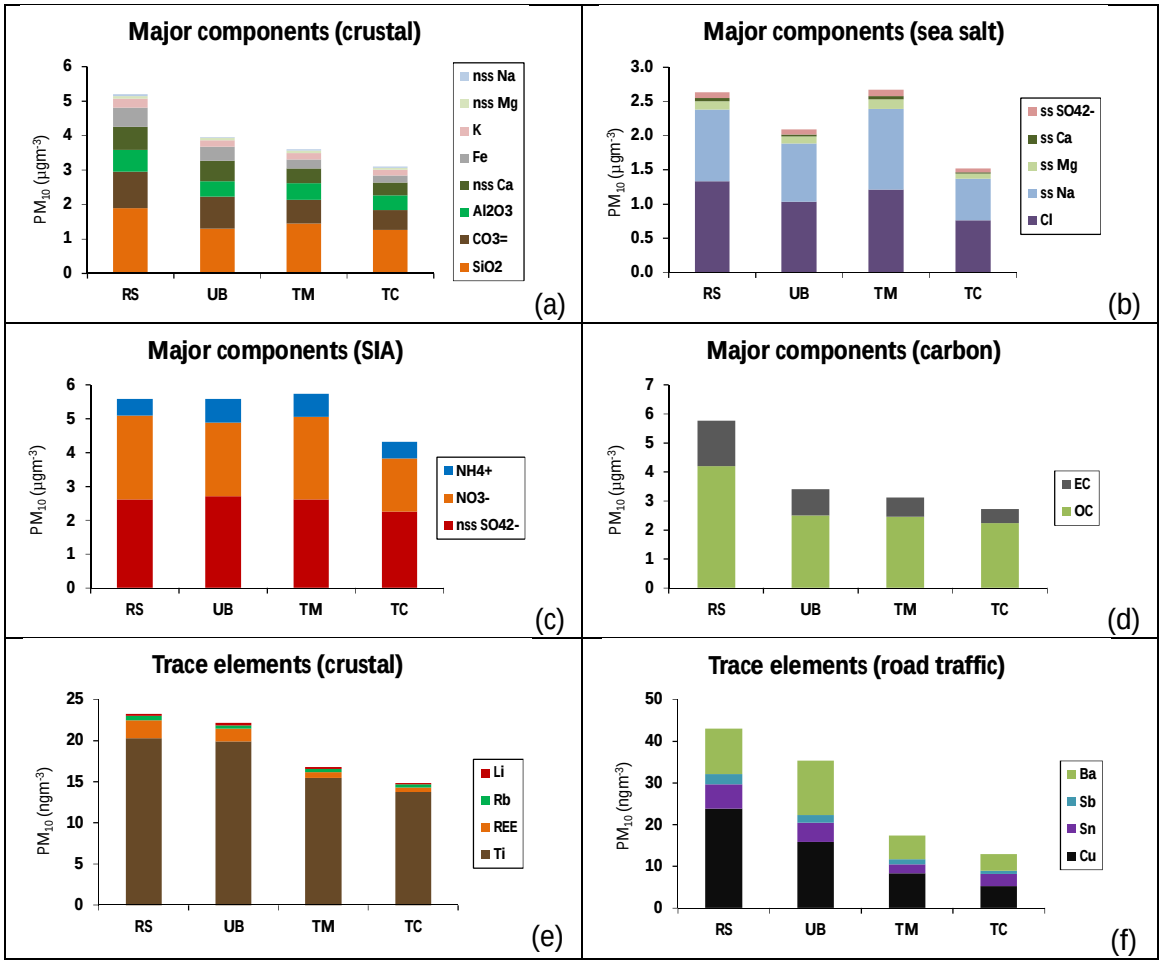

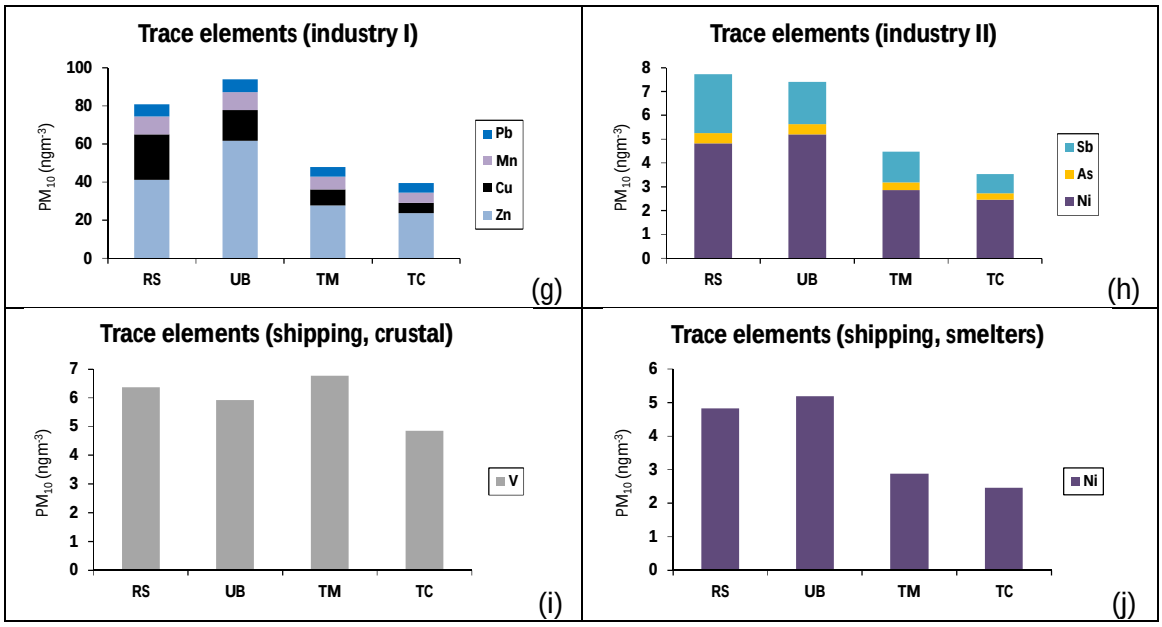

Figure 3.4.3: Average PM_{10} concentration of main and trace elements for different emission sources at each site (RS: Road Site, UB: Urban Background, TM: Torre Mapfre, TC: Torre Collserola). REE denote Rare Earths elements.

The main emission sources affecting the PM_{10} fraction were analysed for each sampling site as they impacted with different intensity over the study area:

- Crustal elements accounted for 14-17% of the mass, which means an unexpectedly homogeneous relative contribution to the total PM_{10} across the Barcelona urban area (see Figure 3.4.2). However, mass concentrations of crustal matter decreased from the city centre sites (5.2 μgm^{-3} at RS) to those located further inland (3.1 μgm^{-3} at TC) (see Figures 3.4.2 and 3.4.3a). .

- Sea salt aerosols relative contribution was homogenous at all sites ranging from 7-11% (1.5-2.7 μgm^{-3}), as can be seen in Figures 3.4.2 and 3.4.3b. The highest concentrations were recorded near the sea side (TM, RS) while a decreasing gradient was recorded towards inland. Despite TM being located a few meters from the sea side, it shows similar concentrations to RS, 4 km distant. This might be due to the elevation of the TM sampling site (150 m a.s.l.) causing dilution of surface pollutants.

- Secondary inorganic aerosols (SIA: sulphate SO_4^{2-}, nitrate NO_3^- and ammonium NH_4^+) display altogether similar concentrations at the city sites (6.3 μgm^{-3} on average at RS, 5.7 μgm^{-3} at UB and 5.8 μgm^{-3} at TM) and decrease around 25%

at TC (4.4 μgm^{-3}) (see Figure 3.4.3c). Sulphate and nitrate contributed in similar proportions at all sites, ranging from 7-10% each (1.6-2.6 μgm^{-3} for nitrate and 2.3-2.8 μgm^{-3} for sulphate), although in absolute concentrations a decrease of 15-35% at the TC was detected. The contribution of ammonium was similar at all sites, around 2-3% (0.5-0.9 μgm^{-3}) of PM_{10} mass. Overall, SIA accounted for 20-23% of the mass (4.4-6.3 μgm^{-3}) (see Figure 3.4.2).

- Elemental carbon (EC) concentration was clearly influenced by traffic sources, as its contribution decreased with the distance to traffic hot spots (RS: 1.4 μgm^{-3}, 5%; UB: 0.9 μgm^{-3}, 4%; TM: 0.7 μgm^{-3}, 3%; TC: 0.5 μgm^{-3}, 2%) (see Figures 3.4.2 and 3.4.3d).

- Organic matter (OM) accounted for 16-21% of the mass and was found in the highest relative proportion at the TC site due to its location on a nearby hill in a suburban environment. The lowest concentrations were observed at UB and TM (4.2 μgm^{-3}), followed by TC (4.6 μgm^{-3}), while the highest ones were recorded at the RS (5.2 μgm^{-3}) (see Figures 3.4.2 and 3.4.3d).

Despite the low contribution of trace elements to the bulk PM_{10} (around 0.1%), their concentrations provide valuable information by tracing specific pollution sources. Figure 3.4.3e-j shows the concentration of a selection of trace elements associated with four known sources affecting the metropolitan area of Barcelona: crustal, road traffic, industry and shipping. The most abundant crustal tracer is Ti followed by far by Rb, Y, Ce, La, Li, Nd, and Ga that were found in higher concentrations at the ground sites (RS and UB) than at the tower sites (TM and TC). This might be due to the dust resuspension by road traffic or other anthropogenic sources such as construction works or parks, thus producing a vertical decreasing gradient. The spatial variability of vehicle wear tracers such as Cu, Sn and Ba (Schauer et al., 2006) is driven by the proximity to traffic sources, being the RS the most polluted site. Out of the industrial emissions tracers for the city of Barcelona Zn, Mn, Pb, As and Ni (Amato et al., 2009) showed higher concentrations at the UB followed by the RS, TM and TC. The higher concentration registered at the UB site might be due to the pollution plume originating from the industrial area along the Llobregat Basin (south-western side of Barcelona

metropolitan area) that first impacts the UB site (Minguillón et al., 2014). On the other hand, the remaining industrial tracers Cu and Sb (showing a decreasing gradient with the distance to traffic sources) might account for both industrial and traffic-related emissions. Both traffic and industrial tracers showed significant higher values at the ground sites respect the tower sites. V and Ni (Figure 3.4.3i-j) are usually associated with shipping emissions (Agrawal et al., 2008; Kim and Hopke, 2008). Indeed, higher V levels were found at the sites closer to the coast (TM and RS), in agreement with findings from Minguillón et al. (2014). However, higher Ni concentrations were recorded at the ground sites (UB and RS) respect to the tower sites (TM and TC), probably due to the contribution of other Ni sources reaching the ground sites (e.g. smelters, Minguillón et al., 2014). Viana et al. (2014) reported a V/Ni ratio associated to shipping emissions of 2.3-4.5. In our study the only site within this range was TM (2.4), located closest to the sea side. RS and UB showed lower ratios (1.3 and 1.1, respectively) probably due to the higher impact of an industrial plume containing Ni. TC ratio was 2.0, which might indicate an additional V loading of crustal origin, due to its location on a nearby hill.

3.4.2 Source apportionment and temporal variability in a 3D scenario

The PMF analysis was applied to the PM_{10} data matrix, which contained 221 samples (56 at RS, 54 at UB, 55 at TM and 56 at TC) and 27 inorganic species. The results of the PMF analysis yielded an 8 factor solution, with a Q (constrained) value of 6627, being the Q/Qexp ratio 1.17, and with an increase dQ of 7.5% with respect to the base run, due to the implementation of auxiliary equations. The eight factors yielded by the PMF ME-2 were: vehicle exhaust and wear, road dust, mineral, aged marine, heavy oil, industrial, sulphate and nitrate (Figure 3.4.4, Tables 3.4.2 and 3.4.3). The road dust source was pulled towards the composition of local road dust (average of city centre samples, as reported by Amato et al., 2009), the Na/Al ration pulled towards the value reported for Earth's crust composition by Mason (1966) in form of auxiliary equations (Paatero and Hopke, 2009). In addition, for selected days, unrealistic differences between RS_{site} and UB_{site} for mineral and road dust factors were minimized.

Table 3.4.2: Mean concentrations (μgm^{-3}) of PMF factors at the Road Site (RS), Urban Background (UB), Torre Mapfre (TM) and Torre Collserola (TC).

PMF Factors (μgm^{-3})	RS	UB	TM	TC
Exhaust & wear	8.7 (27%)	5.0 (17%)	2.9 (11%)	1.9 (10%)
Road dust	3.8 (11%)	3.3 (12%)	2.3 (9%)	1.6 (9%)
Mineral	4.6 (14%)	5.1 (18%)	4.8 (19%)	4.9 (26%)
Aged marine	4.6 (14%)	3.6 (13%)	5.2 (20%)	2.6 (13%)
Heavy oil	0.5 (2%)	0.6 (2%)	0.6 (2%)	0.4 (2%)
Industrial	1.2 (4%)	1.4 (5%)	0.7 (3%)	0.9 (4%)
Sulphate	3.5 (11%)	4.2 (15%)	3.8 (15%)	3.3 (17%)
Nitrate	5.7 (17%)	4.9 (18%)	5.5 (21%)	3.6 (19%)
	32.5 (100%)	28.9 (100%)	25.1 (100%)	21.2 (100%)

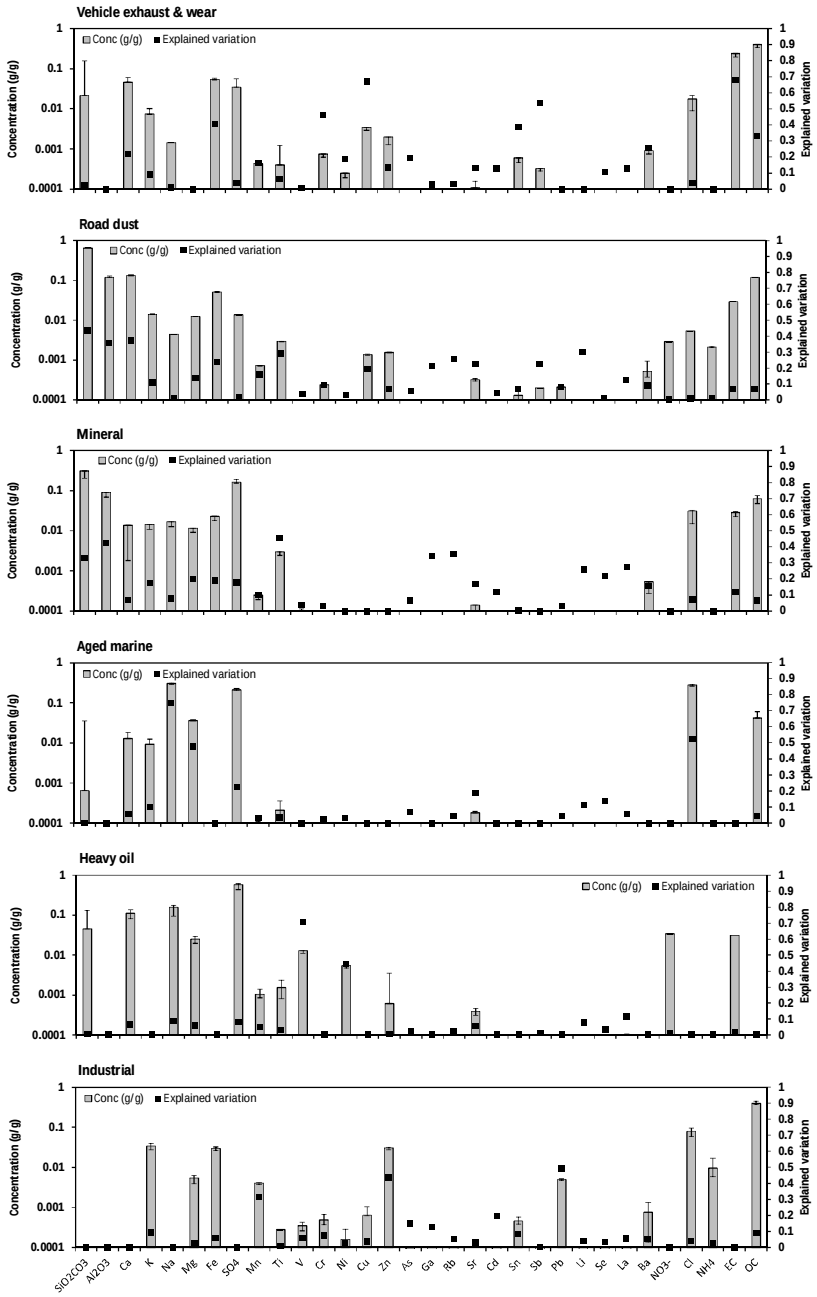

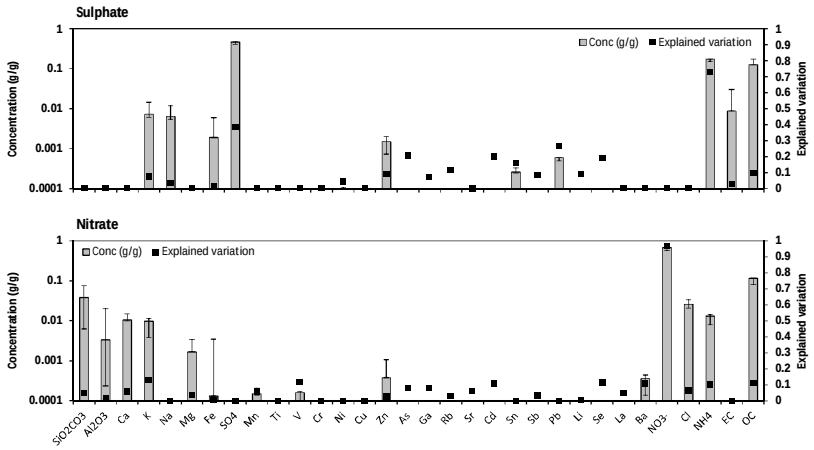

Figure 3.4.4: PMF sources profiles for PM_{10} during the SAPUSS campaign: vehicle exhaust and wear, road dust, mineral, aged marine, heavy oil, industrial, sulphate, nitrate. Uncertainties were obtained by bootstrapping.

Table 3.4.3: Explained variation for each element and each PMF PM_{10} factor. In bold are the species that most contribute to each factor.

	Exhaust &wear	Road dust	Mineral	Aged marine	Heavy oil	Industrial	Sulphate	Nitrate	
	F1	F2	F3	F4	F5	F6	F7	F8	Residuals
PM_{10}	0.16	0.10	0.16	0.15	0.02	0.05	0.13	0.15	0.08
SiO_2CO_3	0.02	**0.43**	**0.33**	0.00	0.01	0.00	0.00	0.05	0.16
Al_2O_3	0.00	**0.35**	**0.42**	0.00	0.00	0.00	0.00	0.02	0.20
Ca	0.22	**0.37**	0.07	0.06	0.07	0.00	0.00	0.06	0.15
K	0.09	0.11	0.18	0.10	0.00	0.10	0.08	0.13	0.23
Na	0.01	0.01	0.08	**0.75**	0.09	0.00	0.03	0.00	0.04
Mg	0.00	0.13	0.20	**0.48**	0.06	0.03	0.00	0.03	0.07
Fe	**0.41**	**0.24**	0.19	0.00	0.00	0.06	0.01	0.00	0.09
SO_4^{2-}	0.04	0.01	0.17	**0.22**	0.08	0.00	**0.39**	0.00	0.08
Mn	0.16	0.16	0.10	0.03	0.05	**0.31**	0.00	0.06	0.13
Ti	0.07	**0.29**	**0.45**	0.03	0.03	0.01	0.00	0.00	0.12
V	0.01	0.03	0.04	0.00	**0.71**	0.06	0.00	0.11	0.04
Cr	**0.46**	0.10	0.03	0.02	0.00	0.07	0.01	0.00	0.30
Ni	0.18	0.03	0.00	0.03	**0.45**	0.03	0.04	0.00	0.24
Cu	**0.67**	**0.19**	0.00	0.00	0.00	0.04	0.00	0.00	0.10
Zn	0.14	0.07	0.00	0.00	0.01	**0.44**	0.09	0.03	0.24
As	0.19	0.05	0.06	0.07	0.02	**0.15**	0.21	0.08	0.17
Ga	0.03	0.21	**0.34**	0.00	0.00	0.13	0.07	0.08	0.13
Rb	0.03	**0.26**	**0.36**	0.04	0.03	0.05	0.12	0.03	0.09
Sr	0.13	**0.23**	0.17	0.18	0.06	0.03	0.00	0.06	0.14
Cd	0.13	0.04	0.12	0.00	0.00	**0.19**	0.20	0.10	0.22
Sn	**0.39**	0.07	0.00	0.00	0.00	0.08	0.16	0.00	0.30
Sb	**0.53**	**0.23**	0.00	0.00	0.01	0.01	0.09	0.03	0.11
Pb	0.00	0.08	0.03	0.05	0.00	**0.50**	0.27	0.00	0.08
Li	0.00	**0.30**	**0.26**	0.11	0.08	0.04	0.09	0.01	0.11
Se	0.10	0.01	**0.22**	0.14	0.04	0.03	0.19	0.12	0.15
La	0.13	0.13	**0.27**	0.06	0.12	0.06	0.00	0.05	0.19

	Exhaust &wear	Road dust	Mineral	Aged marine	Heavy oil	Industrial	Sulphate	Nitrate	
Ba	0.26	0.09	0.15	0.00	0.00	0.05	0.00	0.11	0.34
NO_3^-	0.00	0.00	0.00	0.00	0.01	0.00	0.00	**0.97**	0.02
Cl	0.04	0.01	0.07	**0.52**	0.00	0.04	0.00	0.06	0.25
NH_4^+	0.00	0.01	0.00	0.00	0.00	0.03	**0.73**	0.10	0.13
EC	**0.68**	0.07	0.12	0.00	0.02	0.00	0.03	0.00	0.09
OC	0.33	0.07	0.06	0.04	0.00	0.09	0.10	0.11	0.19

The average concentrations of each factor registered at each site are shown in Figure 3.4.5 and Table 3.4.2, while Figure 3.4.6 displays the temporal variation of each factor for all sites. Figure 3.4.7 shows the average concentrations at each site under the 5 air mass scenarios identified during SAPUSS: Atlantic (ATL), Regional (REG), North African West (NAFW), North African East (NAFE) and European (EUR). To further complete the analysis and interpretation of the results, Figure 3.4.8 present the polar plots, which display the different factors concentrations depending on the blowing wind direction and speed, thus allowing deducing the main pollution sources origin.

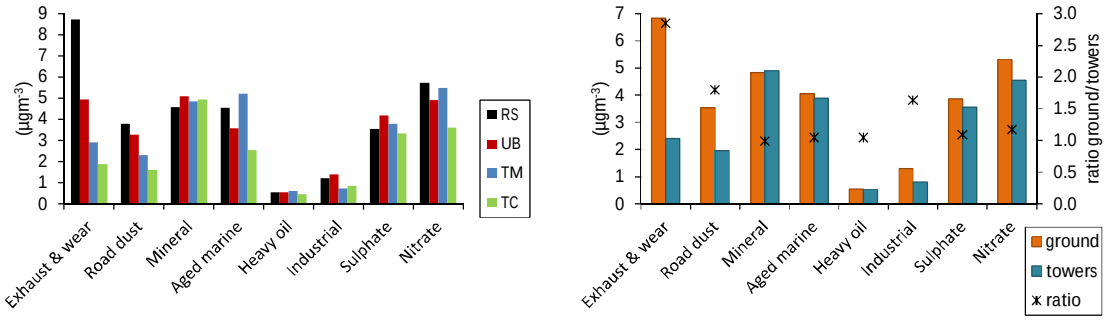

Figure 3.4.5: Contribution to PM_{10} concentration levels of each of the eight factors: a) at each of the 4 sites (RS, UB, TM, TC) and b) at ground (RS and UB) and tower levels (TM and TC) and the concentration ratio between ground and tower sites during the SAPUSS campaign.

The identified factors characteristics are as follows:

- The vehicle exhaust and wear factor was characterized by EC and OC originated from vehicle exhaust emissions, as well as Cu, Sb, Cr, Fe and Sn (67%, 53%, 46%, 41% and 39% of the variation, respectively) which are usually present in the brake and tyre wear (see Figure 3.4.4a) (Sternbeck et al., 2002; Ntziachristos et al., 2007; Amato et al., 2009). Due to its direct traffic origin, this factor accounts for the highest mass contribution at the RS (27%, 8.7 µg m^{-3}), followed by UB (17%, 5.0 µg m^{-3}), TM (11%, 2.9 µg m^{-3}) and TC (10%, 1.9 µg m^{-3})

(see Table 3.4.2 and Figure 3.4.5a). Thus clear horizontal and vertical gradients were evidenced for the contributions to PM_{10} of this source. It originated at the traffic hot spots near RS, UB and TM and was later transported upslope towards TC by the sea breeze, where the maximum concentrations were recorded under SE winds from the city (Figure 3.4.8). Concentrations were 32% higher under REG and NAF_W air masses due to low pollutants dispersion (6.1 μg m^{-3} vs 4.6 μg m^{-3} on average, Figure 3.4.7a-b).

- The road dust factor was constrained using the emission profile reported for the city of Barcelona by Amato et al. (2009) by means of a pulling equation. It contained high concentrations of Al_2O_3, Ca, Fe, Li, Ti but also explained around 20% of the variation of Cu and Sb (Table 3.4.2 and Figure 3.4.4b). As expected, this factor concentration followed also a decreasing trend from RS (11%, 3.8 μg m^{-3}) and UB (12%, 3.3 μg m^{-3}) to TM (9%, 2.3 μg m^{-3}) and TC (9%, 1.6 μg m^{-3}), although the ratio between ground and tower sites was lower than for the vehicle exhaust and wear factor (1.8 vs 2.8, see Figure 3.4.5b). The road dust was transported from the nearby busy streets towards the sites, as seen in Figure 3.4.8. A decrease in concentrations of 90% on average, due to wet deposition and less resuspension, was recorded under EUR air masses, as they were associated with rain during the study period (0.3 μg m^{-3} vs 2.7 μg m^{-3}, see Figure 3.4.7c-d).

- The mineral factor was mainly made up of Al_2O_3, Ti, Rb, La, Li and Se (42%, 45%, 36%, 27%, 26%, 22% of the variation, respectively). Unexpectedly, average absolute concentrations were very homogeneous across the city (4.6 to 5.1 μg m^{-3}, 14-26%) pointing to a source affecting the whole urban area. Under North African air masses (NAF_W and NAF_E), average concentration levels nearly doubled with respect to the average levels for non-African days (9.2 μg m^{-3} vs 4.9 μg m^{-3}, Figure 3.4.5 and 3.4.7e-f). This issue will be further investigated in section 3.4.5.

- The aged marine contribution is characterised by Na and Cl (75% and 52% of the variation, respectively) and also a proportion of Mg and SO_4^{2-} (48% and 22% of the variation, respectively). The ratio SO_4^{2-}/Na exceeded the calculated sea salt ratio, indicating its aged nature. As expected, the highest concentrations were reached at the sites located closer to the sea (TM, 20%, 5.2 μg m^{-3}; RS, 14%, 4.6 μg m^{-3}; UB, 13%, 3.6 μg m^{-3}; TC, 13%, 2.6 μg m^{-3}). It displays a homogeneous temporal variation at the four monitoring sites except under the influence of NAF_E and EUR air masses when aged marine concentrations were more than double (9.2 μg m^{-3} vs 4.0 μg m^{-3} on average, Figure 3.4.7g-h). The trajectory followed by the air masses during these two episodes over the Mediterranean Sea (Dall'Osto et al., 2013a) resulted in high marine loadings transported inland and thus a higher variability between sites, as marine emissions impact decreases with the distance to the emission point (Minguillón et al., 2014). Consequently the highest concentrations at all sites were reached under E-SE blowing winds (caused by sea breeze, Figure 3.4.8).

- The heavy oil factor was characterized by V and Ni (71% and 45% of the variation, respectively) and showed a relevant concentration of SO_4^{2-} and EC. It was attributed to fuel oil combustion from shipping emissions since power generation around Barcelona is only allowed by using natural gas since 2008. Furthermore, 98% of domestic heating systems use natural gas, and the spatial distribution of V concentrations evidenced higher levels as we approach the coast (Figure 3.4.3, Table 3.4.1). Average concentrations varied between 0.4-0.6 μg m^{-3}, representing 2% of the load at each site (Table 3.4.2). Higher concentrations of this factor were found on average under the REG_1 and NAF_W episodes from 30 September to 4 October (1.3 μg m^{-3} vs 0.5 μg m^{-3}, see Figure 3.4.7). REG_1 episode was characterized by the recirculation of air masses in the study area, thus allowing the transport of heavy oil towards the city with the development of the sea breeze, whereas in the REG_2 episode the poor development of the sea breeze minimized the transport of the shipping emissions towards the city (Figure 3.4.9). The variability between sites does not follow a consistent trend, although higher concentrations were often recorded

at TM due to its proximity to the sea side. The cruise and commercial port of the city is located south of the city (Figure 3.4.8), and thus under NAF_W air masses and S-SW winds the highest heavy oil concentrations were recorded at all sites, pointing towards direct port emissions as the main contributor to this factor.

- The industrial factor defined by Pb, Zn, Mn and Cd (50%, 44%, 31% and 19% of the variation, respectively) was related to the smelters and cement kilns located along the nearby Llobregat valley, NW of the city (Amato et al., 2009; Moreno et al., 2011). The emission plume was advected towards the city by the night land breeze (Figure 3.4.8), reaching the ground sites UB and RS in a greater measure due to proximity of the sources (RS, 4%, 1.2 μg m^{-3}; UB, 5%, 1.4 μg m^{-3}; TM, 3%, 0.7 μg m^{-3}; TC, 4%, 0.9 μg m^{-3}). Indeed, the highest peaks (6-8 μgm^{-3}) were recorded for the UB site the 5 October and the 10 October (Figure 3.4.6), being the average concentration 4.0 μgm^{-3}. This is further confirmed by Figure 3.4.8 showing the highest concentrations at all sites under NW winds. Indeed, the highest concentrations were recorded under ATL air mass scenarios, which showed a prevalent N wind direction, and REG, favouring the recirculation of air masses and the accumulation of pollutants (Figure 3.4.7).

- The sulphate factor was traced by SO_4^{2-} and NH_4^+ (39% and 73% of the variation, respectively). OC is also present in significant concentration (around 10%), suggesting the contribution of secondary organic aerosols to this factor. As a consequence of its regional origin and secondary nature, it shows homogeneous concentration values at the four sites (3.5-4.2 μgm^{-3}, 11-17%; see Table 3.4.2). Under REG and NAF_W scenarios, concentrations gradually increase at all sites up to 14 μgm^{-3} (Figures 3.4.6 and 3.4.7), reaching values 60% higher than the average (5.9 vs 3.7 μgm^{-3}), especially during the REG_2 episode (14-17 of October), as possibly an industrial source adds to the loading. At all sites this factor appears to have a regional origin (Figure 3.4.8).

- The nitrate factor was mainly traced by NO_3^- (97% of the variation), but NH_4^+, OC and Cl^- also contributed in a minor proportion (10%, 11% and 6%, respectively). It also shows homogeneous concentration values at the three city sites (around 5.4 μgm^{-3}), whereas at TC concentrations were 33% lower (3.6 $\mu g\ m^{-3}$, see Table 3.4.2). This revealed a dominant local urban origin of this factor, as nitrate was diluted while being transported to the suburban area. Nonetheless, regional nitrate contributed to the loadings under certain scenarios. The highest concentrations were recorded under REG air mass due to the accumulation of pollutants (Figure 3.4.7). Namely, during the REG_2 recirculation episode (14-17 October), nitrate concentrations were doubled (10.7 vs 4.9 μgm^{-3} on average) at the four monitoring sites, reaching occasionally higher levels at the tower sites (TM, TC) than at ground levels (RS, UB). Unlike sulphate, concentrations reached during REG_1 episode were 50% lower compared to REG_2 (5.3 vs 10.7 μgm^{-3}), given the higher ambient temperatures during REG_1 (Figure 3.4.9), which shifted nitrate towards the gas phase (Zhuang et al., 1999).

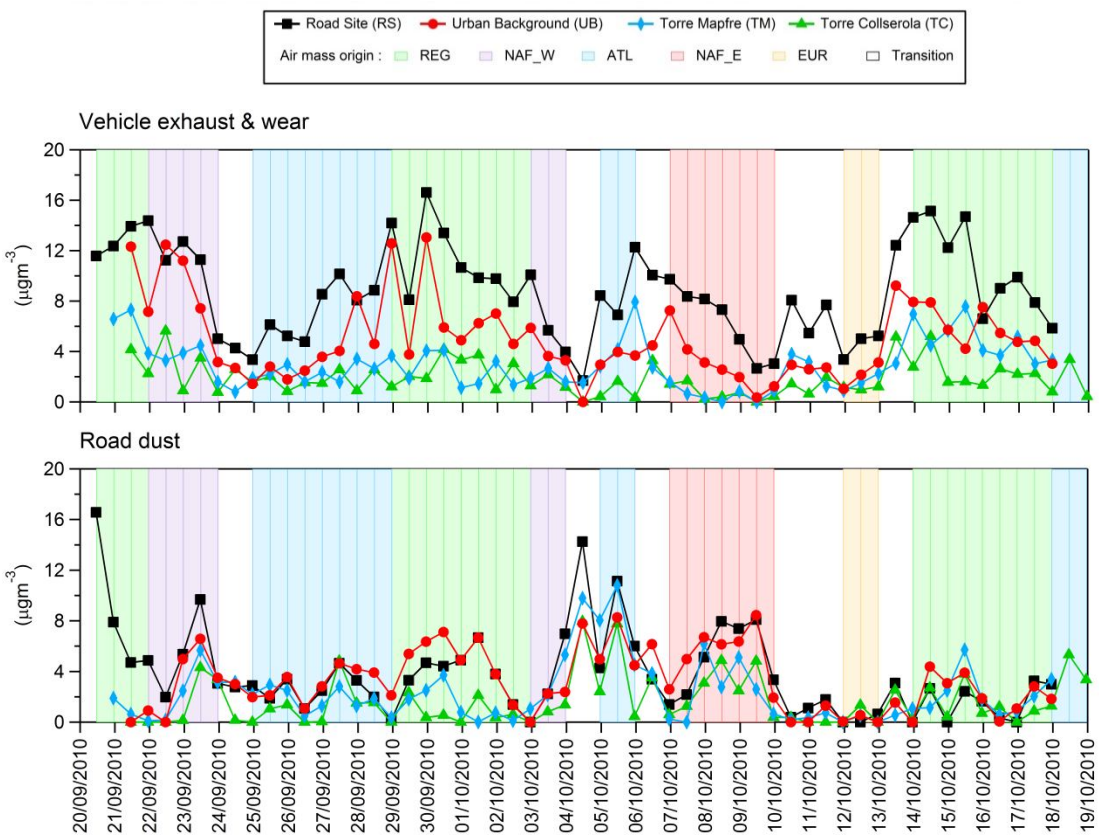

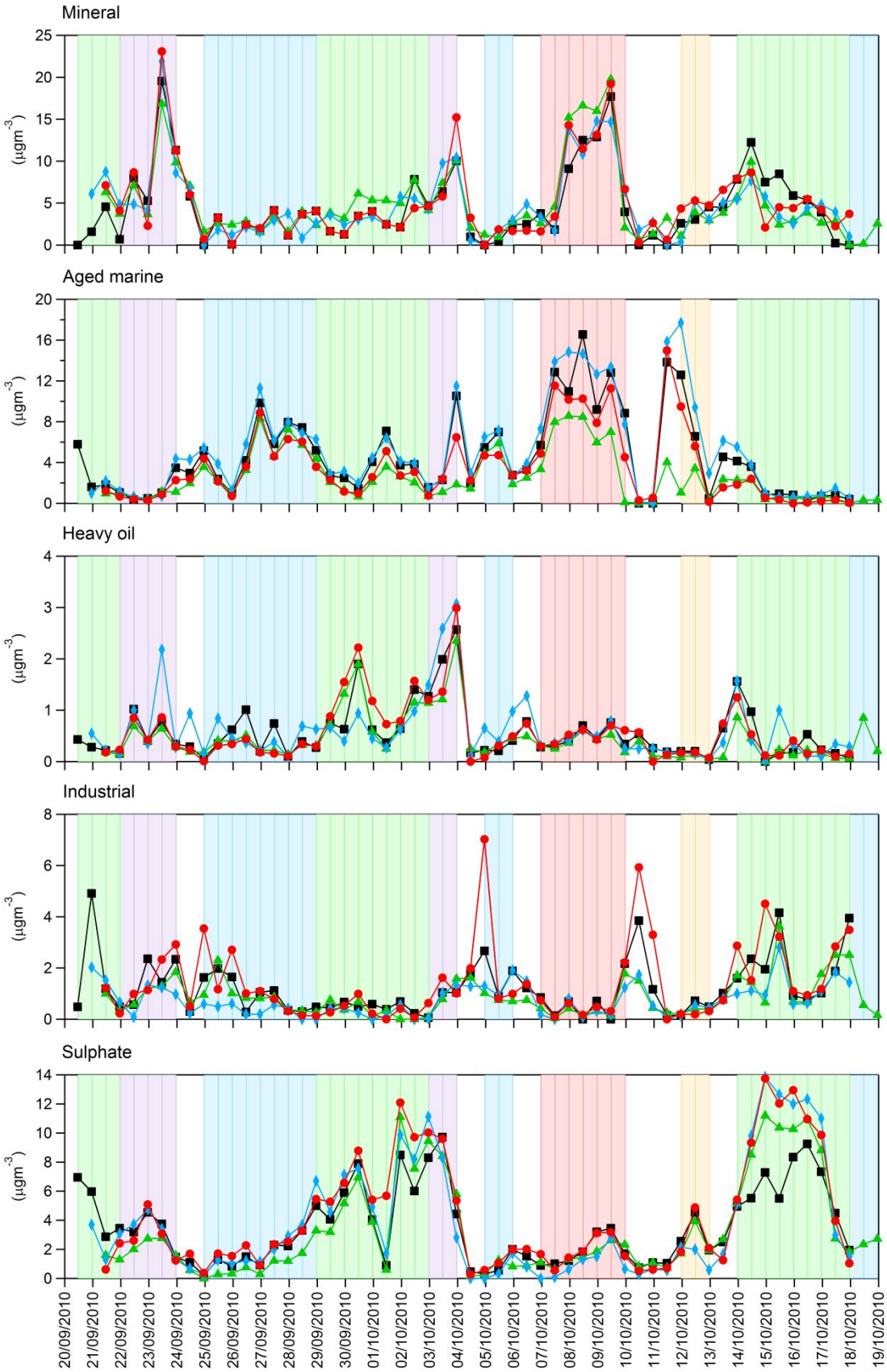
Mineral
Aged marine
Heavy oil
Industrial
Sulphate
(µgm-3)
20/09/2010
21/09/2010
22/09/2010
23/09/2010
24/09/2010
25/09/2010
26/09/2010
27/09/2010
28/09/2010
29/09/2010
30/09/2010
01/10/2010
02/10/2010
03/10/2010
04/10/2010
05/10/2010
06/10/2010
07/10/2010
08/10/2010
09/10/2010
10/10/2010
11/10/2010
12/10/2010
13/10/2010
14/10/2010
15/10/2010
16/10/2010
17/10/2010
18/10/2010
19/10/2010

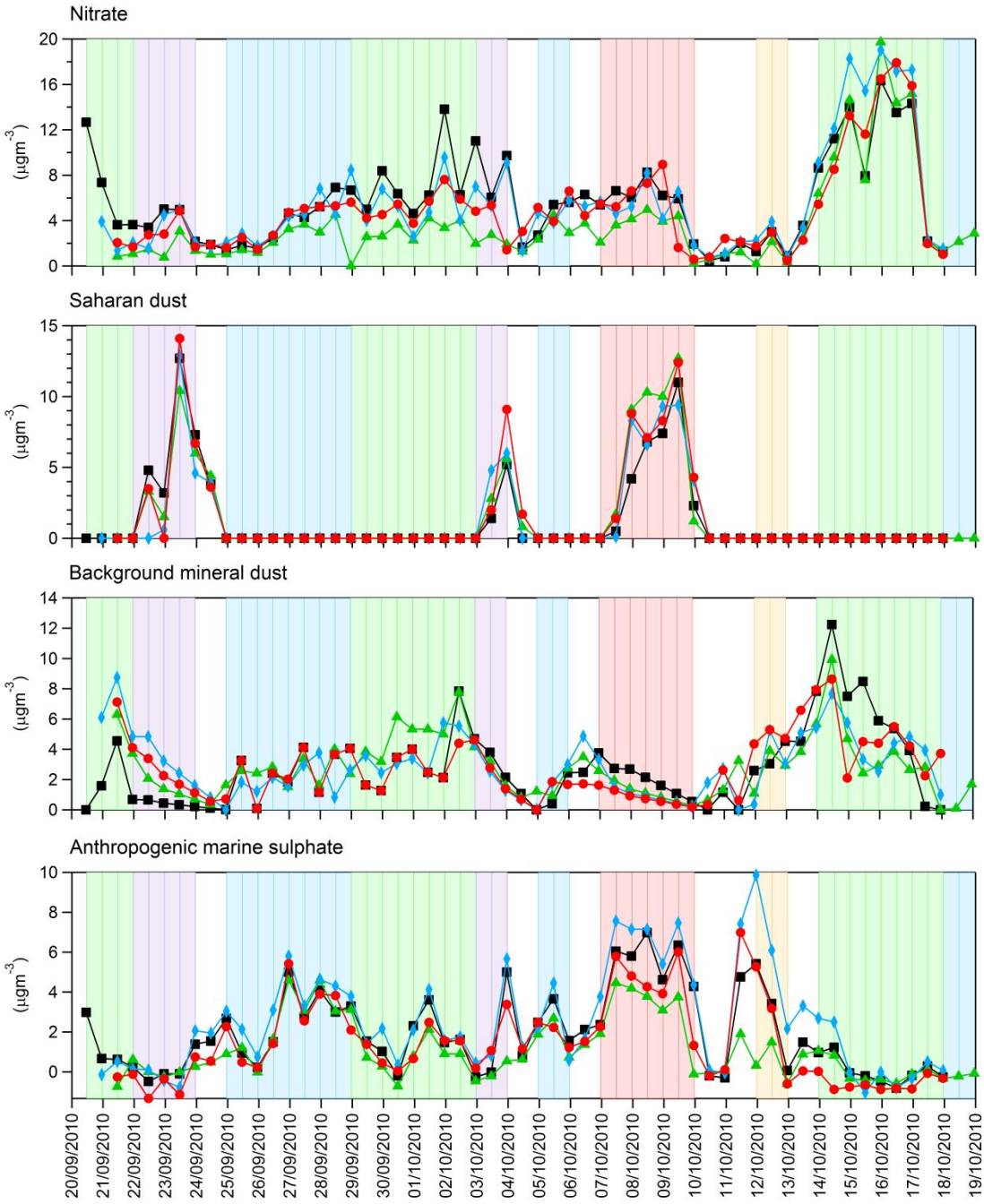

Figure 3.4.6: Temporal variation of the 8 PMF factors (vehicle exhaust and wear, road dust, mineral, marine, heavy oil, industrial, sulphate and nitrate) and the calculated contributions of Saharan dust, background mineral dust and anthropogenic marine sulphate during the study period.

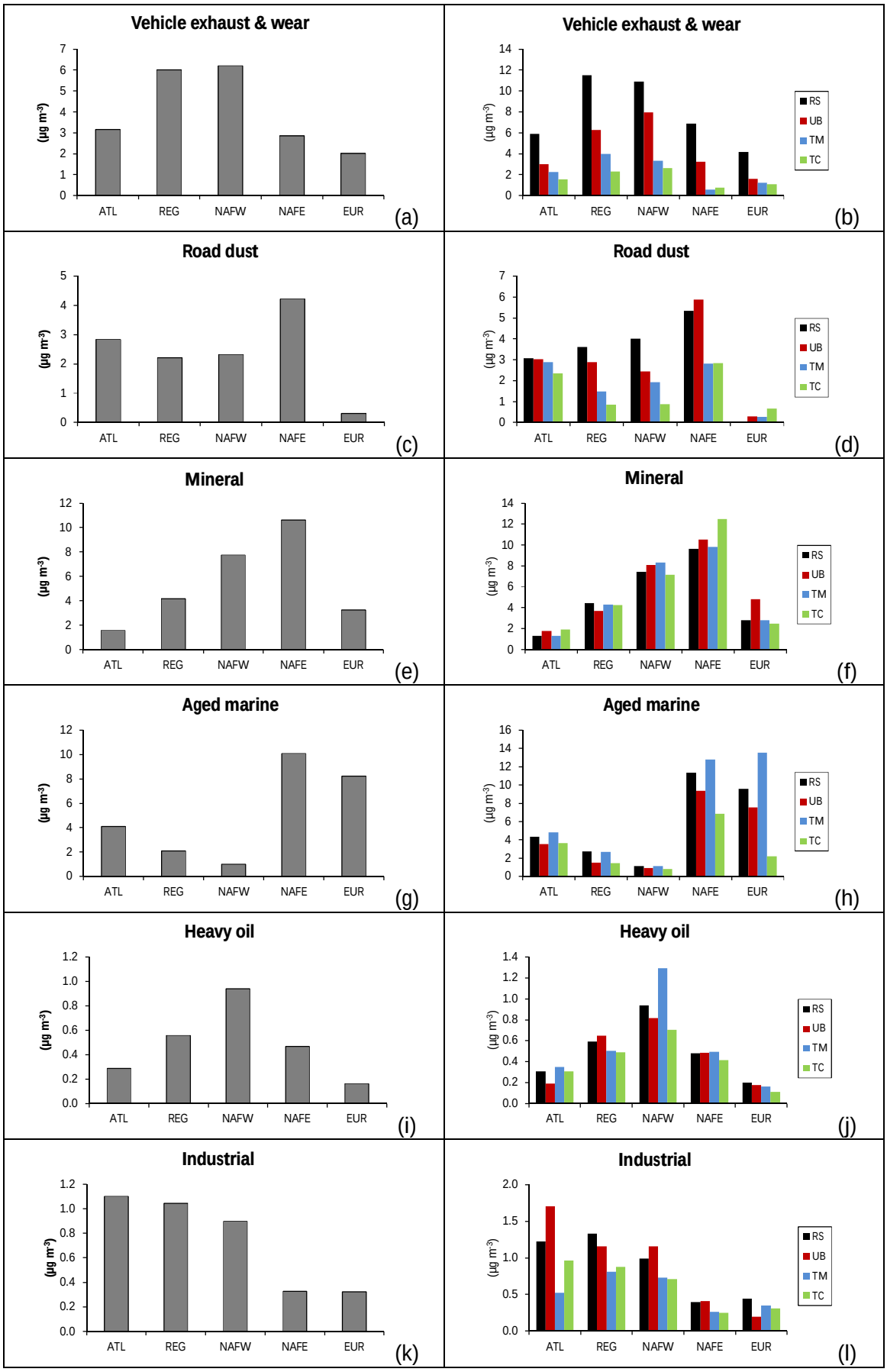
Vehicle exhaust & wear
(μg m-3)
ATL
REG
NAFW
NAFE
EUR
(a)
Vehicle exhaust & wear
RS
UB
TM
TC
(b)
Road dust
(c)
Road dust
(d)
Mineral
(e)
Mineral
(f)
Aged marine
(g)
Aged marine
(h)
Heavy oil
(i)
Heavy oil
(j)
Industrial
(k)
Industrial
(l)

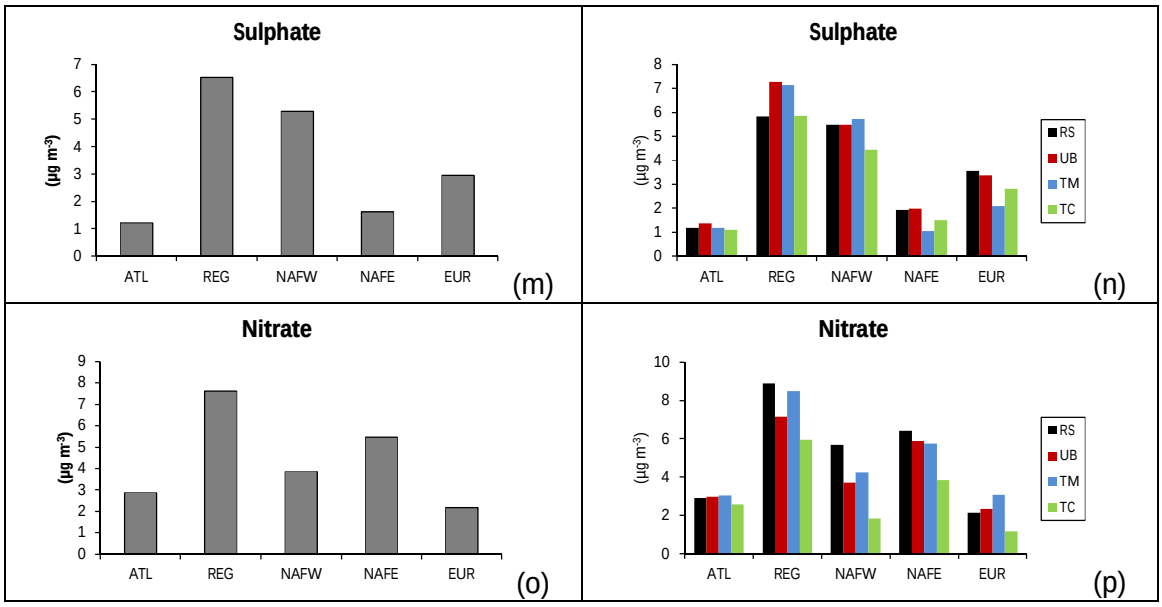

Figure 3.4.7: Average PM_{10} contributions from the eight PMF factors at each of the sites (RS, UB, TM and TC) under different atmospheric scenarios (Atlantic, ATL; Regional, REG; North African West, NAFW; North African East, NAFE and European, EUR) during the SAPUSS campaign: a) and b) Vehicle exhaust and wear, c) and d) road dust, e) and f) mineral, g) and h) marine, i) and j) heavy oil, k) and l) industrial, m) and n) sulphate, o) and p) nitrate.

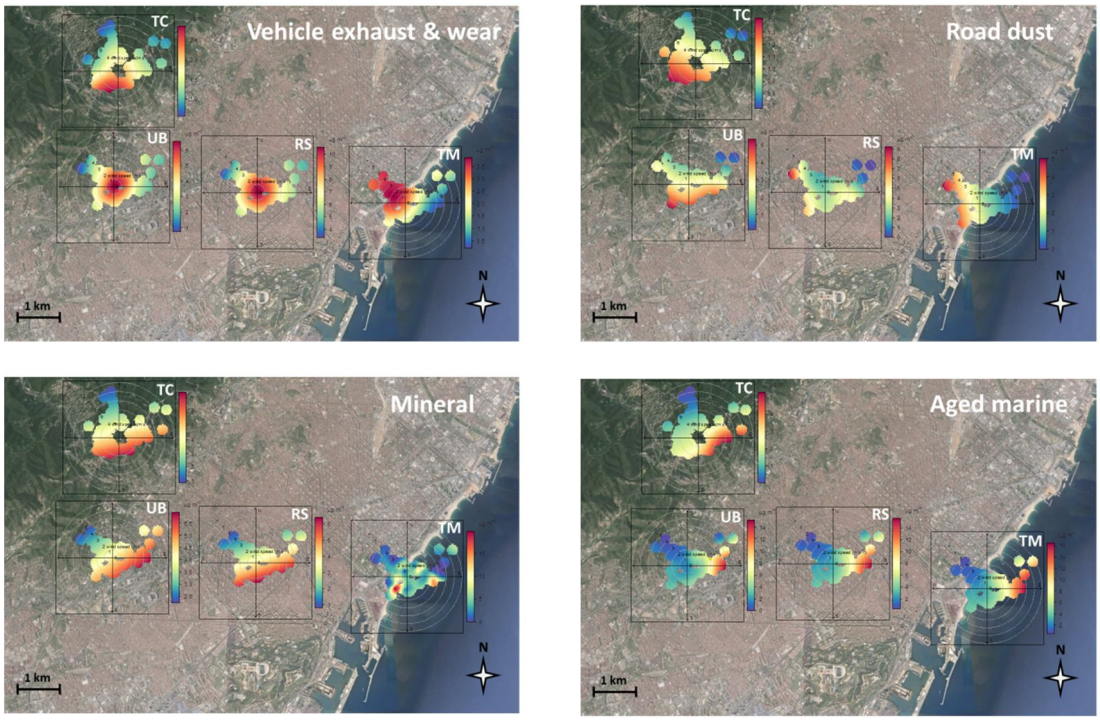

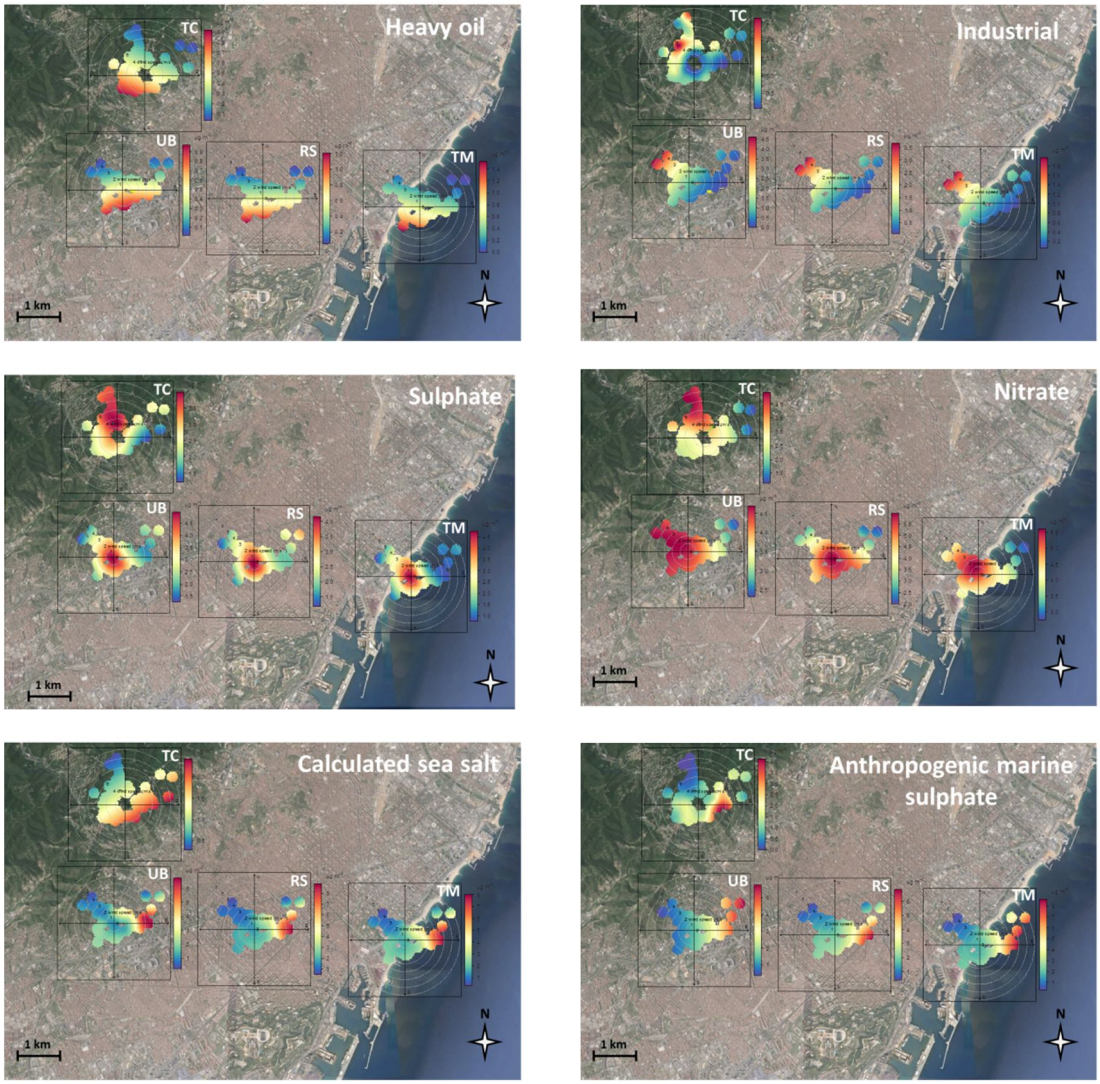

Figure 3.4.8: Polar plots representations for each of the eight PMF factor at each site, calculated sea salt and anthropogenic marine sulphate contributions. Note the different concentration scales.

3.4.3 Variability of aerosol sources across sites and ground-tower ratio

The distance to the emission source strongly influences the concentration levels of certain factors detected at the sampling sites as can be observed in Figure 3.4.5a. This is the case of the exhaust and wear and road dust factors, presenting a decreasing concentration gradient with the distance to the traffic hot spots, as the highest concentrations were found at the RS, followed by UB, TM and TC. Regarding the aged marine factor, the distance to the sea influenced the average concentrations, being highest at TM, followed by RS, UB and TC. In the case of the industrial factor, whose main source is located SW of the city, the UB was the first site impacted by this plume

as it showed the highest concentrations, followed by RS, TC and TM. On the other hand, homogeneous concentrations were recorded at the sites for mineral and heavy oil factors, evidencing that its sources affect the whole urban area. Regarding sulphate, similar concentrations were recorded at the sites, although the higher concentrations displayed at the UB site remain unexplained at this stage. Concerning nitrate, concentrations are found to decrease with the distance to traffic sources from RS to TC; however at TM higher concentrations than at UB are recorded due to the elevation of the tower site above the ground favouring the formation of particulate nitrate.

To further study the vertical variability in the factors concentration, the ratio between the average concentrations at the ground sites (RS, UB) and tower sites (TM, TC) was calculated for each factor (see Figure 3.4.5b). The highest differences were found for the exhaust and wear and road dust factors, where the concentrations at the ground sites were 2.8 and 1.8 times those at the towers, respectively. The industrial factor concentration at the ground sites were on average 1.6 times higher than at the towers, pointing towards the greater impact of the SW industrial plume on ground levels, although a contribution of the small industrial facilities spread within the city should not be discarded. On the other hand, most of the remaining factors (mineral factor, aged marine and heavy oil) showed similar contributions at ground and tower sites, whereas for sulphate and nitrate factors concentrations are slightly higher at the ground than at the tower sites, although as previously registered there is a trend to increase nitrate formation close to traffic and also with altitude.

3.4.4 Aerosol sources variability relative to air mass category

Aerosol concentrations levels of the factors were influenced by air mass origin, due to the different sources (natural and anthropogenic) and formation processes (primary or secondary) affecting the study area. REG and NAF_W air masses were related to recirculation of air masses over the study area, thus favouring the accumulation of both primary (vehicle exhaust and wear factor, industrial) and secondary pollutants (sulphate, nitrate). Air masses with an African origin (NAF_W and NAF_E) influenced mainly the mineral factor, as they transported Saharan dust that contributed to this factors loading (see Figure 3.4.7). Road dust showed the highest

concentrations during NAF_E scenarios due to the increase of its loading and subsequent resuspension. During the study period EUR air masses were related to a rainfall event, thus wet deposition caused a radical decrease in road dust concentrations under this scenario. On the other hand the aged marine factor concentrations were found to increase, due to the trajectory followed by this air mass over the Mediterranean Sea. The NAF_E air mass also crossed the WMB (see Figure 2.13), blowing easterly winds inland and also causing an increase in aged marine aerosols concentration. The high concentrations of heavy oil pollutants registered under NAF_W air mass scenarios might be similarly attributed to advected westerly winds, thus enhancing pollutants transport from their source area (located S-SW of the city area). ATL air masses were generally related to low concentrations for the different factors (due to pollutants dilution) except for the industrial factor, which might be explained similarly by the accompanying westerly winds under this scenario.

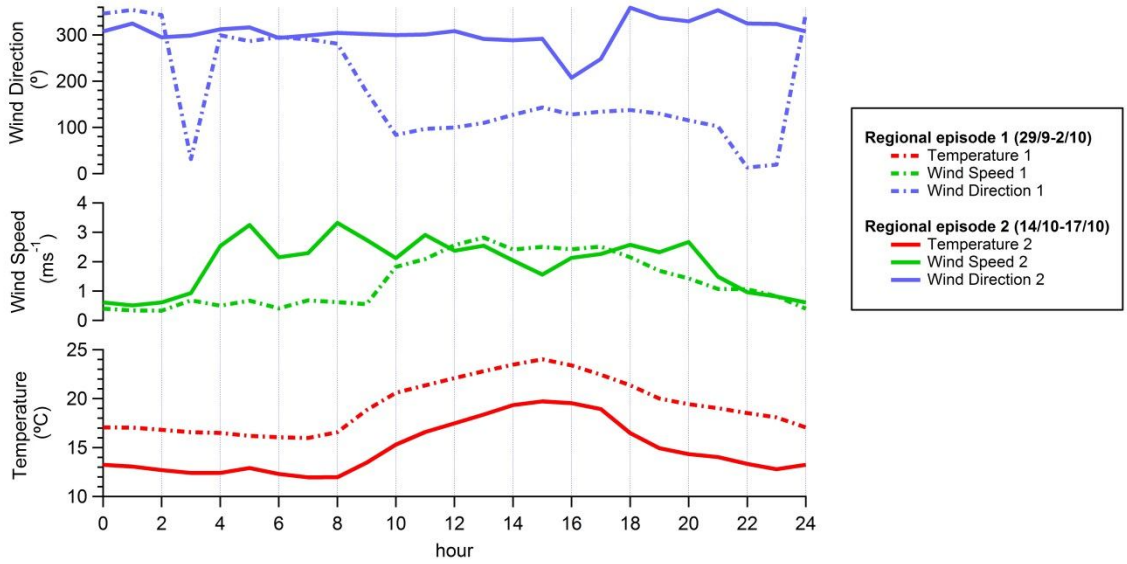

Figure 3.4.9: Average diurnal trends of temperature, wind speed and wind direction during two different regional episodes (REG_1: 29/9-2/10 and REG_2: 14/10-17/10).

3.4.5 Mineral dust sources

Mineral sources in a Mediterranean urban environment are diverse, such as road dust, Saharan dust and background dust of regional/urban origin. In order to elucidate the contributions to ambient PM_{10} concentrations a combination of several techniques were applied. The use of constraints for the source apportionment model by using pulling equations

enabled to quantify the road dust fraction of the mineral dust. The road dust factor was characterised by a clear decreasing concentrations gradient with the distance to traffic sources and it contributed with 1.6 to 3.8 μgm^{-3}.

In addition, different sources of local and regional origin add to the mineral factor loading registered in the study area (Pérez et al., 2008a; Pey et al., 2013). Following the method described in section 2.5.2.3, the average contribution of Saharan dust for the whole study period at the four sites was 2.1 μgm^{-3} (32% of the PM_{10} mineral load). Upon subtraction of the calculated Saharan dust contribution at each site, the remaining mineral loading corresponds to background mineral dust of urban or regional origin, which was 2.5 to 3.0 μgm^{-3}. This relatively narrow concentration range for the four sites (Figure 3.4.10), independently of the height and urban location points towards a regional origin of this background mineral matter.

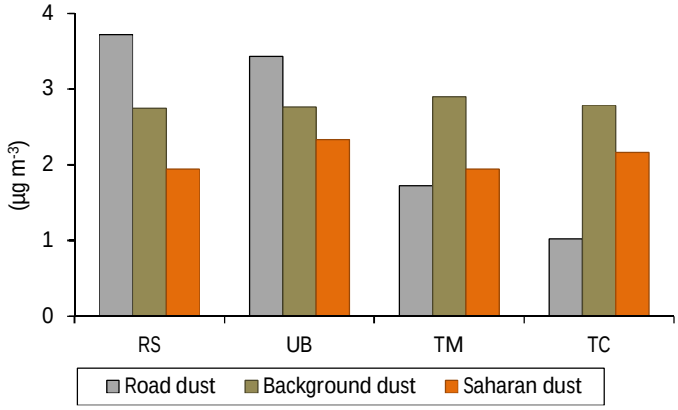

Figure 3.4.10: Average sources contributing to the mineral dust load during SAPUSS at the four monitoring sites RS, UB, TM and TC. Mineral background dust contributes on average 2.6 $\mu g\ m^{-3}$, road dust 1.6 $\mu g\ m^{-3}$ and Saharan dust 2.4 $\mu g\ m^{-3}$.

3.4.6 Sea salt aerosols

Sea salt has a primary and natural origin. However, due to the high impact of anthropogenic activities on the WMB and the frequent recirculation of regional polluted air masses on the region, an interaction between natural and anthropogenic sources was expected (Querol et al., 2009a). Indeed, 22% of the variability of SO_4^{2-} was attributed to the aged marine factor (Figure 3.4.4, Table 3.4.3), therefore evidencing that this factor was internally mixed with anthropogenic pollutants.

The stoichiometrically calculated sea salt concentration for each sample was obtained following the methodology explained in section 2.5.2.3. The difference in

concentration for each sample of the aged marine PMF factor and the calculated sea salt allowed the identification of the anthropogenic marine sulphate contribution, which has a regional origin. Therefore, the PMF marine factor (2.6-5.2 μgm^{-3}) could be broken down into calculated sea salt (1.5-2.7 μgm^{-3}, 51-59%) and anthropogenic marine sulphate of regional origin (1.1-2.5 μgm^{-3}, 41-49%).

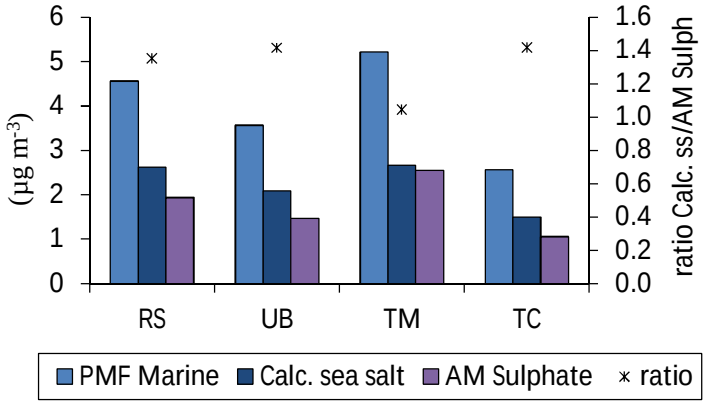

Figure 3.4.11: Average sources contributing to the sea salt factor during SAPUSS at the four monitoring sites RS, UB, TM and TC. Calculated sea salt contributes on average 2.2 $\mu g\ m^{-3}$ and marine sulphate from regional pollution 1.8 $\mu g\ m^{-3}$.

These results evidence that both the calculated sea salt and the anthropogenic marine sulphate aerosols contributed in a similar proportion to the aged marine factor (Figure 3.4.11). The marine sulphate of anthropogenic origin derived from the aged marine factor shows a different origin to the PMF sulphate factor. As can be seen in Figure 3.4.8 the highest concentrations of anthropogenic marine sulphate were recorded under eastern winds at all sites, whereas for the PMF sulphate factor no dominant wind direction was found. Namely, the highest sulphate factor concentrations were recorded under REG air masses while the anthropogenic marine sulphate shows relatively low concentrations. Conversely, under NAF_E air masses the marine sulphate of regional origin shows the highest concentrations, contrarily to the secondary sulphate factor (Figure 3.4.6).

Chapter 4

Discussion

4. Discussion

4.1 Ultrafine particles

Ultrafine particles are very numerous in the urban atmosphere, mainly related with road traffic emissions (Kumar et al., 2014). However, several other sources have been identified to affect these environments (e.g. new particle formation due to photochemical nucleation processes), especially those located in highly insolated regions (Reche et al., 2011). The dynamism of UFP in the urban atmosphere accounts for a high variability in their physical and chemical characteristics, influenced mainly by the transformation processes related with the changing atmospheric conditions or interactions with pre-existing particles and/or gaseous pollutants. The simultaneous sampling of size distributions at four sites in Barcelona during the intensive SAPUSS campaign enables an in depth discussion of the evolution of UFP (grouped in cluster categories) over the urban environment of Barcelona (section 4.1.1). In section 4.1.2 the relationship between primary traffic emissions sampled during SAPUSS and meteorological factors is analysed, due to the fundamental role the variation of this parameters plays on UFP formation and evolution. Using the data sampled during the intensive campaign the correlations of the cluster categories N with air quality parameters are investigated in section 4.1.3. The similar climatic features (e.g. high solar radiation) encountered in many worldwide regions shared with the Mediterranean climate areas influence the atmospheric processes governing aerosol evolution. Therefore, the analysis and comparison of long-term aerosol size distributions sampled in high insolation urban environments enable the study of the common sources and processes affecting such areas, especially urban nucleation events (section 4.1.4). Finally, the main sources affecting the studied urban environments are discussed, with a special focus on the photochemical nucleation events, their types and characteristics in such environments (section 4.1.5).

4.1.1 Evolution of ultrafine particles size distribution in the urban atmosphere of Barcelona during SAPUSS

The results presented in section 3.1 were expected in the sense that the monitoring sites closest to traffic pollution are the ones most influenced by vehicle exhaust emissions (Traffic *k*-means category). In contrast, when moving away from the city centre, the particle size distributions are mainly described by the *k*-means clusters representative of the background conditions (Background Pollution *k*-means category). The dominant clusters at RS_{site} (T_{clus_1} and T_{clus_2}) show very similar size modes in the nucleation and Aitken sizes, centred between 20-35 nm and typical of roadside aerosol size distributions (Charron and Harrison, 2003; Dall'Osto et al., 2011b; Rönkkö et al., 2007) . The finest mode (23±1 nm for T_{clus_1} and 24±1 nm for T_{clus_2}) is well defined (Figure 3.1.2a, b) and can be attributed to particles generated from vehicle exhaust emissions. The Aitken modes, peaking at 33±6 nm and 34±1 nm (T_{clus_1} and T_{clus_2}, respectively), are broader than the nucleation ones (see Figure 3.1.2a, b). This mode is somehow in between the position of the modes at around 20 nm associated with nucleation mode particles generated during dilution of diesel exhaust emissions (Ntziachristos et al., 2007) and at around 50-60 nm corresponding to solid carbonaceous particles from diesel exhaust (Harrison et al., 2011; Shi et al., 2000). Out of the two Traffic clusters at RS_{site}, T_{clus_2} reflects the traffic rush hour diurnal variation (Figure 3.1.3c) and is therefore more representative of fresh vehicle exhaust emissions. By contrast, T_{clus_1} is seen mainly during day time (Figure 3.1.3b) and is more affected by other sources and meteorological conditions (lower RH). T_{clus_1} has a wider nucleation mode area (21%, see Table 3.1.2) whilst T_{clus_2} shows a higher dominance of the Aitken mode (96% of the total area).

When moving away from the traffic hot spot emission sources (RS_{site}), the aerosol size distributions describing such sources showed a strikingly different aerosol size mode. This is well seen in our study of cluster T_{clus_3}, which is the one that best describes the diluted traffic conditions detected at the urban background sites (UB_{site} and TC_{site}). In this case, the nucleation mode peak is found reduced in diameter by 25% (at 15 nm) relative to the nucleation mode detected at the RS_{site}. Moreover, there is a loss of area under the nucleation mode (Figure 3.1.1) which also means a loss of

particle number within the 15-228 nm size range. This suggests that primary particles originating close to traffic sources (around 20 nm mode, like T_{clus_1} and T_{clus_2} nucleation mode peaks) can reduce their sizes by evaporation processes during advection to the urban background site, thus leading to a shift towards smaller size modes (Dall'Osto et al., 2011b; Harrison et al., 2012). On the other hand, the modal diameter of the Aitken mode of cluster T_{clus_3} (42 nm) is larger than the other two traffic clusters (33 nm for T_{clus_1} and 34 nm for T_{clus_2}), suggesting that coagulation and condensation can occur on the Aitken mode. This shows that fine OC mode aerosols (more volatile) tend to evaporate whereas the solid EC aerosols (more stable) do not (Dall'Osto et al., 2011b; Harrison et al., 2012).

The size distribution of cluster UB_{clus_1} suggests that it contains evaporating aerosols (nucleation peak located at 16 nm) but also aged aerosols with an anthropogenic origin (Aitken peak at 53 nm). The latter may also represent the involatile solid graphite particles in vehicle exhaust (Harrison et al., 2011). This cluster describes the urban background pollution, which can reach the suburban (TC_{site}) and regional monitoring (RB_{site}) sites during the afternoon sea breeze circulation (Dall'Osto et al., 2013a). An example of this aerosol transport and evolution of size distributions can be seen for day 28th September 2010 (Table 4.1.1, Figure 4.1.1).

Table 4.1.1: Hourly k-means cluster size distributions for daylight hours of 28th of September 2010 at the four monitoring sites (RS_{site}, UB_{site}, TC_{site}, RB_{site}).

Time	RS_{site}	UB_{site}	TC_{site}	RB_{site}
28/09/2010 08:00	T_{clus_2}	T_{clus_3}	RB_1	
28/09/2010 09:00	T_{clus_2}	T_{clus_3}	UB_{clus_1}	
28/09/2010 10:00	T_{clus_2}	T_{clus_3}	UB_{clus_1}	
28/09/2010 11:00	T_{clus_2}	T_{clus_3}	UB_{clus_1}	
28/09/2010 12:00	T_{clus_2}	T_{clus_3}	T_{clus_3}	
28/09/2010 13:00	T_{clus_2}	T_{clus_3}	T_{clus_3}	
28/09/2010 14:00	T_{clus_1}	T_{clus_3}	NU_{clus}	
28/09/2010 15:00	T_{clus_1}	T_{clus_3}	T_{clus_3}	UB_{clus_1}
28/09/2010 16:00	T_{clus_2}	T_{clus_3}	T_{clus_3}	UB_{clus_1}
28/09/2010 17:00	T_{clus_2}	T_{clus_3}	T_{clus_3}	UB_{clus_1}
28/09/2010 18:00	T_{clus_2}		T_{clus_3}	UB_{clus_1}
28/09/2010 19:00	T_{clus_2}		T_{clus_3}	UB_{clus_1}

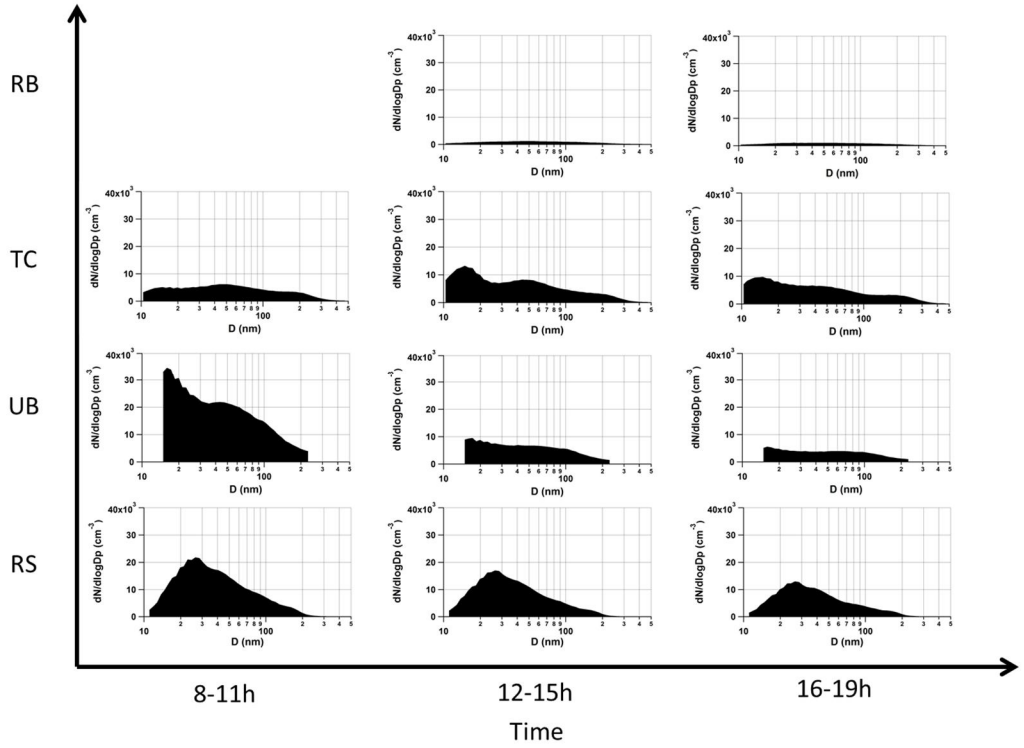

Figure 4.1.1: Aerosol size distributions at daytime during the 28th of September 2010 at the four monitoring sites (RS_{site}, UB_{site}, TC_{site}, RB_{site}).

By contrast, a very different scenario was found at the RB_{site}, dominated by background clusters (RB_{clus_1} and RB_{clus_2}). They all present much lower N in their size distributions in comparison to the Traffic clusters (Figure 3.1.1). The RB_{clus_1} cluster is found under Regional air mass conditions, it shows low N and a dominant accumulation mode, thus pointing to aged anthropogenic aerosols, typical of regional recirculation of air masses. In addition, high PM concentrations are measured for RB_{clus_1} in the urban and rural background stations.

Regarding the minor clusters, the most relevant is the Nucleation cluster, showing that photo-nucleation processes occur in urban environments in southern Mediterranean areas, primarily in urban and suburban background scenarios when the solar radiation is very intense (Dall'Osto et al., 2012; Pey et al., 2009; Reche et al., 2011). This cluster will be further discussed in section 4.1.5.2 as a result of long-term measurements of size distributions in several high insolation urban environments. The Regional Nitrate cluster appears more frequently at the RB_{site} during night time. The Mix cluster was not well defined.

4.1.2 The effect of meteorology on primary traffic emissions and secondary nucleation processes during SAPUSS

The high values of N recorded in the urban area of Barcelona can be mainly attributed to primary vehicle exhaust emissions (Pey et al., 2009). However, Reche et al. (2011) showed that in Barcelona nucleation events can occur in the middle of the day all year round, contributing to an average of 54% of total N (average of year 2009). Indeed, during SAPUSS the particle number concentrations ($N_{>5nm}$) were highly correlated with black carbon (BC, a primary marker for traffic emissions) at all monitoring sites only under strong vehicular traffic influences (Dall'Osto et al., 2013a). By contrast, under cleaner atmospheric conditions three types of nucleation and growth events were identified (regional only, regional all, urban). An in depth study of these new particle formation events during SAPUSS can be found under Dall'Osto et al. (2013a). Overall, during SAPUSS the city centre of Barcelona was found to be a source of non-volatile traffic primary particles (29-39% of $N_{>5\ nm}$), but other sources, including secondary freshly nucleated particles contributed up to 61-71% of particle number ($N_{>5nm}$) at all sites (Dall´Osto et al., 2013a).

However, previous studies considering only particles larger than 13 nm found that photochemically induced nucleation particles make only a small contribution to the total particle number concentration (2–3% of the total, Dall´Osto et al., 2012). Considering aerosol size distributions above 15 nm ($N_{>15nm}$), a small percentage of N (<2% of the total number) was associated with nucleation events, calculated by considering the percentage of time the Nucleation cluster occurred (5%, see Table 3.1.1) and the nucleation mode area in it (16%, see Table 3.1.2). In other words, within clean Atlantic air masses, nucleation processes strongly affect $N_{>5nm}$ concentrations (Reche et al., 2011; Dall´Osto et al., 2013a). However, such particles often fail to grow above the SMPS detection limit of 13 nm (Dall'Osto et al., 2012) or 15 nm (this study) in the Mediterranean urban environment.

Less is known on the effect of meteorology on freshly emitted traffic-related ultrafine aerosols in the Mediterranean region. Hence, this section aims to investigate

the effect of meteorology on primary traffic emissions. Our objective is to investigate the effect of meteorological parameters on freshly emitted particles from vehicles for a given primary traffic aerosol size distribution. For this purpose, we consider only the traffic hot spot monitoring site (RS_{site}). We therefore monitor a specific SMPS cluster (T_{clus_2}, Figure 3.1.1) which best represents traffic emissions and also shows a good correlation with traffic counts at the RS reported in the SAPUSS overview (R^2 = 0.9; Dall'Osto et al., 2013a). We additionally removed from this analysis the days dominated by nucleation events (25th September, 5th October, 17th October 2010) and rain episodes (11th October 2010), thus obtaining a homogeneous dataset representative of the average fresh traffic emissions (26 days in total). In other words, we only considered hourly data characterised by a specific aerosol size distribution (SMPS cluster T_{clus_2}) sampled in a road site hot spot (RS_{site}). This is a unique query which allows us to study how meteorological parameters affect the total N (measured by CPC, $N_{5\text{-}1000nm}$) for a given aerosol size distributions (measured by an SMPS, $N_{15\text{-}228nm}$).

In order to do so, we plotted the ratio of N measured by the CPC ($N_{>5nm}$) and the SMPS ($N_{15\text{-}228nm}$) deployed at the road site (RS_{site}) versus key meteorological parameters (Wind Speed, Solar Radiation, Temperature and Relative Humidity). The ratio $N_{>5nm}/N_{15\text{-}228nm}$ accounts for particles with diameters mainly between 5 and 15 nm. Perhaps surprisingly, no meteorological variable was found to give a significant correlation with the total particle number ratio, despite earlier studies (e.g. Charron and Harrison, 2003) finding an inverse relationship to temperature, and a positive relationship with wind speed. It therefore appears likely that other factors such as the road traffic composition and local condensation sink are more important in influencing the nanoparticle number concentration at the RS_{site}. Figure 4.1.2 shows hourly values of RH versus $N_{5\text{-}1000}/N_{15\text{-}228}$, were the solid circle points are also coloured as a function of the air mass origin (ATL, REG, NAF_W and NAF_E).

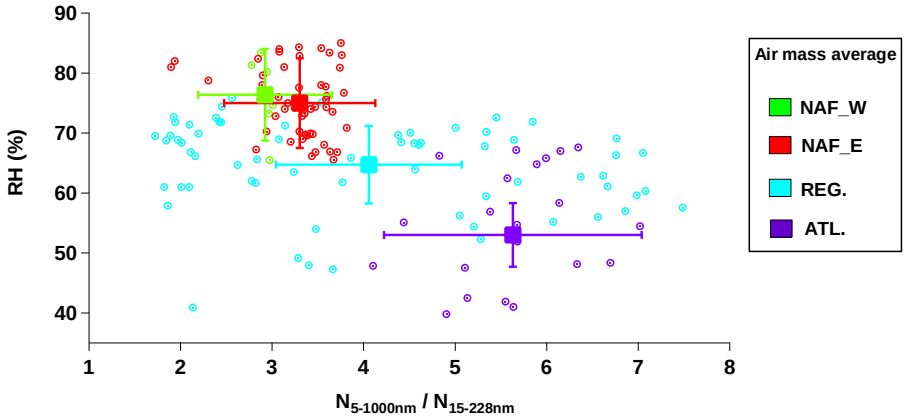

Figure 4.1.2: Particle number concentration ratio of $N_{5\text{-}1000nm}$/ $N_{15\text{-}228nm}$ versus relative humidity (RH). Colour plot indicates the four different air mass types encountered. Please note that only hourly data characterised by a specific size distributions (Traffic 2) at a specific hot spot road site (RS_{site}) are considered in this analysis. Regional nucleation and raining event days are not taken into account.

Figure 4.1.2 suggests that for a specific aerosol size distribution associated with primary traffic emissions (T_{clus_2}), there is a very high variability of ultrafine particles in the range 5-15 nm. However, the trend is not significant (R^2<0.1) for the hourly values (Figure 4.1.2). These findings highlight the difficulty of establishing meaningful standards for vehicle emissions based upon particle number concentration given the highly remarkable dynamics of traffic related particles in the urban atmosphere (Dall'Osto et al., 2011b; Fujitani et al., 2012; Li et al., 2013).

4.1.3 Correlations of N with air quality parameters during SAPUSS

The current European directive on air quality (2008/50/CE) is based on particle mass although mass concentration limit values do not protect against high N (Atkinson et al., 2010). Figure 4.1.3 shows several plots of $N_{15\text{-}30nm}$ and $N_{15\text{-}228nm}$ versus selected air pollutant concentrations (NO_2, BC, $PM_{2.5}$ and $PM_{2.5\text{-}10}$). Each point shows the average value of N_x versus an average of a specific air quality parameter for each of the *k*-means clusters obtained at each monitoring site. Average parameters that presented less than 30 total counts for each *k*-mean cluster were omitted from the diagrams presented in Figure 4.1.3. Figure 4.1.3 shows that the current SMPS SAPUSS datasets can be greatly simplified, allowing a better description of the airborne particle number concentrations and their correlations with other air quality parameters.

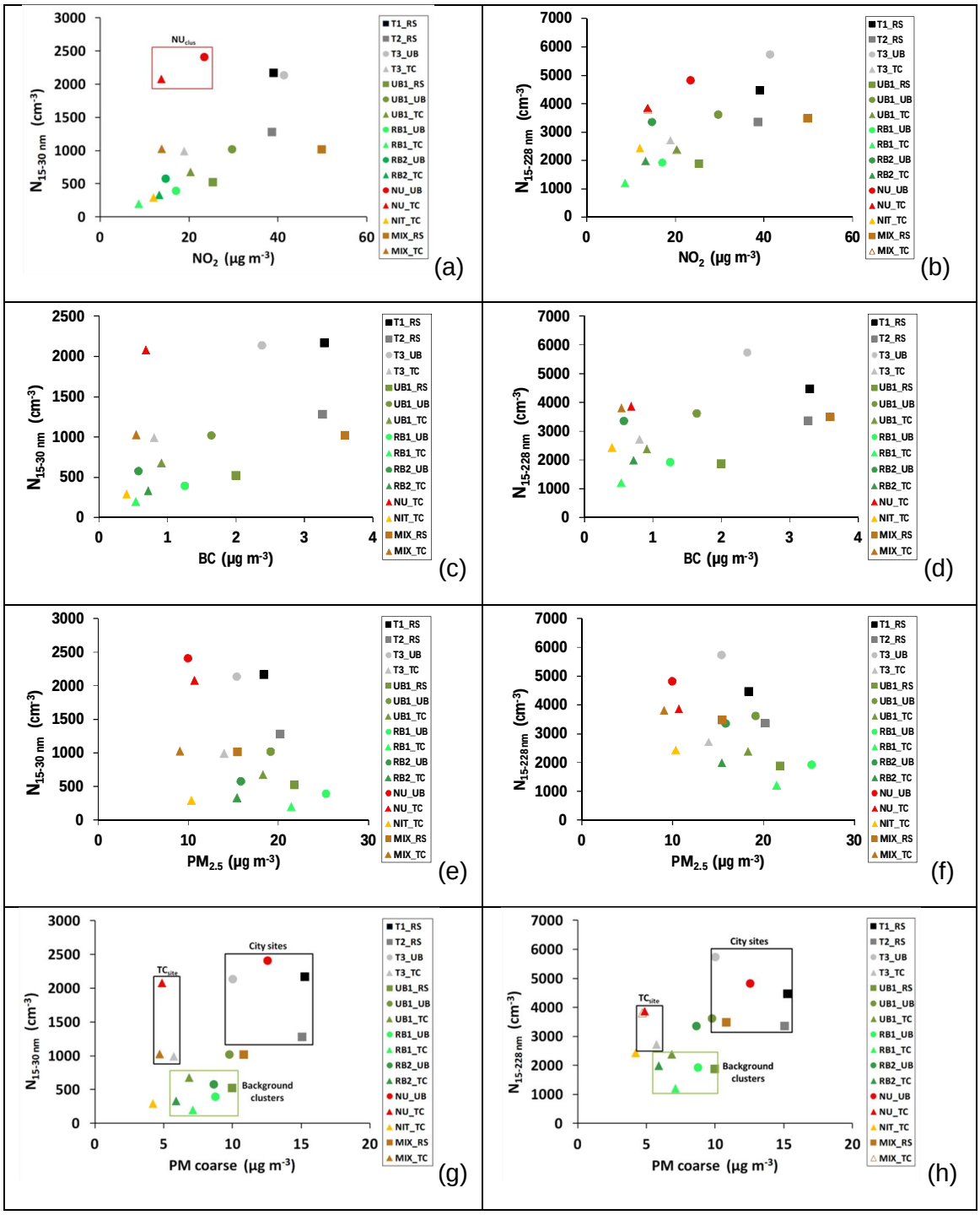

Figure 4.1.3: Regressions of particle number concentration (N) against air quality parameters and other pollutants. The "Traffic" *k*-means cluster category at all monitoring sites is represented with grey-black dots, the "Background" *k*-means cluster category is coloured in green (light and dark) and the "special cases" *k*-means cluster category in brown (light and dark).: a) $N_{15\text{-}30\ nm}$ vs NO_2, b) $N_{15\text{-}228\ nm}$ vs NO_2, c) $N_{15\text{-}30\ nm}$ vs BC, d) $N_{15\text{-}228\ nm}$ vs BC, e) $N_{15\text{-}30\ nm}$ vs $PM_{2.5}$, f) $N_{15\text{-}228\ nm}$ vs $PM_{2.5}$, g) $N_{15\text{-}30\ nm}$ vs PM_{coarse}, h) $N_{15\text{-}228\ nm}$ vs PM_{coarse}. PM_{coarse} refers to the fraction PM_{10}-$PM_{2.5}$. N concentrations are calculated from the SMPS data.

Figure 4.1.3a and 4.1.3b shows the NO_2 concentrations correlating with N, given that the most polluted clusters are the Traffic ones (black spots), followed by UB_{clus_1},

RB_{clus_1} and RB_{clus_2}. It should be noted that the main difference between N_{15-30} / NO_2 and N_{15-228} / NO_2 is given by the location of the NU_{clus}. These clusters show a high average N (2000-2500 cm^{-3}) but an intermediate NO_2 concentration (15-25 µg m^{-3}), confirming nucleation events are a source of N not directly related to primary traffic emissions (Dall'Osto et al., 2013b). A similar conclusion - although less clear - can be drawn if BC is used as an air quality parameter (Figure 4.1.3c, 4.1.3d). The same applies to CO (although not shown). $PM_{2.5}$ is regulated by the 2008/50/CE Directive. Figure 4.1.3e and 4.1.3f show that RB_{clus_1} and RB_{clus_2} clusters are the ones that recorded the highest $PM_{2.5}$ levels and lower N concentrations in both cases. UB_{clus_1}, T_{clus_1-3} and NU_{clus} show lower $PM_{2.5}$ and higher N concentrations progressively, this trend being clearer for the total fraction $N_{15-228nm}$ (Figure 4.1.3f). Figures 4.1.3g and 4.1.3h show the corresponding graphs for PM_{coarse}, the mass concentration of PM between 2.5 and 10 µm. Both figures clearly show three main groups: a first one enclosing the city monitoring sites (UB_{site}, RS_{site}), a second one associated with the background hill urban site (TC_{site}) and a third one containing Background Pollution clusters. In both figures, the Traffic and Nucleation clusters associated with the city sites (UB_{site}, RS_{site}) are located at the top right corner. When considering the same clusters but for TC_{site}, although they still show high N, they contain less coarse particles than at the RS_{site} and UB_{site}, implying the city is a source of urban dust coarse aerosols not found in the background monitoring sites. This clearly suggests that the coarse dust detected in the city mostly arises from anthropogenic sources found in the city (UB_{site}, RS_{site}) but not in the suburban areas (TC_{site}). The discussion regarding the coarse fraction will be further developed in section 4.2.2. Finally, in the bottom part of the graphs we find the Regional Background clusters. They show low values of N and moderate values of coarse particle mass.

4.1.4 Ultrafine particles sources in 5 high insolation urban environments

The study of the evolution of UFP in the previous sections provides a deeper knowledge of the dynamics of UFP in a typical Mediterranean urban environment. However, to fully apportion the sources and processes affecting such environments, longer sampling periods are needed, due to the seasonal variability affecting sources and processes of UFP. Therefore in this section we will focus on the discussion of the

results presented in section 3.2. The clustering results for the cities of BCN, MAD and BNE (representative of high insolation urban environments) can be summarised and simplified in three main categories:

- Traffic: this category includes all clusters directly related to traffic emission sources. It contains 3 subcategories (Traffic 1-Traffic 3) ranging from fresh traffic emissions to aerosols that have been affected by atmospheric processes after emission, such as coagulation, condensation or evaporation (Dall'Osto et al., 2011b). This is the dominant category at all sites, showing the high prevalence of traffic emissions in the ultrafine N concentration in urban background sites. This category was found to be the main one in all the studied cities, ranging from 44% in Brisbane to 63% in Barcelona (see Table 4.1.2). The average Traffic size distribution shows a main peak in the Aitken mode at 31±1 nm and a minor one in the accumulation mode at 120±2 nm (see Figure 4.1.4 and Table 4.1.3). According to vehicle emission studies, the Aitken mode corresponds with grown nucleated particles associated with the dilution of vehicle exhausts (Kittelson et al., 2006; Ntziachristos et al., 2007), while the larger mode is associated with solid carbonaceous compounds from exhausts (Shi et al., 2000; Harrison et al., 2011). The clusters included in this category are characterised by the highest levels of traffic-related pollutants, such as NO, NO_2, CO and BC. These values are usually higher for clusters T1 and T2 and decrease for T3 (see Figure 3.2.4).

- Nucleation events: they accounted for 14-19% of the hourly observations, with an average of 16% of the time, indicating nucleation as an important source of UFP in high insolation urban areas (see Table 4.1.2). The average Nucleation size distribution (Figure 4.1.4) is characterised by a high N nucleation mode peak at 17±1 nm and a lower N peak in the Aitken mode at 53±7 nm (Table 4.1.3). It occurs under intense solar irradiance, clean air conditions (high wind speed and low concentrations of CO, NO and NO_2), low relative humidity and relatively high levels of SO_2, although still low SO_2 levels in absolute concentration values (see Figure 3.2.4). It presents the highest N (12000±8000

cm^{-3}) of all categories (see Figure 4.1.4). In the case of Madrid, the nucleation peak coincides with a decrease in N at the end of the morning rush hour.

- Background pollution and Specific cases. These clusters characterise the urban background and regional background pollution of the sites. They are likely composed of a mixture of aerosol particle types with different sources and origins. The Urban Background cluster usually describes the cleanest conditions encountered at the urban sites, ranging from 6 to 22% of the time (note that this cluster is common to all sites, see Table 3.2.2). The resulting average spectra for all Urban Background clusters (Figure 4.1.4) show a trimodal size distribution, with two peaks in the Aitken mode (at 38±3 nm and 72±2 nm) and a minor one in the accumulation mode at 168±14 nm, reflecting aged aerosols mostly of an anthropogenic origin (see Table 4.1.2). Specific cases were associated with "Nitrate" containing aerosol particles, "Growth" of new particle formation events and “Summer Background” conditions. The Nitrate cluster was observed in Madrid and Barcelona, the Summer Background was typical of Madrid, whereas the Growth clusters were only seen in Brisbane. Each cluster represents around 10% of the time at their respective sites (see Table 3.2.2). The difference in the Nitrate size distributions of Barcelona and Madrid might be due to the urban site characteristics of this cluster in Barcelona, while in Madrid it is also enriched with Background clusters (see Figure 3.2.1b-c). The Growth clusters reflect the size mode increase of nucleation particles due to subsequent growth (see Table 3.2.1), since they are recorded after nucleation episodes. The Summer Background reflects the lower pollution levels recorded during summer in Madrid.

Table 4.1.2: Cluster categories (Traffic, Nucleation, Background and Specific case (SC)) and their occurrence at the main sites.

Category	Barcelona	Madrid	Brisbane
Traffic	63%	58%	44%
Nucleation	15%	19%	14%
Background and SC	22%	23%	42%
	100%	100%	100%

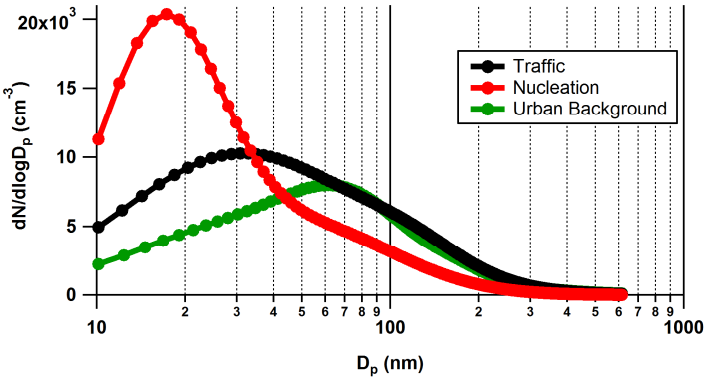

Figure 4.1.4: Average aerosol size distributions for the main *k*-Means cluster category: Traffic, Nucleation and Urban Background. Only the main cities BCN, MAD and BNE were considered.

Table 4.1.3: *k*-Means cluster categories average size distribution size mode peaks and corresponding area percentage. Only the main cities BCN, MAD and BNE were considered. Note the 2 Aitken modes for Urban Background.

Category	Nucleation	Aitken	Accumulation
Traffic	-	31±1 nm (86%)	120±2 nm (14%)
Nucleation	17±1 nm (43%)	53±7 nm (57%)	-
Urban Background	-	38±3 nm (71%), 72±2 nm (25%)	168±14 nm (4%)

4.1.5 Main sources of ultrafine particles in high insolation developed urban environments

4.1.5.1 Road traffic emissions

As previously discussed in section 4.1.4, traffic is a main source of UFP in the urban atmosphere, accounting for 44-63% of the time. The quantified particle number concentration contribution of motor vehicle emissions was also the major source in other urban locations: 47.9% in Beijing (Liu et al., 2014), 69% in Barcelona (Pey et al., 2009; Dall´Osto et al., 2012), 65% in London (Harrison et al., 2011; Beddows et al., 2015), 69% in Helsinki (Wegner et al., 2012), 42% in Pittsburgh and 45% in Rochester (Woo et al., 2001; Stanier et al.,2004). Recent source contributions of ultrafine particles in the Eastern United States also identified gasoline automobiles being responsible for 40% of the ultrafine particle number emissions, followed by industrial sources (33%), non-road diesel (16%), on-road diesel (10%), and 1% from biomass burning and dust (Posner and Pandis, 2015). Vehicle emissions consist of hot gases and

primary particles, which are a highly dynamic and reactive in nature mixture (Kumar et al., 2011), resulting in rapid physical and chemical transformations of the emitted particles following atmospheric dilution and cooling. There is a need for more field studies to map traffic related particle number concentrations and to understand the particle dynamics and their dispersion in urban areas (Goel and Kumar, 2014).

4.1.5.2 Photochemical nucleation

Secondary nucleation processes attain for a relevant contribution to UFP, overall dominating the size distribution for 16% of the time on average, resulting in the second major source of ultrafine particles in the urban atmosphere of the developed urban areas herein presented (see section 4.1.4). Overall, this represented on average 21% of total N (Barcelona 22%, Madrid 13% and Brisbane 28% of total N). The evolution of photochemically newly formed particles in urban environments does not follow the same patterns as in regional ones, which usually show a banana-shape (Kulmala et al., 2004). Figure 4.1.5 shows that new particle formation events in high-insolation urban environments often fail to grow to sizes larger than 30-40 nm (Figure 4.1.5a-c). Further growth of these nucleated particles in urban environments following a banana-like shape is probably constrained by the decrease in solar radiation intensity and the prevalence of traffic emitted particles in the evening.

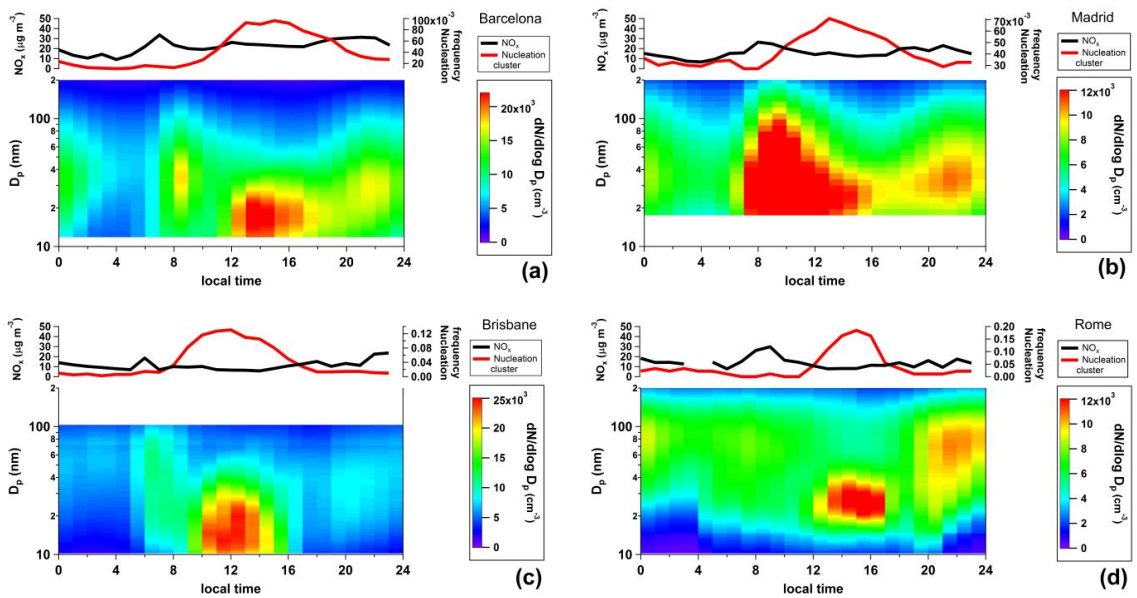

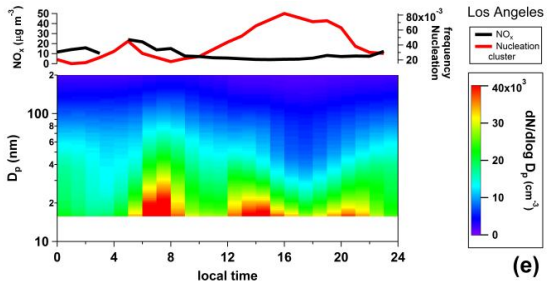

Figure 4.1.5: Mean SMPS size distributions on a nucleation day at each selected city, NO_x average concentration and the frequency of occurrence of the Nucleation cluster for: a) Barcelona, b) Madrid, c) Brisbane, d) Rome and e) Los Angeles. Please note that NO_x concentrations for Madrid represent $NO_x/2$ and for Los Angeles $NO_x/10$. These values are 30-65% lower on nucleation days than the corresponding sampling period average levels.

Although only three months of data are available, the same conclusion can be extracted from the urban Los Angeles site, whereas aged nucleated particles downwind of Rome (20-40 nm) reach the Rome regional site in the early afternoon (Figure 4.1.5d-e). Figure 4.1.6 shows aerosol size distribution data collected in Barcelona, Madrid and Brisbane during the days when nucleation events were detected (as *k*-Means cluster NU). Additionally, temperature, relativity humidity, solar radiation and nitrogen oxide gaseous concentrations are plotted. A clear burst of particles can be seen at midday when gaseous pollutants are diluted and maximum insolation occurs.

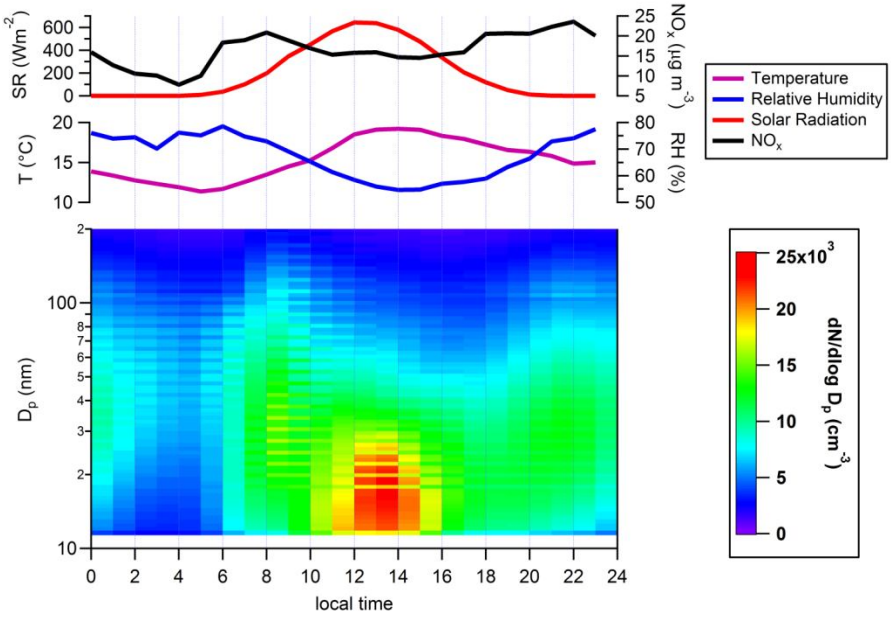

Figure 4.1.6: Daily average N size distribution, temperature, relative humidity, solar radiation and NO_x levels on a nucleation day using data from Barcelona, Madrid and Brisbane.

It is common in the literature to refer to the frequency of nucleation events as the percentage of days such an event has been detected. The size distribution time series need to be visually inspected to certify that a distinct new mode starting in the nucleation range appears, that the mode prevails over some hours and that it shows signs of growth (Dal Maso et al., 2005). This methodology has been proven to be very useful to detect "banana-like" nucleation events, where distinct nucleation events and subsequent particle growth can be observed. However, this is not the most common nucleation event type detected in the studied urban environments, where an increase in the particle condensation sink due to traffic emissions might constrain the growth of nucleated particles. Instead, nucleation events consist of particle bursts lasting for 3-4 hours with particle growth limited to 20-40 nm (see Figures 4.1.5 and 4.1.6). Therefore, to adapt this methodology to our current scenario, the percentage of days that presented nucleation events were classified considering the prevalence of the Nucleation cluster from 2 up to 4 consecutive hours for each site. The results were found to be very homogeneous among the main sampling sites (see Table 4.1.5). Nucleation events were detected for 53-58% of the days lasting for two hours or more, decreasing to 37-43% for 3 hours or more and 27-30% for 4 hours or more. The decrease in occurrence of long nucleation events is a consequence of the limitation for nucleated particles to grow in high-insolation urban environments. Interrupted nucleation events were not considered, which may have led to slightly higher occurrence if considered.

Table 4.1.5: Percentage of nucleation event days at the main cities BCN, MAD and BNE, and the uninterrupted time prevalence of these events.

City	2 h or more	3 h or more	4 h or more
Barcelona	54%	43%	28%
Madrid	58%	41%	30%
Brisbane	53%	37%	27%

It is important to remember that nucleation events in Northern European urban areas are found to be infrequent. In the Helsinki urban atmosphere they are usually observed during noon hours with a maximum during spring and autumn (Hussein et al., 2008), and overall representing only about 2% of the time (Wegner et al., 2012).

Additionally, these events were regional because they were observed at Hyytiälä (250 km north of Helsinki). By contrast, in Southern Europe, Reche et al. (2011) showed that new particle formation events occur more frequently than in Northern Europe. However, only N was reported in that study, making it harder to link aerosol sources and processes. Nonetheless, this study clearly shows how new particle formation events impact the urban areas studied. In order to discuss this further, we link our discussion to that reported in (Dall'Osto et al., 2013b). At least two main different main types of new particle formation events can be seen in the Mediterranean urban environment:

(1) A regional type event, originating over the whole study region and impacting almost simultaneously the city and the surrounding urban background area;

(2) An urban type event, which originates only within the city centre but whose growth continues while transported away from the city to the regional background.

The main difference between these two types resides in the origin of the nucleation events (regional scale in type 1 and urban origin in type 2). Moreover, the regional events are found to start earlier in the morning than the urban type and usually display the typical banana shape implying that photochemically nucleated particles experience subsequent growth. On the other hand, the urban type nucleated particles experience less growth, reaching sizes of 30-40 nm, as clearly shown in Figure 4.1.6.

The city of Brisbane exhibits new particle formation events starting in the morning (see Figure 4.1.5c), similar to the regional nucleation event types discussed in Dall´Osto et al. (2013b) as they are often followed by particle growth showing a banana-shape (Cheung et al., 2011). This may be due to the fact that the Brisbane site is located in a relatively clean environment. By contrast we find that the majority of new particle formation events detected in the other cities occur under the highest solar irradiance

and thus around noon. Such events are characterised by a burst of particles lasting for about 3-4 h (Figure 4.1.5, 4.1.6), as reported in Dall´Osto et al. (2013b).

It should be noted that many urban areas exposed to high insolation are also characterised by high condensation sinks. This is the case of many developing urban areas, where new particle formation events are limited. For example, particle bursts in the nucleation mode size range (5-25 nm), followed by a sustained growth in size were observed very rarely (only 5 out of 79 observation days) in a tropical Southern India site, less frequently than at most other locations around the world during May-July (Kanawade et al., 2014a). New particle formation at two distinct Indian sub-continental urban locations were observed with lower frequency at Kampur (14%) than that at Pune (26%), due to the presence of pre-existing large particles at the former site (Kanawade et al., 2014b). Observations of new aerosol particle formation in a tropical urban atmosphere (Betha et al., 2013) were also found to be suppressed by very high pre-existing particle concentrations during haze periods (Betha et al., 2014). Zhu et al. (2014) reported fewer new particle formation events in a severely polluted atmosphere (Qingdao, China) than in Toronto (Canada). Long-term measurements of particle number size distributions in urban Beijing and in the North China Plain showed homogeneous nucleation events characterized by the co-existence of a stronger source of precursor gases and a higher condensational sink of pre-existing aerosol particles than European cities (Wang et al., 2013a, b).

Ragettli et al. (2014) recently reported spatio-temporal variation of urban ultrafine particle number concentrations, showing that the most important predictor for all models was the suburban background UFP concentration, explaining 50% and 38% of the variability of the median and mean, respectively. Frequencies of new particle formation (NPF) events in China were much higher at urban and regional sites than at coastal sites and during open ocean cruise measurements (Peng et al., 2014). Regional nucleation events were found to occur more frequently over the weekend in urban areas (Sabaliauskas et al., 2013).

The occurrence of nucleation events has important implications because the city seems to be not only a source of primary UFP but also a driver for nucleation events

occurring only in the city. Indeed, if the daily N cycles for the five cities are considered, three distinct peaks can be clearly seen at Barcelona, Brisbane and Los Angeles, two mirroring rush hour road traffic emissions and a third one at midday reflecting NPF due to photochemical nucleation processes (Figure 4.1.7a, c, e). In the case of Madrid the nucleation peak coincides with the decrease of the morning traffic rush hour (around 12 p.m.) and in Rome a minor peak can be observed at 3 p.m. when the nucleated particles downwind of Rome reach the sampling site (Figure 4.1.7b, d, respectively).

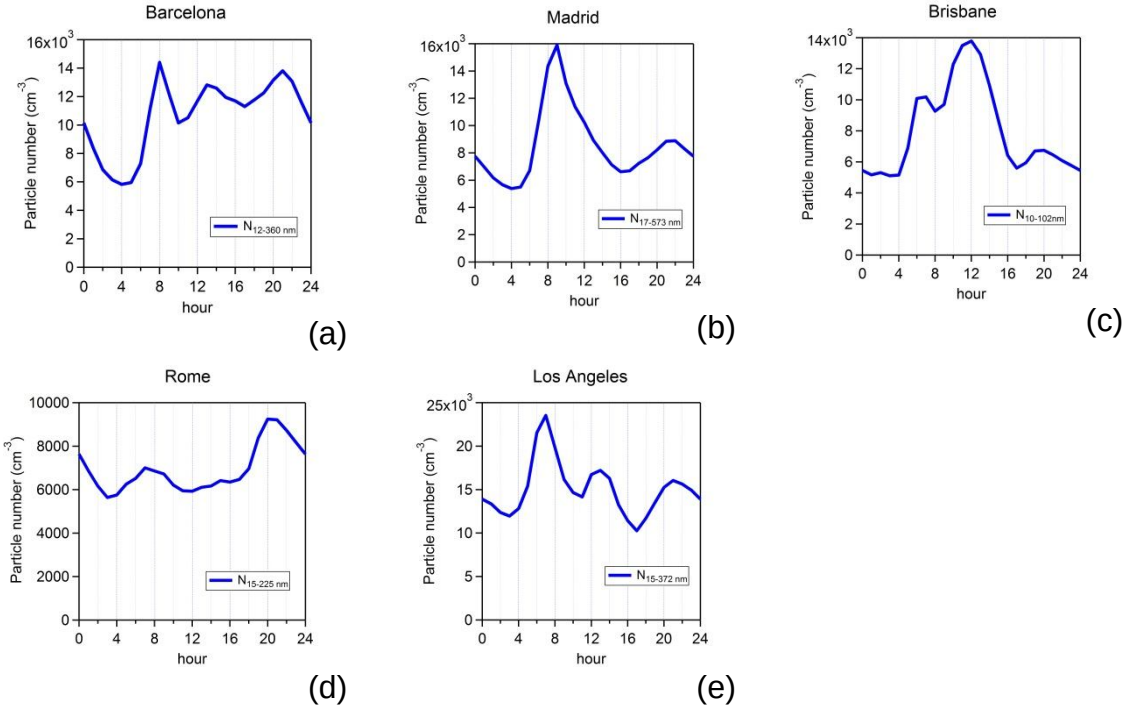

Figure 4.1.7: Average daily particle number concentration for the study periods at each city: a) Barcelona, b) Madrid, c) Brisbane, d) Rome and e) Los Angeles.

4.2 Source apportionment of fine and coarse aerosols during SAPUSS

Particulate matter in the fine and coarse fractions in an urban environment is not only apportioned by anthropogenic sources, but also by natural ones, especially in the PM_{10} fraction. The simultaneous sampling during SAPUSS at several sites within the urban environment of Barcelona enables the study of the sources evolution in horizontal (for PM_1, see section 4.2.1) and also in vertical levels (for PM_{10}, see section 4.2.2). Regarding PM_1, inorganic and organic species were analysed and a joint source apportionment study was carried out. Source factors obtained were further compared to other source apportionment studies during SAPUSS that only comprised one type of species (see section 4.2.1.1-4.2.1.3). Source apportionment of PM_{10} is discussed in section 4.2.2, focusing on the estimation of the contribution of natural and anthropogenic sources to the mineral dust and aged sea salt factors.

4.2.1 PM_1

Previous studies have reported the main sources affecting fine aerosols during the SAPUSS campaign at RS and UB sites (PM_1 organic compounds, 12 h resolution: Alier et al., 2013; $PM_{2.5}$ PIXE measurements, 1 h resolution: Dall'Osto et al. 2013c). Source apportionment methods were applied, being MCR-ALS the preferred one for the PM_1 organic and PMF for the $PM_{2.5}$ aerosols. This resulted in 6 and 9 factors respectively, representing the aerosol sources affecting each fraction. For the first time organic and inorganic species were obtained for the PM_1 fraction in the Barcelona urban environment, as previous studies had reported them separately (inorganic: Amato et al., 2009; organic: van Drooge et al. 2012). In order to investigate the different sources obtained by combining organic and inorganic compounds or treating them separately, comparative analyses were carried out (Table 4.2.1). Section 4.2.1.1 compares the sources obtained by Alier et al. (2013), which only considered organic compounds, with the present study, in which the levels of around 40 inorganic elements or species in PM_1 were specifically determined for a combined organics&inorganic source apportionment. The following section (4.2.1.2) investigates the differences between the PMF solutions for organic&inorganic compounds and only inorganic. Furthermore, Dall'Osto et al. (2013c) carried out a source apportionment study of hourly $PM_{2.5}$

concentrations of inorganic compounds, whose factors concentrations have been averaged to 12 h resolution in order to compare them with the results from this thesis (section 4.2.1.3). Finally, section 4.2.1.4 summarises the similarities and differences between the factors obtained by the different source apportionment studies.

Table 4.2.1: Comparison of source apportionment results of PM_1 organics&inorganics (this study) with MCR-ALS PM_1 Organics (Alier et al., 2013), PMF PM_1 Inorganics (this study) and PMF $PM_{2.5}$ (Dall'Osto et al., 2013c). Road Site results are shown in black while Urban Background site results are marked in blue.

	Sources	PM_1 organics&inorganics (this study)								
		PM_1 Fresh traffic	PM_1 OUM	PM_1 Nitrate	PM_1 Ind. NE&sea salt	PM_1 Ind. SW&pin	PM_1 Shipping	PM_1 SIA	PM_1 Bio SOA	PM_1 Biomass burning
PM_1 Organics (Alier et al., 2013)	POA Urban	R^2=0.86 R^2=0.92	-	-	-	-	-	-	-	-
	OOA Urban	-	R^2=0.45 R^2=0.43	-	-	-	-	-	-	-
	SOA BIO PIN	-	-	-	-	R^2=0.16 R^2=0.55	-	-	-	-
	SOA Aged	-	-	-	-	-	-	R^2=0.50 R^2=0.78	-	-
	SOA ISO	-	-	-	-	-	-	-	R^2=0.88 R^2=0.87	-
	BBOA Regional	-	-	-	-	-	-	-	-	R^2=0.88 R^2=0.94
PM_1 Inorganics (this study)	$Traffic_{\_i}$	R^2=0.47 R^2=0.58	-	-	-	-	-	-	-	-
	$Nitrate_{\_i}$	-	-	R^2=0.99 R^2=0.96	-	-	-	-	-	-
	$Shipping_{\_i}$	-	-	-	-	-	R^2=0.67 R^2=0.77	-	-	-
	Sul.&Ind. NE &aged sea $salt_{\_i}$	-	-	-	-	-	-	-	-	-
	$Ind.\ SW_{\_i}$	-	-	-	-	R^2=0.50 R^2=0.83	-	-	-	-
$PM_{2.5}$ Inorganics (Dall'Osto et al., 2013c)	Sulphate	-	-	-	-	-	-	R^2=0.32 R^2=0.38	-	-
	Sea salt	-	-	-	-	-	-	-	-	-
	Biomass burning	-	-	-	-	-	-	-	-	R^2=0.49 R^2=0.13
	Industrial	-	-	-	-	R^2=0.43 R^2=0.63	-	-	-	-
	Oil combustion	-	-	-	-	-	R^2=0.81 R^2=0.48	-	-	-
	Waste incinerator	-	-	-	-	-	-	-	-	-
	Brake dust	R^2=0.22 R^2=0.40	-	-	-	-	-	-	-	-
	Soil dust	-	-	-	-	-	-	-	-	-
	Urban dust	-	-	-	-	-	-	-	-	-

4.2.1.1 Comparison of PMF profiles of PM_1 organics & inorganics and PM_1 organics

Organic compounds in the PM_1 fraction collected at the RS and UB sites during the SAPUSS campaign have been thoroughly discussed in Alier et al. (2013). The corresponding source apportionment study yielded 6 factors contributing to the RS and UB with different intensity. They reported two main factors related to anthropogenic emissions: POA Urban, which accounted mainly for primary traffic emissions and OOA Urban, which represented a mixture of sources related to the urban lifestyle, such as traffic emissions, tobacco smoke and cooking aerosols. As expected, higher concentrations of both factors were recorded at the RS than at the UB. On the other hand, the UB site was more influenced by secondary organic aerosols, as reflected by the prevalence of SOA ISO, SOA BIO PIN and SOA Aged factors. The first two were represented by isoprene and α-pinene oxidation products, while the third reflected more oxidized products of both biogenic and anthropogenic nature. A minor factor, BBOA Regional, accounting for the biomass burning emissions was also presented.

By including both inorganic and organic compounds in the source apportionment analysis, a higher number of factors were obtained (9 factors). The majority of these factors were characterised by a mixture of organic and inorganic species, although some of them were dominated by one type.

A high similarity was found between the Fresh traffic and POA Urban factors (R^2=0.86 at the RS and R^2=0.92 at the UB, Table 4.2.1). The Fresh traffic factor contained the organic tracers of the POA Urban factor (PAHs) in addition to high EC and OC concentrations as well as Sb, Cu and Fe which are typical brake and road wear tracers (Amato et al., 2009). The organic urban mix (OUM) and OOA Urban shared organic tracers, such as PAH (related to vehicle emissions) and C_7-C_9 DCA, pointing towards cooking aerosol contribution. Additionally the nicotine signal was more relevant for the OUM (75% of the specie) compared to OOA Urban. EC and OC concentrations were also found to significantly contribute to OUM. Altogether, a good correlation was also found between the OUM and OOA Urban factors (R^2=0.45 at the RS and R^2=0.43 at the UB, Table 4.2.1).

The biomass burning factor and BBOA Regional factors were found to share an almost identical temporal trend (R^2=0.88 at the RS and R^2=0.94 at the UB, Table 4.2.1), given that the anhydro saccharids mannosan, galactosan and levoglucosan were the main species contributing to both factors.

The Bio SOA factor and the SOA Isoprene also presented a high similarity in their temporal trends (R^2=0.88 at the RS and R^2=0.87 at the UB, Table 4.2.1), as the main contributors were organic isoprene oxidation products, although an additional 30% of cis-pinonic acid was also found in the Bio SOA factor.

Regarding the SIA and SOA Aged factors, although the chemical profiles differed, both factors contained DCA linked to secondary oxidation products such as tricarballytic, 3 hidroxyglutaric, malonic and tartaric acids (R^2=0.50 at the RS and R^2=0.78 at the UB, Table 4.2.1).

The industrial SW + pinene and SOA BIO PIN factors were found to share a higher degree of similarity at the UB than at the RS (R^2=0.16 at the RS and R^2=0.55 at the UB, Table 4.2.1). This is due to the higher impact of non-traffic sources at the UB than the RS, as well as the UB being located closer to the industrial area and the Collserola park.

The nitrate, industrial NE & sea salt and shipping factors were not associated to any organic factor, mainly due to being dominated by inorganic species, especially the nitrate and shipping factors. The organic elements contributing to the industrial NE & sea salt factor were probably not strong enough to form a new factor, and thus remained distributed among the other factors.

4.2.1.2 Comparison of PMF profiles of PM_1 organics & inorganics and PM_1 inorganics

The source apportionment study for the inorganic compounds done in this study (see section 3.3.2) resulted in 5 factors: sulphate & industrial NE & aged sea $salt_{\_i}$, $traffic_{\_i}$, $nitrate_{\_i}$, $shipping_{\_i}$ and industrial $SW_{\_i}$ (Figure 3.3.5).

The factor with less contribution of organic aerosols was nitrate (see Figure 3.3.1), resulting in a very high correlation between nitrate and $nitrate_{\_i}$ factors (R^2=0.99 at the RS and R^2=0.96 at the UB, Table 4.2.1). On the other hand, the contribution of PAH and

hopanes to the fresh traffic factor differentiated it from the traffic_i factor (R^2=0.47 at the RS and R^2=0.58 at the UB, Table 4.2.1). The shipping and shipping_i factors showed a good correlation, as their components were mainly inorganic (V, Ni and SO_4^{2-}), with only a light contribution of hopanes (R^2=0.67 at the RS and R^2=0.77 at the UB, Table 4.2.1). The industrial SW_i factor showed a good correlation with the industrial SW & pin factor, especially at the UB (R^2=0.50 at the RS and R^2=0.83 at the UB, Table 4.2.1). The sulphate & industrial NE & aged sea salt_i factor was not found to correlate with any factor (see Table 4.2.1).

The factors with a higher contribution of organic aerosols, such as organic urban mix, bio SOA and biomass burning did not match any of the PM_1 inorganic factors, owing to their strong organic nature. The industrial NE & sea salt and the SIA factors inorganic species mass was probably included in the sulphate & industrial NE & aged sea salt_i factor, which was a mixture of different sources and showed the highest contribution to PM_1 mass (see Table 3.3.2).

4.2.1.3 Comparison of PMF profiles of PM_1 organics & inorganics and $PM_{2.5}$ inorganics

The comparison of the profiles obtained by Dall'Osto et al. (2013c) of hourly $PM_{2.5}$ PIXE analysis with the PM_1 fraction of organic and inorganic species concentrations may be helpful in determining the common sources contributing to fine aerosols at both the RS and UB sites. Dall'Osto et al. (2013c) reported 9 factors, which could be further grouped in 3 categories: regional (regional sulphate, sea salt and biomass burning), anthropogenic activities (industrial activities, oil combustion and waste incinerator) and dust (brake dust, soil dust and urban dust).

The highest correlations were obtained for two of the industrial factors: the shipping factor showed a good agreement with the oil combustion factor (R^2=0.81 at the RS and R^2=0.48 at the UB, Table 4.2.1), whereas the industrial NW & pin correlated with the industrial activities factor (R^2=0.43 at the RS and R^2=0.63 at the UB, Table 4.2.1). On the other hand, the industrial NE & sea salt factor did not correlate with the

$PM_{2.5}$ Pb_Cl factor as might be expected, as Cl was also a main contributor to the industrial NE & sea salt factor related to waste incineration plant emissions.

The fresh traffic factor presented similarities in its temporal trend with the $PM_{2.5}$ brake dust factor, both being characterised by Fe and Cu (R^2=0.22 at the RS and R^2=0.40 at the UB, Table 4.2.1). On the other hand, the soil dust and urban dust factors did not present any significant correlation with any of the PM_1 factors, thus emphasizing their coarser nature.

Regarding the regional factors, the $PM_{2.5}$ sea salt did not correlate with the industrial NE & sea salt factor, evidencing that the latter factor was dominated by anthropogenic emissions and the contribution of sea salt aerosols to PM_1 was minimal. A weak correlation was detected between SIA and the regional sulphate (R^2=0.32 at the RS and R^2=0.38 at the UB, Table 4.2.1) as well as both biomass burning factors (R^2=0.49 at the RS and R^2=0.13 at the UB, Table 4.2.1).

The soil and urban dust factors detected in the $PM_{2.5}$ fraction did not match any of the PM_1 factors, evidencing their coarser nature. The organic urban mix and bio SOA PM_1 factors did not correlate with any $PM_{2.5}$ factor, owing to the relevant contribution from organic species to those factors. Given that the nitrate contribution to $PM_{2.5}$ could not be analysed with the PIXE technique, the nitrate PM_1 factor found no match in any of the $PM_{2.5}$ factors. The industrial NE & sea salt did not correlate with the $PM_{2.5}$ waste incinerator factor, although both sources were related to the industrial emissions from the area NE of Barcelona.

4.2.1.4 Summary of PM_1 comparison analysis

The traffic factor related to fresh primary emissions (Fresh traffic, POA Urban, Traffic_i and Brake dust) was present in all studies, due to being characterised by both inorganic and organic species. On the other hand, the other factor related to traffic, the Organic Urban Mix was only reflected in the analysis of organics (OOA Urban) due to the relevant contribution of smoking and cooking aerosols to it, which are traced by organic compounds. The nitrate factor was prevalently inorganic, and thus was only detected in the inorganic study.

The industrial SW coupled with α-pinene oxidation products factor was also present in all studies (SOA BIO PIN, Industrial $SW_{\_i}$ and Industrial), either characterised by the organic or inorganic fractions only. On the other hand, the Industrial NE & sea salt factor was not correlated with any other factor. Although it is associated with industrial emissions such as waste incineration plants it did not correlated with the waste incinerator $PM_{2.5}$ factor, maybe due to the different techniques applied and the size fraction differences. Moreover, the $PM_{2.5}$ waste incinerator factor was associated also to Pb, which only showed 13% of the specie in the Industrial NE & sea salt factor (see Table 3.3.2). A positive correlation between the Industrial NE & sea salt factor and the inorganic sulphate & industrial NE & aged sea $salt_{\_i}$ would be expected. However, the contribution of SO_4^{2-} in the inorganic factor was double that of the Industrial NE & sea salt factor (50% and 23% of the specie, respectively), thus influencing the factor's concentration. The shipping factor was dominated by inorganic species (V and Ni) and thus correlated positively with the inorganic $shipping_{\_i}$ factor and the $PM_{2.5}$ oil combustion factor.

The SIA and SOA Aged factors presented a positive correlation as they shared the organic tracers of aged organic aerosols. A less positive relationship was found between SIA and the $PM_{2.5}$ sulphate factor, as more chemical species also contribute to the SIA factor. Being the BIO SOA a factor mainly related to organic aerosols, only the SOA ISO showed a positive correlation with it. In the case of the biomass burning factor, in addition to the correlation with the organic BBOA Regional it was also related to the $PM_{2.5}$ biomass burning, which was characterised by K.

4.2.1.5 Horizontal variability of PM_1 sources containing organic&inorganic species

The concurrent sampling in two urban environments within Barcelona, one heavily influenced by road traffic emissions (RS) while the other represented an urban background environment (UB) enabled the study of the horizontal variability of PM_1 levels within the city. Moreover, the joint source apportionment analysis yielded the opportunity of studying the sources intensities at each site.

Table 4.2.2: Concentration ratio RS/UB for each PMF factor.

PMF PM_1 factors	Ratio
Fresh traffic	2.3
Organic Urban Mix	15.2
Nitrate	2.2
Industrial NE & sea salt	1.2
Industrial SW & pin	0.6
Shipping	0.9
SIA	0.6
Bio SOA	0.4
Biomass burning	0.5

The organic urban mix factor shows the highest concentration ratio between RS and UB (15.2, see Table 4.2.2), being associated with road traffic emissions, cooking activities and tobacco smoke, a complex urban mix typically encountered in the city centre and thus at the RS. The fresh traffic and nitrate factors, which are directly related to road traffic emissions, show more than two times higher concentrations at the RS than the UB, emphasizing their local urban nature and their dependence on the proximity to emission sources (ratio 2.3 and 2.2, respectively, see Table 4.2.2).

The industrial NE & sea salt and the shipping factors show similar concentrations at both sites, although for the industrial factor they are higher at the RS and for the shipping factor at the UB (ratio 1.2 and 0.9, respectively, Table 4.2.2), also mirroring their proximity to their respective emission sources.

On the other hand, the industrial SW & pin, SIA, biomass burning and bio SOA factors display on average half the concentration at the RS than at the UB. Being the UB site less influenced by road traffic, secondary aerosols are found in higher concentrations, while its proximity to the SW industrial area explains the prevalence of the industrial source.

4.2.2 PM_{10}

During SAPUSS, a decreasing PM_{10} concentration gradient from road traffic hot spots to the background areas was recorded. Thus higher PM_{10} levels were recorded at the RS, followed by UB, TM and TC. Nevertheless, the atmospheric scenarios exerted an impact on the PM_{10} concentrations, and therefore both the proximity to traffic

sources and the type of scenario influences overlap, leading to a wide variability in concentrations and chemical composition of PM_{10} at a regional scale. Hence, during the regional air mass recirculation episode (REG_2) in the last days of the campaign (14-17 October), the formation of secondary aerosols increased PM_{10} concentrations. Higher PM_{10} concentrations were also recorded under North African air masses as the transported Saharan dust contributed to the PM_{10} loadings. By contrast, rainy periods as well as air mass change favoured a decrease in pollution levels (see Figure 3.4.1). During the periods when low concentrations were measured, a homogeneous distribution among the sampling sites evidenced the existence of background concentrations affecting the whole study area.

Mineral dust and organic matter were the main contributors to average PM_{10} loadings at all sites, indicating that the city might be a relevant emission source for such aerosols. The contributions from sea salt, sulphate and nitrate were similar and homogeneous across the city (7-11%). The secondary emission factors identified by PMF showed a higher homogeneity across the sites than expected, reflecting the efficient pollutants mixing in the boundary layer both in horizontal and vertical levels. On the other hand the contributions from the primary emissions factors vehicle exhaust and wear, and road dust displayed a horizontal and vertical spatial variability related to the proximity to the emission source. Certainly, higher concentrations were recorded at the RS, followed by UB, TM and TC. Amato et al. (2011) and Minguillón et al. (2014) also reported a horizontal variability for trace elements concentrations related to vehicle exhaust and wear emissions and road dust with the distance to road traffic sources.

The trajectory followed by certain air masses (NAF_E and EUR) over the Mediterranean Sea enhanced the incorporation of sea salt aerosols to their loadings, increasing the aged marine aerosol concentrations at the sites, although a decreasing gradient reflecting the sites distance to the sea side could be observed. The incursion of NAF_W air masses also caused the advection of shipping emissions from the harbour into the city, as concentration peaks of heavy oil were recorded at all sites, especially at the TM site, being closest to the sea. Recirculation of air masses during the regional episode REG_1 also accounted for an increase in heavy oil concentrations.

The emissions from high temperature industrial processes (smelters and cement kilns located in the industrial area along the Llobregat valley) impacted the city under NW winds. The impact was larger at the ground sites, causing concentration spikes, especially at the UB site, as they were the ones located closest to the source (Figure 3.4.6).

Both the sulphate and nitrate source contributions were mainly driven by the atmospheric scenarios. The increase of the contributions of these factors was favoured under REG air mass due to recirculation, enhancing the formation of nitrate and sulphate (Figure 3.4.6). However, a significant difference could be observed between the REG_1 and REG_2 episodes. Very high concentrations of both nitrate and sulphate were recorded under REG_2 episode, which was characterised by higher wind speed than REG_1, an almost constant NW advection and a lower temperature than REG_1 (Figures 3.4.7 and 3.4.9). The temperature difference between these two periods accounted for the lower nitrate levels registered during REG_1, as the higher temperature recorded under this episode caused the volatilization of part of the nitrate, thus reducing its concentration in the solid phase.

Unexpectedly, the mineral dust PMF factor concentrations showed a low spatial variability among the sites. However, several sources were found to contribute to the total mineral load and have been grouped in the following categories:

1) Road dust: the concentrations decreased from RS to TC, contributing 3.8-1.6 μgm^{-3} on average (35% of the mineral dust in PM_{10} during the study period).

2) Saharan dust: African air mass incursions occurred on 20% of the days during the study period. Under this scenario, the excess dust from the PMF mineral factor was extracted and attributed to Saharan dust, thus obtaining an average Saharan dust contribution of 2.1 μgm^{-3} (28% of the mineral dust in PM_{10} in the study period).

3) Background dust: it presented a homogeneous distribution among the sampling sites and was thus attributed to background mineral dust with a possible urban or regional origin. A regional origin is thought to be more

probable due to the uniform distribution of this dust type at both horizontal and vertical levels for the whole study area. Average concentrations during the SAPUSS study ranged from 2.7 to 2.9 μgm^{-3}, resulting in the mineral source with the highest contribution (37% of the mineral dust in PM_{10} in the study period).

The estimation of the ss Na allowed for the calculation of the theoretical sea salt (attaining to its chemical composition ratios respect Na) and the measured concentrations at the sites. Their comparison with the PMF aged marine factor led to the identification of the following sources or processes:

1) Calculated sea salt: presented a homogeneous relative contribution among the sampling sites, accounting for the majority of the aged marine load mass (51-59%, 1.5-2.7 μgm^{-3}).

2) Anthropogenic marine sulphate of regional origin: presented a homogenous relative contribution among the sampling sites, accounting for 41-49% of the mass load (1.1-2.5 μgm^{-3}). The anthropogenic marine sulphate showed a different origin than the PMF sulphate and heavy oil factors. This pointed towards the possible contribution of the WMB background sulphate concentrations due to maritime transport and other industrial sources located near the Mediterranean coasts, in agreement with Querol et al. (2009a).

However, the elevation of the sampling sites might also affect the variability of factors concentrations between ground and tower measurements. Due to the location of the TM site (influenced by two nearby roads), vehicle exhaust and wear particles emitted at street level might evaporate and coagulate while being advected upwards to the sampling site (150 m a.s.l.). The elevation of the site might partially account for the decrease in concentrations levels for this factor registered at TM in comparison to the urban background site UB. In the case of the suburban TC site (415 m a.s.l.), high relative sulphate concentrations were recorded, although the marine sulphate of regional origin affected the TM site more intensely due to its closeness to the sea side (see Figure 4.2.2). Due to the predominantly urban origin of nitrate, concentrations registered at TC were considerably lower, although the location of the TM site (150 m a.s.l. within the city) favoured higher concentrations than at UB. Therefore, even in

vertical levels within a city environment, the exact location of the site still has a high influence on the pollution's impact.

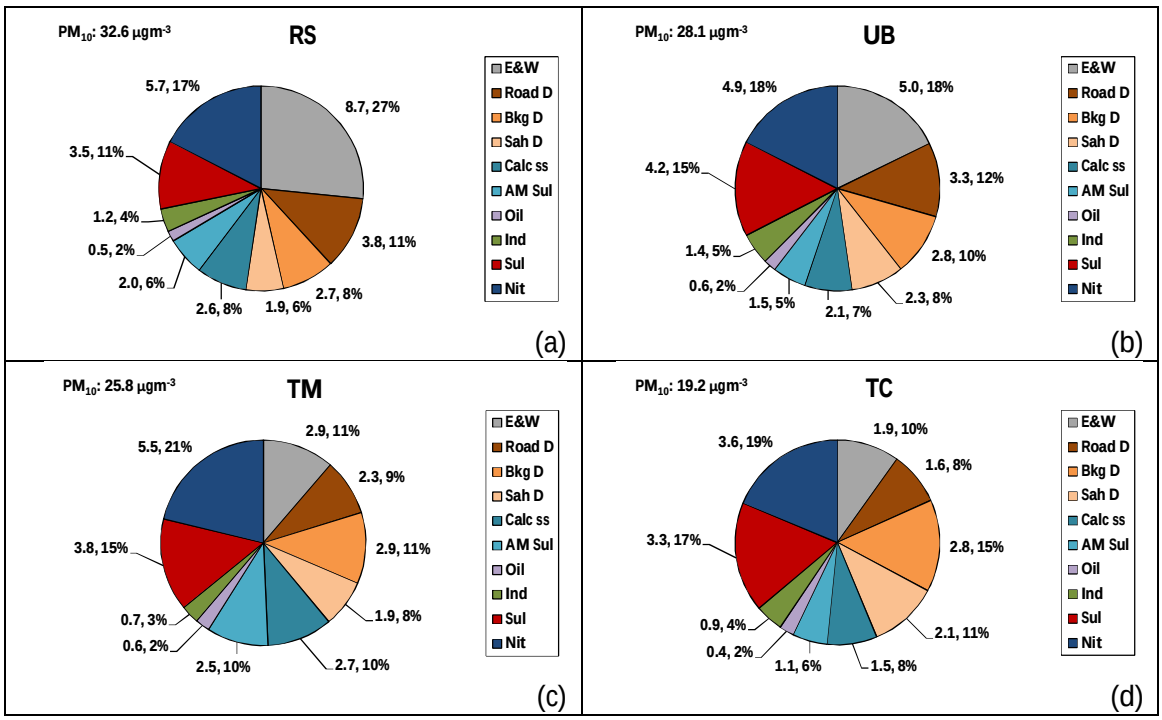

Figure 4.2.2: Sources contributing to the PM_{10} load extracted with the PMF tool and subcomponents at each monitoring: a) RS, b) UB, c) TM and d) TC. Exhaust&Wear (E&W), Road dust (Road D), Heavy oil (Oil), Industrial (Ind), Sulphate (Sul) and Nitrate (Nit) are direct PMF factors. The mineral factor was broken into Background dust (Bkg D) and Saharan dust (Sah D) and the aged marine factor into Calculated sea salt (Calc ss) and Anthropogenic marine sulfate of regional origin (AM Sul). Data are given in μgm^{-3} and %. The average PMF PM_{10} concentration are represented at the top right of each graph for each site.

Chapter 5

Conclusions

5. Conclusions

A detailed study of aerosol sources and processes in the Western Mediterranean Basin urban environment of Barcelona was performed, ranging from ultrafine to coarse particles. This geographical region presents unique and complex characteristics, which have been investigated in a number of studies over the last years (see the introduction section). However, the evolution of aerosols within the urban atmosphere both in horizontal and vertical levels, their sources and processes and the influence of meteorological and climatological features characteristic of the area needed further study. For this reason, an intensive sampling campaign named SAPUSS (20th Septembre-20th October 2010) was developed in the Barcelona urban environment, which consisted on concurrent aerosol sampling in 6 sites by different methods and techniques, in order to obtain a detailed picture of aerosols features in this area (Dall'Osto et al., 2013a). Moreover, long term measurements of particle number size distribution were also measured in the urban background of Barcelona and were further compared with other worldwide developed cities characterised by intense solar radiation. This allowed for the comparison between sources and processes affecting ultrafine particles in similar climatic environments around the globe, focusing on urban nucleation events.

Concerning ultrafine particles, measurements of particle size distribution were performed in the Barcelona urban area during the SAPUSS campaign. Four SMPSs were simultaneously deployed at four different monitoring sites: a road site (RS_{site}), two urban background sites (UB_{site} and TC_{site}) and a regional background station (RB_{site}). Measurement size ranges for all monitoring sites were harmonised, resulting in a homogenous dataset with particle sizes between 15 nm and 228 nm at one hour resolution.

- A *k*-means clustering analysis was performed on the combined four datasets, resulting in nine size distributions that described the overall aerosol

population: Traffic 1, Traffic 2, Traffic 3, Urban Background 1, Regional Background 1, Regional Background 2, Nucleation, Regional Nitrate and Mix. Three clusters account for traffic conditions (30% of the time), three account for background pollution (54% of the time) and three described specific special cases (16% of the time).

- Traffic emissions heavily impact the closest sites, while the sites located in the urban background are more influenced by background clusters. Atmospheric and meteorological conditions play a key role in the evolution of ultrafine particles.

- Evaporation of traffic-related ultrafine aerosols occurs when the air mass moves away from the traffic hot spot. This process had been reported in an urban northern European environment under different cimatological conditions (London, Dall'Osto et al., 2011b), and is shown for the first time in a southern European urban environment.

- The smallest ultrafine particles (between 5 and 15 nm in size) show the most complex behaviour. On the one hand, new non-traffic particles formed in cities often fail to grow above 15 nm. On the other hand, 20-30 nm primary traffic particles shrink to smaller sizes soon after emission.

- Moreover, photochemical nucleation events under high solar radiation conditions is a common feature in southern European cities and contributes to increase N, although such particles often fail to grow to sizes above 10-15 nm, being detected only 5% of the time, on average, during SAPUSS. This behaviour points out the extremely dynamic nature of ultrafine particles, especially of the smaller sized ones, and how meteorological features influence their evolution in the urban atmosphere.

The analysis of the long term size segregated particle number enabled the study of the main sources and processes dominating similar urban environments to Barcelona worldwide, including Madrid, Brisbane, Rome and Los Angeles. A k-means clustering analysis was performed for each data set, which allowed the comparison of the

sources characteristics at each city. Data sets from Rome and Los Angeles were used to complement the study, although the main conclusions were reached considering only Barcelona, Madrid and Brisbane.

- Traffic and nucleation events are reported as the two most relevant sources of ultrafine particles (44-63% and 14-19% of the time, respectively). Minor sources were Urban Background pollution and other specific clusters of each location.

- The nucleation cluster represented on average 16% of the time. For the SAPUSS study, the nucleation cluster only represented 5% of the time as the campaign had a one month duration in autumn, while if 1 year of measurements is considered the prevalence of this cluster is three times higher.

- On average, nucleation particles accounted for 21% of total N, evidencing the importance of nucleation processes to total concentrations of ultrafine particles in high insolation urban areas.
- The urban nucleation events detected in these cities consist on particles bursts starting around midday and lasting 3-4 hours while growing to 20-40 nm. Further growing of these particles in a banana shape (regional nucleation type) is probably constrained by the increase of the condensation sink due to traffic emitted particles in the evening coinciding with a decrease in the solar radiation intensity. Therefore, the detected events represent a source of new particle formation restricted to urban areas, whereas the regional nucleation events show different characteristics and affect a wide area.

- On average, nucleation events lasting for two hours or more were detected in 55% of the days, this extending to over four hours in 28% of the days, demonstrating that the atmospheric conditions in urban environments do not favour photochemically nucleated particle growth.

- The urban nucleation events described in this thesis presumably have an anthropogenic origin, or at least are influenced by anthropogenic precursors,

due to the fact that such events are seen initiating in city hot spots and not in the nearby background (Dall'Osto et al., 2013b).

Regarding particulate mass, the concurrent analysis of inorganic and organic PM_1 species allowed the study of the main sources contributing to this factor in two distinct urban environments (RS and UB) during the SAPUSS campaign.

- The PMF analysis performed yielded 9 factors representative of the aerosol sources affecting both sites: Fresh traffic, Organic Urban Mix, Nitrate, Industrial NE & sea salt, Industrial SW & pin, Shipping, SIA, Bio SOA and Biomass burning. The proximity to emission sources had an impact on the concentrations registered at the sites, being RS more influenced by traffic emissions (39% of PM_1) and the UB by industrial sources (51% of PM_1) and secondary species (24% of PM_1).

- On average, traffic sources ranged between 23-36%% of the PM_1 mass (minimum contribution calculated as the sum of fresh traffic and 60% of the nitrate factor and maximum adding the organic urban mix factor), whereas 42% was related to industrial activities and shipping emissions. Secondary aerosols accounted for 29% of the PM_1 mass, while the biomass burning contribution was minimal (1%).

- The industrial NE & sea salt factor was identified for the first time in the PM_1 fraction in the study area, thanks to the inclusion of organic species concentrations in the PMF matrix.

- The comparison of the obtained factors with other studies using either organic or inorganic species in the source apportionment was carried out. The joint analysis of both species led to a higher number of identified sources (9 sources) than if the study had been carried out separately for each specie (yielding 6 organic sources and 5 inorganic sources, respectively), resulting in a more complete and realistic study of the aerosol sources in the urban environment of Barcelona.

In the case of the PM_{10} fraction only inorganic species were analysed. However, the sampling sites were increased to four, with the aim of assessing and evaluating the spatial variability in vertical and horizontal levels of PM_{10}. Therefore, two of the sites were at the ground level (RS and UB), while two more were located at a certain height, one at the rooftop of Torre Mapfre (TM, 150 m a.s.l.) close to the sea side, and a suburban one located on the hills surrounding Barcelona, Torre Collserola (415 m a.s.l., TC).

- The PMF analysis optimal solution contained 8 factors: Vehicle exhaust and wear, Road dust, Mineral, Aged marine, Heavy oil, Industrial, Sulphate and Nitrate. Overall, primary traffic emissions (Exhaust and wear and Road dust) accounted for 19-38% of PM_{10} mass, primary inorganic aerosols (Mineral dust and Aged marine) 28-39%, industry (Heavy oil and Industrial) 5-7% and secondary aerosols (Sulphate and Nitrate) 28-36%.

- Most of the factors showed a homogeneous distribution among the sampling sites, although primary traffic emissions displayed a decreasing gradient from the traffic sites to the suburban background (RS, UB, TM and TC).

- Vehicle exhaust & wear, road dust and industrial factors showed around two times higher concentrations at the ground sites (RS and UB) than at the tower sites (TM and TC), evidencing that distance to pollution sources and atmospheric vertical dilution lead to a decrease in concentrations with height.

- The main factors influencing the different sources concentration at each site were: proximity to the emission source, air mass origin and meteorological parameters, such as wind speed and direction (influencing the sea breeze development for both dispersion and transport of specific pollutants) or temperature (causing the volatilization of nitrate under high temperatures). Air mass recirculation due to regional episodes enhanced the formation of secondary inorganic aerosols, such as sulphate and nitrate, or heavy oil. On the other hand, precipitation and air mass transition periods were found to favour a decrease in concentration levels due to wet deposition and low resuspension in the first case and atmospheric dilution in the second scenario.

- A special focus was made on the mineral dust and aged marine aerosols, as they were both mainly found in the PM_{10} fraction and were a complex mixture of anthropogenic and natural components. The mineral dust factor was heavily influenced by the Saharan dust intrusions, causing the concentration levels to be two times higher. By extracting the contribution of this natural aerosol to the factor, the remaining concentrations were found to show homogeneous levels at all sites, thus indicating the existence of a background mineral dust source that affected the whole urban area.

- Therefore, three sources of mineral dust were identified in the urban area of Barcelona: road dust (3.8-1.6 μgm^{-3} and 35% on average of the mineral load in PM_{10}), Saharan dust (2.1 μgm^{-3} and 28% on average) and mineral dust of regional origin (2.7-2.9 μgm^{-3} and 37% on average).

- Regarding the aged marine factor, it was found to be internally mixed with sulphate of regional origin, as the calculated sea salt (2.2 μgm^{-3}, 56% of the aged marine load) was aged by the mixing with anthropogenic marine sulphate of regional origin (1.8 μgm^{-3}, 44% of the aged marine load).

- The anthropogenic marine sulphate contribution was attributed to the intense maritime traffic and industrial emissions in the coast of the WMB, as it showed a relative homogeneous distribution at the sites and did not correlate with the PMF sulphate factor as it was related to inland industrial sources.

5.1 From ultrafine to coarse: concluding remarks and implications for air quality

The study of aerosols in an urban environment of the Western Mediterranean Basin, ranging from the smallest particles (ultrafine particles, described by particle number) to the coarsest ones (PM_{10}, dominated by particle mass) carried out in this thesis allows for a general understanding of the main sources and processes affecting aerosols.

Considering the results obtained from the SAPUSS campaign, traffic sources dominate the ultrafine particles size distribution for 30% of the time and range between 23-36%% of the PM_1 mass (minimum contribution calculated as the sum of

fresh traffic and 60% of the nitrate factor and maximum adding the organic urban mix factor) and 36% of PM_{10} on average (calculated as the sum of the vehicle exhaust and wear, road dust factors and 60% of the concentration of the nitrate factor), evidencing its impact in all size ranges, both to N and PM. The second most important source contributing to ultrafine particles was urban nucleation events, also occurring in similar climatic worldwide urban environments, which cause an abrupt increase in N but have a negligible effect on PM. Relevant sources to the PM_1 fraction were industrial emissions and shipping, which accounted for 42% of the mass on average, whereas in PM_{10} they only explained 6% of the mass. This difference between fractions might be due to the industrial factors in the PM_1 fraction incorporating other anthropogenic sources before reaching the sampling site (industrial NE & sea salt factor) and the addition of pinene and other bioaerosols to the load (industrial SW & pin factor). Secondary aerosols, such as nitrate and sulphate, were present in all size ranges, as the nitrate cluster was detected in the ultrafine particles size range, occurring 6% of the time during SAPUSS and 7% of the time in Barcelona on an annual basis. Moreover, they contributed similarly to PM_1 and PM_{10} mass (on average 29% and 33%, respectively). Primary aerosols, including mineral sources and sea salt, had a relevant contribution to PM_{10}, representing on average 34% of PM_{10} mass. Finally, biomass burning aerosols were detected in the PM_1 fraction, but their contribution to PM was only 1%.

According to this, it is clear that abatement strategies should focus on reducing anthropogenic emissions, especially from traffic and industrial sources. The reduction of primary emissions however, might cause a decrease of the condensation sink and thus enhance nucleation processes, leading to the formation of a high number of newly formed particles with little mass (Wichmann et al., 2000). Therefore, further investigation is required in better understanding the secondary new particle formation processes, their precursors and formation mechanisms to better assess effective strategies that might lead to pollution reduction and consequently improve air quality.

According to the results obtained in this thesis, the following recommendations should be taken into consideration regarding air pollution studies and the improvement of air quality in urban environments:

- Concerning the establishment of ultrafine particles standards for air quality, although road traffic is the main source of ultrafine particles, it has to be taken into account that in high insolation developed urban environments new particle formation through nucleation processes can highly influence total particle number concentrations (e.g. in Barcelona it represents 22% of the total N), especially in highly insolated regions (on average, $N_{nucleation}$=12000±8000 cm^{-3} and $N_{traffic}$=10000±5000 cm^{-3}). As a result, particle number concentration as an air quality parameter would be affected by different sources depending on the region. However, BC measurements specifically point to road traffic emissions and would therefore represent a more accurate parameter to monitor them than particle number concentration.

- Regarding epidemiological studies, it would be advisable to study the morbidity and mortality associated with the daily N concentration, differentiating between the nucleation particles and the traffic related ones, as they are thought to affect human helth differently.

- The need to include both organic and inorganic species in the source apportionment studies by PMF, providing a more accurate description of the emission sources, which can be dominated by inorganic or organic elements or be a mixture of the two.
- The identification of the industrial area NE of Barcelona for the first time in the PM_1 fraction as a relevant pollution source, due to the joint analysis of organic and inorganic species.
- The need to reduce mineral dust of anthropogenic urban origin because it represents an important contribution to PM_{10} levels (38% of the mineral load).
- The anthropogenic marine sulphate of regional origin attributed to the maritime traffic background pollution of the Mediterranean basin is a relevant contributor to total sulphate levels in Barcelona (32% of the sulphate load).

Chapter 6

Future studies

6. Future studies

The research carried out in this thesis leaves many open questions that may lead to additional research in urban environments in the Western Mediterranean Basin.

- It is highly interesting to obtain long-term concurrent measurements of particle size distribution data at the urban background, regional background and continental background monitoring sites, in order to further investigate the nucleation events affecting the study area, especially to assess urban and regional nucleation events.
- The incorporation of particle number size distributions measurements from 1 to 15 nm, in order to assess new particle formation events and growth, especially in an urban background environment.
- The simultaneous analysis of long time series of air pollutants, as well as N, size segregated N, and BC will allow investigating its association with mortality and morbidity, and study the health effects of ultrafine particles and to discriminate between effects of traffic-related ultrafine particles and newly formed particles from photochemical processes.
- The chemical characterization of nucleation processes and subsequent particle growth is highly relevant to be resolved considering the high contribution of secondary particles to particle number and its derived health problems.
- Study the vertical distribution of N and size distributions of UFP in order to elucidate the atmospheric dynamics that enhance new particle formation events by using a airborne measurements.
- A better understanding of the factors influencing nucleation events would enable for better decision making regarding the design and implementation of air quality monitoring networks (Duyzer et al., 2015).
- Shipping emissions should be quantified in detail to evaluate its contribution to the urban pollution scenario, especially SO_2 emissions, which play a key role in the growth of nucleated particles. It might also form sulphate aerosols and contribute to PM_1 and $PM_{2.5}$ concentration levels, especially in the

Mediterranean basin where intense maritime traffic occurs. It is relevant in coastal sites to discriminate between the regional marine and the harbour contributions.

- Further investigation of the emissions of the industrial area NE of Barcelona, whose pollution plume has been detected in the PM_1 (this thesis) and $PM_{2.5}$ fraction (Dall'Osto et al., 2013c).
- Deepen the knowledge of organic aerosols fractions, and quantify the contribution of possible cooking emissions and secondary organic aerosols.
- Investigate the SOA in the urban environment, in order to elucidate if it has urban or regional origin and deepen into the formation and transformation processes governing these aerosols.
- Study the interaction of SOA, SIA and gaseous pollutants, especially NO_x, VOCs and O_3 in urban environments.
- Further investigate the mineral background sources contributing to the PM_{10} fraction, such as construction dust, and investigate effectiveness of specific abatement strategies.

Chapter 7

Scientific contributions

7. Scientific contributions

Brines, M., Dall'Osto, M., Beddows, D. C. S., Harrison, R. M. and Querol, X.: Simplifying aerosol size distributions modes simultaneously detected at four monitoring sites during SAPUSS, Atmos. Chem. Phys., 14(6), 2973–2986, doi:10.5194/acp-14-2973-2014, 2014.

Brines, M., Dall'Osto, M., Beddows, D. C. S., Harrison, R. M., Gómez-Moreno, F., Núñez, L., Artíñano, B., Costabile, F., Gobbi, G. P., Salimi, F., Morawska, L., Sioutas, C. and Querol, X.: Traffic and nucleation events as main sources of ultrafine particles in high-insolation developed world cities, Atmos. Chem. Phys., 15(10), 5929–5945, doi:10.5194/acp-15-5929-2015, 2015.

Dall'Osto, M., Querol, X., Alastuey, a., Minguillon, M. C., Alier, M., Amato, F., **Brines, M**., Cusack, M., Grimalt, J. O., Karanasiou, a., Moreno, T., Pandolfi, M., Pey, J., Reche, C., Ripoll, a., Tauler, R., Van Drooge, B. L., Viana, M., Harrison, R. M., Gietl, J., Beddows, D., Bloss, W., O'Dowd, C., Ceburnis, D., Martucci, G., Ng, N. L., Worsnop, D., Wenger, J., Mc Gillicuddy, E., Sodeau, J., Healy, R., Lucarelli, F., Nava, S., Jimenez, J. L., Gomez Moreno, F., Artinano, B., Prévôt, a. S. H., Pfaffenberger, L., Frey, S., Wilsenack, F., Casabona, D., Jiménez-Guerrero, P., Gross, D. and Cots, N.: Presenting SAPUSS: Solving aerosol problem by using synergistic strategies in Barcelona, Spain, Atmos. Chem. Phys., 13(17), 8991–9019, doi:10.5194/acp-13-8991-2013, 2013a.

Minguillón, M. C., **Brines, M.**, Pérez, N., Reche, C., Pandolfi, M., Fonseca, a. S., Amato, F., Alastuey, a., Lyasota, a., Codina, B., Lee, H.-K., Eun, H.-R., Ahn, K.-H. and Querol, X.: New particle formation at ground level and in the vertical column over the Barcelona area, Atmos. Res., 165, 118–130, doi:10.1016/j.atmosres.2015.05.003, 2015.

Moreno, T., Reche, C., Rivas, I., Cruz Minguillón, M., Martins, V., Vargas, C., Buonanno, G., Parga, J., Pandolfi, M., **Brines, M**., Ealo, M., Fonseca, A.S., Amato, F., Sosa, G., Capdevila, M., de Miguel, E., Querol, X. and Gibbons, W.: Urban air quality

comparison for bus, tram, subway and pedestrian commutes in Barcelona, Environ. Res., 142, 495–510, doi:10.1016/j.envres.2015.07.022, 2015.

Reche, C., Viana, M., **Brines, M.**, Pérez, N., Beddows, D., Alastuey, A. and Querol, X.: Determinants of aerosol lung-deposited surface area variation in an urban environment, Sci. Total Environ., 517, 38–47, doi:10.1016/j.scitotenv.2015.02.049, 2015.

Chapter 8

References

8. References

Agrawal, H., Malloy, Q.G.J., Welch, W.A., Wayne Miller, J. and Cocker, D.R.: In-use gaseous and particulate matter emissions from a modern ocean going container vessel, Atmos. Environ., 42(21), 5504–5510, doi:10.1016/j.atmosenv.2008.02.053, 2008.

Alam, A., Shi, J.P. and Harrison, R.M.: Observations of new particle formation in urban air, J. Geophys. Res., 108 (D3), 4093, doi: 10.1029/2001JD001417, 2003.

Alastuey A.: Caracterización mineralógica y alterológica de morteros de revestimiento en edificios de Barcelona, Universitat de Barcelona, PhD thesis, 1994.

Alier, M., Van Drooge, B.L., Dall'Osto, M., Querol, X., Grimalt, J.O. and Tauler, R.: Source apportionment of submicron organic aerosol at an urban background and a road site in Barcelona (Spain) during SAPUSS, Atmos. Chem. Phys., 13(20), 10353–10371, doi:10.5194/acp-13-10353-2013, 2013.

Alier, M.: Desenvolupament i aplicació de metodologies analítiques i quimiomètriques per a l'estudi de la contaminació atmosfèrica, Universitat de Barcelona, PhD Thesis, 2014.

Alier, M., Osto, M.D., Lin, Y.H., Surratt, J.D., Tauler, R., Grimalt, J.O. and van Drooge, B.L.: On the origin of water-soluble organic tracer compounds in fine aerosols in two cities: the case of Los Angeles and Barcelona, Environ. Sci. Pollut. Res., 1–12, doi:10.1007/s11356-013-2460-9, 2014.

Alves, C.A., Gonçalves, C., Pio, C.A., Mirante, F., Caseiro, A., Tarelho, L., Freitas, M.C. and Viegas, D.X.: Smoke emissions from biomass burning in a Mediterranean shrubland, Atmos. Environ., 44(25), 3024–3033, doi:10.1016/j.atmosenv.2010.05.010, 2010.

Amato, F., Pandolfi, M., Escrig, A., Querol, X., Alastuey, A., Pey, J., Perez, N. and Hopke, P. K.: Quantifying road dust resuspension in urban environment by Multilinear

Engine: A comparison with PMF2, Atmos. Environ., 43(17), 2770–2780, doi:10.1016/j.atmosenv.2009.02.039, 2009.

Amato, F.: Particulate Matter Resuspensión from Urban Paved Roads: Impact on Air Quality and Abatement Strategies, Universitat Politècnica de Catalunya, PhD Thesis, 2010.

Amato, F., Viana, M., Richard, A., Furger, M., Prévôt, A. S. H., Nava, S., Lucarelli, F., Bukowiecki, N., Alastuey, A., Reche, C., Moreno, T., Pandolfi, M., Pey, J. and Querol, X.: Size and time-resolved roadside enrichment of atmospheric particulate pollutants, Atmos. Chem. Phys., 11(6), 2917–2931, doi:10.5194/acp-11-2917-2011, 2011.

Amato, F., Alastuey, A., De La Rosa, J., Sánchez De La Campa, A.M., Pandolfi, M., Lozano, A., Contreras González, J. and Querol, X.: Trends of road dust emissions contributions on ambient air particulate levels at rural, urban and industrial sites in southern Spain, Atmos. Chem. Phys., 14(7), 3533–3544, doi:10.5194/acp-14-3533-2014, 2014.

Andreae, M.O. and Rosenfeld, D.: Aerosol-cloud-precipitation interactions. Part 1. The nature and sources of cloud-active aerosols, Earth-Science Rev., 89(1-2), 13–41, doi:10.1016/j.earscirev.2008.03.001, 2008.

Atkinson, R.W., Fuller, G.W., Anderson, H.R., Harrison, R.M. and Armstrong, B.: Urban particle metrics and health: A time series analysis, Epidemiology, 21, 501-511, 2010.

Australian Bureau of Statistics, 2014: http://www.abs.gov.au/ausstats/abs@.nsf/mf/9309.0

Ávila A., Alarcón M. and Queralt I.: The chemical composition of Dust transported in Red Rains: its contribution to the Biogeochemical Cycle of a holm oak forest in Catalonia (Spain), Atmos. Environ., 32, 179-191, 1998.

Basagaña, X., Jacquemin, B., Karanasiou, A., Ostro, B., Querol, X., Agis, D., Alessandrini, E., Alguacil, J., Artiñano, B., Catrambone, M., de la Rosa, J. D., Díaz, J., Faustini, A., Ferrari, S., Forastiere, F., Katsouyanni, K., Linares, C., Perrino, C., Ranzi, A., Ricciardelli, I., Samoli, E., Zauli-Sajani, S., Sunyer, J. and Stafoggia, M.: Short-term effects of particulate matter constituents on daily hospitalizations and mortality in five South-European cities: Results from the MED-PARTICLES project, Environ. Int., 75, 151–158, doi:10.1016/j.envint.2014.11.011, 2015.

Beddows, D. C. S., Dall'Osto, M. and Harrison, R. M.: Cluster analysis of rural, urban, and curbside atmospheric particle size data, Environ. Sci. Technol., 43(13), 4694–4700, doi:10.1021/es803121t, 2009.

Beddows, D. C. S., Dall'Osto, M., Harrison, R. M., Kulmala, M., Asmi, A., Wiedensohler, A., Laj, P., Fjaeraa, A. M., Sellegri, K., Birmili, W., Bukowiecki, N., Weingartner, E., Baltensperger, U., Zdimal, V., Zikova, N., Putaud, J. P., Marinoni, A., Tunved, P., Hansson, H. C., Fiebig, M., Kivekäs, N., Swietlicki, E., Lihavainen, H., Asmi, E., Ulevicius, V., Aalto, P. P., Mihalopoulos, N., Kalivitis, N., Kalapov, I., Kiss, G., De Leeuw, G., Henzing, B., O'Dowd, C., Jennings, S. G., Flentje, H., Meinhardt, F., Ries, L., Denier Van Der Gon, H. A. C. and Visschedijk, A. J. H.: Variations in tropospheric submicron particle size distributions across the European continent 2008-2009, Atmos. Chem. Phys., 14(8), 4327–4348, doi:10.5194/acp-14-4327-2014, 2014.

Beddows, D. C. S., Harrison, R. M., Green, D. C., and Fuller, G. W.: Receptor modelling of both particle composition and size distribution from a background site in London, UK, Atmos. Chem. Phys. Discuss., 15, 10123-10162, doi:10.5194/acpd-15-10123-2015, 2015.

Besombes, J. L., Maître, A., Patissier, O., Marchand, N., Chevron, N., Stoklov, M. and Masclet, P.: Particulate PAHs observed in the surrounding of a municipal incinerator, Atmos. Environ., 35(35), 6093–6104, doi:10.1016/S1352-2310(01)00399-5, 2001.

Betha, R., Spracklen, D. V. and Balasubramanian, R.: Observations of new aerosol particle formation in a tropical urban atmosphere, Atmos. Environ., 71, 340–351, doi:10.1016/j.atmosenv.2013.01.049, 2013.

Betha, R., Zhang, Z. and Balasubramanian, R.: Influence of trans-boundary biomass burning impacted air masses on submicron number concentrations and size distributions, Atmos. Environ. 92, 9-18, 2014.

Birch, M. E. and Cary, R. A.: Elemental carbon-based method for monitoring occupational exposures to particulate diesel exhaust, Aerosol Science and Technolody, 25, 221-241, 1996.

Birmili, W. and Wiedensohler, A.: New particle formation in the continental boundary layer: Meteorological and gas phase parameter influence, Geophys. Res. Letts., 27, 20, 3325-3328, 2000.

von Bismarck-Osten, C., Birmili, W., Ketzel, M., Massling, A., Petäjä, T., Weber, S.: Characterization of parameters influencing the spatio-temporal variability of urban particle number size distributions in four European cities, Atmos. Environ., 77, 415-429, 2013.

Biswas, S., Fine, P. M., Geller, M. D., Hering, S. V. and Sioutas, C.: Performance Evaluation of a Recently Developed Water-Based Condensation Particle Counter, Aerosol Sci. Technol., 39(5), 419–427, doi:10.1080/027868290953173, 2005.

Blumenthal D. L., White W. H. and Smith T. B.: Anatomy of a Los Angeles smog episode: pollutant transport in the daytime sea breeze regime. Atmos. Environ.,12, 893-907, 1978.

Bobak, M., Pikhart, H. and Leon, D.: Air pollution, low birth weight and prematurity, , 1(2) [online] Available from: http://discovery.ucl.ac.uk/89222/, 1999.

Bond, T. C., Doherty, S. J., Fahey, D. W., Forster, P. M., Berntsen, T., Deangelo, B. J., Flanner, M. G., Ghan, S., Kärcher, B., Koch, D., Kinne, S., Kondo, Y., Quinn, P. K.,

Sarofim, M. C., Schultz, M. G., Schulz, M., Venkataraman, C., Zhang, H., Zhang, S., Bellouin, N., Guttikunda, S. K., Hopke, P. K., Jacobson, M. Z., Kaiser, J. W., Klimont, Z., Lohmann, U., Schwarz, J. P., Shindell, D., Storelvmo, T., Warren, S. G. and Zender, C. S.: Bounding the role of black carbon in the climate system: A scientific assessment, J. Geophys. Res. Atmos., 118(11), 5380–5552, doi:10.1002/jgrd.50171, 2013.

Boy, M. and Kulmala, M.: Nucleation events in the continental boundary layer: Influence of the physical and meteorological parameters, Atmos. Chem. Phys., 2, 1-16, 2002.

Brimblecombe P.: Urban air pollution. In The Urban Atmosphere and Its Effects (Brimblecombe P. and Maynard R., eds.). Vol 1, Air Pollution Reviews, Imperial College Press, London, UK, 2001.

Brunekreef, B. and Forsberg, B.: Epidemiological evidence of effects of coarse airborne particles on health, Eur. Respir. J., 26(2), 309–318, doi:10.1183/09031936.05.00001805, 2005.

Carslaw, D.C. and K. Ropkins: Openair --- an R package for air quality and data analysis, Environmental Modelling & Software, 27-28, 52-61, 2012.

Castillo, S.: Impacto de las masas de aire africano sobre los niveles y composición del material particulado atmosférico en Canarias y el NE de la Península Ibérica. Universidad Autónoma de Barcelona, PhD Thesis, 2006.

Cavalli, F., Viana, M., Yttri, K.E., Genberg, J., and Putaud, J.-P., 2010. Toward a standardised thermal-optical protocol for measuring atmospheric organic and elemental carbon: the EUSAAR protocol. Atmospheric Measurement Techniques, 3, 79–89, doi:10.5194/amt-3-79-2010.

CEN: Air quality – Determination of the PM10 fraction of suspended particulate matter. Reference method and field test procedure to demonstrate reference equivalence of measurement methods, EN12341:1999, 1999.

Charron, A. and Harrison, R. M.: Primary particle formation from vehicle emissions during exhaust dilution in the roadside atmosphere, Atmos. Environ., 37(29), 4109–4119, doi:10.1016/S1352-2310(03)00510-7, 2003.

Chester, R., Nimmo, M. Keyse, S.; The influence of Saharan and Middle Eastern Desert-Derived dust on the Trace Metal Composition of Mediterranean Aerosols and Rainwater: an overview. In The Impact of Desert Dust across the Mediterranean, Vol. 11 (ed. S Guerzoni and R. Chester), 253-273, 2006.

Cheung, H. C., Morawska, L. and Ristovski, Z. D.: Observation of new particle formation in subtropical urban environment, Atmos. Chem. Phys., 11(8), 3823–3833, doi:10.5194/acp-11-3823-2011, 2011.

Cheung, H. C., Chou, C. C.-K., Huang, W.-R., and Tsai, C.-Y.: Characterization of ultrafine particle number concentration and new particle formation in an urban environment of Taipei, Taiwan, Atmos. Chem. Phys., 13, 8935-8946, doi:10.5194/acp-13-8935-2013, 2013.

Ciccioli, P., Brancaleoni, E. and Frattoni, M.: Reactive Hydrocarbons in the Atmosphere at Urban and Regional Scales, React. Hydrocarb. Atmos., 159–207, 1999.

Claeys, M., Graham, B., Vas, G.,Wang,W., Vermeylen, R., Pashynska, V., Cafmeyer, J., Guyon, P., Andrae, M. O., Artaxo, P., and Maenhaut, W.: Formation of secondary organic aerosols through photooxidation of isoprene, Science, 303, 1173–1176, 2004.

Claeys, M., Szmigielski, R., Kourtchev, I., Van der Veken, P., Vermeylen, R., Maenhaut, W., Jaoui, M., Kleindienst, T., Lewandowski, M., Offenberg, J., and Edney, E.: Hydroxydicarboxylic Acids: Markers for Secondary Organic Aerosol from the Photooxidation of _-Pinene, Environ. Sci. Technol., 41, 1628–1634, 2007.

Colbeck, I., Lazaridis, M.: Aerosol Science: technology and Application. First Edition © 2014 John Wiley & Sons, Ltd. ISBN: 978-1-119-97792-6.

Costabile, F., Birmili, W., Klose, S., Tuch, T., Wehner, B., Wiedensohler, A., Franck, U., König, K. and Sonntag, A.: Spatio-temporal variability and principal components of the particle number size distribution in an urban atmosphere, Atmos. Chem. Phys. Discuss., 8(5), 18155–18217, doi:10.5194/acpd-8-18155-2008, 2008.

Costabile, F., Amoroso, A. and Wang, F.: Sub-μm particle size distributions in a suburban Mediterranean area. Aerosol populations and their possible relationship with HONO mixing ratios, Atmos. Environ., 44(39), 5258–5268, doi:10.1016/j.atmosenv.2010.08.018, 2010.

Cusack, M.: Physical and chemical processes affecting atmospheric aerosols in the Western Mediterranean regional background, Universitat Autónoma de Barcelona, PhD Thesis, 2013.

Cusack, M., Pérez, N., Pey, J., Alastuey, A. and Querol, X.: Source apportionment of fine PM and sub-micron particle number concentrations at a regional background site in the western Mediterranean: A 2.5 year study, Atmos. Chem. Phys., 13(10), 5173–5187, doi:10.5194/acp-13-5173-2013, 2013a.

Cusack, M., Pérez, N., Pey, J., Wiedensohler, A., Alastuey, A. and Querol, X.: Variability of sub-micrometer particle number size distributions and concentrations in the Western Mediterranean regional background, Tellus, Ser. B Chem. Phys. Meteorol., 65(1), 1–19, doi:10.3402/tellusb.v65i0.19243, 2013b.

Dal Maso, M., Kulmala, M., Riipinen, I., Wagner, R., Hussein, T., Aalto, P. P. and Lehtinen, K. E. J.: Formation and growth of fresh atmospheric aerosols: Eight years of aerosol size distribution data from SMEAR II, Hyyti??l??, Finland, Boreal Environ. Res., 10(5), 323–336, 2005.

Dall'Osto, M., Monahan, C., Greaney, R., Beddows, D. C. S., Harrison, R. M., Ceburnis, D. and O'Dowd, C. D.: A statistical analysis of North East Atlantic (submicron)

aerosol size distributions, Atmos. Chem. Phys., 11(24), 12567–12578, doi:10.5194/acp-11-12567-2011, 2011a.

Dall'Osto, M., Thorpe, A., Beddows, D. C. S., Harrison, R. M., Barlow, J. F., Dunbar, T., Williams, P. I. and Coe, H.: Remarkable dynamics of nanoparticles in the urban atmosphere, Atmos. Chem. Phys., 11(13), 6623–6637, doi:10.5194/acp-11-6623-2011, 2011b.

Dall'Osto, M., Beddows, D. C. S., Pey, J., Rodriguez, S., Alastuey, A., M. Harrison, R. and Querol, X.: Urban aerosol size distributions over the Mediterranean city of Barcelona, NE Spain, Atmos. Chem. Phys., 12(22), 10693–10707, doi:10.5194/acp-12-10693-2012, 2012.

Dall'Osto, M., Querol, X., Alastuey, A., Minguillon, M. C., Alier, M., Amato, F., Brines, M., Cusack, M., Grimalt, J. O., Karanasiou, A., Moreno, T., Pandolfi, M., Pey, J., Reche, C., Ripoll, A., Tauler, R., Van Drooge, B. L., Viana, M., Harrison, R. M., Gietl, J., Beddows, D., Bloss, W., O'Dowd, C., Ceburnis, D., Martucci, G., Ng, N. L., Worsnop, D., Wenger, J., Mc Gillicuddy, E., Sodeau, J., Healy, R., Lucarelli, F., Nava, S., Jimenez, J. L., Gomez Moreno, F., Artinano, B., Prévôt, A. S. H., Pfaffenberger, L., Frey, S., Wilsenack, F., Casabona, D., Jiménez-Guerrero, P., Gross, D. and Cots, N.: Presenting SAPUSS: Solving aerosol problem by using synergistic strategies in Barcelona, Spain, Atmos. Chem. Phys., 13(17), 8991–9019, doi:10.5194/acp-13-8991-2013, 2013a.

Dall'Osto, M., Querol, X., Alastuey, A., O'Dowd, C., Harrison, R. M., Wenger, J. and Gómez-Moreno, F. J.: On the spatial distribution and evolution of ultrafine particles in Barcelona, Atmos. Chem. Phys., 13(2), 741–759, doi:10.5194/acp-13-741-2013, 2013b.

Dall'Osto, M., Querol, X., Amato, F., Karanasiou, A., Lucarelli, F., Nava, S., Calzolai, G. and Chiari, M.: Hourly elemental concentrations in PM2.5 aerosols sampled simultaneously at urban background and road site during SAPUSS -diurnal variations and PMF receptor modelling, Atmos. Chem. Phys., 13(8), 4375–4392, doi:10.5194/acp-13-4375-2013, 2013c.

Davidson, C., Phalen, R. and Salomon, P.: Airborne particulate matter and human health: a review, Aerosol Sci. Technol., 39, 737-749, 2005.

Deng X., Tie X., Wu D., Zhou X., Bi X., Tan H., Li F. and Jiang C.: Long-term trend of visibility and its characterizations in the Pearl River Delta (PRD) region, China. Atmospheric Environment 42, 7, 1424-1435, 2008.

Dirección General de Tráfico (DGT), 2015: http://www.dgt.es/es/seguridad-vial/estadisticas-e-indicadores/parque-vehiculos/prov-y-tipos-vehiculos/ (last entry July 2015)

Dockery, D.W., Pope III, C.A., Xu, X., Spengler, J.D., Ware, J.H., Fay. M., Ferris, B.G. and Speizer, F.E.: An association between Air Pollution and Mortality in Six U.S. Cities, New England Journal of Medicine, 329, 1753, 1759, 1993.

Dockery, D. W. and Pope, C. A: Acute respiratory effects of particulate air pollution, Annu. Rev. Public Health, 15, 107–132, doi:10.1146/annurev.pu.15.050194.000543, 1994.

DOGC 1995: Forest fire prevention, Catalunya, Ordinance 64/1995.

Dorevitch, S., Demirtas, H., Perksy, V. W., Erdal, S., Conroy, L., Schoonover, T. and Scheff, P. A: Demolition of high-rise public housing increases particulate matter air pollution in communities of high-risk asthmatics., J. Air Waste Manag. Assoc., 56(7), 1022–1032, doi:10.1080/10473289.2006.10464504, 2006.

Draxler, R. R. and Rolph, G. D.: Hysplit (hybrid single-particle lagrangian integrated trajectory) model http://www.Arl.Noaa.Gov/ready/hysplit4.Html), in, NOAA Air Resources Laboratory, Silver Spring, MD, USA, 2003.

van Drooge, B. L., Crusack, M., Reche, C., Mohr, C., Alastuey, A., Querol, X., Prevot, A., Day, D. A., Jimenez, J. L. and Grimalt, J. O.: Molecular marker characterization of the organic composition of submicron aerosols from Mediterranean urban and rural environments under contrasting meteorological conditions, Atmos. Environ., 61, 482–489, doi:10.1016/j.atmosenv.2012.07.039, 2012.

van Drooge, B. L. and Grimalt, J. O.: Particle size-resolved source apportionment of primary and secondary organic tracer compounds at urban and rural locations in Spain, Atmos. Chem. Phys., 15(13), 7735–7752, doi:10.5194/acp-15-7735-2015, 2015.

Durant, A. J., Bonadonna, C., Horwell, C. J.: Atmospheric and environmental impacts of volcanic particulates, Elements, 6, 235-240, 2010.

Duyzer, J., van der Hout, D., Zandveld, P. and van Ratingen, S: Representativeness of air quality monitoring networks, Atmos. Environ., 104, 88-101, 2015.

EEA Report Air Quality in Europe, No 5/2014, 2014.

Eeftens, M., Tsai, M. Y., Ampe, C., Anwander, B., Beelen, R., Bellander, T., Cesaroni, G., Cirach, M., Cyrys, J., de Hoogh, K., De Nazelle, A., de Vocht, F., Declercq, C., Dedele, A., Eriksen, K., Galassi, C., Gražulevičiene, R., Grivas, G., Heinrich, J., Hoffmann, B., Iakovides, M., Ineichen, A., Katsouyanni, K., Korek, M., Krämer, U., Kuhlbusch, T., Lanki, T., Madsen, C., Meliefste, K., Mölter, A., Mosler, G., Nieuwenhuijsen, M., Oldenwening, M., Pennanen, A., Probst-Hensch, N., Quass, U., Raaschou-Nielsen, O., Ranzi, A., Stephanou, E., Sugiri, D., Udvardy, O., Vaskövi, É., Weinmayr, G., Brunekreef, B. and Hoek, G.: Spatial variation of PM2.5, PM10, PM2.5 absorbance and PMcoarse concentrations between and within 20 European study areas and the relationship with NO2 - Results of the ESCAPE project, Atmos. Environ., 62, 303–317, doi:10.1016/j.atmosenv.2012.08.038, 2012.

Efron, B. and Tibshirani, R.: Bootstrap methods for standard errors, confidence intervals, and other measures of statistical accuracy, Statistical Science 1, 54–75, 1986.

Ehrlich, C., Noll, G., Kalkoff, W. D., Baumbach, G. and Dreiseidler, a.: PM10, PM2.5 and PM1.0-Emissions from industrial plants-Results from measurement programmes in Germany, Atmos. Environ., 41(29), 6236–6254, doi:10.1016/j.atmosenv.2007.03.059, 2007.

Escrig Vidal, A., Monfort, E., Celades, I., Querol, X., Amato, F., Minguillón, M.C., Hopke, P.K., 2009. Application of optimally scaled target factor analysis for assessing source contribution of ambient PM10, Journal of the Air and Waste Management Association, 59, 1296-1307, 2009.

Escudero, M., Castillo, S., Querol, X., Avila, A., Alarcón, M., Viana, M. M., Alastuey, A., Cuevas, E. and Rodríguez, S.: Wet and dry African dust episodes over eastern Spain, J. Geophys. Res. D Atmos., 110(18), 1–15, doi:10.1029/2004JD004731, 2005.

Escudero, M.: Suspended Particulate Matter and Wet Deposition Fluxes in Regional Background Stations of the Iberian Peninsula, Universitat de Barcelona, PhD Thesis, 2006.

Escudero, M., Querol, X., Pey, J., Alastuey, A., Pérez, N., Ferreira, F., Alonso, S., Rodríguez, S. and Cuevas, E.: A methodology for the quantification of the net African dust load in air quality monitoring networks, Atmos. Environ., 41(26), 5516–5524, doi:10.1016/j.atmosenv.2007.04.047, 2007.

EU, 2012. Commissions Regulation (EU) No. 459/2012. Official Journal of the European Union. http://eur-lex.europa.eu/legal-content/EN/TXT/?uri=celex:32012R0459 (accessed on 08 Apr 2014).

Fernández-Camacho, R., Rodríguez, S., De La Rosa, J., Sánchez De La Campa, A. M., Viana, M., Alastuey, A. and Querol, X.: Ultrafine particle formation in the inland sea breeze airflow in Southwest Europe, Atmos. Chem. Phys., 10(19), 9615–9630, doi:10.5194/acp-10-9615-2010, 2010.

Fine, P. M., Cass, G. R., and Simoneit, B. R. T.: Chemical characterization of fine particle emissions from the fireplace combustion of wood types grown in the Midwestern and Western United States, Environ. Eng. Sci., 21, 387–409, 2004.

Finlaysson-Pitts, B. and Pitts, J.N.: Chemistry of the Upper and Lower Atmosphere – Theory, Experiments and Applications, Elsevier, ISBN: 978-0-12-257060-5, 2000.

Fujitani, Y., Kumar, P., Tamura, K., Fushimi, A., Hasegawa, S., Takahashi, K., Tanabe, K., Kobayashi, S. and Hirano, S.: Seasonal differences of the atmospheric particle size distribution in a metropolitan area in Japan, Sci. Total Environ., 437, 339–347, doi:10.1016/j.scitotenv.2012.07.085, 2012.

Fusco, D., Forastiere, F., Michelozzi, P., Spadea, T., Ostro, B., Arcà, M. and Perucci, C. A.: Air pollution and hospital admissions for respiratory conditions in Rome, Italy, Eur. Respir. J., 17(6), 1143–1150, doi:10.1183/09031936.01.00005501, 2001.

Gentner, D.R., Isaacman, G., Worton, D.R., Chan, A.W.H., Dallmann, T.R., Davis, L., Liu, S., Day, D.A., Russell, L.M., Wilson, K.R., Weber, R., Guha, A., Harley, R.A., Goldstein, A.H., Elucidating secondary organic aerosol from diesel and gasoline vehicles through detailed characterization of organic carbon emissions, Proceeding of the National Academy of Science, 109, 45, 18318-18323, 2012.

Gieré, R. and Querol, X.: Solid particulate matter in the atmosphere, Elements, 6(4), 215–222, doi:10.2113/gselements.6.4.215, 2010.

Ginoux, P., Prospero, J. M., Gill, T. E., Hsu, N. C. and Zhao, M.: Global-Scale Attribution of Anthropogenic and Natural Dust Sources and Their Emission Rates Based on Modis Deep Blue Aerosol Products, 1–36, doi:10.1029/2012RG000388.1.INTRODUCTION, 2012.

Goel, A. and Kumar, P.: A review of fundamental drivers governing the emissions, dispersion and exposure to vehicle-emitted nanoparticles at signalised traffic intersections, Atmos. Environ. 97, 316-331, 2014.

Goldberg, E. D.: Black carbon in the environment: properties and distribution, John Wiley & Sons Inc., 1985.

Gómez-Moreno, F. J., Núñez, L., Plaza, J., Alonso, D., Pujadas, M. and Artíñano, B.: Annual evolution and generation mechanisms of particulate nitrate in Madrid, Atmos. Environ., 41(2), 394–406, doi:10.1016/j.atmosenv.2006.07.040, 2007.

Gómez-Moreno, F. J., Pujadas, M., Plaza, J., Rodríguez-Maroto, J. J., Martínez-Lozano, P. and Artíñano, B.: Influence of seasonal factors on the atmospheric particle number concentration and size distribution in Madrid, Atmos. Environ., 45(18), 3169–3180, doi:10.1016/j.atmosenv.2011.02.041, 2011.

El Haddad, I., D'Anna, B., Temime-Roussel, B., Nicolas, M., Boreave, A., Favez, O., Voisin, D., Sciare, J., George, C., Jaffrezo, J. L., Wortham, H. and Marchand, N.: Towards a better understanding of the origins, chemical composition and aging of oxygenated organic aerosols: Case study of a Mediterranean industrialized environment, Marseille, Atmos. Chem. Phys., 13(15), 7875–7894, doi:10.5194/acp-13-7875-2013, 2013.

Harris, S. J. and Maricq, M. M.: Signature size distributions for diesel and gasoline engine exhaust\rparticulate matter, J. Aerosol Sci., 32, 749–764, 2001.

Harrison, R. M. and Yin, J.: Particulate matter in the atmosphere: which particle properties are important for its effects on health?, Sci. Total. Environ., 249, 85-101, 2000.

Harrison, R. M., Stedman, J. and Derwent, D.: New Directions: Why are PM10 concentrations in Europe not falling?, Atmospheric Environment, 42(3), 603–606, doi:10.1016/j.atmosenv.2007.11.023, 2008.

Harrison, R. M., Beddows, D. C. S. and Dall'Osto, M.: PMF analysis of wide-range particle size spectra collected on a major highway, Environ. Sci. Technol., 45(13), 5522–5528, doi:10.1021/es2006622, 2011.

Harrison, R. M., Dall'Osto, M., Beddows, D. C. S., Thorpe, a. J., Bloss, W. J., Allan, J. D., Coe, H., Dorsey, J. R., Gallagher, M., Martin, C., Whitehead, J., Williams, P. I., Jones, R. L., Langridge, J. M., Benton, a. K., Ball, S. M., Langford, B., Hewitt, C. N., Davison, B., Martin, D., Petersson, K. F., Henshaw, S. J., White, I. R., Shallcross, D. E., Barlow, J. F., Dunbar, T., Davies, F., Nemitz, E., Phillips, G. J., Helfter, C., Di Marco, C. F. and Smith, S.: Atmospheric chemistry and physics in the atmosphere of a developed megacity (London): An overview of the REPARTEE experiment and

its conclusions, Atmos. Chem. Phys., 12, 3065–3114, doi:10.5194/acp-12-3065-2012, 2012.

HEI Review Panel on Ultrafine Particles, Understanding the Health Effects of Ambient Ultrafine Particles, HEI Perspectives 3, Health Effects Institute, Boston, MA. 2013

Hendricks, J., Kärcher, B., Döpelheuer, A., Feichter, J., Lohmann, U. and Baumgardner, D.: Simulating the global atmospheric black carbon cycle: a revisit to the contribution of aircraft emissions, Atmos. Chem. Phys. Discuss., 4(3), 3485–3533, doi:10.5194/acpd-4-3485-2004, 2004.

Hidy, G. M.: Atmospheric sulfur and nitrogen oxides: Eastern North American source receptor relationships, Academic Press, San Diego, pp. 447, 1994.

Holman, C., Harrison, R. and Querol, X.: Review of the efficacy of low emission zones to improve urban air quality in European cities, Atmos. Environ., 111, 161–169, doi:10.1016/j.atmosenv.2015.04.009, 2015.

Hoyle, C. R., Boy, M., Donahue, N. M., Fry, J. L., Glasius, M., Guenther, A., Hallar, A. G., Huff Hartz, K., Petters, M. D., Petäjä, T., Rosenoern, T. and Sullivan, A. P.: A review of the anthropogenic influence on biogenic secondary organic aerosol, Atmos. Chem. Phys., 11(1), 321–343, doi:10.5194/acp-11-321-2011, 2011.

Huang, L., Gong, S. L., Gordon, M., Liggio, J., Staebler, R. M., Stroud, C. A., Lu, G., Mihele, C., Brook, J. R. and Jia, C. Q.: Aerosol-CFD modelling of ultrafine and black carbon particle emission, dilution, and growth near roadways, Atmos. Chem. Phys. Discuss., 14(8), 12235–12278, doi:10.5194/acpd-14-12235-2014, 2014.

Hudda, N., Cheung, K., Moore, K. F. and Sioutas, C.: Inter-community variability in total particle number concentrations in the eastern Los Angeles air basin, Atmos. Chem. Phys., 10(23), 11385–11399, doi:10.5194/acp-10-11385-2010, 2010.

Husar R. B., Holloway J. M., Patterson D. E., Wilson W. E.: Spatial and temporal pattern of eastern U.S. haziness: A summary. Atmospheric Environment 15, 10-11, 1919-1928, 1981.

Hussein, T., Puustinen, A., Aalto, P.P., Mäkelä , J.M., Hämeri, K. and Kulmala, M.: Urban aerosol number size distributions, Atmos. Chem. Phys. 4, 391–411, 2004.

Hussein, T., Karppinen, A., Kukkonen, J., Härkönen, J., Aalto, P.P., Hämeri, K., Kerminen, V.M. and Kulmala, M.: Meteorlogical dependence of size fractioned number concentration of urban aerosol particles, Atmos. Environ., 40, 1427-1440, 2006.

Hussein, T., Martikainen, J., Junninen, H., Sogacheva, L., Wagner, R., Maso, M.D., Riipinen, I., Aalto, P.P., Kulmala, M.,: Observation of regional new particle formation in the urban atmosphere, Tellus B, 60, 509-521, 2008.

Idescat, 2014: http://www.idescat.cat/pub/?id=aec&n=250&t=2014&x=9&y=5 (last entry: July 2015).

IPCC. Climate Change 2007: The Physical Science Basis. Contribution of Working Group I to the fourth Assessment Report of the IPCC (ISBN 978 0521 88009-1 Hardback; 9780521 070596-7 Paperback), 2007.

IPCC. Climate Change 2013: The Physical Science Basis. Contribution of Working Group I to the fifth Assessment Report of the IPCC (ISBN 978-1-107-05799-1 hardback; ISBN 978-1-107-66182-0 paperback), 2013.

Istituto Nazionali di Statistica, 2009: Annuari di Statistiche Ambientali 2009, n.11-2009, http://www3.istat.it/dati/catalogo/20091130_00/ann_09_11statistich_%20ambientali09.pdf

Jickells T. D., An Z. S., Andersen K. K., Baker A. R., Bergametti G., Brooks N., Cao J. J., Boyd P. W., Duce R. A., Hunter K. A., Kawahata H., Kubilay N., laRoche J., Liss P. S., Mahowald N., Prospero J. M., Ridgwell A. J., Tegen I. and Torres R.: Global Iron Connections between Desert Dust, Ocean Biogeochemistry and Climate. Science 308, 5718, 67–71, 2005.

Jimenez, J. L., Canagaratna, M. R., Donahue, N. M., Prevot, A. S. H., Zhang, Q., Kroll, J. H., DeCarlo, P. F., Allan, J. D., Coe, H., Ng, N. L., Aiken, A. C., Docherty, K. S.,

Ulbrich, I. M., Grieshop, A. P., Robinson, A. L., Duplissy, J., Smith, J. D., Wilson, K. R., Lanz, V. A., Hueglin, C., Sun, Y. L., Tian, J., Laaksonen, A., Raatikainen, T., Rautiainen, J., Vaattovaara, P., Ehn, M., Kulmala, M., Tomlinson, J. M., Collins, D. R., Cubison, M. J., Dunlea, E. J., Huffman, J. A., Onasch, T. B., Alfarra, M. R., Williams, P. I., Bower, K., Kondo, Y., Schneider, J., Drewnick, F., Borrmann, S., Weimer, S., Demerjian, K., Salcedo, D., Cottrell, L., Griffin, R., Takami, A., Miyoshi, T., Hatakeyama, S., Shimono, A., Sun, J. Y., Zhang, Y. M., Dzepina, K., Kimmel, J. R., Sueper, D., Jayne, J. T., Herndon, S. C., Trimborn, A. M., Williams, L. R., Wood, E. C., Middlebrook, A. M., Kolb, C. E., Baltensperger, U. and Worsnop, D. R.: Evolution of organic aerosols in the atmosphere, Science, 326(5959), 1525–1529, doi:10.1126/science.1180353, 2009.

Jorba, O., Pandolfi, M., Spada, M., Baldasano, J. M., Pey, J., Alastuey, A., Arnold, D., Sicard, M., Artiñano, B., Revuelta, M. A. and Querol, X.: Overview of the meteorology and transport patterns during the DAURE field campaign and their impact to PM observations, Atmos. Environ., 77, 607–620, doi:10.1016/j.atmosenv.2013.05.040, 2013.

Kanawade, V. P., Shika, S., Pöhlker, C., Rose, D., Suman, M.N.S., Gadhavi, H., Kumar, A., Shiva Nagendra, S.M., Ravikrishna, R., Yu, H., Sahu, L.K., Jayaraman, A., Andreae, M.O., Pöschl, U. and Gunthe, S.S: Infrequent occurrence of new particle formation at a semi-rural location, Gadanki, in tropical Southern India, Atmos. Environ., 94, 264-273, 2014a.

Kanawade, V.P., Tripathi, S.N., Siingh, D., Gautam, A.S., Srivastava, A.K., Kamra, A.K., Soni, V.K. and Sethi, V.: Observations of new particle formation at two distinct Indian subcontinental urban locations, Atmos. Environ., 96, 370-379, 2014b.

Kim, E. and Hopke, P. K.: Source characterization of ambient fine particles at multiple sites in the Seattle area, Atmos. Environ., 42(24), 6047–6056, doi:10.1016/j.atmosenv.2008.03.032, 2008.

Kim, K., Kabir, E. and Kabir, S.: A review on the human health impact of airborne particulate matter, Environ. Int., 74, 136–143, doi:10.1016/j.envint.2014.10.005, 2015.

Kittelson, D. B.: Engines and nanoparticles: A review, J. Aerosol Sci., 29(5-6), 575–588, doi:10.1016/S0021-8502(97)10037-4, 1998.

Kittelson, D. B., Watts, W. F. and Johnson, J. P.: On-road and laboratory evaluation of combustion aerosols-Part1: Summary of diesel engine results, J. Aerosol Sci., 37(8), 913–930, doi:10.1016/j.jaerosci.2005.08.005, 2006.

Knippertz P., Stuut J.-B.W.: Mineral dust: a key player in the earth system, Springer, ISBN 978-94-017-8978-3, 2014.

Kulmala, M., Pirjola, L. and Makela, J.: Stable sulphate clusters as a source of new atmospheric particles, Nature, 404(6773), 66–9, doi:10.1038/35003550, 2000.

Kulmala, M., Vehkamäki, H., Petäjä, T., Dal Maso, M., Lauri, A., Kerminen, V. M., Birmili, W. and McMurry, P. H.: Formation and growth rates of ultrafine atmospheric particles: A review of observations, J. Aerosol Sci., 35(2), 143–176, doi:10.1016/j.jaerosci.2003.10.003, 2004.

Kulmala, M. and Kerminen, V.-M.: On the formation and growth of atmospheric nanoparticles, Atmos. Res., 90(2-4), 132–150, doi:10.1016/j.atmosres.2008.01.005, 2008.

Kulmala, M., Kontkanen, J., Junninen, H., Lehtipalo, K., Manninen, H. E., Nieminen, T., Petäjä, T., Sipilä, M., Schobesberger, S., Rantala, P., Franchin, A., Jokinen, T., Järvinen, E., Äijälä, M., Kangasluoma, J., Hakala, J., Aalto, P. P., Paasonen, P., Mikkilä, J., Vanhanen, J., Aalto, J., Hakola, H., Makkonen, U., Ruuskanen, T., Mauldin, R. L., Duplissy, J., Vehkamäki, H., Bäck, J., Kortelainen, A., Riipinen, I., Kurtén, T., Johnston, M. V, Smith, J. N., Ehn, M., Mentel, T. F., Lehtinen, K. E. J., Laaksonen, A., Kerminen, V.-M. and Worsnop, D. R.: Direct observations of atmospheric aerosol nucleation., Science, 339(6122), 943–946, doi:10.1126/science.1227385, 2013.

Kumar, P., Ketzel, M., Vardoulakis, S., Pirjola, L. and Britter, R.: Dynamics and dispersion modelling of nanoparticles from road traffic in the urban atmospheric environment-A review, J. Aerosol Sci., 42(9), 580–603, doi:10.1016/j.jaerosci.2011.06.001, 2011.

Kumar, P., Morawska, L., Birmili, W., Paasonen, P., Hu, M., Kulmala, M., Harrison, R. M., Norford, L. and Britter, R.: Ultrafine particles in cities, Environ. Int., 66, 1–10, doi:10.1016/j.envint.2014.01.013, 2014.

Laden, F., Neas, L. M., Dockery, D. W. and Schwartz, J.: Association of fine particulate matter from different sources with daily mortality in six U.S. cities [In Process Citation], Env. Heal. Perspect, 108(10), 941–947, doi:10.1289/ehp.00108941, 2000.

Lelieveld, J., Berresheim, H., Borrmann, S., Crutzen, P. J., Dentener, F. J., Fischer, H., Feichter, J., Flatau, P. J., Heland, J., Holzinger, R., Korrmann, R., Lawrence, M. G., Levin, Z., Markowicz, K. M., Mihalopoulos, N., Minikin, A., Ramanathan, V., De Reus, M., Roelofs, G. J., Scheeren, H. a, Sciare, J., Schlager, H., Schultz, M., Siegmund, P., Steil, B., Stephanou, E. G., Stier, P., Traub, M., Warneke, C., Williams, J. and Ziereis, H.: Global air pollution crossroads over the Mediterranean., Science, 298(5594), 794–799, doi:10.1126/science.1075457, 2002.

Levin, Z. and Cotton, W.R.: Aerosol pollution impact on precipitation – A scientific review, Springer, ISBN 978-1-4020-8690-8, 2009.

Li, T., Chen, X. and Yan, Z.: Comparison of fine particles emissions of light-duty gasoline vehicles from chassis dynamometer tests and on-road measurements, Atmos. Environ., 68, 82–91, doi:10.1016/j.atmosenv.2012.11.031, 2013.

Lighty, J. S., Veranth, J. M. and Sarofim, A. F.: Combustion aerosols: factors governing their size and composition and implications to human health., J. Air Waste Manag. Assoc., 50(9), 1565–1618; discussion 1619–1622, doi:10.1080/10473289.2000.10464197, 2000.

Lim, S. S., Vos, T., Flaxman, A. D., Danaei, G., Shibuya, K., Adair-rohani, H., Almazroa, M. A., Amann, M., Barker-collo, S., Baxter, A., Bell, M. L., Blore, J. D., Blyth, F., Bonner, C., Borges, G., Bourne, R., Boussinesq, M., Brauer, M., Brooks, P., Bruce, N. G., Brunekreef, B., Bryan-hancock, C., Bucello, C., Buchbinder, R., Bull, F., Burnett, R. T., Byers, T. E., Calabria, B., Carapetis, J., Carnahan, E., Chafe, Z., Charlson, F., Chen, H., Chen, J. S., Cheng, A. T., Child, J. C., Cohen, A., Colson, K. E., Cowie, B. C., Darby, S., Darling, S., Davis, A., Degenhardt, L., Dentener, F., Jarlais, D. C. Des, Devries, K., Dherani, M., Ding, E. L., Dorsey, E. R., Giovannucci, E., Gmel, G., Graham, K., Grainger, R., Grant, B., Gunnell, D., Gutierrez, H. R., Hall, W., Room, R., Rosenfeld, L. C., Roy, A., Rushton, L., Salomon, J. A., Sampson, U., Sanchez-riera, L., Sanman, E., Stapelberg, N. J. C., Steenland, K., Stöckl, H., Stovner, L. J., Straif, K., Straney, L., Thurston, G. D., Tran, J. H., Whiteford, H., Wiersma, S. T., Wilkinson, J. D., Williams, H. C., Williams, W., Wilson, N., Woolf, A. D., Yip, P., Zielinski, J. M., Lopez, A. D., Murray, C. J. L. and Ezzati, M.: A comparative risk assessment of burden of disease and injury attributable to 67 risk factors and risk factor clusters in 21 regions , 1990 – 2010 : a systematic analysis for the Global Burden of Disease Study 2010, The Lancet , 380, 1990–2010, doi:10.1016/S0140-6736(12)61766-8, 2012.

Lin, Y. H., Zhang, Z., Docherty, K. S., Zhang, H., Budisulistiorini, S. H., Rubitschun, C. L., Shaw, S. L., Knipping, E. M., Edgerton, E. S., Kleindienst, T. E., Gold, A., and Surratt, J. D.: Isoprene epoxydiols as precursors to secondary organic aerosol formation: Acid-catalyzed reactive uptake studies with authentic compounds. Environ. Sci. Technol., 46, 250–258, 2012.

Liu, G., Tong, Y., Luong, J. H. T., Zhang, H. and Sun, H.: A source study of atmospheric polycyclic aromatic hydrocarbons in Shenzhen, South China, Environ. Monit. Assess., 163(1-4), 599–606, doi:10.1007/s10661-009-0862-4, 2010.

Liu, Z.R., Hu, B., Liu, Q., Sun, Y., Wang, Y.S.: Source apportionment of urban fine particle number concentration during summertime in Beijing, Atmos. Environ., 95, 359-369, 2014.

Lu, R. and Turco, R. P.: Air pollutant transport in a coastal environment -II. Three dimensional simulations over Los Angeles basin, Atmos. Environ., 29(13), 1499–1518, 1995.

Magee Scientific: Aethalometer book 2005.07, 2005.

Maître, A., Collot-Fertey, D., Anzivino, L., Marques, M., Hours, M. and Stoklov, M.: Municipal waste incinerators: air and biological monitoring of workers for exposure to particles, metals, and organic compounds, Occup. Environ. Med., 60(8), 563–569, doi:10.1136/oem.60.8.563, 2003.

Mason, B.: Principles of Geochemistry, 3rd ed. Wiley, New York, 1966.

McCreanor, J., Cullinan, P., Nieuwenhuijsen, M. J., Stewart-Evans, J., Malliarou, E., Jarup, L., Harrington, R., Svartengren, M., Han, I.-K., Ohman-Strickland, P., Chung, K. F. and Zhang, J.: Respiratory effects of exposure to diesel traffic in persons with asthma., N. Engl. J. Med., 357(23), 2348–2358, doi:10.1056/NEJMoa071535, 2007.

McMurry, P.: A review of atmospheric aerosol measurements, Atmos. Environ., 34, 1959–1999, doi:10.1016/S1352-2310(99)00455-0, 2000.

Mészáros, E.: Fundamentals of Atmospheric Aerosol Chemistry, Akadémiai Kiado, 1999.

Mildford, J. B. and Davidson, C. I.: The sizes of particulate sulphate and nitrate in the Atmosphere: A review, Journal of Air Pollution Control Association, 37, 2, 125-134, 1987.

Millán, M., Salvador, R., Mantilla, E. and Kallos, G.: Photo-oxidant dynamics in the Mediterranean basin in summer: results from European research projects, Journal of Geophysical Research, 102, 8811-8823, 1997.

Millán, M., Mantilla, E., Salvador, R., Carratala, A., Sanz, M. J., Alonso, L., Gangoiti, G., and Navazo, M.: Ozone cycles in the western Mediterranean basin: interpretation of monitoring data in complex coastal terrain, J. Appl. Meteorol., 39, 487–508, 73–83, 2000.

Minguillón, M.C.: Composicion del material particulado atmosferico en la zona ceramica de Castellon: Impacto de la introducción de las mejoras tecnicas disponibles. Universidad Jaume I de Castellon, PhD Thesis, 2007.

Minguillón, M. C., Cirach, M., Hoek, G., Brunekreef, B., Tsai, M., de Hoogh, K., Jedynska, A., Kooter, I. M., Nieuwenhuijsen, M. and Querol, X.: Spatial variability of trace elements and sources for improved exposure assessment in Barcelona, Atmos. Environ., 89, 268–281, doi:10.1016/j.atmosenv.2014.02.047, 2014.

Minguillón, M. C., Perron, N., Querol, X., Szidat, S., Fahrni, S. M., Alastuey, A., Jimenez, J. L., Mohr, C., Ortega, A. M., Day, D. A., Lanz, V. A., Wacker, L., Reche, C., Cusack, M., Amato, F., Kiss, G., Hoffer, A., Decesari, S., Moretti, F., Hillamo, R., Teinilä, K., Seco, R., Peñuelas, J., Metzger, A., Schallhart, S., Müller, M., Hansel, A., Burkhart, J. F., Baltensperger, U. and Prévót, A. S. H.: Fossil versus contemporary sources of fine elemental and organic carbonaceous particulate matter during the DAURE campaign in Northeast Spain, Atmos. Chem. Phys., 11(23), 12067–12084, doi:10.5194/acp-11-12067-2011, 2011.

Morawska, L., Thomas, S., Bofinger, N., Wainwright, D. and Neale, D.: Comprehensive characterization of aerosols in a subtropical urban atmosphere, Atmos. Environ., 32(14-15), 2467–2478, doi:10.1016/S1352-2310(98)00023-5, 1998.

Morawska, L., Thomas, S., Jamriska, M. and Johnson, G.: The modality of particle size distributions of environmental aerosols, Atmos. Environ., 33(27), 4401–4411, doi:10.1016/S1352-2310(99)00217-4, 1999.

Morawska, L., Keogh, D. U., Thomas, S. B. and Mengersen, K.: Modality in ambient particle size distributions and its potential as a basis for developing air quality regulation, Atmos. Environ., 42(7), 1617–1628, doi:10.1016/j.atmosenv.2007.09.076, 2008.

Moreno, T., Querol, X., Alastuey, A., Reche, C., Cusack, M., Amato, F., Pandolfi, M., Pey, J., Richard, a., Prévt, a. S. H., Furger, M. and Gibbons, W.: Variations in time and

space of trace metal aerosol concentrations in urban areas and their surroundings, Atmos. Chem. Phys., 11(17), 9415–9430, doi:10.5194/acp-11-9415-2011, 2011.

Moreno, T., Querol, X., Castillo, S., Alastuey, A., Cuevas, E., Herrmann, L., Mounkaila, M., Elvira, J. and Gibbons, W.: Geochemical variations in aeolian mineral particles from the Sahara-Sahel Dust Corridor, Chemosphere, 65(2), 261–270, doi:10.1016/j.chemosphere.2006.02.052, 2006.

Müller, T., Henzing, J. S., de Leeuw, G., Wiedensohler, A., Alastuey, A., Angelov, H., Bizjak, M., Collaud Coen, M., Engström, J. E., Gruening, C., Hillamo, R., Hoffer, A., Imre, K., Ivanow, P., Jennings, G., Sun, J. Y., Kalivitis, N., Karlsson, H., Komppula, M., Laj, P., Li, S.-M., Lunder, C., Marinoni, A., Martins dos Santos, S., Moerman, M., Nowak, A., Ogren, J. A., Petzold, A., Pichon, J. M., Rodriquez, S., Sharma, S., Sheridan, P. J., Teinilä, K., Tuch, T., Viana, M., Virkkula, A., Weingartner, E., Wilhelm, R. and Wang, Y. Q.: Characterization and intercomparison of aerosol absorption photometers: result of two intercomparison workshops, Atmos. Meas. Tech., 4(2), 245–268, doi:10.5194/amt-4-245-2011, 2011.

Norman, M. and Johansson, C.: Studies of some measures to reduce road dust emissions from paved roads in Scandinavia, Atmos. Environ., 40(32), 6154–6164, doi:10.1016/j.atmosenv.2006.05.022, 2006.

Ntziachristos, L., Ning, Z., Geller, M. D. and Sioutas, C.: Particle concentration and characteristics near a major freeway with heavy-duty diesel traffic, Environ. Sci. Technol., 41(7), 2223–2230, doi:10.1021/es062590s, 2007.

O'Dowd, C., Monahan, C. and Dall'Osto, M.: On the occurrence of open ocean particle production and growth events, Geophys. Res. Lett., 37(19), 2–6, doi:10.1029/2010GL044679, 2010.

Oberdorster, G., Oberdorster, E. and Oberdorster, J.: Nanotoxicology: An emerging discipline evolving from studies of ultrafine particles, Environmental Health Perspectives, 113, 7, 823-839, 2005.

Olivares, G., Johansson, C., Ström, J. and Hansson, H.C.: The role of ambient temperature for particle number concentrations in a street canyon, Atmos. Environ., 41, 2145-2155, 2007.

Ostro, B.D., Broadwin, R., Lipsett, M.J.: Coarse and fine particles and daily mortality in the Coachella Valley, California: a follow-up study, J. Expo. Anal. Environ. Epidemiol., 10, 412– 419, 2000.

Ostro, B., Tobias, A., Querol, X., Alastuey, A., Amato, F., Pey, J., Pérez, N. and Sunyer, J.: The Effects of Particulate Matter Sources on Daily Mortality : A Case-Crossover Study of Barcelona, Spain, Environmental Health Perspectives, 119, 12, 2011.

Pandolfi, M., Gonzalez-Castanedo, Y., Alastuey, A., de la Rosa, J. D., Mantilla, E., de la Campa, A. S., Querol, X., Pey, J., Amato, F. and Moreno, T.: Source apportionment of PM10 and PM2.5 at multiple sites in the strait of Gibraltar by PMF: Impact of shipping emissions, Environ. Sci. Pollut. Res., 18(2), 260–269, doi:10.1007/s11356-010-0373-4, 2011.

Pandolfi, M., Martucci, G., Querol, X., Alastuey, A., Wilsenack, F., Frey, S., O'Dowd, C. D. and Dall'Osto, M.: Continuous atmospheric boundary layer observations in the coastal urban area of Barcelona during SAPUSS, Atmos. Chem. Phys., 13(9), 4983–4996, doi:10.5194/acp-13-4983-2013, 2013.

Pandolfi, M., Querol, X., Alastuey, A., Jimenez, J. L., Jorba, O., Day, D., Ortega, A., Cubison, M. J., Comerón, A., Sicard, M., Mohr, C., Prévôt, A. S. H., Minguillón, M. C., Pey, J., Baldasano, J. M., Burkhart, J. . F., Seco, R., Peñuelas, J., van Drooge, B. L., Artiñano, B., Di Marco, C., Nemitz, E., Schallhart, S., Metzger, A., Hansel, A., Lorente, J., Ng, S., Jayne, J. and Szidat, S.: Effects of sources and meteorology on particulate matter in the Western Mediterranean Basin: An overview of the DAURE campaign, J. Geophys. Res. Atmos., 119, 4978–5010, doi:10.1002/2013JD021079.Received, 2014.

Paatero, P. and Tapper, U.: Positive matrix factorization: a non-negative factor model with optimal utilization of error estimates of data values, Environmetrics, 5, 111-126, 1994.

Paatero, P.: The multilinear engine – a table-driven, least squares program for solving multilinear problems, including the n-way parallel factor analysis model, J. Comput. Graph. Stat., 8, 854-888, 1999.

Paatero, P.: End User's Guide to Multilinear Engine Applications, 2007.

Paatero, P. and Hopke, P.K.: Rotational tools for factor analytic models. Journal of Chemometrics 23 (2), 91–100, 2009.

Pant, P. and Harrison, R. M.: Estimation of the contribution of road traffic emissions to particulate matter concentrations from field measurements: A review, Atmos. Environ., 77, 78–97, doi:10.1016/j.atmosenv.2013.04.028 Review, 2013.

Park, Y. K., Kim, W. and Jo, Y. M.: Release of harmful air pollutants from open burning of domestic municipal solid wastes in a metropolitan area of Korea, Aerosol Air Qual. Res., 13(4), 1365–1372, doi:10.4209/aaqr.2012.10.0272, 2013.

Peng, J. F., Hu, M., Wang, Z. B., Huang, X. F., Kumar, P., Wu, Z. J., Guo, S., Yue, D. L., Shang, D. J., Zheng, Z., and He, L. Y.: Submicron aerosols at thirteen diversified sites in China: size distribution, new particle formation and corresponding contribution to cloud condensation nuclei production, Atmos. Chem. Phys., 14, 10249-10265, doi:10.5194/acp-14-10249-2014, 2014.

Perez, L., Tobias, A., Querol, X., Künzli, N., Pey, J., Alastuey, A., Viana, M., Valero, N., González-Cabré, M. and Sunyer, J.: Coarse particles from Saharan dust and daily mortality., Epidemiology, 19(6), 800–807, doi:10.1097/EDE.0b013e31818131cf, 2008.

Pérez, N., Pey, J., Castillo, S., Viana, M., Alastuey, a and Querol, X.: Interpretation of the variability of levels of regional background aerosols in the Western

Mediterranean, Sci. Total Environ., 407(1), 527–540, doi:10.1016/j.scitotenv.2008.09.006, 2008a.

Pérez, N., Pey, J., Querol, X., Alastuey, A., López, J. M. and Viana, M.: Partitioning of major and trace components in PM10-PM2.5-PM1 at an urban site in Southern Europe, Atmos. Environ., 42(8), 1677–1691, doi:10.1016/j.atmosenv.2007.11.034, 2008b.

Pérez, N.: Variability of atmospheric Aerosols at urban, regional and continental backgrounds in the western Mediterranean Basin, Universitat Autónoma de Barcelona, PhD Thesis, 2010.

Pérez, N., Pey, J., Cusack, M., Reche, C., Querol, X., Alastuey, A. and Viana, M.: Levels and Speciation: Influence of Road Traffic Emissions on Urban Air Quality, Aerosol Sci. Technol., 44(7), 487–499, doi:10.1080/02786821003758286, 2010.

Petäjä, T., Kerminen, V.-M., Dal Maso, M., Junninen, H., Koponen, I. K., Hussein, T., Aalto, P. P., Andronopoulos, S., Robin, D., Hämeri, K., Bartzis, J. G., and Kulmala, M.: Sub-micron atmospheric aerosols in the surroundings of Marseille and Athens: physical characterization and new particle formation, Atmos. Chem. Phys., 7, 2705-2720, doi:10.5194/acp-7-2705-2007, 2007.

Pey, J.: Caracterización físico-química de los aerosoles atmosféricos en el Mediterráneo Occidental. Universitat Politecnica de Catalunya, PhD Thesis, 2007.

Pey, J., Rodríguez, S., Querol, X., Alastuey, A., Moreno, T., Putaud, J. P. and Van Dingenen, R.: Variations of urban aerosols in the western Mediterranean, Atmos. Environ., 42(40), 9052–9062, doi:10.1016/j.atmosenv.2008.09.049, 2008.

Pey, J., Querol, X., Alastuey, A., Rodríguez, S., Putaud, J. P. and Van Dingenen, R.: Source apportionment of urban fine and ultra-fine particle number concentration in a Western Mediterranean city, Atmos. Environ., 43(29), 4407–4415, doi:10.1016/j.atmosenv.2009.05.024, 2009.

Pey, J., Querol, X. and Alastuey, A.: Discriminating the regional and urban contributions in the North-Western Mediterranean: PM levels and composition, Atmos. Environ., 44(13), 1587–1596, doi:10.1016/j.atmosenv.2010.02.005, 2010.

Pey, J., Alastuey, A. and Querol, X.: PM10 and PM2.5 sources at an insular location in the western mediterranean by using source apportionment techniques, Sci. Total Environ., 456-457, 267–277, doi:10.1016/j.scitotenv.2013.03.084, 2013.

Pope III, C.A., Dockery, D.W. and Schwartz, J.: Review of epidemiological evidence of health effects of particulate air pollution, Inhalation Toxicology, 7, 1-18, 1995.

Pope III, C.A., Burnett, R.T., Thun, M.J., Calle, E.E., Krewski, D., Ito, K., Thurnston, G.D.: Lung cancer, cardiopulmonary mortality, and long-term exposure to fine particulate air pollution. Journal of the American Medical Association, 287 (9), 1132-1141, 2002.

Pope III, C.A. and Dockery, D.W.: Health effects of fine particulate air pollution: lines that connect, Journal of the Air and Waste Management Association, 56, 709-742, 2006.

Pope III, C.A., Ezzati, M. and Dockery, D.W.: Fine particulate air pollution and US county life expectancies, N. Engl. J. Med., 360, 4, 376-386, 2009.

Posner, L. N. and Pandis, S. N.: Sources of ultrafine particles in the Eastern United States, Atmos. Environ., 111, 103-112, 2015.

Prospero J. M.: Long range transport of mineral dust in the global atmosphere: impact of African dust on the environment of the south-eastern United States. Proceedings of the National Academy of Science USA, 96, 3396-3403, 1999.

Prospero, J. M.: Environmental characterization of global sources of atmospheric soil dust identified with the NIMBUS 7 Total Ozone Mapping Spectrometer (TOMS) absorbing aerosol product, Reviews of Geophysics, 40(1), 1002, doi:10.1029/2000RG000095, 2002.

Putaud, J.-P., Raes, F., Van Dingenen, R., Brüggemann, E., Facchini, M.-C., Decesari, S., Fuzzi, S., Gehrig, R., Hüglin, C., Laj, P., Lorbeer, G., Maenhaut, W., Mihalopoulos, N., Müller, K., Querol, X., Rodriguez, S., Schneider, J., Spindler, G., Brink, H. Ten, Tørseth, K. and Wiedensohler, A.: A European aerosol phenomenology—2: chemical characteristics of particulate matter at kerbside, urban, rural and background sites in Europe, Atmospheric Environment, 38(16), 2579–2595, doi:10.1016/j.atmosenv.2004.01.041, 2004.

Putaud, J. P., Van Dingenen, R., Alastuey, A., Bauer, H., Birmili, W., Cyrys, J., Flentje, H., Fuzzi, S., Gehrig, R., Hansson, H. C., Harrison, R. M., Herrmann, H., Hitzenberger, R., Hüglin, C., Jones, A. M., Kasper-Giebl, A., Kiss, G., Kousa, A., Kuhlbusch, T. A. J., Löschau, G., Maenhaut, W., Molnar, A., Moreno, T., Pekkanen, J., Perrino, C., Pitz, M., Puxbaum, H., Querol, X., Rodriguez, S., Salma, I., Schwarz, J., Smolik, J., Schneider, J., Spindler, G., ten Brink, H., Tursic, J., Viana, M., Wiedensohler, A. and Raes, F.: A European aerosol phenomenology - 3: Physical and chemical characteristics of particulate matter from 60 rural, urban, and kerbside sites across Europe, Atmos. Environ., 44(10), 1308–1320, doi:10.1016/j.atmosenv.2009.12.011, 2010.

Puxbaum, H., Caseiro, A., Sánchez-Ochoa, A., Kasper-Giebl, A., Claeys, M., Gelencsér, A., Legrand, M., Preunkert, S. and Pio, C. A.: Levoglucosan levels at background sites in Europe for assessing the impact of biomass combustion on the European aerosol background, J. Geophys. Res. Atmos., 112(23), 1–11, doi:10.1029/2006JD008114, 2007.

Querol, X., Alastuey, A., Lopez-Soler, A., Mantilla, E., Plana, F.: Mineral composition of atmospheric particulates around a large coal-fired power station, Atmos. Environ., 30, 3557-3572, 1996.

Querol, X., Alastuey, A. S., Puicercus, J. A., Mantilla, Ruiz, C.R., Lopez-soler, A. and Plana-, F, Juan, R.: Seasonal evolution of suspended particles around a large coalfired power station: chemical characterization, Atmospheric Environment, 32(4), 719-731, 1998a.

Querol, X., Alastuey, A. S., Puicercus, J. A., Mantilla, E., Miro, J. V, Lopez-soler, A. and Plana-, F.: Seasonal evolution of suspended particles around a large coal-fired power station: particulate levels and sources, Atmospheric Environment, 32(11), 1963-1978, 1998b.

Querol, X., Alastuey, A., Rodriguez, S., Plana, F., Mantilla, E. and Ruiz, C. R.: Monitoring of PM10 and PM2.5 around primary particulate anthropogenic emission sources, Atmos. Environ., 35(5), 845–858, doi:10.1016/S1352-2310(00)00387-3, 2001.

Querol, X., Alastuey, A., Rosa, J. D. La, Sánchez-de-la-Campa, A., Plana, F. and Ruiz, C. R.: Source apportionment analysis of atmospheric particulates in an industrialised urban site in southwestern Spain, Atmospheric Environment, 36(19), 3113–3125, doi:10.1016/S1352-2310(02)00257-1, 2002.

Querol, X., Alastuey, A., Rodríguez, S., Viana, M. M., Artíñano, B., Salvador, P., Mantilla, E., Do Santos, S. G., Patier, R. F., De La Rosa, J., De La Campa, a. S., Menéndez, M. and Gil, J. J.: Levels of particulate matter in rural, urban and industrial sites in Spain, Sci. Total Environ., 334-335(2004), 359–376, doi:10.1016/j.scitotenv.2004.04.036, 2004a.

Querol, X., Alastuey, A., Ruiz, C. R., Artiñano, B., Hansson, H. C., Harrison, R. M., Buringh, E., Ten Brink, H. M., Lutz, M., Bruckmann, P., Straehl, P. and Schneider, J.: Speciation and origin of PM10 and PM2.5 in selected European cities, Atmos. Environ., 38(38), 6547–6555, doi:10.1016/j.atmosenv.2004.08.037, 2004b.

Querol, X., Alastuey, A., Pey, J., Cusack, M., Pérez, N., Mihalopoulos, N., Theodosi, C., Gerasopoulos, E., Kubilay, N. and Koçak, M.: Variability in regional background aerosols within the Mediterranean, Atmos. Chem. Phys. Discuss., 9(2), 10153–10192, doi:10.5194/acpd-9-10153-2009, 2009a.

Querol, X., Pey, J., Pandolfi, M., Alastuey, A., Cusack, M., Pérez, N., Moreno, T., Viana, M., Mihalopoulos, N., Kallos, G. and Kleanthous, S.: African dust contributions to mean ambient PM10 mass-levels across the Mediterranean Basin, Atmos. Environ., 43(28), 4266–4277, doi:10.1016/j.atmosenv.2009.06.013, 2009b.

Ragettli, M.S., Ducret-Stich, R.E., Foraster, M., Morelli, X., Aguilera, I., Basagaña, X., Corradi, E., Ineichen, A., Tsai, M.-Y., Probst-Hensch, N., Rivera, M., Slama, R., Künzli, N. and Phuleria, H.C.: Spatio-temporal variation of urban ultrafine particle number concentrations : Spatio-temporal variation of urban ultrafine particle number concentration, Atmos. Environ.,96, 275-283, 2014.

Reche, C., Querol, X., Alastuey, A., Viana, M., Pey, J., Moreno, T., Rodríguez, S., González, Y., Fernández-Camacho, R., De La Campa, A. M. S., De La Rosa, J., Dall'Osto, M., Prévôt, a. S. H., Hueglin, C., Harrison, R. M. and Quincey, P.: New considerations for PM, Black Carbon and particle number concentration for air quality monitoring across different European cities, Atmos. Chem. Phys., 11(13), 6207–6227, doi:10.5194/acp-11-6207-2011, 2011.

Reche, C.: Sources and processes affecting urban aerosols in a coastal Mediterranean environment, Universitat Autónoma de Barcelona, PhD Thesis, 2012.

Reche, C., Viana, M., Amato, F., Alastuey, A., Moreno, T., Hillamo, R., Teinilä, K., Saarnio, K., Seco, R., Peñuelas, J., Mohr, C., Prévôt, A. S. H. and Querol, X.: Biomass burning contributions to urban aerosols in a coastal Mediterranean City, Sci. Total Environ., 427-428, 175–190, doi:10.1016/j.scitotenv.2012.04.012, 2012.

Revuelta, M. A., Harrison, R. M., Núñez, L., Gomez-Moreno, F. J., Pujadas, M. and Artíñano, B.: Comparison of temporal features of sulphate and nitrate at urban and rural sites in Spain and the UK, Atmos. Environ., 60, 383–391, doi:10.1016/j.atmosenv.2012.07.004, 2012.

Rimnácová, D., Ždímal, V., Schwarz, J., Smolík, J. and Rimnác, M.: Atmospheric aerosols in suburb of Prague: The dynamics of particle size distributions, Atmos. Res., 101(3), 539–552, doi:10.1016/j.atmosres.2010.10.024, 2011.

Ripoll, A.: Physical, optical and chemical properties of atmospheric aerosols in the western Mediterranean continental background, Universitat de Barcelona, PhD Thesis, 2015.

Ripoll, A., Minguillón, M. C., Pey, J., Pérez, N., Querol, X., and Alastuey, A.: Joint analysis of continental and regional background environments in the western Mediterranean: PM_1 and PM_{10} concentrations and composition, Atmos. Chem. Phys., 15, 1129-1145, doi:10.5194/acp-15-1129-2015, 2015.

Ritz, B., Ritz, B., Yu, F., Yu, F., Fruin, S., Fruin, S., Chapa, G., Chapa, G., Shaw, G. M., Shaw, G. M., Harris, J. a and Harris, J. a: Ambient air pollution and risk of birth defects in Southern California., Am. J. Epidemiol., 155(1), 17–25 [online] Available from: http://www.ncbi.nlm.nih.gov/pubmed/11772780, 2002.

Robinson, A. L., Subramanian, R., Donahue, N. M., Bernardo-Bricker, A., and Rogge, W. F.: Source apportionment of molecular markers and organic aerosol – 3. food cooking emissions, Environ. Sci. Technol., 40, 7820–7827, 2006.

Rodríguez, S., Querol, X., Alastuey, A. and Plana, F.: Sources and processes affecting levels and composition of atmospheric aerosol in the western Mediterranean, J. Geophys. Res. Atmos., 107(24), 1–14, doi:10.1029/2001JD001488, 2002.

Rodríguez, S., Querol, X., Alastuey, A., Viana, M. M., Alarcón, M., Mantilla, E. and Ruiz, C. R.: Comparative PM10-PM2.5 source contribution study at rural, urban and industrial sites during PM episodes in Eastern Spain, Sci. Total Environ., 328(1-3), 95–113, doi:10.1016/S0048-9697(03)00411-X, 2004.

Rogge, W. F., Hildemann, L. M., Mazurek, M. A., Cass, G. R., and Simoneit, B. R. T.: Sources of fine organic aerosol. 2. Noncatalyst and catalyst-equipped automobiles and heavy duty diesel trucks, Environ. Sci. Technol., 27, 636–651, 1993.

Rönkkö, T., Virtanen, A., Kannosto, J., Keskinen, J., Lappi, M. and Pirjola, L.: Nucleation mode particles with a nonvolatile core in the exhaust of a heavy duty diesel vehicle, Environ. Sci. Technol., 41(18), 6384–6389, doi:10.1021/es0705339, 2007.

Sabaliauskas, K., Jeong, C., Yao, X., Jun, Y. and Evans, G.: Cluster analysis of roadside ultra fi ne particle size distributions, Atmos. Environ., 70, 64–74, doi:10.1016/j.atmosenv.2012.12.025, 2013.

Salimi, F., Ristovski, Z., Mazaheri, M., Laiman, R., Crilley, L. R., He, C., Clifford, S. and Morawska, L.: Assessment and application of clustering techniques to atmospheric particle number size distribution for the purpose of source apportionment, Atmos. Chem. Phys. Discuss., 14(10), 15257–15281, doi:10.5194/acpd-14-15257-2014, 2014.

Salma, I., Borsòs, T., Weidinger, T., Aalto, P., Hussein, T., Dal Maso, M. and Kulmala, M.: Production, growth and properties of ultrafine atmospheric aerosol particles in an urban environment, Atmos. Chem. Phys., 11(3), 1339–1353, doi:10.5194/acp-11-1339-2011, 2011.

Salma, I., Füri, P., Németh, Z., Balásházy, I, Hofmann, W. and Farkas, A.: Lung burden and deposition distribution of inhaled atmospheric urban ultrafine particles as the first step in their health risk assessment, Atmos. Environ. 104, 39-49, 2015

Schauer, J. J., Lough, G. C., Shafer, M. M., Christensen, W. F., Arndt, M. F., Deminter, J. T. and Park, J.: Research Report Characterization of Metals Emitted from Motor Vehicles, Health Effects Institute, (133), 2006.

Schwartz, J.: Is Daily Mortality Associated Specifically with Fine Particles?, Journal of the Air and Waste management association, 46, 927-939, 1996.

Seaton, A., Godden, D., MacNee, W. and Donaldson, K.: Particulate air pollution and acute health effects, Lancet, 345, 176-178, 1995.

Seinfeld, J. H. and Pandis, S. N.: Atmospheric chemistry and physics: From air pollution to climate change, 2nd Edition. 1232 pp., ISBN: 978-0-471-72018-8, September 2006.

Sellegri, K., Laj, P., Venzac, H., Boulon, J., Picard, D., Villani, P., Bonasoni, P., Marinoni, A., Cristofanelli, P., and Vuillermoz, E.: Seasonal variations of aerosol size distributions based on long-term measurements at the high altitude Himalayan site of Nepal Climate Observatory-Pyramid (5079 m), Nepal, Atmos. Chem. Phys., 10, 10679-10690, doi:10.5194/acp-10-10679-2010, 2010.

Shi, J. P. and Harrison, R. M.: Investigation of ultrafine particle formation during diesel exhaust dilution, Environ. Sci. Technol., 33(21), 3730–3736, doi:10.1021/es981187l, 1999.

Shi, J. P., Mark, D. and Harrison, R. M.: Characterization of particles from a current technology heavy-duty diesel engine, Environ. Sci. Technol., 34(5), 748–755, doi:10.1021/es990530z, 2000.

Sicard, M., Rocadenbosch, F., Reba, M. N. M., ComerÓn, a., Tomás, S., García-Vízcaino, D., Batet, O., Barrios, R., Kumar, D. and Baldasano, J. M.: Seasonal variability of aerosol optical properties observed by means of a Raman lidar at an EARLINET site over Northeastern Spain, Atmos. Chem. Phys., 11(1), 175–190, doi:10.5194/acp-11-175-2011, 2011.

Simoneit, B. R. T.: Biomass burning – a review of organic tracers for smoke from incomplete combustion, Appl. Geochem., 17, 129–162, 2002.

Simpson, D., Winiwarter, W., Börjesson, G., Cinderby, S., Ferreiro, A., Guenther, A., Hewitt, C. N., Janson, R., Khalil, M. A. K., Owen, S., Pierce, T. E., Puxbaum, H., Shearer, M., Skiba, U., Steinbrecher, R., Tarrasón, L., Öquist, M. G.: Inventorying emissions from nature in Europe, Journal of Geophysical Research, 104 (D7), 8113–8152, doi:10.1029/98JD02747, 1999.

Somers, C. M., McCarry, B. E., Malek, F. and Quinn, J. S.: Reduction of particulate air pollution lowers the risk of heritable mutations in mice., Science, 304(5673), 1008–1010, doi:10.1126/science.1095815, 2004.

Stanier, C.O., Khlystov, A.Y. and Pandis, S.N.: Nucleation events during the Pittsburgh air quality study: description and relation to key meteorological, gas phase, and aerosol parameters, Aerosol Sci. Tech., 38 (S1):253-264, 2004.

Sternbeck, J., Sjödin, A., Andréasson, K.: Metal emissions from road traffic and the influence of resuspension results from two tunnel studies, Atmos. Environ. 36, 4735-4744. 2002.

Surratt, J. D., Chan, A. W. H., Eddingsaas, N. C., Chan, M. N., Loza, C. L., Kwan, A. L., Hersey, S. P., Flagan, R. C.,Wennberg, P. O., and Seinfeld, J. H.: Reactive intermediates revealed in secondary organic aerosol formation from isoprene, P. Natl. Acad. Sci. USA, 107, 6640–6645, 2010.

Swietlicki, E., Hansson, H.-C., Hämeri, K., Svenningsson, B., Massling, A., McFinnigans, G., McMurray, P.H., Petäjä, T., Tunved, P., Gysel, M., Topping, D., Weingartner, E., Baltensperger. U., Rissler, J., Wiedensohler, A. and Kulmala, M.: Hygroscopic properties of submicrometer atmospheric aerosol particles measured with H-TDMA instruments in various environments-a review, Tellus, 60B, 432-469, 2008.

Szmigielski, R., Surratt, J.D., Gómez-González, Y., Van der Veken, P., Kourtchev, I., Vermeylen, R., Blockhuys, F., Jaoui, M., Kleindienst, T. E., Lewandowski, M., Offenberg, J. H., Edney, E. O., Seinfeld, J. H., Maenhaut, W., and Claeys, M.: 3-Methyl-1,2,3-butanetricarboxylic acid: an atmospheric tracer for terpene secondary organic aerosol, Geophys. Res. Lett., 34, L24811, doi:10.1029/2007GL031338, 2007.

Tobías, A., Pérez, L., Díaz, J., Linares, C., Pey, J., Alastruey, A. and Querol, X.: Short-term effects of particulate matter on total mortality during Saharan dust outbreaks: A case-crossover analysis in Madrid (Spain), Sci. Total Environ., 412-413, 386–389, doi:10.1016/j.scitotenv.2011.10.027, 2011.

Tolis, E. I., Gkanas, E. I., Pavlidou, E., Skemperi, A., Pey, J., Pérez, N. and Bartzis, J. G.: Microstuctural analysis and determination of PM10 emission sources in an industrial Mediterranean city, Cent. Eur. J. Chem., 12(10), 1081–1090, doi:10.2478/s11532-014-0549-8, 2014.

Torfs, K. and Van Grieken, R.: Chemical relations between atmospheric aerosols, deposition and stone decay layers on historic buildings at the Mediterranean coast, Atmos. Environ., 31(15), 2179–2192, doi:10.1016/S1352-2310(97)00038-1, 1997.

Tukey, J.W.: Bias and confidence in not-quite large samples, Ann. of Math. Stat., 29, 2, 614, 1958.

Uhrner, U., von Löwis, S., Vehkamäki, H., Wehner, B., Bräsel, S., Hermann, M., Stratmann, F., Kulmala, M. and Wiedensohler, a.: Dilution and aerosol dynamics within a diesel car exhaust plume-CFD simulations of on-road measurement conditions, Atmos. Environ., 41(35), 7440–7461, doi:10.1016/j.atmosenv.2007.05.057, 2007.

Väänänen, R., Kyrö, E.-M., Nieminen, T., Kivekäs, N., Junninen, H., Virkkula, A., Dal Maso, M., Lihavainen, H., Viisanen, Y., Svenningsson, B., Holst, T., Arneth, A., Aalto, P. P., Kulmala, M., and Kerminen, V.-M.: Analysis of particle size distribution changes between three measurement sites in northern Scandinavia, Atmos. Chem. Phys., 13, 11887-11903, doi:10.5194/acp-13-11887-2013, 2013.

Vakkari, V., Laakso, H., Kulmala, M., Laaksonen, A., Mabaso, D., Molefe, M., Kgabi, N., and Laakso, L.: New particle formation events in semi-clean South African savannah, Atmos. Chem. Phys., 11, 3333-3346, doi:10.5194/acp-11-3333-2011, 2011.

Viana, M.: Niveles, Composición y Origen del Material Particulado Atmosférico en los sectores Norte y Este de la Península Ibérica y Canarias. Universitat de Barcelona, PhD Thesis, 2003.

Viana, M., Hammingh, P., Colette, A., Querol, X., Degraeuwe, B., Vlieger, I. De and Aardenne, J. Van: Impact of maritime transport emissions on coastal air quality in Europe, Atmos. Environ., 90, 96–105, doi:10.1016/j.atmosenv.2014.03.046, 2014.

Waked, a., Favez, O., Alleman, L. Y., Piot, C., Petit, J. E., Delaunay, T., Verlinden, E., Golly, B., Besombes, J. L., Jaffrezo, J. L. and Leoz-Garziandia, E.: Source apportionment of PM10 in a north-western Europe regional urban background site (Lens, France) using positive matrix factorization and including primary biogenic emissions, Atmos. Chem. Phys., 14(7), 3325–3346, doi:10.5194/acp-14-3325-2014, 2014.

Wang, Z. B., Hu, M., Sun, J. Y., Wu, Z. J., Yue, D. L., Shen, X. J., Zhang, Y. M., Pei, X. Y., Cheng, Y. F., and Wiedensohler, A.: Characteristics of regional new particle formation in urban and regional background environments in the North China Plain, Atmos. Chem. Phys., 13, 12495-12506, doi:10.5194/acp-13-12495-2013, 2013a.

Wang, Z. B., Hu, M., Wu, Z. J., Yue, D. L., He, L. Y., Huang, X. F., Liu, X. G., and Wiedensohler, A.: Long-term measurements of particle number size distributions and the relationships with air mass history and source apportionment in the summer of Beijing, Atmos. Chem. Phys., 13, 10159-10170, doi:10.5194/acp-13-10159-2013, 2013b.

Wegner, T., Hussein, T., Hämeri, K., Vesala, T., Kulmala, M. and Weber, S.: Properties of aerosol signature size distributions in the urban environment as derived by cluster analysis, Atmos. Environ., 61, 350–360, doi:10.1016/j.atmosenv.2012.07.048, 2012.

Wehner, B., Birmili, W., Gnauk, T. and Wiedensohler, a: Particle number size distributions in a street canyon and their transformation into the urban background: Measurements and a simple model study, Atmos., Environ., 36, 2215–22232002a9174, 2002.

Wehner, B., Siebert, H., Stratmann, F., Tuch, T., Wiedensohler, A., Petäjä, T., Dal Maso, M. and Kulmala, M.: Horizontal homogeneity and vertical extent of new particle formation events, Tellus, Ser. B Chem. Phys. Meteorol., 59(3), 362–371, doi:10.1111/j.1600-0889.2007.00260.x, 2007.

Wehner, B., Uhrner, U., von Löwis, S., Zallinger, M. and Wiedensohler, a.: Aerosol number size distributions within the exhaust plume of a diesel and a gasoline passenger car under on-road conditions and determination of emission factors, Atmos. Environ., 43(6), 1235–1245, doi:10.1016/j.atmosenv.2008.11.023, 2009.

WHO. Health effects of Black Carbon, Regional Office for Europe, World Health Organization, 2012.

Wichmann, H. E., Spix, C., Tuch, T., Wölke, G., Peters, a, Heinrich, J., Kreyling, W. G. and Heyder, J.: Daily mortality and fine and ultrafine particles in Erfurt, Germany part I: role of particle number and particle mass., Res. Rep. Health. Eff. Inst., (98), 5–86; discussion 87–94, 2000.

Wiedensohler, A., Wehner, B., Birmili, W.: Aerosol number concentrations and size distributions at mountain-rural, urban-influenced rural, and urban-background sites in Germany, Journal of Aerosol Medicine-Deposition Clearance and Effects in the Lung, 15 (2), 237–243, 2002.

Woo, K.S., Chen, D.R., Pui, D.Y.H and McMurry, P.H.: Measurement of Atlanta aerosol size distributions: observations of ultrafine particle events, Aerosol Sci. Tech., 34, 75-87, 2001.

Wu D., Tieb X., Li C., Ying Z., Kai-Hon Lau A., Huang J., Deng X. and Bi X.: An extremely low visibility event over the Guangzhou region: A case study. Atmospheric Environment 39, 6568–6577, 2005.

Wu, Z., Hu, M., Lin, P., Liu, S., Wehner, B. and Wiedensohler, A.: Particle number size distribution in the urban atmosphere of Beijing, China, Atmos. Environ., 42(34), 7967–7980, doi:10.1016/j.atmosenv.2008.06.022, 2008.

Yang, H. H., Lee, W. J., Chen, S. J. and Lai, S. O.: PAH emission from various industrial stacks, J. Hazard. Mater., 60(2), 159–174, doi:10.1016/S0304-3894(98)00089-2, 1998.

Yin, J., Allen, a. G., Harrison, R. M., Jennings, S. G., Wright, E., Fitzpatrick, M., Healy, T., Barry, E., Ceburnis, D. and McCusker, D.: Major component composition of urban PM10 and PM2.5 in Ireland, Atmos. Res., 78(3-4), 149–165, doi:10.1016/j.atmosres.2005.03.006, 2005.

Yin, J. and Harrison, R. M.: Pragmatic mass closure study for PM1.0, PM2.5 and PM10 at roadside, urban background and rural sites, Atmos. Environ., 42(6), 980–988, doi:10.1016/j.atmosenv.2007.10.005, 2008.

Zhu, Y., Hinds, W. C., Kim, S. and Sioutas, C.: Concentration and size distribution of ultrafine particles near a major highway., J. Air Waste Manag. Assoc., 52(9), 1032–1042, doi:10.1080/10473289.2002.10470842, 2002.

Zhu, Y., Sabaliauskas, K., Liu, X., Meng, H., Gao, H., Jeong, C.-H., Evans, G.J. and Yao, X.: Comparative analysis of new particle formation events in less and severely polluted urban atmosphere, Atmos. Environ., 98, 655-664, 2014.

Zhuang, H., Chan, C. K., Fang, M. and Wexler, A. S.: Size distributions of particulate sulfate, nitrate, and ammonium at a coastal site in Hong Kong, Atmos. Environ., 33(6), 843–853, doi:10.1016/S1352-2310(98)00305-7, 1999.

Zielinska, B., Sagebiel, J., McDonald, J. D., Whitley, K., and Lawson, D. R.: Emission rates and comparative chemical composition from selectedin-use diesel and gasoline-fueled vehicles, J. Air Waste Manage. Assoc., 54, 1138–1150, 2004.

Zwack, L. M., Paciorek, C. J., Spengler, J. D. and Levy, J. I.: Modeling spatial patterns of traffic-related air pollutants in complex urban terrain, Environ. Health Perspect., 119(6), 852–859, doi:10.1289/ehp.1002519, 2011.

Chapter 9

Acknowledgements

9. Acknowledgements

I would like to thank both my supervisors Xavier Querol and Manuel Dall'Osto, for their constant support and infinite patience with me, for teaching me many things about science and life; I finish this thesis much wiser than I started.

Gracias al resto de investigadores del grupo Andrés, Mar, Tere, Mari Cruz, Fulvio, Angeliki y Marco por ser tan buena gente, por estar siempre disponibles y dispuestos a ayudarme y por vuestro apoyo.

A mis compañeros de despacho, ha sido un placer ser vuestra secretaria. Muchas gracias Noemí, por ser siempre la voz de la razón, por tu infinita sabiduría, por las risas compartidas, por todas las cosas que me has enseñado de aerosoles, y por responder siempre a mis preguntas (de ciencia). Sofia, siempre un torbellino de energía y alegría, estoy segura de que todo te va a ir muy bien! Roy, thanks for bringing teas and sweets from all around the world, it was always a pleasure to chat with you. Al resto de las immaduras, Ioar, Cristina, Anna, Iria, Vânia y Marina muchas gracias por las charlas durante la comida, no hubiera sido lo mismo sin vosotras. Patri, muchas gracias por estar siempre ahí, a pesar de la distancia y mucha suerte en todo!

A la gent del laboratori Mercè, Rafa, Silvia, Natalia, Rebeca, Jesús, Oriol i Jordi per la vostra simpatía i les converses mantingudes al llarg dels anys, ha estat un plaer tenir-vos com a companys. Gracias también a Garay y Cristina por las risas de cada dia, hacéis la vida más facil.

I would like to thank the people from the University of Birmingham for the great three-months period that I spent there, especially Professor Roy Harrison and Dr. David Beddows. I learned a lot from you, thank you for your selfless help. Muchas gracias Mary por hacer las cosas más fáciles.

Als meus amics, en especial a Sandra, Neus, Vero, Sara, Teresa, Alba, Vicent, Tarsi, Sento i David perquè sempre m'heu escoltat, recolzat i animat durant aquesta (de vegades complicada) tesi, moltes gràcies. Kasia, danke schön for the skype calls from Down Under, they really made my day(s), see you really soon! Katerina, Lisa, Christina,

David and Edin thanks for your friendship and support. To all the fantastic people I met during my stay in Birmingham both at the University and at the Wesley House, we spent such a wonderful time together and you always made me feel at home.

A la meua familia, en especial als meus pares pel seu recolzament i ajuda en tot moment, per estimar-me.

A Arnau, perquè aquests 4 anys a Barcelona han estat molt intensos, moltes gràcies per estar al meu costat, pels infinits consells i per obrir-me els ulls a tot un mon de noves aventures i possibilitats, t'ho agrairé sempre.

This thesis was done with the financial support of a *Formación de Personal Investigador* (FPI) predoctoral fellowship (BES-2011-046110) funded by the *Ministerio de Economía y Competitividad* (MINECO) and FEDER funds under the projects of *Variabilidad temporal y espacial de aerosoles en el Mediterráneo Occidental: combinación de instrumentación de última generación en caracterización de aerosoles a nivel de superficie.* (VAMOS, CGL2010-19464) A three-month stay in the Division of Environmental Health & Risk Management of the School of Geography, Earth & Environmental Sciences at the University of Birmingham was supported by a *Estancias Breves* fellowship (EEBB-I-13-06027) funded by the MINECO.